

Statistical analysis of till geochemistry in the Nelson River area, northeastern Manitoba:  
implications for Quaternary glacial stratigraphy

by

Ying Wang

A thesis  
presented to the University of Waterloo  
in fulfillment of the  
thesis requirement for the degree of  
Master of Science  
in  
Earth Sciences

Waterloo, Ontario, Canada, 2018

©Ying Wang 2018

## **AUTHOR'S DECLARATION**

I hereby declare that I am the sole author of this thesis. This is a true copy of the thesis, including any required final revisions, as accepted by my examiners.

I understand that my thesis may be made electronically available to the public.

## **Abstract**

The Hudson Bay Lowland (HBL) contains a unique sedimentary record extending beyond the penultimate glaciation of the Quaternary. The complex interplay between two major ice dispersal centres (the Keewatin in the north and the Quebec-Labrador centre in the east) produced multiple till sheets in northeastern Manitoba containing Canadian Shield and carbonate rock detritus in variable proportions. In the Gillam area, the existing till stratigraphic framework consists of four tills: the Sundance Till, the Amery Till, the Long Spruce Till, and the Sky Pilot Till. This till classification is based on clast lithology, matrix color, matrix carbonate content, and clast fabric. One important aspect of this classification is that it has been established at sites where rare interstadial or interglacial organic beds separate certain tills, which facilitated their identification. The main problems are A- these organic beds seldom occur away from type sections and B- the tills show considerable overlap in their sedimentary characteristics. In addition, descriptive inconsistencies exist in the literature and different criteria have been used by various researchers over time. Altogether, these problems make it challenging to use the existing till stratigraphic framework to describe new till sections, understand the regional glacial sedimentary record, and help drift exploration. New approaches need to be tested to verify the stratigraphic framework, determine provenance of the tills and help with regional interpretations.

Till matrix geochemistry contains information which can be used to discriminate till units and determine their provenance, but it has not been used widely in the HBL region in previous till studies. The aim of this thesis is to assess whether tills can be discriminated on the basis of their matrix geochemistry.

To this end, multivariate statistical analysis is applied to a till geochemistry dataset. The methods used include k-means clustering and principal component analysis (PCA) to gain insights into spatial and compositional trends. The integration of cluster analysis and PCA, and spatial visualization of results in ArcGIS, allow for the classification and examination of till groups statistically and spatially.

The number of clusters was determined through visual inspection of a scree plot based on the sum of squared error (SSE) in the dataset. The PCA configuration of the six geochemical

clusters (groups) was then examined and the groups were analyzed and interpreted in terms of composition and possible provenance. While five of the six groups have a relatively clear compositional signature near their centroid in multivariate space, the majority of samples (n=80) fall within a mixed group that considerably overlap in the overall PCA configuration with all other groups. This means that while specific till samples have distinct compositions, several samples within each group are not clearly separated from the large mixed group, suggesting a till composition continuum and a complex (mixed) provenance for most till samples.

Based on this thesis, it can be concluded that 1) considerable overlap in till matrix composition exists across and within all identified till sheets; and 2) stratigraphic correlations away from type sections are thus greatly hindered by the compositional variations/continuum. Tills within the Manitoba HBL are interpreted as a palimpsest product of sediment provenance overprinting and inheritance related to a long glacial history and complex changes in ice flow and subglacial conditions responsible for till production and re-entrainment through time. Till matrix geochemistry, however, provides complementary information on the proportion of shield vs platform contributions in tills and this is useful for the interpretation of till and the glacial history alongside other data such as clast lithology and till fabrics.



## **Acknowledgements**

This project was funded by Natural Resources Canada through a Geo-Mapping for Energy and Minerals Phase 2 (GEM II) research grant to Dr. Martin Ross (UW). First, I would like to thank both of my supervisors, Dr. Martin Ross and Dr. Michelle Gauthier (MGS) for their immense guidance and support over this project. Quaternary group members including Tyler, Aaron, Shawn, Jessey, Amanda, Sam made my graduate life at Waterloo an even better experience. Sam is especially thanked for his help and knowledge through the project. Dr. Brian Kendall and Dr. Eric Grunsky are thanked for being my committee members and providing their comments and insightful thoughts on the project. Tyler Hodder and Daniel Shaw are thanked for their field work and assistance. Tian You is thanked for her excellent statistical knowledge and learning R together with me. Lingyi Kong is thanked for her knowledge of geochemical lab methodology. Finally, I thank my mom, my friends and Han for their support during my MSc project.

## Table of Contents

AUTHOR'S DECLARATION .....	ii
Abstract .....	iii
Acknowledgements .....	v
Table of Contents .....	vi
List of Figures .....	ix
List of Tables .....	xiii
Chapter 1 Introduction.....	1
1.1 Research problem.....	1
1.2 State of Knowledge .....	3
1.2.1 Physiography.....	3
1.2.2 Bedrock Geology.....	4
1.2.3 Continental-scale erratics .....	6
1.3 Quaternary till stratigraphy of the HBL – previous work.....	7
1.4 Problems.....	13
1.5 Thesis Objectives .....	16
1.6 Methodology overview and author's contributions.....	16
1.7 Thesis Structure.....	17
Chapter 2 A strategy and workflow for analyzing and interpreting till matrix geochemical data in a multi-till stratigraphy context .....	18
2.1 Introduction .....	18
2.2 Field Work.....	18
2.2.1 Stratigraphic logging .....	18
2.2.2 Fabric Measurements .....	19
2.2.3 Till Sampling.....	20
2.3 Sample Preparation and Analytical Work .....	22
2.4 Quality Assurance and Quality Control.....	22
2.4.1 Scatterplots .....	23
2.4.2 Thompson-Howarth method.....	24
2.5 Analysis of Geochemical Data .....	25
2.5.1 Elemental ratios and first-order associations.....	26
2.6 Dataset Preparation for Multivariate Analysis .....	26

2.6.1 Censored Data .....	27
2.6.2 Compositional Data and Closure Problem .....	29
2.7 Multivariate Analysis .....	30
2.7.1 K-means Cluster Analysis .....	32
2.7.2 Principal Component Analysis .....	33
2.7.3 Integration of results and interpretation approach .....	35
Chapter 3 Statistical analysis of till geochemistry in northeastern Manitoba .....	37
Overview .....	37
3.1 Introduction .....	37
3.1.1 Physiography and Surficial Geology .....	40
3.1.2 Bedrock .....	41
3.1.3 Manitoba HBL four till stratigraphy .....	44
3.2 Methods .....	48
3.2.1 Field and Laboratory Work and QA/QC .....	48
3.2.2 Multivariate Analysis .....	49
3.3 Results .....	53
3.3.1 Cluster analysis results .....	53
3.3.2 Grain size results .....	53
3.3.3 Principal Component Analysis .....	54
3.3.4 Integrating the methods .....	55
3.3.5 Comparison with single element concentrations .....	59
3.4 Discussion .....	63
3.4.1 Interpreting the source of the six till-geochemistry groups .....	63
3.4.2 Vertical stratigraphic trends in Moondance section .....	71
3.4.3 Implications .....	77
3.5 Conclusion .....	78
Chapter 4 Conclusion .....	80
4.1 Statistical analysis of the till geochemistry of the Gillam area .....	80
4.1.1 Thesis Contributions .....	80
Bibliography .....	82
Appendix A R code .....	91
Appendix B .....	94

Appendix C Examples for Thompson-Howarth Plot .....	102
Appendix D Boxplots of some elements .....	104
Appendix E.....	108

## List of Figures

Figure 1-1 A map of ice mass extent in North America during Last Glacial Maximum (LGM), depicting the location of the Laurentide, Innuitian, Cordilleran, and Greenland Ice Sheets. Highlighted on this map are the extent of the Precambrian Shield (covered by ice during the LGM), and the location of the Hudson Bay Lowland in red font (modified from Dyke et al., 2002).....	1
Figure 1-2 Location of the study area with elevation. Historical sections discussed in this thesis are highlighted in the black box. Major hydraulic dams are in orange. Background hillshade image was generated using a Shuttle Radar Topography Mission (United States Geological Survey, 2002) digital elevation model. ....	4
Figure 1-3 Major bedrock geology in the study area (unpublished digital bedrock geology compilation from MGS, 2016). Black solid line shows the boundary between Precambrian shield and Hudson Bay carbonate platform. Black dashed line shows a small part of the Fox River belt.....	5
Figure 1-4 Map showing distinctive bedrock geology in northern and central Canada (from Dredge and McMartin, 2011).....	7
Figure 1-5 Quaternary stratigraphic framework of the Hudson Bay Lowlands of northeastern Manitoba (from Dredge and McMartin (2011)). ....	8
Figure 1-6 Sundance section exposed on Nelson River. a: carbonate bedrock, b: Sundance Till, c: Amery Till and d: postglacial sediments (from Dredge and McMartin, 2011). ....	10
Figure 1-7 a) Sequence exposed at the Henday section; A: Amery Till; B: Nelson River Sediments; C: Long Spruce Till and D: Lake Agassiz and Tyrrell Sea sediments (Nielsen et al., 1986) b) Sequence exposed along Gods River; 1: Lower till; 2: Gods River sediment; 3: middle till; 4: upper till; 5: Tyrrell Sea sediments (Klassen, 1986).....	11
Figure 2-1 An elongated clast or pebble with its three principal and orthogonal axes (a, b, c) and associated planar surfaces (ab, ac, bc) (Benn, 2007).....	19
Figure 2-2 Example of a sampling site and general sampling approach. The section is first cleaned with an unpainted shovel to remove any slumped or weathered material. The sample is extracted using a plastic trowel (not shown) and put in a thick plastic bag with a sample number.....	21
Figure 2-3 Locations of the till sample sites (red dots are surficial samples and blue stars indicate where section samples are collected). Background hillshade image was generated using a Shuttle Radar Topography Mission (United States Geological Survey, 2002) digital elevation model.....	21
Figure 2-4 An example of a scatterplot where the original sample is plotted vs. the duplicate sample. The orange solid line is the 1:1 control line which means original data is equal to duplicate data. The	

blue dashed line is the 15% precision line. Since the majority of data points are within the chosen precision lines, with some outside scatter, this suggests the data is moderately precise with no bias at a level of 15% precision (modified from Piercey, 2014). ..... 24

Figure 2-5 Thompson-Howarth plot. Control line is set at 95<sup>th</sup> percentile. No points are above the control line suggesting data is acceptable for the desired precision. .... 25

Figure 2-6 An example for how censored data look in the report. Detection limit (DL) is 0.1 ppm. Censored values are indicated in red. .... 27

Figure 2-7 zPatterns indicate censored values graphically. In this example, 20.32% of Bi values are below the detection limit. All other elements in the dataset have values above their detection limit. . 29

Figure 2-8 Scree plot for choosing the number of clusters; red rectangle shows the “elbow” shape (known as the point of inflexion). In this example, the chosen number of clusters is 4. .... 33

Figure 2-9. Graphic plot of first principal component (red line) and second principal component (yellow line) regenerated from Detlefs (2016). .... 34

Figure 2-10 Workflow chart summarizing the methodological approach of this study. The workflow is generated from an online drawing software “Processon” (<https://www.processon.com>, only available in Chinese). .... 36

Figure 3-1 A map of ice mass extent in North America during Last Glacial Maximum (LGM), depicting the location of the Laurentide, Innuitian, Cordilleran, and Greenland Ice Sheets. Highlighted on this map are the extent of the Precambrian Shield (covered by ice during the LGM), and the location of the Hudson Bay Lowland in red font (modified from Dyke et al., 2002). .... 38

Figure 3-2 Location of study area. The main road is marked as a thick black line, and railway is the thin interlaced black line. The location of five important historical sections (Moondance, Henday, Limestone, Birds’ Island and Sundance) is included in this map. Background hillshade image was generated using a Shuttle Radar Topography Mission (United States Geological Survey, 2002) digital elevation model. .... 41

Figure 3-3 Major bedrock geology in the study area (unpublished digital bedrock geology compilation from MGS, 2016) ..... 42

Figure 3-4 Map showing distinctive bedrock geology in northern and central Canada (from Dredge and McMartin, 2011). .... 44

Figure 3-5 Simplified stratigraphic column from northeastern Manitoba (modified from Dredge and McMartin, 2011). .... 45

Figure 3-6 K-means sum of squared errors (SSE) plot. SSE associated with each number of clusters is shown on the y-axis. The less number of clusters has the bigger SSE. The inflexion point here is at number 6 which is applied in this study. .... 51

Figure 3-7 Principal Component Analysis (PCA) scree plot. Eigenvalues associated with each principal component is shown on the y-axis. First principal component has the largest eigenvalue which explains the most variance within the dataset (e.g. Grunsky, 2010). The inflexion point (“elbow” shape) here is at number 3 which is used in this study. .... 52

Figure 3-8 Ternary plots of grain size results for each group..... 54

Figure 3-9 K-means clusters (colored) plotted on graphs that compare PCs: A) PC1 vs. PC2, B) PC1 vs. PC3. Number of samples in each group: Group a ( $n=2$ ), Group b ( $n=80$ ), Group c ( $n=31$ ), Group d ( $n=41$ ), Group e ( $n=24$ ), Group f ( $n=67$ ). The position of an individual labelled element is plotted in R according to its loading value away from (0,0) and its eigenvector. Centroids from k-mean clustering analysis are black solid dots. .... 59

Figure 3-10 Color-coded geochemical groups classified from till matrix geochemistry by k-means cluster analysis: scatterplot of carb ratio vs. sum of REEs. Group a: lowest in carb ratio and medium value of sum of REEs; Group b: medium values in both carb ratio and REEs; Group c: highest value in carb ratio with a large spread, and a large spread in REEs; Group d: high in carb ratio and lowest in REEs; Group e: large spreads in both carb ratio and REEs; Group f: low- medium value in carb ratio and highest in REEs. .... 67

Figure 3-11 The spatial distribution of till-geochemistry groups. Locations of sections are denoted by hollow triangles, and stacked dots show individual till samples with those sections (unpublished digital bedrock geology compilation from MGS, 2016). .... 69

Figure 3-12 A) Spatial characteristics within Group f (yellow stars) showing only those samples with PC3 scores  $<0$  and PC2 scores  $>0$ ; B) spatial relationship between Group f and Group c of samples with PC3 scores  $>0$  and PC2 scores  $<0$  (unpublished digital bedrock geology compilation from MGS, 2016)..... 71

Figure 3-13 Moondance section till-clast units logged by research team and till-geochemistry units based on the multivariate analysis (this study) compared with stratigraphy generated from Roy (1998). Sample locations are revealed by their labels (e.g. 1 to 10)..... 73

Figure 3-14 PCA biplots show the position of samples collected from Moondance section. .... 76

Figure 3-15 Concentration plots for carbonate ratio and certain REEs (Gd, Nd, Pr, Sm) with Hf and Zr for the Moondance samples. Orange dashed lines indicate the contacts between the major till units according to Roy (1998)..... 77



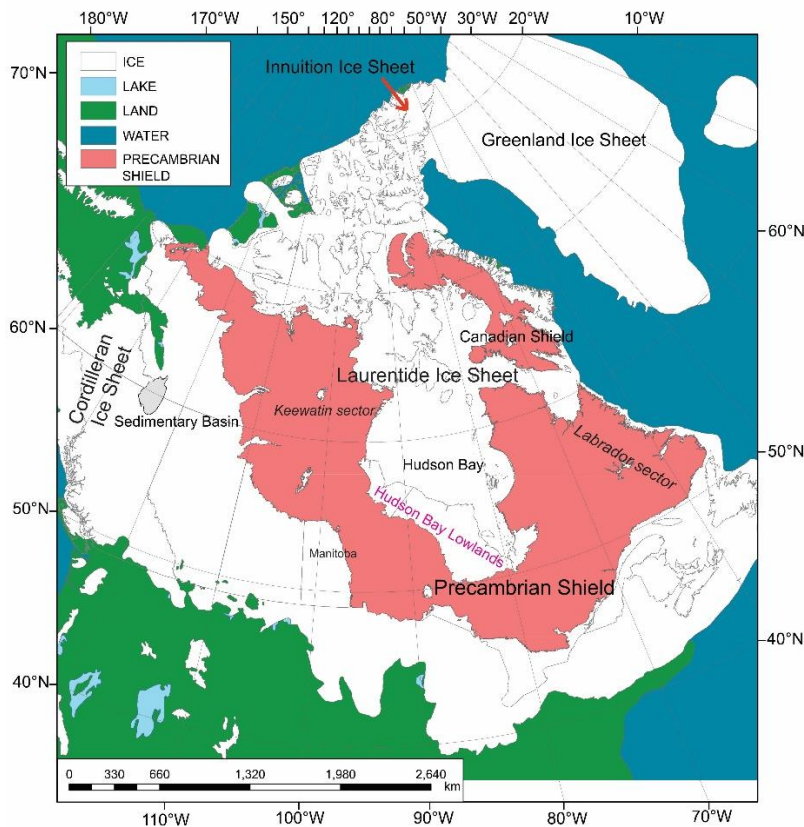
## List of Tables

Table 1-1 Summary table showing till unit descriptions by different authors .....	15
Table 2-1 Total digestion detection limit of all analyzed elements reported from SRC. ....	28
Table 3-1 Results from k-means method.....	53
Table 3-2 Summary of principal components .....	57
Table 3-3 Individual element loadings of first 3 PCs. Loadings of $\pm 0.5$ is the threshold for elements that contribute strongly to PCs (red bold fonts). ....	57
Table 3-4 Summary table of the average concentration and standard deviation of each element, calculated for each of the six till-geochemistry groups. Rare earth elements (REE) are highlighted in yellow, and are included as a summed group at the end of the table. Light orange shaded boxes delimit the highest mean concentrations of a specific element, relative to the six till-geochemistry groups. Light green shaded boxes likewise delimit the lowest mean concentrations of a specific element, relative to the six till-geochemistry groups. Box plots are plotted for several elements (Appendix D).....	60

# Chapter 1 Introduction

## 1.1 Research problem

The Quaternary stratigraphic record of the Hudson Bay Lowlands (HBL) is an important geological archive of glacial and interglacial cycles in North America (e.g. Andrews et al. 1983; Nielsen et al. 1986; Dredge et al. 1990; Thorleifson et al. 1992; Parent et al. 1995; Veillette et al. 1999; Roy et al. 2009; Dubé-Loubert et al. 2012). Firstly, it is a key record of ice sheet evolution and dynamics related to two major ice centres or ice domes; namely the Keewatin sector and the Quebec-Labrador sector of the Laurentide Ice Sheet (LIS), which expanded and contracted in concert with the nearby Innuitian and Cordilleran Ice Sheets (Figure 1-1).



**Figure 1-1** A map of ice mass extent in North America during Last Glacial Maximum (LGM), depicting the location of the Laurentide, Innuitian, Cordilleran, and Greenland Ice Sheets. Highlighted on this map are the extent of the Precambrian Shield (covered by ice during the LGM), and the location of the Hudson Bay Lowland in red font (modified from Dyke et al., 2002).

The sediment successions in the HBL have long been identified for their potential to capture the main changes in LIS configuration (e.g. Shilts 1982). Using a specific pebble lithology, in this case Dubawnt erratics, Shilts (1982) determined that till within northern Nunavut and the Manitoba HBL had been derived at least partially from Baker Lake - a distance of more than 600 km to the north/northwest. Similarly, using greywacke erratics with calcareous concretions (Omars), Prest et al. (2000) showed that part of the tills within the Manitoba HBL was derived from the Belcher Island Group - a distance of more than 800 km to the east.

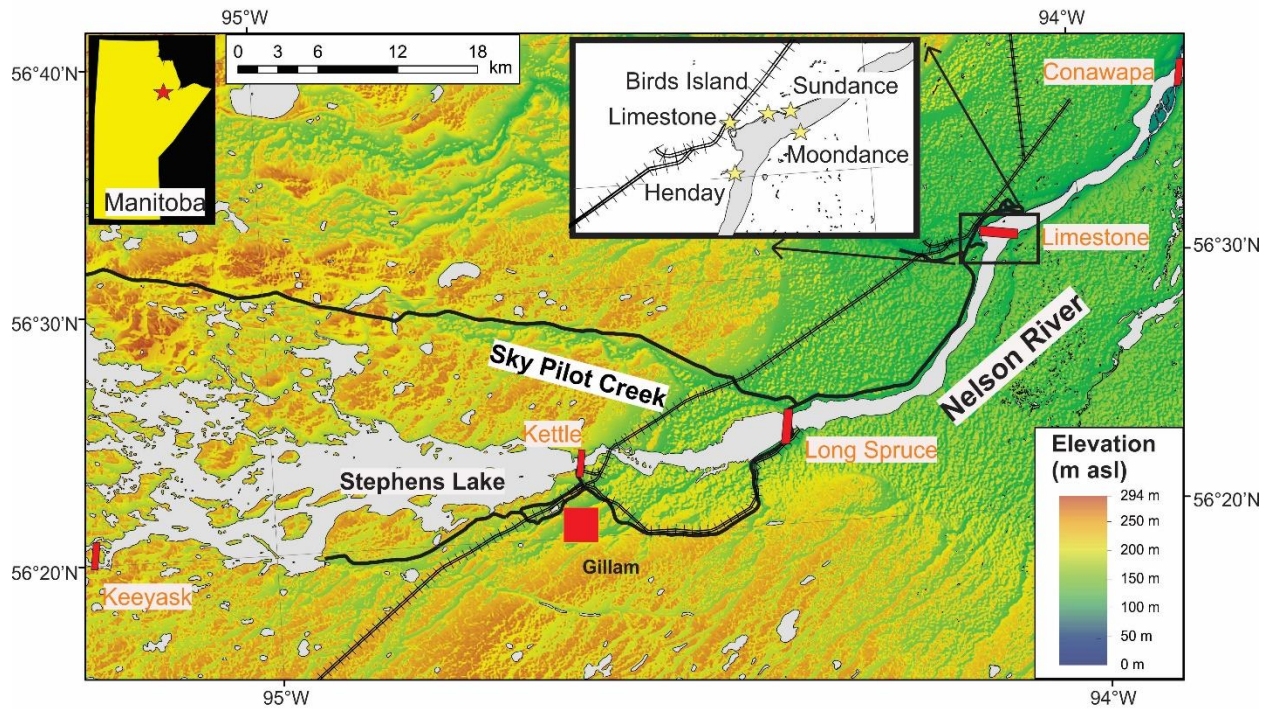
In northeastern Manitoba, the Quaternary sediment successions of the HBL have been the subject of numerous studies (e.g. Nielsen and Dredge, 1982; Nielsen et al. 1986; Dredge and Nielsen, 1987; Klassen, 1986; Roy, 1998; Trommelen, 2013) that aimed at 1) developing understanding of the regional Quaternary history including the preliminary till stratigraphy, as well as more thorough documentation of nonglacial units; and 2) better understanding LIS evolution and dynamics (e.g. Shilts, 1982; Klassen, 1986; Thorleifson et al., 1992). These studies focused on characterizing the sub-till nonglacial units, and attempting to apply ages to those units. Roy (1998) was the first to systematically apply quantitative analyses to the till units, using detailed till-clast lithology counts, geochemistry of the till matrix, and clast-fabric analyses. Unfortunately, his M.Sc. thesis involved work on only four Quaternary sections. These early Quaternary studies named and described a sequence of four layered tills, sometimes separated by nonglacial sorted sediment units. The preliminary work completed by Roy (1998) shows that the data is more variable and cannot easily be separated into four distinct till sheets. This was also shown by Trommelen (2013), which led to the need for this M.Sc. thesis. Tills were characterized in previous work based on simplified clast lithology, matrix color, matrix carbonate content, clast fabric, and microfossils (e.g. Nielsen and Dredge, 1982; Klassen, 1986; Nielsen et al., 1986). In most cases, however, the facies descriptions overlap or are based on different methodologies between studies. In addition, the studies that named and described stratigraphic till sheets for the Manitoba HBL are based on sections within just 6 km<sup>2</sup> – and are not regionally representative. Additionally, the sub – till sorted sediment units are of uncertain ages (Roy, 1998) and not found at every section. These problems limit unit correlations between different sediment exposures.

New developments in till classification have involved integrating facies analysis (e.g. clast fabric, clast lithology) with provenance studies based on various combinations of indicator minerals, high-dimensional visualization and geochemistry (e.g. Grünfeld, 2007; Grunsky and Kjarsgaard, 2008; Boston et al., 2010; Dempster et al., 2013; McMartin et al., 2016). Such integrated approaches have yet to be applied to the glacial stratigraphy of northeastern Manitoba. The key question is thus: Can quantitative multi-variate statistical analyses of till matrix geochemistry be used to differentiate tills in the Manitoba HBL where the qualitative field descriptions shows inconsistencies and conflicts? The objectives of this thesis are to 1) examine till matrix geochemistry using multivariate statistical techniques, and 2) compare to the existing four-layered till stratigraphy, and 3) carefully analyze what the results may mean in terms of provenance and glacial dynamics. This represents an important step towards establishing a more quantitative Quaternary till stratigraphic framework for the HBL.

## **1.2 State of Knowledge**

### **1.2.1 Physiography**

The study area is located in the Hudson Bay Lowlands (HBL) of northeastern Manitoba (Figure 1-1, Figure 1-2). The HBL is characterized by flat topography and thick Quaternary sediments. Elevation ranges from 21 m to 294 m above sea level (asl) (Figure 1-2). The terrain is poorly to moderately-drained and is dominated by swamps and spruce bogs (Bostock, 1970). Bedrock outcrop in the study area is rare, and only occurs at the base of a few river sections. Along the Nelson River, logged sections contain multiple stratigraphic layers recording glacial and interglacial events of the Quaternary (Nielsen and Dredge, 1982). Because of train and road connections to the town, as well as the constructions of several dams, this is an accessible area where geologists can study the stratigraphic sequences of the HBL. The main study area for this master's thesis project is near Gillam (Figure 1-2).



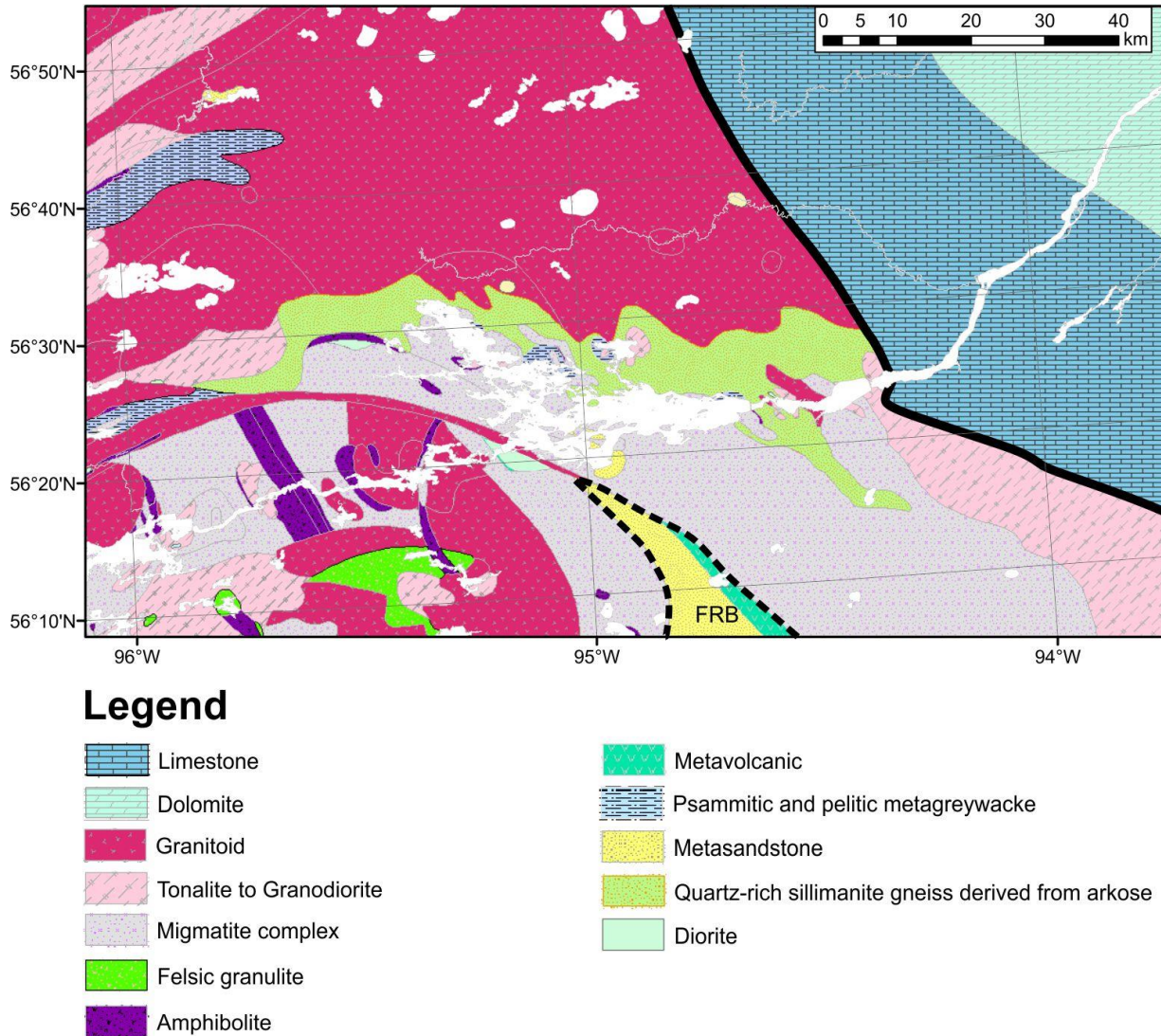
**Figure 1-2** Location of the study area with elevation. Historical sections discussed in this thesis are highlighted in the black box. Major hydraulic dams are in orange. Background hillshade image was generated using a Shuttle Radar Topography Mission (United States Geological Survey, 2002) digital elevation model.

### 1.2.2 Bedrock Geology

The study area crosses the Paleozoic platform in Hudson Bay in the east and Precambrian Shield in the west (Manitoba Energy and Mines, 1992). Main bedrock lithologies in the region are shown in Figure 1-3: 1) Precambrian shield (west of black solid line) contains felsic granulite, granites, granodiorite, tonalite, amphibolite, metavolcanic rocks, migmatite, and metasedimentary rocks such as metagraywacke (Manitoba Energy and Mines, 1992; Rinne, 2016). The geochemical contrast may be limited locally within Precambrian Shield lithologies since many of the rock types are compositionally similar (e.g. felsic); 2) Paleozoic platform in Hudson Bay (east of black solid line) is mainly composed of limestone and dolomite (Manitoba Energy and Mines, 1992). A northwestern part of Fox River Belt (denoted as “FRB” in Figure 1-3) is situated in the south of the study area, and contains layered ultramafic-mafic intrusions and sedimentary rocks (e.g.



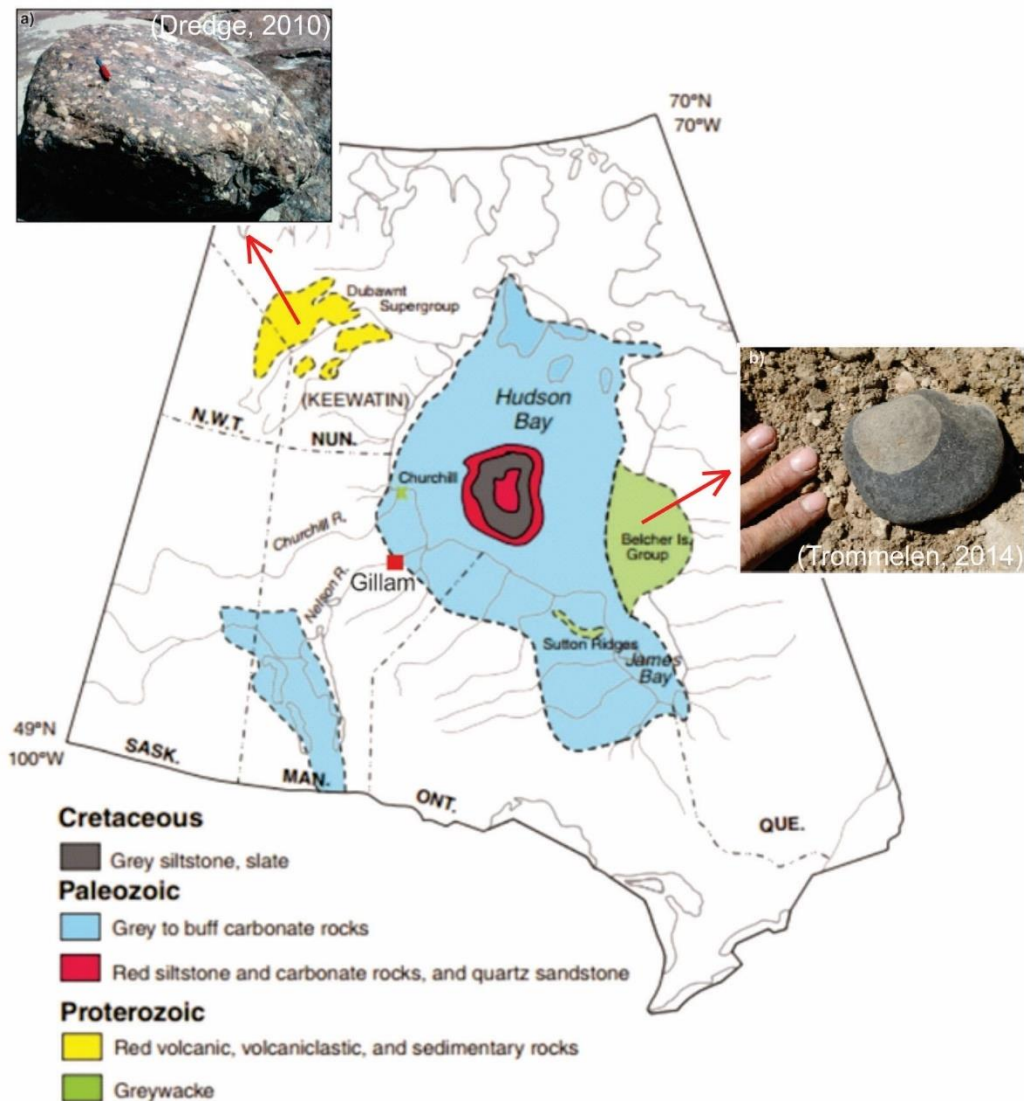
Scoates, 1981; 1990; Manitoba Energy and Mines, 1992; Peck et al., 1999). The major rock types associated with the ultramafic-mafic intrusions are komatiitic basalt and basalt (Peck et al., 1999, 2000). The sedimentary rocks mainly compromise clastic sedimentary rocks including mudstone, argillite, greywacke and siltstone (Peck et al., 1999, 2000).



**Figure 1-3** Major bedrock geology in the study area (unpublished digital bedrock geology compilation from MGS, 2016). Black solid line shows the boundary between Precambrian shield and Hudson Bay carbonate platform. Black dashed line shows a small part of the Fox River belt.

### **1.2.3 Continental-scale erratics**

The map shown in Figure 1-4 includes several distinct bedrock lithologies in some parts of Canada including northern and central Manitoba. Glacial erratics (far - transported rocks in glaciated terrain) have been regarded as important indicators for ice flow history and ice provenance (e.g. Doornbos et al., 2009; Dredge and McMartin, 2011; Plouffe et al., 2011). According to Nielsen and Dredge (1982), the provenances for the glacial erratics from the coarse fraction of tills in the Gillam area can be divided into two groups: northern provenance and eastern provenance. The reddish volcanic and sedimentary rocks are found in tills, and are most likely sourced from the Dubawnt Supergroup in the District of Keewatin (Nielsen and Dredge, 1982). The fact that lithic clasts of the Dubawnt Supergroup indicate that the transport of the glacial material is significant, and this is the evidence for reworking and long-distance transport. Their presence in the study area indicates ice flow from the north. The greywacke with light concretions (also called omars), which have often eroded away and left circular holes, are found in tills, and are most likely sourced from the Omarolluk Formation in the Belcher Island Group (Nielsen and Dredge, 1982). Their presence in the study area indicates ice flow from the west and southwest (Nielsen and Dredge, 1982; Prest et al., 2000).



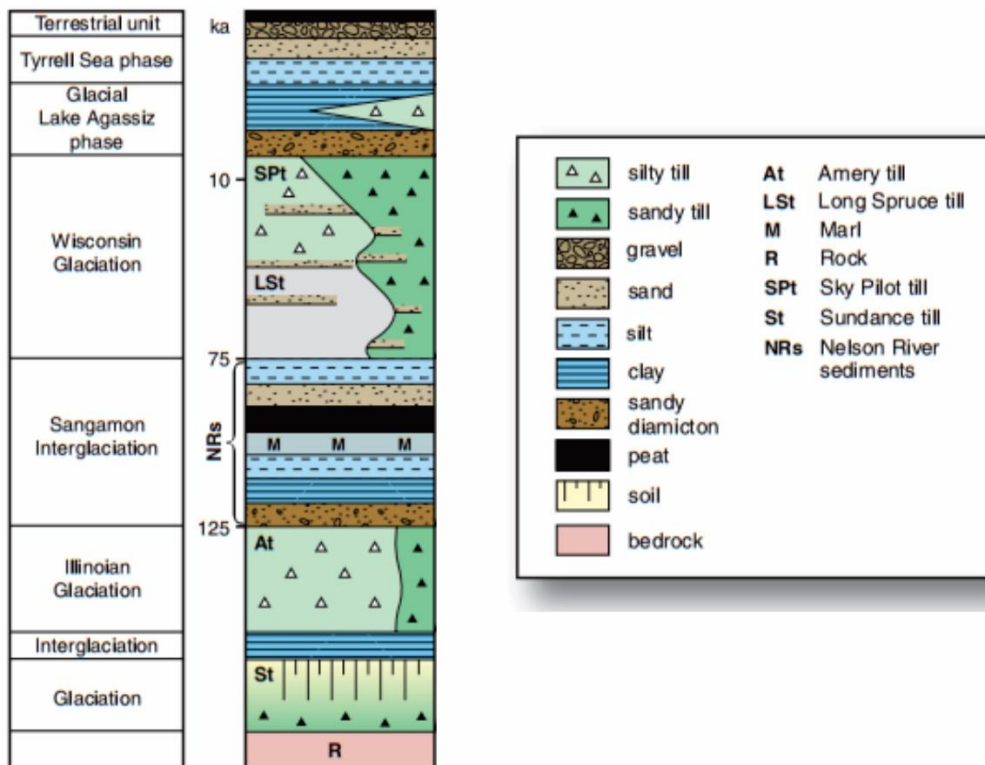
**Figure 1-4** Map showing distinctive bedrock geology in northern and central Canada (from Dredge and McMartin, 2011).

### 1.3 Quaternary till stratigraphy of the HBL – previous work

The HBL region contains numerous Quaternary sediment exposures along the main rivers flowing into Hudson Bay (cf. Dredge and Cowan, 1989). Although HBL region covers three provinces (e.g. Manitoba, Ontario and Quebec), this thesis focuses on the Manitoba part. Four tills have been named during previous work in Manitoba: Sundance Till, Amery Till, Long Spruce Till and Sky Pilot Till (Figure 1-5). This succession of tills is overlain at most sites by glacial lake and



glaciomarine sediment. Figure 1-5 is a composite stratigraphic summary, and it is important to note that this entire succession has not been found at any of the known exposures to date. Instead, it is a product of stratigraphic analysis and correlation based on research done over many years by several workers. The sub-sections below summarize the main characteristics of each of the named till units, while highlighting the nature of the overlaps and the correlation issues away from the type sections. The main descriptions for each till unit are summarized in Table 1-1.

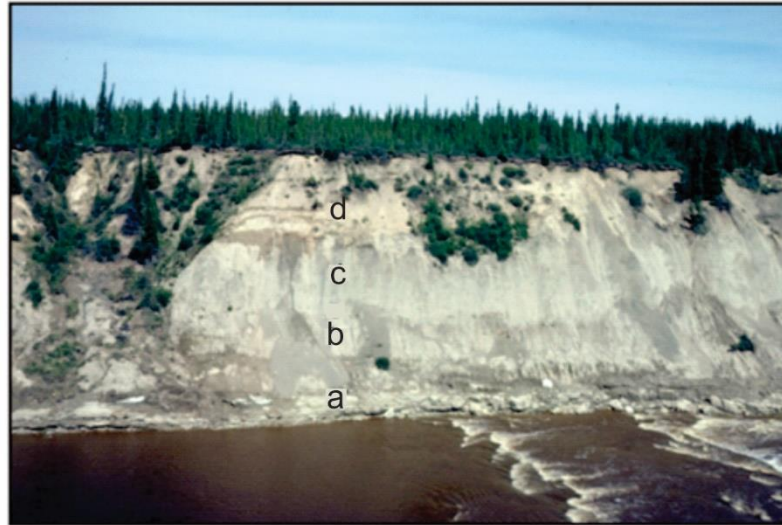


**Figure 1-5** Quaternary stratigraphic framework of the Hudson Bay Lowlands of northeastern Manitoba (from Dredge and McMartin, 2011).

### 1.3.1.1 Sundance Till

The till at the base of the Sundance section (Figure 1-2, Figure 1-6) rests on carbonate bedrock and is considered the oldest till in the area (Nielsen and Dredge, 1982). The Sundance Till is described as light olive grey (5Y 5/2), with a relatively high proportion of sand (45-47%) (cf. Nielsen et al. 1986). Clast lithology is characterized by a high percentage (45-53%) of

undifferentiated Precambrian igneous clasts and 40-55% weight percent carbonate clasts of interpreted local source (Nielsen and Dredge, 1982; Nielsen et al., 1986; Roy, 1998; Dredge and McMartin, 2011). The latter interpretation is based on the lack (or trace amount) of distinctive erratics of eastern Hudson Bay provenance, such as greywacke of the Omarolluk Fm (Nielsen et al., 1986) and low foraminifer content. The less than 63 microns fraction contains from 16 to 31 wt. percent carbonate (Nielsen et al., 1986; Dredge and McMartin, 2011). Ice flow erosional indicators on bedrock underlying Sundance Till are indicative of southwest-trending ice flow (245°), but upstream of Sundance section there are ice flow erosional indicators (miniature crag-and-tails) that trend southeast (145°) (Nielsen et al., 1986; Dredge and McMartin, 2011). Fabric data also suggest SE-trending ice flow during till deposition (Nielsen et al., 1986). Overall, the till has been interpreted to be the product of Keewatin ice (northwest provenance; cf. Figure 1-1), but with minor incorporation of pre-existing material of eastern provenance due to the small number of foraminifera in the till and the striae that underlies the Sundance Till at the Sundance section (Dredge and McMartin, 2011). At the Sundance section, a paleosol is developed at the top of the Sundance Till (Nielsen and Dredge, 1982; Roy, 1998). The paleosol (Table 1-1) is described as a 30 cm leached zone characterized by depletion of labile metals (e.g. Zn, Ni) overlying a zone of metal enrichment (Nielsen et al., 1986; Dredge et al., 1990). The paleosol also has pollen content indicative of tundra vegetation (Dredge and Cowan, 1989). The paleosol was also documented at Moondance section by Roy (1998) where it developed in the upper part of the Sundance Till as a ~1 m thick zone of weathering. A till found and described at the Moondance section, as well as Birds' Island has been correlated to the Sundance Till due to the similar clast lithology, same stratigraphic position and southeast ice flow from fabric data (Roy, 1998; Nielsen, 2002b).

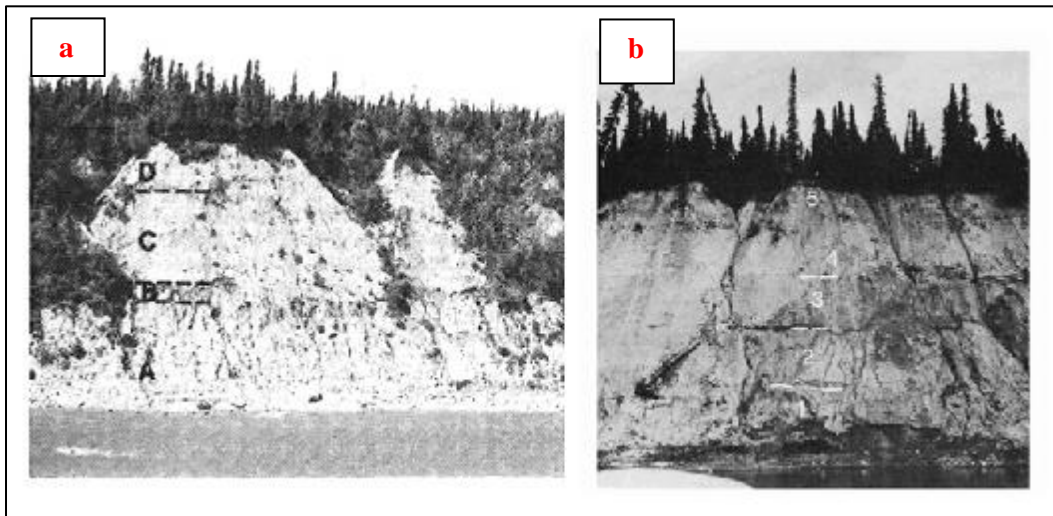


**Figure 1-6** Sundance section exposed on Nelson River. a: carbonate bedrock, b: Sundance Till, c: Amery Till and d: postglacial sediments (from Dredge and McMartin, 2011).

#### 1.3.1.2 Amery Till

At the Henday Section (Figure 1-2) along the Nelson River, a lower till in contact with bedrock is overlain by an interglacial unit, which is in turn overlain by glacial (Wisconsinan) layers and Holocene layers (Klassen, 1986; Figure 1-7a). This lower till, referred to as the Amery Till (Nielsen et al., 1986), is described as a compact, fissile, and jointed light olive grey (5Y 6/1) till. The color is also described as olive grey (5Y 4/2) and olive brown (2.5Y 4/4) by Roy (1998) and olive grey (5Y 5/2) by Klassen (1986). It also shows oxidation along the joint surfaces (Dredge and McMartin, 2011). Amery Till contains more silt (less sand) than the Sundance Till (Table 1-1). The composition is different than the Sundance till, as the Amery Till contains about 66-87 percent carbonate clasts, 9-24 percent igneous clasts and up to 20 percent greywacke clasts from the Omarolluk Fm (Omars) in eastern Hudson Bay (Nielsen et al., 1986). The fine matrix (<63  $\mu\text{m}$ ) contains about 25 to 40 wt. percent carbonate (Nielsen et al., 1986; Table 1-1). Till fabrics indicate ice flow ranging from southwest-trending to northwest-trending directions depending on the site and authors (cf. Dredge and McMartin, 2011), but that combined with the occurrence of Omars have been used to interpret ice flow from the Quebec-Labrador Sector (Figure 1-1) during the deposition of Amery Till. The Amery Till has also been described as containing marine shell

fragments (e.g. *Hiatella arctica*) and abundant microfossils, mainly foraminifers, which has been used to further support an eastern (Hudson Bay) source for the till (Nielsen et al., 1986). Another till with similar characteristics as the Amery Till is found at the base of the God's River section (Figure 1-7b) where it also underlies interglacial sediments (e.g. Klassen, 1986). It has also been identified at other sections including the Moondance section, Limestone section, and Birds' Island section (Roy, 1998). At the Moondance section, the Amery Till was described as olive brown (2.5Y 4/4) and contained marine shell fragments. The Amery Till is separated from the underlying Sundance Till by the occurrence of paleosol (Roy, 1998). At the other two sections (Limestone section and Bird's Island section) described in Roy (1998), the Amery Till has the same color as shown in Moondance section, and they have similar matrix texture and contain marine shell fragments. The age of this till has been assigned to the Illinoian glaciation based on its stratigraphic position beneath Sangamonian age (e.g. Missinaibi Formation; Skinner, 1973) interglacial sediments (Nielsen et al., 1986).



**Figure 1-7** a) Sequence exposed at the Henday section; A: Amery Till; B: Nelson River Sediments; C: Long Spruce Till and D: Lake Agassiz and Tyrrell Sea sediments (Nielsen et al., 1986) b) Sequence exposed along Gods River; 1: Lower till; 2: Gods River sediment; 3: middle till; 4: upper till; 5: Tyrrell Sea sediments (Klassen, 1986)

### 1.3.1.3 Long Spruce Till

At a number of sites (e.g. Klassen, 1986; Dredge and Nielsen, 1985; Dredge and Nielsen, 1987; Nielsen et al., 1986; Roy, 1998; Dredge and McMartin, 2011), a carbonate-rich till is found overlying organic-rich sediments that have been assigned to the last (Sangamonian) interglacial (Nelson River sediments, Figure 1-5). Along the Nelson River, this till is referred to as the Long Spruce Till, whereas a comparable till in a similar stratigraphic position along the Gods River is referred to as “the lower till” of the Wigwam Formation (Klassen, 1986). The Long Spruce Till shows a range of color including a light olive grey (5Y 6/1) color (Nielsen and Dredge, 1982), dark grey (5Y 4/1) color (Roy, 1998) and olive grey (Dredge and McMartin, 2011). Clast fabric data from Long Spruce Till has been interpreted as NW-, W-, and SW – trending (Nielsen and Dredge, 1982; Nielsen et al., 1986; Roy, 1998; Nielsen, 2001; Dredge and McMartin, 2011). Its grain size and clast lithology are similar to that of the Amery Till (Table 1-1). The two can be distinguished based on their stratigraphic position relative to the interglacial bed, but that can only be achieved at a limited number of sites where interglacial sediments are exposed.

Long Spruce Till overlies Amery Till or Nelson River Sediments. However, the separation between Long Spruce Till and Amery Till is not easy to clarify. It has been argued that Long Spruce Till has a lower average abundance of foraminifers than Amery Till (Nielsen et al., 1986), but a close look at the Nielsen et al. (1986) data shows the difference is due to only one outlier “Amery Till” sample with an anomalously high count. If this one sample is removed from the dataset, the averages become similar. Furthermore, no statistical test of the mean has been applied, making this criterion speculative. Nielsen et al. (1986) suggested that an anomalously high percentage (23%) of Omars at some sites suggests that more than one grey till may overlie the Nelson River sediments, since other Long Spruce Till sites only have 5% Omars. However, Omar clasts have also been identified in the Amery Till, Sky Pilot Till (see below), as well as some of the surficial undifferentiated tills.

### 1.3.1.4 Sky Pilot Till

Several till sheets stratigraphically positioned above interglacial sediments have been documented by previous workers. These tills are often interbedded with sand and gravel layers and

have been traditionally separated into grey and brown tills (Dredge and Cowan, 1989). According to legacy work, the grey tills (e.g. Long Spruce) are found below brown tills (Nielsen and Dredge, 1982) and the brown tills have been lumped together into a single unit referred to as the Sky Pilot Till (Nielsen et al. 1986). The tills are fractured and contain oxidation rinds (Nielsen & Dredge, 1982). Descriptions vary among different authors. The lower unit is described as clast-rich and silty, compact, and calcareous, while the upper unit is less stony, and less compact (Dredge & McMartin, 2011). The ice flow history associated with these two brown tills includes a shift in ice flow from W-trending to SW-trending which are based on the till fabric measurement and the orientation of drumlins (Nielsen et al., 1986; Dredge & McMartin, 2011). However, Trommelen (2013), Trommelen et al. (2014) and Gauthier et al. (2016, 2017) have shown that the youngest till along the Sky Pilot Creek is associated with a transition from west-trending to northwest-trending ice flow.

#### **1.4 Problems**

At least 3 glacial cycles occurred in Hudson Bay Lowlands (HBL) as evidenced by the presence of nonglacial intervals (Nielsen and Dredge, 1982; Nielsen et al., 1986; Roy, 1998). Moreover, the glacial dynamics that occurred as each of those glacial cycles advanced and retreated from at least 2 different source areas of the LIS (e.g. Keewatin and Quebec-Labrador sectors) likely led to complex changes in ice-flow directions over time. The resultant deposition, transportation, and erosion of till is likely complex as well. The palimpsest nature of till production is seen in the qualitative, field – based four till stratigraphy described above, as parameters typically used in facies analysis (e.g. texture, colour, clast lithology, fabric) show overlaps, inconsistencies, and conflicting descriptions from different authors between the described till units (Table 1-1). Other than the stratigraphic position, where glacial units are separated by a nonglacial sorted sediment and/or organic unit at a limited number of sites, none of the criteria that have been used to discriminate between Amery and Long Spruce tills are unique. Moreover, the ice flow direction associated with the Long Spruce Till and Amery Till are variable among different authors (Table 1-1). As for the Sky Pilot Till, it appears from the literature that the texture, fabric, and physical properties of these surficial till sheets vary considerably with major overlaps between the properties of the surficial till and other named tills. Nielsen et al. (1986) recognized two different

brown tills based on the content of greywacke clasts; the lower till sheet contains 20% Omars versus 5% for the upper till. However, they do not specify the number of samples or the standard error associated to these average values. The identification of Omars in certain grain size fractions may also be difficult and it is possible that in some cases it is confused with other lithologies (Hodder et al., 2015). Assigning these upper till sheets to a single stratigraphic unit (Sky Pilot Till) is likely a major, and perhaps misleading, simplification.

The main issue in the study area is that previous researchers focused on the non-glacial stratigraphic units, and preliminarily named four tills based on only a few samples from a few sections along the Nelson River. Examining the published data shows that there are no clear distinctions between the upper 3 tills (Amery Till, Long Spruce Till and Sky Pilot Till). In their stratigraphic summary of Manitoba, Dredge and McMartin (2011) acknowledged that previous efforts to discriminate till sheets into separate stratigraphic units in the HBL of northeastern Manitoba have “met with limited success” because of the considerable compositional variability within tills. Additionally, quantitative analysis on till matrix geochemistry hasn’t been applied to the studied area. However, there is uncertainty about till recognition because of petrographic similarities and ambiguities. It is possible that till-matrix geochemistry would be affected by the same limitations, because of the complex shifts in ice sheet configuration which caused sediment re-entrainment and mixing of bedrock detritus from multiple sources during till production (Dredge and McMartin 2011).



**Table 1-1** Summary table showing till unit descriptions by different authors

Unit Name		Sediment Type	Color	Structure	Fossils	Typical Clast Lithology	Matrix Texture	Matrix total Carbonate	Manganese Staining	Clast-fabric Orientation
Brown Clay Till/ Sky Pilot Till	Till C	Clayey Till	Pale yellowish (10YR 6/2); brown (10YR 4/3), dark greyish brown (10YR 4/2) or dark brown (7.5YR 4/2)	Vary between compact and fissile; relatively soft and unoxidized; no oxidation evidence	Shell fragments	Carbonate: 59-99%, 70.75-72.57% (red carb. 3.2-4.46%),75% Precambrian: 1-29%, 11.94-15.00%, Greywacke: 0-31%; 5.89-9.6%, 5-20%	Gravel: 2-23%, Sand: 13-48%, 7.78-17.14%,15% Silt: 35-61%,73.31-82.43%, 75% Clay: 12-46%, 8.32-9.78%, 10%	N/A; N/A; 38.56%, 38%	YES	West-trending, west-trending and southwest-trending; 218° (southwest-trending); ice flow shift between two brown tills; west-southwest-trending and west-trending; west-trending to southwest-trending
Upper Grey Till/ Long Spruce Till	Twin Creeks sediments Till B	Till	Light olive grey (5Y 6/1); dark grey (5Y 4/1); dark olive grey (5Y 3/2)	Highly fissile with faint light brown oxidation rinds	Abraded shell fragments; poorly fossiliferous	Carbonate: 62-82%, 76%, 62.00-78.56% (red carb.0-0.65%), 70% Precambrian: 8-25%, 19%, 13.76-26.60%,28% Greywacke: 2-26%, 5%, 6.32-10.55%, 8%	Gravel: 4-11%,9% Sand: 22-33%, 25%, 17.658-27.278%,25% Silt: 38-48%, 39%, 65.977-72.336%,68% Clay: 24-37%, 27%, 5.905-10.746%, 8%	N/A; 24%; 31.60%, 24 40%	YES, but relatively less	Northwest-trending; west-trending;300° (North-trending); southwest-trending
Interglacial Deposits/Nelson River sediment	Gods River sediments	Sand, silt and clay mixture with minor ice-rafted detritus	N/A	thinly bedded	spruce wood (Picea)	N/A	N/A	N/A	N/A	N/A
Middle Grey Till/Amery Till	Till A	Till	Light olive grey (5Y 6/1); olive gray (5Y 4/2); olive gray (5Y 5/2 or 5Y 4/2)	Highly fractured with oxidation rinds	Shell fragments are common; abundant marine shell fragment	Carbonate: 66-87%, 79%, 76.38-80.15% (red carb. 0-0.60%), 77% Precambrian: 9-24%, 14%, 1.96-4.33%, 23% Greywacke: 3-10%, 7%, 16.80-20.10%	Gravel: 9-12%, 8% Sand: 25-31%, 27%, 24.054-34.043%,28% Silt: 36-47%, 40%, 60.14-69.931%, 66% Clay: 22-39%, 25%, 4.444-7.35%, 7%	N/A; 25%; 37.61%, 25-40%	YES	Northwest-trending; southwest-trending and west-trending; 238° (southwest-trending); southwest-trending and southeast-trending; southwest-trending
Paleosol/Sundance paleosol		Paleosol	N/A	Consist of 30cm thick carbonate leach zone	N/A	N/A;	N/A;	N/A;	N/A	N/A
Lower Grey Till/Sundance Till		Till	Light olive grey (5Y 5/2); dark grayish brown color (2.5Y 5/2)	Some oxidation shown	N/A; lack of fossils	Carbonate: 52% or 42%, 47%, 40.33-46.72% (red carb. 0%), 55% Precambrian: 45% or 53%, 53%, 0.13-0.88%, 45% Greywacke: 3% or 5%, 0%, 51.2-58.40%	Gravel: 14% or 6%,10% Sand: 49% or 55%,47%, 30.786-54.594%, 45% Silt: 38% or 33%, 32%, 42.696-63.008%,45% Clay: 13% or 12%; 11%, 2.328-13.29%, 10%	N/A; 16%; 37.61%; 16-31%	YES	Striae: 245°, fabric: southeast-trending; southeast-trending;149° (southeast-trending); southeast-trending
(Netterville, 1974) and (Klassen, 1986)	(Nielsen & Dredge, 1982)	(Nielsen et al., 1986)	(Nielsen, 2001, 2002)	(Roy, 1998)	McMartin and Dredge, 2011					



## **1.5 Thesis Objectives**

One possible solution to the problem in this study is to integrate till geochemistry, using multivariate statistical techniques (Grunsky, 2010; Grunsky and Kjarsgaard, 2016), with traditional facies analysis (e.g. color, clast lithology, texture, fabric) of the till. As mentioned in Section 1.1, the scope of this research is not to complete the full facies analysis integration, but rather to examine till matrix geochemistry in detail to see what information it can provide that traditional facies analysis methods cannot. The primary objectives are to:

- Determine whether till-matrix geochemical groups form a continuum (hybrid groups overlapping with end-members) or distinct groups (clear groups with unique geochemical makeup).
- Identify and interpret vertical trends in selected key sections as well as horizontal spatial patterns.
- Interpret potential causes for the groups and trends.

This thesis is part of a collaborative project involving the Manitoba Geological Survey and the University of Waterloo. The research team will use the results and interpretation of this thesis to develop the overall, more comprehensive, till stratigraphy of the study area.

## **1.6 Methodology overview and author's contributions**

Field work was conducted in 2014 and 2015 by the author and project team members. Field work involved till sampling, section logging, and fabric measurements. The stratigraphic logs were completed by the MGS team (thesis co-supervisor Dr. Michelle Trommelen and Tyler Hodder) in Winnipeg and used in this thesis for the purpose of providing a framework of major unit contacts and general facies. This is useful to put the results of this research thesis into a general descriptive stratigraphic framework (major bounding surfaces and textural descriptions). A total of 254 till samples were collected from tills at surface and outcropping in section. All samples were processed at the Saskatchewan Research Council Geoanalytical Laboratory (SRC). Geochemical data were prepared, analyzed, and interpreted by the author of the thesis in Waterloo under the guidance of Dr. Martin Ross (co-supervisor) and Dr. Samuel Kelley (post-doc) using statistical methods

through the software program R (<https://www.r-project.org>). A more detailed method section is found in Chapter 2.

## **1.7 Thesis Structure**

This thesis contains four parts: An introduction chapter (Chapter 1) describing the rationale for the study as well as the main objectives; a method chapter (Chapter 2), which describes the details of field work, sampling, analytical work, data processing and statistical analysis; a paper format main body chapter (Chapter 3), which presents the main findings and interpretation; and, finally, a conclusion chapter (Chapter 4), which summarizes the thesis work and the main contributions.

## **Chapter 2 A strategy and workflow for analyzing and interpreting till matrix geochemical data in a multi-till stratigraphy context**

### **2.1 Introduction**

This Chapter describes the necessary ordered set of activities, or workflow, required to achieve the project's objectives as stated in Chapter one. It also provides background information about the rationale for choosing certain methods as well as the preliminary steps to prepare data before initiating the analysis presented in details in Chapter 3. The sub-sections below present the details of the workflow.

### **2.2 Field Work**

Field work was a team effort (see acknowledgments) and it consisted primarily of documenting observations from exposed stratigraphic sections, collecting clast fabric measurements, and sampling till for geochemical analysis. This work builds upon existing published literature (cf. Nielsen & Dredge, 1982; Klassen, 1986; Nielsen et al., 1986; Dredge & Nielsen, 1987; Roy, 1998; Dredge & McMartin, 2011 for stratigraphic descriptions; cf. Nielsen & Dredge, 1982; Roy, 1998 for fabric measurements; cf. Roy, 1998; Dredge and Pehrsson, 2006; Trommelen, 2013 for till sampling). In total, approximately two months were spent in the field including 45 days and 14 days spent in 2014 and 2015, respectively. The field sites are located within the 7,380 km<sup>2</sup> study area and were accessed by truck, helicopter, or boat.

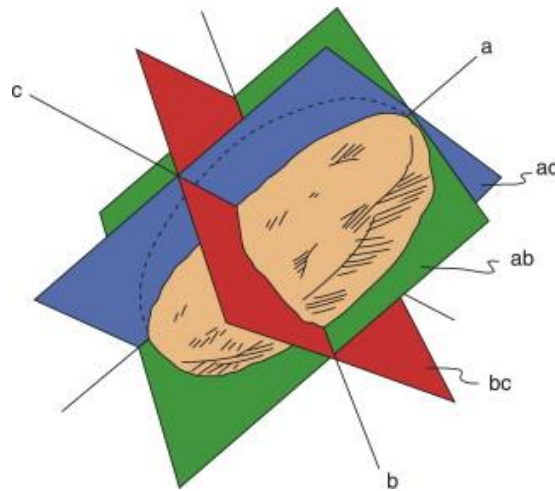
#### **2.2.1 Stratigraphic logging**

Stratigraphic logging consisted of identifying along natural exposures (mainly river sections) visible bounding surfaces separating stratigraphic beds. The vertical thickness of each identified stratigraphic bed was measured and their sedimentary facies described, such as texture and color of sediments, as well as clast content and sedimentary structures. The nature of the contact (e.g., sharp, diffuse) and any apparent facies trends were noted. Clast fabrics were completed at 19 stratigraphic sections, in order to help determine the ice flow orientations associated with till samples. The stratigraphic and fabric analyses are used for comparison with the chemostratigraphy developed in this thesis and to support part of the interpretation. Details

about the stratigraphic and fabric analyses can be found in Trommelen, (2013), Trommelen et al., (2014), and Kelley et al., (2015) at the Manitoba Geological survey. Only a brief summary of the concept is described below.

### 2.2.2 Fabric Measurements

Elongated clasts in a matrix-supported till can have a preferred orientation reflecting stress and strain at time of deposition and this information can be used to derive past ice flow direction associated to that till. Measurement of clast macrofabrics are conducted routinely during investigations of past glacial activity (Evans et al., 2007). Individual elongated clasts can be described by three orthogonal axes and their associated planes (Figure 2-1). The dip and dip-direction of the long a-axis of in situ clasts are always measured and for a 3D fabric, the intermediate b-axis or the ab plane is also measured. The short c-axis can be derived from the measurements of the other two. The shape of the clasts is thus an important criterion to consider. In order to facilitate the identification of the different axes and make accurate measurements, a minimum length difference between them is necessary. The ratio between the length of the a- and b-axes of a clast needs to be greater than 1.5 (Benn 2007).



**Figure 2-1** An elongated clast or pebble with its three principal and orthogonal axes (a, b, c) and associated planar surfaces (ab, ac, bc) (Benn, 2007).

In order to complete a clast fabric in the field, a working surface needs to be prepared at selected sites. To reduce bias in the selection of the clasts to be measured, it is recommended to

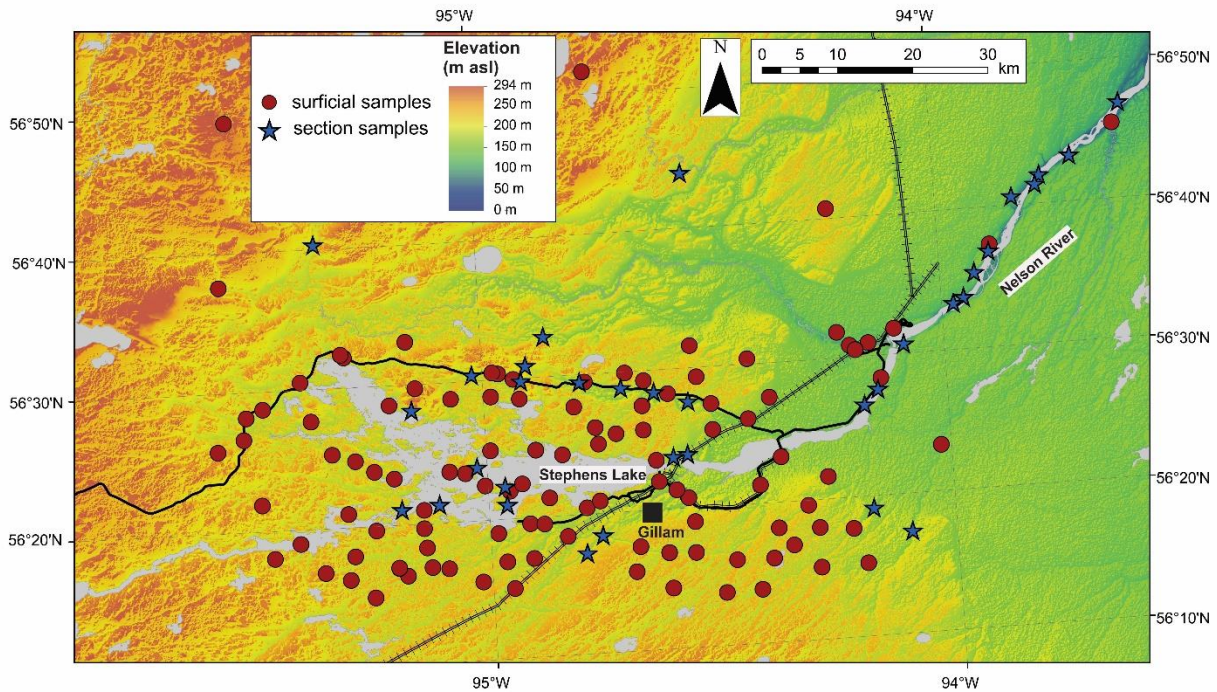
prepare at each site a clean horizontal surface; generally, a 30 cm\*30 cm square surface is sufficient) instead of a vertical surface because clasts in lodgement till (i.e. till that has moderate-strong fabric anisotropy good for ice flow analysis) tend to have a shallow dip and a vertical face could lead to an xy orientation bias in the sampling. A minimum number of measurements is needed to get representative fabrics, and most studies in the literature recommend about 50 clasts for a single fabric (Benn, 2007). However, this can be difficult to achieve in matrix-rich, clast-poor, tills and due to time, budget considerations, and previous work in Manitoba comparing clast fabrics with different sample populations (Hart and Smith, 1997; Nielsen, 2001; Nielsen, 2002b), a minimum of 30 clasts was considered acceptable for this study. These measurements are then used to investigate the spatial arrangement of clasts in the till matrix and determine whether there is a preferred orientation that could be a record of past ice flow at the time of deposition.

### **2.2.3 Till Sampling**

A total of 254 till samples were collected from cleaned sections along the Nelson River and from hand-dug pits at the surface across the field area (Figure 2-3). A clean unpainted shovel and/or dutch auger were used to collect samples of till (Figure 2-2). For surface samples, the minimum depth of sampling was 40 cm in order to be within the parent material (c-horizon) and thus minimize the complexities related to shallower soil forming processes and the risk of contamination from any anthropogenic activity (McMartin and McClenaghan, 2001). Each till sample weighed about 2 to 3 kilograms, which meets the minimum recommended weight (2 kg) for till matrix geochemistry surveys in northern Canada (McMartin and Campbell, 2009). About half of the total weight of each sample was kept at the MGS for archiving. The sample splits were sent to the Saskatchewan Research Council (SRC) Geoanalytical Laboratory, to separate out the <63  $\mu\text{m}$  grain size fraction – which was then used for the analysis of trace element geochemistry. The >2 mm size fraction was also separated at SRC, and sent back to the MGS where the 2–80 mm clasts were classified by lithology.



**Figure 2-2** Example of a sampling site and general sampling approach. The section is first cleaned with an unpainted shovel to remove any slumped or weathered material. The sample is extracted using a plastic trowel (not shown) and put in a thick plastic bag with a sample number.



**Figure 2-3** Locations of the till sample sites (red dots are surficial samples and blue stars indicate where section samples are collected). Background hillshade image was generated using a Shuttle Radar Topography Mission (United States Geological Survey, 2002) digital elevation model.

## 2.3 Sample Preparation and Analytical Work

The fine fraction (< 63  $\mu\text{m}$ ) underwent both partial (HCl: HNO<sub>3</sub>) and total digestions (HF: HNO<sub>3</sub>: HClO<sub>4</sub>). The two digestion methods provide different information useful for the analysis and interpretation. Specifically, partial digestion is useful in exploration because it can dissolve certain minerals that are of economic interest such as sulphide minerals. Partial digestion can also dissolve carbonates and other soft minerals that can be of interest to various provenance studies. The total digestion is a more aggressive digestion that can dissolve most minerals including the more resistant silicate minerals. Results from total digestion provide a more complete set of information about the composition of a sample. Since this study is mostly about discriminating till units on the basis of their overall composition, the results based on the total digestion are the ones used in the statistical analysis. At SRC, the product of total digestion was analyzed using a Perkin Elmer Optima 5300DV inductively coupled plasma-emission spectrometer (ICP-OES) and inductively coupled plasma mass spectrometry (ICP-MS). The partial digestion was analyzed using ICP-MS. The commercial laboratory also provided percentages of calcite (CaCO<sub>3</sub>), dolomite (CaMg (CO<sub>3</sub>)<sub>2</sub>), and total carbonate (CO<sub>3</sub><sup>2-</sup>) based on Ca and Mg results and calculations (all in weight percent) using several equations (e.g. Dolomite (%) = Mg (%) \* 7.5852).

Grain size analysis was done on the materials less than 2 mm by SRC. Samples were dried and sieved. An aliquot of materials less than 2 mm were deflocculated using Calgon<sup>®</sup> and sieved through a 2 mm screen into a graduated cylinder, and then an aliquot of the sample was removed at once. After settling occurred, another aliquot of sample was removed from the cylinder to determine the grain size distribution. The aliquots of materials and sieved sand were dried and re-weighed.

## 2.4 Quality Assurance and Quality Control

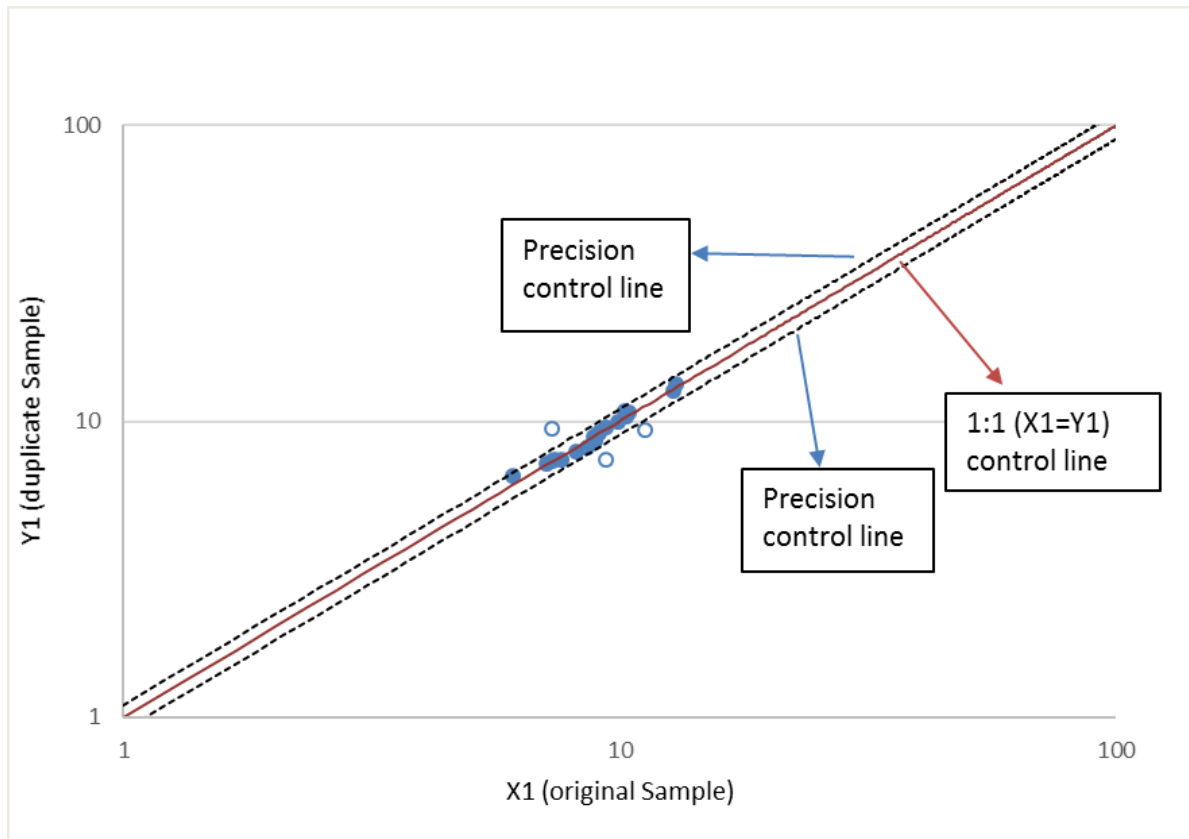
Field duplicates and lab duplicates are used for the quality control. This is important in order to test reproducibility of results, as well as to identify any changes in the performance of the laboratory equipment during the analysis of a sample batch. In total, 12 lab duplicates (samples are separated into two parts in the lab) and 9 field duplicates (samples are repeatedly collected in the field), as well as 12 standard samples from SRC were inserted in the batches. The QA/QC

procedure (e.g. Piercey, 2014) involves comparing results of duplicates for identification of discrepancies.

#### **2.4.1 Scatterplots**

Scatterplots are a tool plotting original data as  $X_1$  and duplicate data as  $Y_1$  with a given precision level (Piercey, 2014; Figure 2-4). If data points are plotted within the precision line, they are precise to the chosen precision (e.g. blue solid dots; Figure 2-4). If the points are not within the precision line, then they are not considered precise to the certain precision level (e.g. blue hollow dots; Figure 2-4). Scatterplots were produced in Microsoft Excel (Appendix B). In this study, the comparison of results for the SRC standard samples shows the average relative standard deviation (%RSD) is 2.92%, which indicates good precision for geologic interpretation according to Jenner (1996) and Abzalov (2008). For the duplicate samples (both field and lab duplicates), results show a precision of 10% for the major oxides and between 10-15% for trace elements (Appendix B). The precision for the duplicate samples is likely due to intrinsic heterogeneities of the split samples; one sample aliquot containing a slightly different mineral blend than the other aliquot will reduce the precision relative to the standard samples. Nonetheless, this level of precision was deemed reasonable for the purpose of this study.



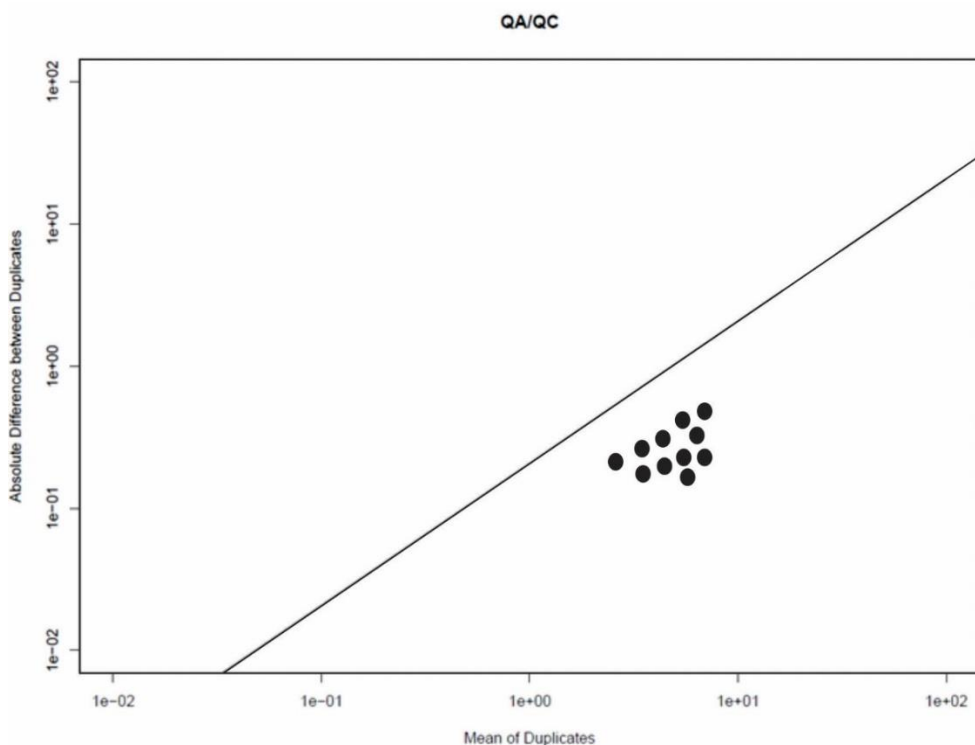


**Figure 2-4** An example of a scatterplot where the original sample is plotted vs. the duplicate sample. The orange solid line is the 1:1 control line which means original data is equal to duplicate data. The blue dashed line is the 15% precision line. Since the majority of data points are within the chosen precision lines, with some outside scatter, this suggests the data is moderately precise with no bias at a level of 15% precision (modified from Piercey, 2014).

#### 2.4.2 Thompson-Howarth method

The Thompson-Howarth method (Thompson & Howarth, 1978) of QA/QC involves plotting data on a control graph with a control line (e.g. 95th percentile or 90th percentile) (Thompson & Howarth, 1978; Stanley, 2003; Piercey, 2014). The process is conducted using a function which is created for the R program (see Garrett and Grunsky, 2003). The x axis is the mean  $((X_1+X_2)/2)$  of original data ( $X_1$ ) and duplicate data ( $X_2$ ), while the y axis is the absolute difference  $(|X_1-X_2|)$  between original data ( $X_1$ ) and duplicate data ( $X_2$ ). With a chosen precision, if the data points are below the control line, then the data are precise at this precision or even better

(Figure 2-5). If the data points are all above the control line, then the data are not precise and should not be used (Thompson & Howarth, 1978; Piercey, 2014). In this study, all elements plotted below the 95<sup>th</sup> percentile line, except Yb (Appendix C). Therefore, Yb was not used for further analysis.



**Figure 2-5** Thompson-Howarth plot. Control line is set at 95<sup>th</sup> percentile. No points are above the control line suggesting data is acceptable for the desired precision.

## 2.5 Analysis of Geochemical Data

The statistical analysis of geochemical data is the main approach used to achieve objective 1, which is to determine whether different till units can be recognized on the basis of till matrix geochemistry (cf. Sect. 1.5). Geochemical results received from SRC were processed using the R programming software. R is open source software widely used for statistical computing and graphics (<https://www.r-project.org>).

Since the study location (Figure 2-3) is underlain by two contrasting geological domains (a carbonate platform to the east and shield rocks to the west), the geochemical signature of these two domains is important for establishing provenance, especially in the regional context of

multiple tills and ice flow shifts (cf. Chapter 1). It is expected that most tills will have a mixed provenance and it is thus important to use techniques that can discriminate tills characterized by mixed sources. Different methods were used herein, to ascertain which methods work best, but also to capture and represent different characteristics of the data. The first group of techniques is based on the use of elemental ratios and groups of elements that are characteristic of a specific source. The second group of techniques involves the multivariate analysis of the complete dataset treated as individual elements.

### **2.5.1 Elemental ratios and first-order associations**

Combining elements into ratios is useful for examining mineral content of till (e.g. Ross et al., 2011; Dredge & McMartin, 2011, McMartin et al., 2016). For example, Ross et al. (2011) and Dredge and McMartin (2011) used ratios to discriminate Ca and Mg from carbonates versus Ca derived from plagioclase (feldspars) and Mg derived from ferromagnesian silicate minerals. Unlike carbonates, plagioclase contains Al and Na. Other feldspars, such as alkali feldspars (e.g. orthoclase), contain K and Na, and ferromagnesian minerals also have abundant Al. Therefore, a ratio of Ca and Mg with these elements (Al, Na, K) helps separate a carbonate source from a silicate source. In this study, the  $\text{Ca+Mg/Na+K+Al}$  ratio is used to determine the carbonate v. feldspathic relative contributions in till. In addition, Rare Earth Elements (REE) in till are good indicators of a shield provenance because they belong to the group of lithophile elements which are concentrated in silicate rocks of the Precambrian Shield (e.g. Dredge and Pehrsson, 2006; Dredge & McMartin, 2011; McMartin et al., 2016); carbonates have comparatively low REE content (Rose et al. 1979). In this study, the  $\text{Ca+Mg/Na+K+Al}$  ratio and total REE were plotted alongside selected till stratigraphic logs (cf. Chapter 3) as a first-order analysis of carbonate versus shield proportion and provenance in tills.

### **2.6 Dataset Preparation for Multivariate Analysis**

Two important pre-processing steps should be applied to data before using statistical methods. The first step involves results that are below the instrument detection limit (censored data). The second step is to address a common problem with compositional data that sum up to a constant; also referred to as the ‘closure’ problem (e.g. Grunsky, 2010).

### 2.6.1 Censored Data

Geochemical data reported from SRC contain censored values (Sanford et al., 1993; Grunsky, 2010). These values are reported as “< lower detection limit” (Figure 2-6) and every element has its own detection limit for a particular instrument or analytical approach (Table 2-1). If an element has a high proportion of censored values, it is better to drop that element from the dataset before applying statistical analyses. In the case where only a small proportion of the values are censored, it may be useful to find a replacement value for these few censored values.

Bi (ppm)
DL=0.1
<0.1
0.1
<0.1
0.2
<0.1
0.1
<0.1

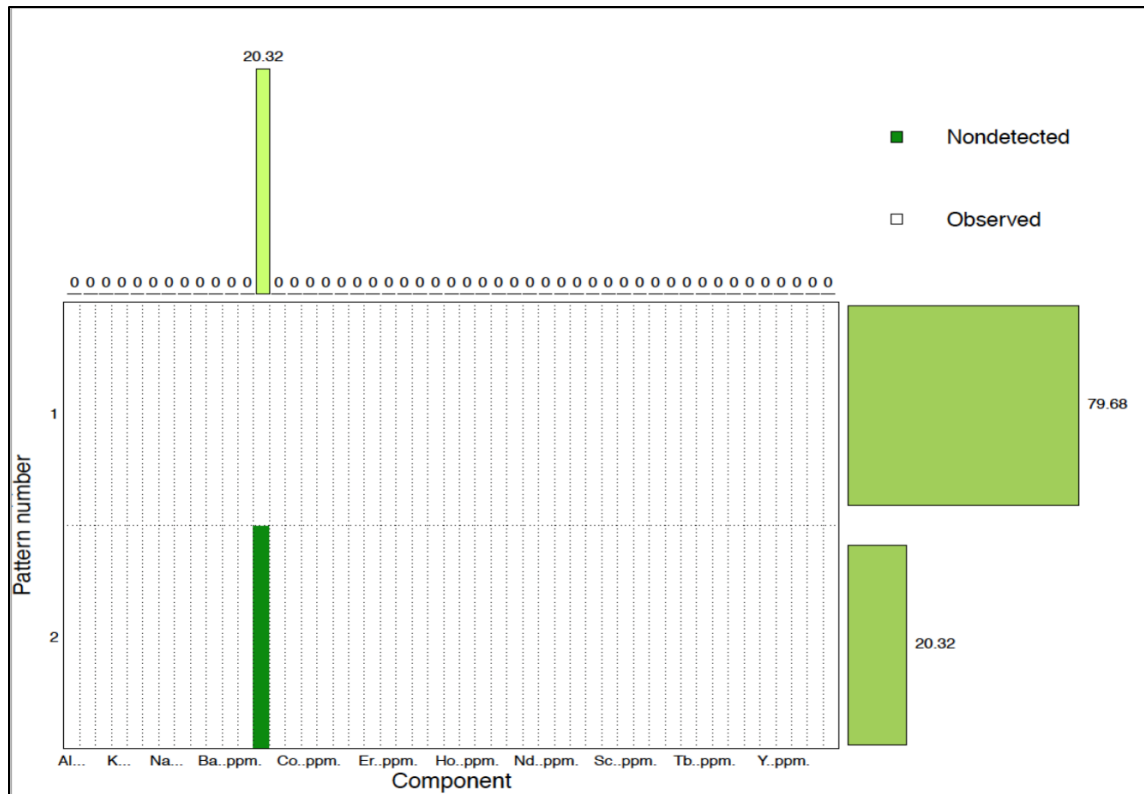
**Figure 2-6** An example for how censored data look in the report. Detection limit (DL) is 0.1 ppm. Censored values are indicated in red.

Total Digestion Detection Limit									
Major Elements (%)		Trace Elements (ppm)							
Al <sub>2</sub> O <sub>3</sub>	0.01	Ag	0.02	Er	0.02	Pb	0.02	V	0.1
CaO	0.01	Ba	1	Eu	0.02	Pr	0.1	W	0.1
Cr <sub>2</sub> O <sub>3</sub>	0.002	Be	0.1	Ga	0.1	Rb	0.1	Y	0.1
Fe <sub>2</sub> O <sub>3</sub>	0.01	Bi	0.1	Gd	0.1	Sc	0.1	Yb	0.02
K <sub>2</sub> O	0.002	Cd	0.1	Hf	0.1	Sm	0.1	Zn	5
MgO	0.001	Ce	0.1	Ho	0.02	Sn	0.02	Zr	0.1
MnO	0.001	Co	0.2	La	1	Sr	1		
Na <sub>2</sub> O	0.01	Cs	0.1	Li	1	Ta	0.02		
P <sub>2</sub> O <sub>5</sub>	0.002	Cr	1	Mo	0.02	Tb	0.02		
TiO <sub>2</sub>	0.001	Cu	0.1	Nb	0.1	Th	0.02		
LOI	0.1	Dy	0.02	Nd	0.1	U	0.02		

**Table 2-1** Total digestion detection limit of all analyzed elements reported from SRC.

There are many approaches to handle censored data. Two methods have been considered in this research: 1) divide the lower detection limit by the square root of 2 and use that value as a replacement value (e.g. Dinse et al., 2014); 2) use the *zCompositions*, an R package developed by Palarea-Albaladejo and Martín-Fernández (2015) to identify elements with censored values and remove the ones that have a high proportion of censored values (Grunsky, 2010). In the first empirical method, all censored values are replaced with a single value. This method introduces bias into the dataset, and may influence later analysis (Dinse et al., 2014). It was decided not to use the first method in this study. The second method (*zCompositions*) allows the R program to target censored values in one dataset and perform imputation for censored data (cf. Palarea-Albaladejo & Martín-Fernández, 2015). This method of dealing with censored data is thought to produce a more realistic and representative distribution of very low values than the first method. The workflow for *zCompositions* starts with the use of another R package (*zPatterns*). The latter summarizes in a graphical format all the censored values within one dataset (Figure 2-7). After plotting the *zPatterns* for the total digestion dataset, only bismuth (dark green rectangle in Figure 2-7) is found to have many censored values (20.32%), and most of the other values are also close to the detection limit for that element. Bismuth was thus dropped from the datasets prior to the

statistical analysis. This also helped increase the degree of freedom in the dataset by reducing the number of elements relative to the total number of samples.



**Figure 2-7** zPatterns indicate censored values graphically. In this example, 20.32% of Bi values are below the detection limit. All other elements in the dataset have values above their detection limit.

### 2.6.2 Compositional Data and Closure Problem

Geochemical data is a type of compositional data and can be visualized using various plots, such as bivariate plots and ternary diagrams, to recognize different compositional assemblages. However, geochemical data are generally reported as proportions (e.g. weight %, parts per million, parts per billion) that sum to a ‘closed’ constant (e.g. 100%), which can lead to spurious correlations and other statistical issues. Closure can be exemplified by looking at elemental values, where all the major elements are reported as weight percent (%). This means the total of all major elemental values remains constant at or very near 100%. Hence, when some elemental values increase, the others decrease to balance the sum. This internal relationship between compositional data is known as the constant-sum or closure problem (Aitchison, 1984), and is a problem because

abundance of one element in a particular sample can make another element seem less abundant when in reality it has not changed relative to other samples. In addition, compositional geochemical data are reported in real positive number space, whereas the standard statistical analysis requires independent variables to freely range from  $+\infty$  to  $-\infty$ ; statistical results may thus not be valid leading to incorrect interpretations (Grunsky, 2010). Aitchison (1984) introduced the use of centred-logratio transformations for statistical analysis of compositional data by converting a concentration (e.g. ppm) into a vector in the Euclidean space using ratios. The transformation projects compositional data into the real number space, allowing the standard statistical process to be used (Grunsky, 2010). The most recent developments in the theory and application of the use of centred-logratios are described by Egozcue et al. (2003), Buccianti et al. (2006), and Pawlowsky-Glahn and Egozcue (2006).

The dataset for this research comprises both major oxides and trace elements. Oxides are reported as weight percent (%), whereas trace elements are reported as parts per million (ppm). To avoid the closure problem, we apply the centred-logratio transformation (Equation 1) to the dataset. The centred-logratio transformation was done together on oxides and trace elements. Oxides were first recalculated to their single element contents (e.g.  $Ca = CaO * \left(\frac{Ca}{Ca+O}\right)$ ; Ca and CaO are in wt. %, Ca and O are the atomic mass of these elements) and applied with transformation. Hence, all the data was converted to a common unit (ppm) for statistical analysis.

$$z = clr(x) = \left[ \log \left\{ \frac{x_1}{g(x)} \right\}, \dots, \log \left\{ \frac{x_D}{g(x)} \right\} \right] \quad (2)$$

**Equation 1.** Centred- logratio transformation (from Aitchison, 1982).  $X_1$  and  $X_d$  are the first number of the data and the Dth number of the data.  $g(x)$  is the geomean of the data.

## 2.7 Multivariate Analysis

A single till sample contains numerous elements (e.g. 49 elements in our dataset) and there can be 100s or 1000s of samples in a database. Multivariate analysis is an effective approach to handling this type of dataset (Grunsky, 2010). Multivariate analysis is a family of advanced statistical techniques designed to reduce dimensionality to analyze large sample datasets described by multiple variables. These techniques can be subdivided into two broad groups: the unsupervised

and supervised classification techniques. The unsupervised techniques are used to develop an understanding of the general structure of the data and to identify groups or clusters in multivariate space that may have a geological meaning, for example. Common techniques include principal component analysis (PCA), k-means clustering, self-organizing maps, and hierarchical clustering (Mellinger, 1987; Grunsky, 2010). Supervised classification techniques are used to label a class of observations of interest, referred to as ‘training data’, characterize it, and predict that class in the dataset. Techniques such as weights of evidence and decision trees are among the most commonly used machine learning techniques to carry out supervised classification (Harris and Grunsky, 2015). It is out of the scope of this thesis to describe in detail all these techniques.

As for the process discovery (e.g. Grunsky and Kjarsgaard, 2016), in the context of this thesis and considering the limited understanding of surficial sediment geochemical composition in the study area prior to this research, and the lack of detailed bedrock lithochemical maps for high level provenance fingerprinting, it is considered most appropriate to focus on developing a general understanding of the structure of compositional data in the region and use that to achieve the thesis objectives at that level of understanding (identify groups, trends, and propose possible geological meanings). The strategy of the thesis is thus to focus on the application of unsupervised techniques to describe the compositional data and analyze clusters and trends in an attempt to extract meaningful information that will help describe and understand the glacial record of the study area. The main advantage of this strategy is that it proposes to increase step-by-step the level of understanding of compositional variations in the study area and to extract possible geological meanings before a higher order understanding can be attained. It is, however, important to also recognize the limitations of this strategy and of the thesis; the results of the analysis may not be sufficient to establish with confidence a formal chemostratigraphic framework and determine specific bedrock sources with a high degree of certainty. Nonetheless, the hope is that the thesis will lay the foundation to develop a higher level of understanding, perhaps using advanced supervised techniques to see how well certain observations of interest can be predicted.

After the initial process discovery phase, it was determined that PCA and k-means clustering would be appropriate to analyze the data. No detailed investigation or comparison of all the available classification techniques was carried out as this was deemed to be beyond the scope

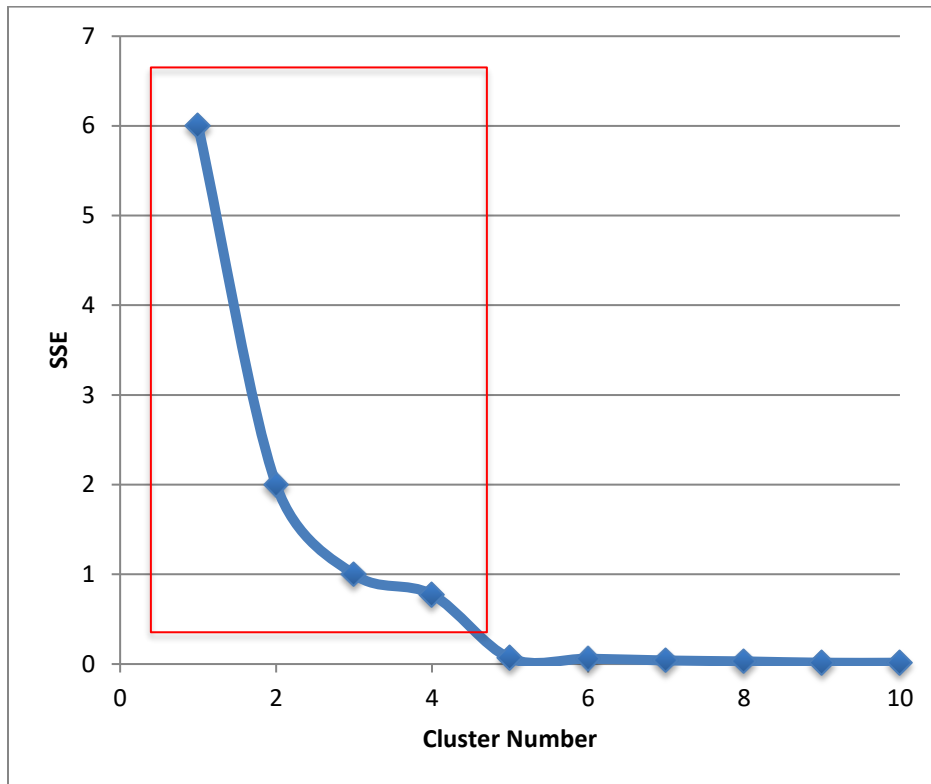


of this research. In addition, the use of k-means clustering and PCA separately or in combination have been successfully applied to the analysis of compositional data to address a variety of geoscience problems (e.g. Grünfeld, 2007; Boston et al., 2010; Grunsky, 2010; Refsnider and Miller, 2013; Gamboa et al., 2017) and should provide the necessary insights to achieve the thesis objectives. These two techniques are further described below.

### **2.7.1 K-means Cluster Analysis**

The k-means clustering technique uses multivariate proximities, instead of the similarities among individual samples which the hierarchical clustering techniques use (Grunsky, 2010). The k-means clustering method aims to partition  $n$  observations into  $k$  ( $\leq n$ ) clusters or sets  $S = \{S_1, S_2, \dots, S_k\}$  to minimize the distance of each point ( $x_i$ ) in the cluster  $j$  to the  $k$  centroid ( $c_j$ ) (Tan et al., 2005). The first step of the algorithm consists in randomly assigning  $k$  ‘mean’ centroids ( $c_j$ ). In the second step, clusters are formed so that every observation ( $x_i$ ) is assigned to the closest  $k$  ‘mean’ centroid. In the third step, new  $k$  ‘means’ are calculated based on the distances between the points  $x_i$  within each cluster and steps 2-3 are repeated until the squared distance is minimized for each point; i.e. when the best  $k$  centroids are found. R code for the k-means method is included in Appendix A.

In the R program, the total number of clusters is determined by consulting a scree plot (Figure 2-8). The trend on the scree plot shows an inflection point based on the relationship between the number of clusters and the sum of squares. The idea is to find that inflection point on the scree plot, and choose that cluster number. For example, in Figure 2-8, the first 4 clusters account for over 90% sum of squared error (SSE) in the dataset; hence, 4 clusters would be an appropriate number of clusters to run the mean K clustering technique on this data.

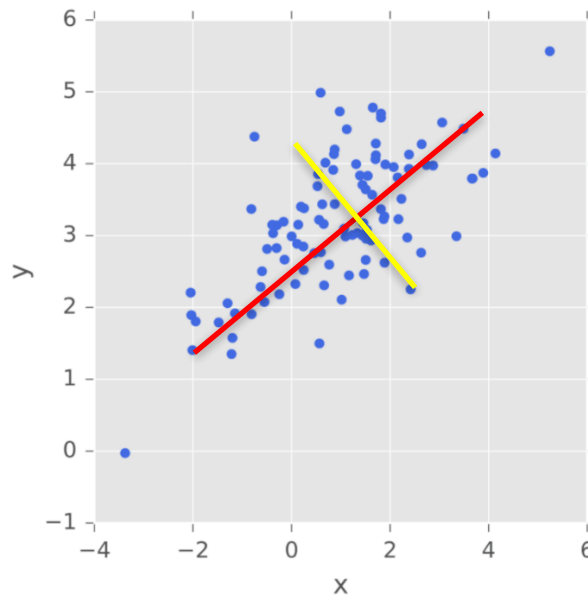


**Figure 2-8** Scree plot for choosing the number of clusters; red rectangle shows the “elbow” shape (known as the point of inflexion). In this example, the chosen number of clusters is 4.

## 2.7.2 Principal Component Analysis

The PCA is another dimension reduction technique useful to examine the relationships between elements within a large multivariate dataset and to determine which elements are most responsible for the variance in the data. PCA has been used for the study of tills by extracting multi-elemental information on a spatial map (Grünfeld, 2007; Refsnider and Miller, 2013; McMartin et al., 2016). PCA is a multivariate method that consists of a linear transformation with  $x$  original variables and  $y$  new variables, where each new variable is a linear combination of the old variable (Grunsky, 2010). The PCA method generates a new coordinate system for the dataset by using eigenvectors and eigenvalues of the covariance matrix of the log-transformed data (Jeong et al., 2016). The eigenvectors and eigenvalues will determine how one variable differs from another and where the original samples are located in the new coordinate system defined by the selected principal components (e.g. PC1 v. PC2, PC1 v. PC3, and so on). The first principal

component (PC1) is the axis which contains the most variability of a dataset (Davies & Fearn, 2004). Second and higher components represent the lower variability compared to PC1 within the data and are plotted orthogonal to PC1 (Davies & Fearn, 2004, Figure 2-9). There are two outputs from running PCA in the R program: one is called "score", and the other one is called "loading". Scores are the new values of samples plotting on the new coordinate system (Davies & Fearn, 2004). Loadings are derived by multiplying the eigenvector matrix by a diagonal matrix of eigenvalues (e.g. Jolliffe & Cadima, 2016; Grunsky, 2010). A score plot shows the data points distribution on the axes of PCs. The loading plot displayed as a barplot showing values of the variables were negative or positive for each principal component, which is useful for determining which variables are controlling variability in each PC. PCA can be very useful in discriminating different geological processes by identifying patterns and relationships between several geochemical elements (Grunsky, 2010).



**Figure 2-9** Graphic plot of first principal component (red line) and second principal component (yellow line) regenerated from Detlefs (2016).

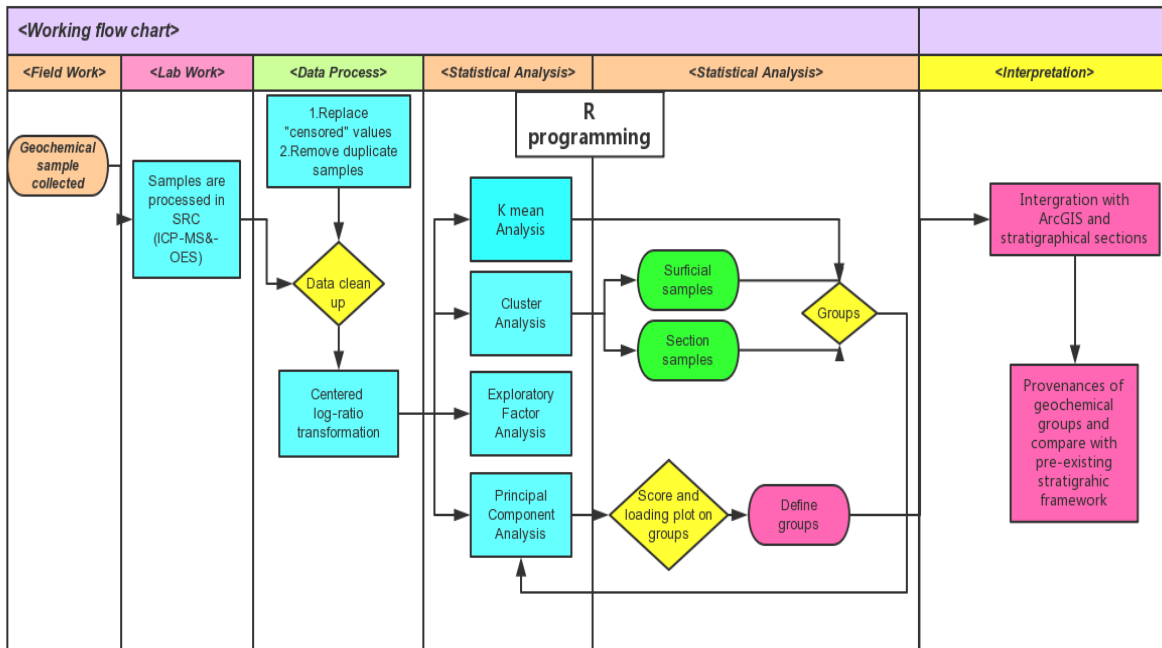
PCA is best suited for finding the driving variables which are demonstrated based on the absolute loading values of each variable in the PC space. If one variable has a large positive or negative value under one of the PCs, then this variable is the driving variable under the

corresponding PC. Sample compositional clusters can be identified, but only if they separate well on a PC plot. PCA results can be plotted on a map (e.g. using GIS) or vertically along stratigraphic logs to identify possible spatial (horizontal and vertical) relationships. In this study, the PCA was done using the *ggbiplot* package in R (Vu, 2016).

### **2.7.3 Integration of results and interpretation approach**

The geochemical dataset in this study was first illustrated by k-means clustering, classifying 6 clusters out of all samples (see Chapter 3). Next, these 6 clusters were projected in PC space, and the PCA added driving variables for each cluster and gave each sample new values (scores) under the PC spaces. The combination of k-means and PCA provided a description of the general structure of the data. After the statistical analysis, these results were then analyzed spatially on maps using ArcGIS (“Geospatial Coherence”; Grunsky and Kjarsgaard, 2016) as well as vertically along stratigraphic logs to detect possible meaningful patterns and trends that can be interpreted in terms of the bedrock provenance. Additionally, six geochemical groups are compared to the pre-existing stratigraphic framework at one type section in order to determine whether these two classifications are similar.

A summary workflow of the methods described and discussed above is presented in Figure 2-10.



**Figure 2-10** Workflow chart summarizing the methodological approach of this study. The workflow is generated from an online drawing software “Processon” (<https://www.processon.com>, only available in Chinese).

# **Chapter 3 Statistical analysis of till geochemistry in northeastern Manitoba**

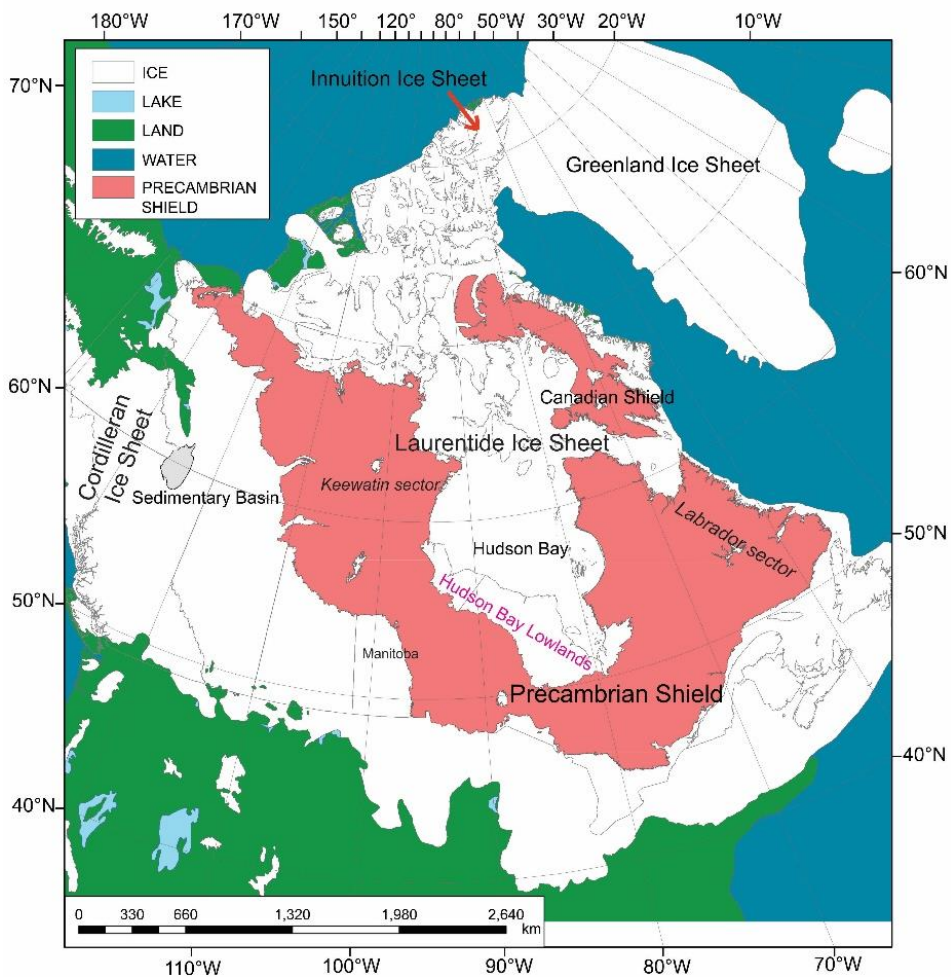
## **Overview**

The Quaternary stratigraphy of Manitoba Hudson Bay Lowland (HBL) contains valuable information about past glacial cycles. Previous research has identified four till units that outcrop in the region: Sundance Till, Amery Till, Long Spruce Till, and Sky Pilot Till. These tills are thought to have been deposited during the Pre-Illinoian, the Illinoian, and the Wisconsin glaciations. However, applying this four till stratigraphy to new stratigraphic sections over a larger region of the HBL has proven difficult. This is because the descriptions are mainly qualitative, and there are inconsistencies between different studies. Multivariate statistical analysis, including cluster analysis and principal component analysis, of till matrix geochemistry is applied to the Quaternary tills of the HBL near Gillam, Manitoba, to quantify the local till classification and gain understanding about the genesis of different till units. Six statistical till-geochemistry groups are identified first by examining a scree plot based on the sum of squared error in the dataset and then by applying k-means clustering and PCA analysis. An attempt is made to determine the provenance of these 6 groups, as their compositions are sourced from the mineralogy of original eroded rocks, as well as any re-entrained glacial or nonglacial sediments. There are fuzzy boundaries between the statistical till-geochemistry groups, and considerable overlap in the element signatures. Based on these results, tills within the Manitoba HBL are interpreted as a palimpsest product of overprinting and inheritance and cannot easily be separated and correlated into regionally-widespread layered till sheets based on their geochemistry and the previously proposed four-till stratigraphy.

## **3.1 Introduction**

The Quaternary stratigraphic record of the Hudson Bay Lowland (HBL) preserves valuable information from past glacial and interglacial cycles (e.g. Andrews et al., 1983; Nielsen et al., 1986; Dredge et al., 1990; Thorleifson et al., 1992). The sedimentary records provide key information about ice sheet evolution and dynamics related to two major ice centres; namely the Keewatin Sector and the Quebec-Labrador Sector of the Laurentide Ice Sheet (LIS) (Figure 3-1).

The sediment successions in the HBL have long been identified for their potential to capture the main changes in LIS configuration (e.g. Shilts, 1982). Using a specific pebble lithology, in this case Dubawnt erratics, Shilts (1982) determined that till within northern Nunavut and the Manitoba HBL had been derived at least partially from Baker Lake - a distance of more than 600 km to the north/northwest. Similarly, using greywacke erratics with calcareous concretions (Omars), Prest et al. (2000) showed that part of the tills within the Manitoba HBL was derived from the Belcher Island Group - a distance of more than 800 km to the east.



**Figure 3-1** A map of ice mass extent in North America during Last Glacial Maximum (LGM), depicting the location of the Laurentide, Innuitian, Cordilleran, and Greenland Ice Sheets. Highlighted on this map are the extent of the Precambrian Shield (covered by ice during the LGM), and the location of the Hudson Bay Lowland in red font (modified from Dyke et al., 2002).

In northeastern Manitoba, the Quaternary sediment successions of the HBL have been the subject of numerous studies (e.g. Nielsen and Dredge, 1982, 1985; Nielsen et al., 1986; Klassen, 1986; Roy, 1998) aimed at better understanding: 1) the regional Quaternary history such as glacial and interglacial cycles, but also possibly interstadial events, and 2) the LIS evolution and dynamics (e.g. Shilts, 1982; Klassen, 1986; Thorleifson et al., 1992). The till classification framework that resulted from these studies is largely based on visual field observations and related sediment facies descriptions. However, it is difficult to differentiate tills and correlate them from section to section on the basis of sediment facies descriptions alone because of the apparent homotaxy of tills and the lack of laterally extensive marker beds; organic beds separating similar tills at type sections, for example, are highly discontinuous. Moreover, while previous researchers have measured clast fabrics (e.g. Nielsen and Dredge, 1982; Nielsen et al., 1986; Roy, 1998) and simplified till-clast composition (Roy, 1998), these results were assigned to a qualitative four till stratigraphy rather than used quantitatively. Our research involves revisiting and sampling historical sections, documenting and sampling new stratigraphic sections, as well as collecting surficial till samples away from river sections. This paper focuses on the statistical aspect of the sampled till matrix geochemistry. Detailed studies are being conducted on the stratigraphy, till-clast composition and clast fabrics, concurrently to this paper.

Analysis of till matrix geochemistry has been successfully applied to understand the till provenance and dispersal patterns in Canada and Europe (Shilts, 1995; Garrett and Thorleifson, 1996; Boston et al., 2010; Grunsky, 2010; Dempster et al., 2013; Salmirinne et al., 2012; Grunsky and Kjarsgaard, 2016; Kääriäinen, 2016; McMartin et al., 2016) hence, this technique is regarded as a useful tool to determine if different till units can be distinguished (cf. Boston et al., 2010). Multivariate statistical analysis of till-matrix geochemistry has the potential to reveal important vertical and/or lateral trends, which together may provide important new insights into till provenance and related glacial processes (e.g. erosion, sediment re-entrainment). Such analysis can contribute to improving the existing till stratigraphic framework. This study applies till-matrix geochemical analyses to tills sampled within the Manitoba HBL.

The specific goals of this study are: 1) to determine whether till geochemical groups form a continuum (no clear end-members), have both end-members and hybrid groups, or consist of

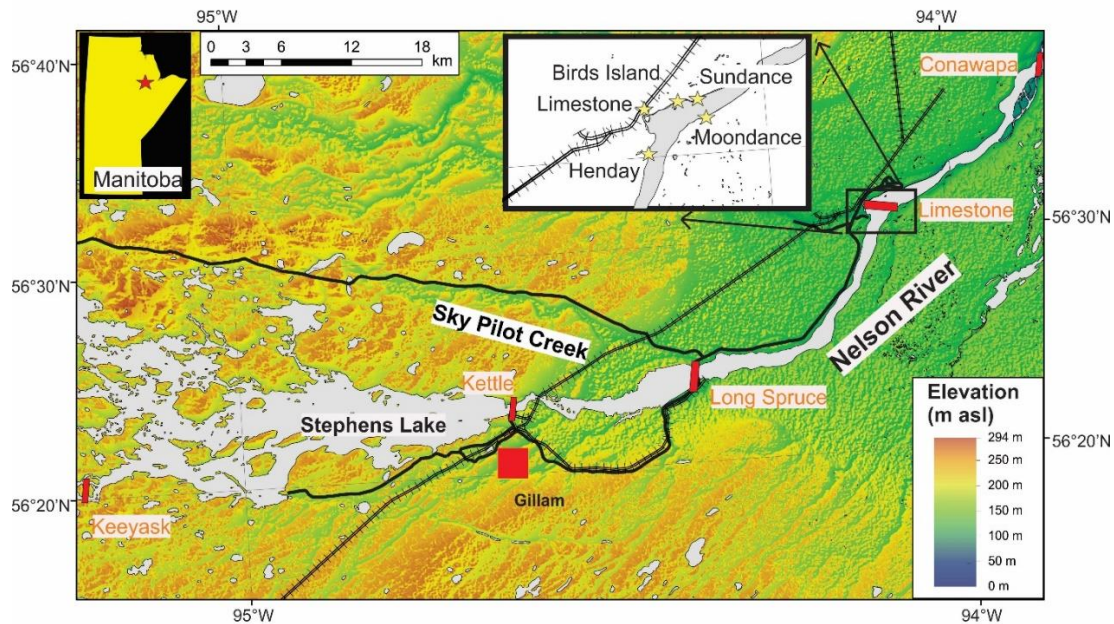


distinct groups (limited overlap; clear groups with unique geochemical makeup); 2) apply the groups spatially, and examine the data for evidence of vertical and lateral trends; and 3) determine whether the statistical groups can be linked to changes in glacial process such as provenance shifts, sediment re-entrainment, or advance/retreat cycles (time gaps).

### **3.1.1 Physiography and Surficial Geology**

The study area is centred on Gillam, northeastern Manitoba (Figure 3-2). Elevation varies from 21 to 294 m above sea level, with 30+ m bluffs along the Nelson River. Nelson River is the main northeast drainage channel into Hudson Bay. The region is dominated by spruce bogs. Permafrost is commonly near surface. The presence of bedrock is rare in the eastern half of the study area.

The surficial geology of Gillam area has been discussed by Nielsen and Dredge (1982) and Trommelen (2013) and Trommelen et al. (2014). Main types of sediment deposits are 1) glaciofluvial and sandy diamicton deposits (e.g. Nielsen and Dredge, 1982; Trommelen, 2013); 2) glaciolacustrine deposits; 3) marine sediments; 4) till. The glaciolacustrine deposits including silt and clay rhythmites, clay, and waterlain till were situated west of the Long Spruce hydroelectric dam and in the valley of Sky Pilot Creek (Nielsen and Dredge, 1982; Trommelen, 2013). The marine sediments consist of 1) sand and gravel situated along the road between Long Spruce and Conawapa hydroelectric dam sites, and 2) laminated silt was situated east of the Long Spruce hydroelectric dam, generally 0.5 to 5 m thick (Trommelen, 2013). A detailed literature review on till description is discussed in Section 3.1.3. The study area is in a zone where a transition occurs from a thin till on the Precambrian Shield to the west to multi-till stratigraphy (30-50 m in depth) in the HBL to the east (e.g. Kelley et al., 2015; Gauthier et al., 2016). The glaciofluvial and sandy diamicton deposits were likely deposited by glaciofluvial outwash and debris flow when the ice retreated eastwardly (Nielsen and Dredge, 1982; Nielsen et al., 1986; Trommelen, 2013; Trommelen et al., 2014).

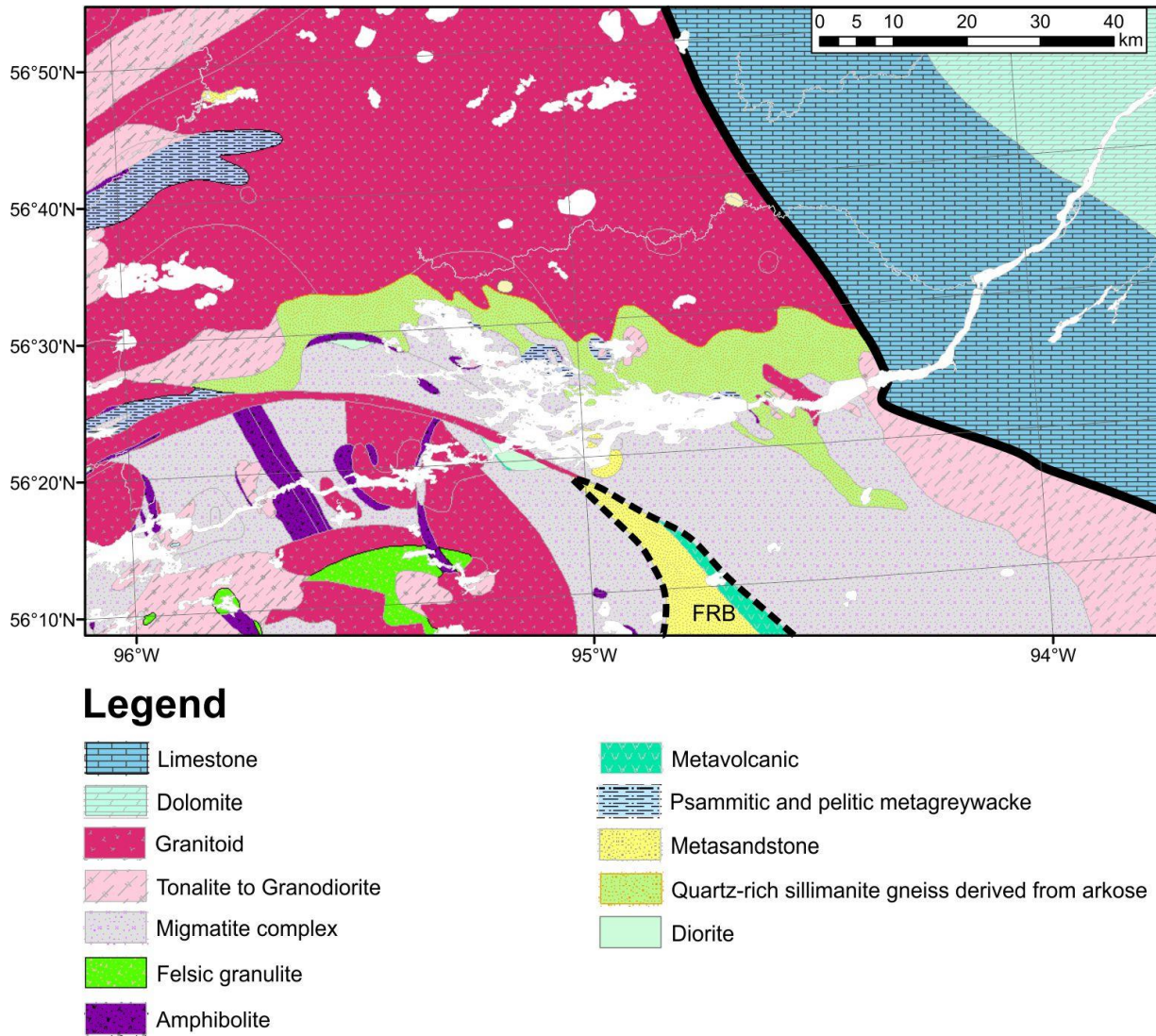


**Figure 3-2** Location of study area. The main road is marked as a thick black line, and railway is the thin interlaced black line. The location of five important historical sections (Moondance, Henday, Limestone, Birds’ Island and Sundance) is included in this map. Background hillshade image was generated using a Shuttle Radar Topography Mission (United States Geological Survey, 2002) digital elevation model.

### 3.1.2 Bedrock

The study area crosses the Paleozoic platform in Hudson Bay in the east and the Precambrian Shield in the west (Manitoba Energy and Mines, 1992). Main bedrock lithologies in the region are shown in Figure 3-3: 1) Precambrian shield (west of black solid line) contains felsic granulite, granites, granodiorite, tonalite, amphibolite, metavolcanic rocks, migmatite, and metasedimentary rocks such as metagraywacke (Manitoba Energy and Mines, 1992; Rinne, 2016). The geochemical contrast may be limited locally within Precambrian Shield lithologies since many of the rock types are compositionally similar (e.g. felsic); 2) Paleozoic platform in Hudson Bay (east of black solid line) is mainly composed of limestone and dolomite (Manitoba Energy and Mines, 1992). A northwestern part of the Fox River Belt (denoted as “FRB” in Figure 3-3) is situated in the south of the study area, and contains layered ultramafic-mafic intrusions and sedimentary rocks (e.g. Scoates, 1981; 1990; Manitoba Energy and Mines, 1992; Peck et al., 1999). The major rock types associated with the ultramafic-mafic intrusions are komatiitic basalt and

basalt (Peck et al., 1999, 2000). The sedimentary units mainly compromise clastic sedimentary rocks including mudstone, argillite and siltstone (Peck et al., 1999, 2000).



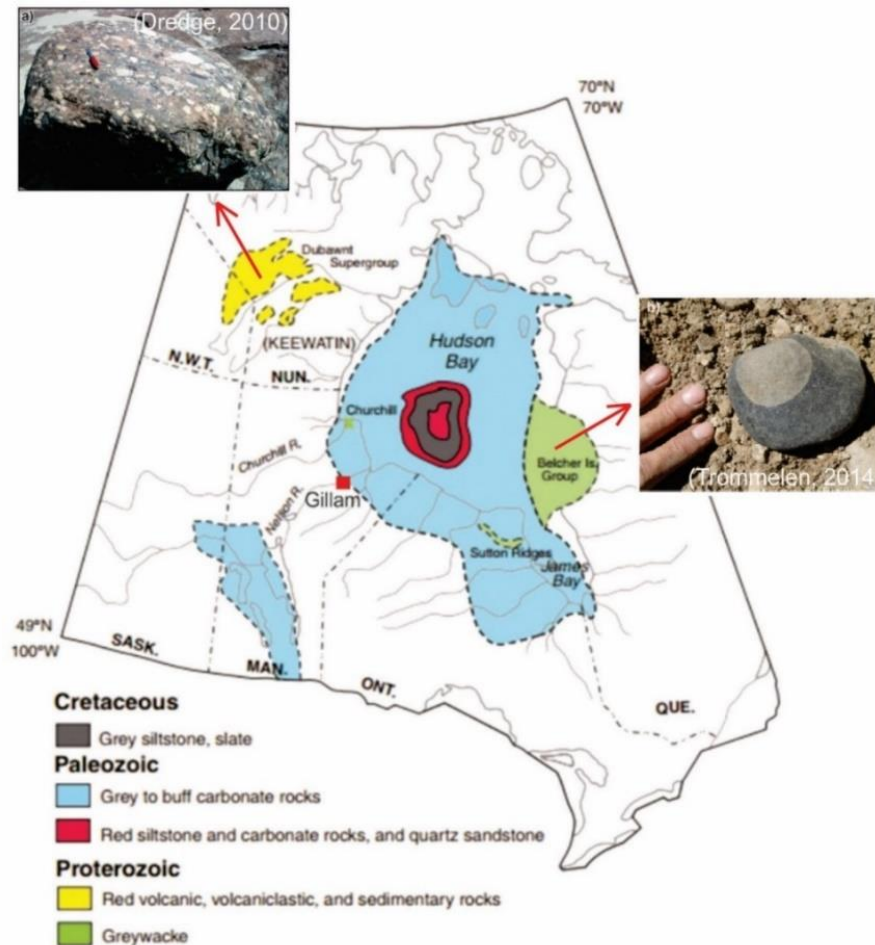
**Figure 3-3** Major bedrock geology in the study area (unpublished digital bedrock geology compilation from MGS, 2016)

### 3.1.2.1 Erratics

The map shown in Figure 3-4 includes several distinct bedrock lithologies in some parts of Canada including northern and central Manitoba. Glacial erratics (far - transported rocks in glaciated terrain) have been regarded as important indicators for ice flow history and ice

provenance (e.g. Doornbos et al., 2009; Dredge and McMartin, 2011; Plouffe et al., 2011). According to Nielsen and Dredge (1982), the provenances for the glacial erratics from the coarse fraction of tills in the Gillam area can be divided into two groups: northern provenance and eastern provenance. The reddish volcanic and sedimentary rocks are found in tills, and are most likely sourced from the Dubawnt Supergroup in the District of Keewatin (Nielsen and Dredge, 1982). Their presence in the study area indicates ice flow from the north. The fact that lithic clasts of the Dubawnt Supergroup indicate that the transport of the glacial material is significant, and this is the evidence for reworking and long-distance transport. The greywacke with light concretions (also called omars), which have often eroded away and left circular holes, are found in tills, and are most likely sourced from the Omarolluk Formation in the Belcher Island Group (Nielsen and Dredge, 1982). Their presence in the study area indicates ice flow from the west and southwest (Nielsen and Dredge, 1982; Prest et al., 2000).

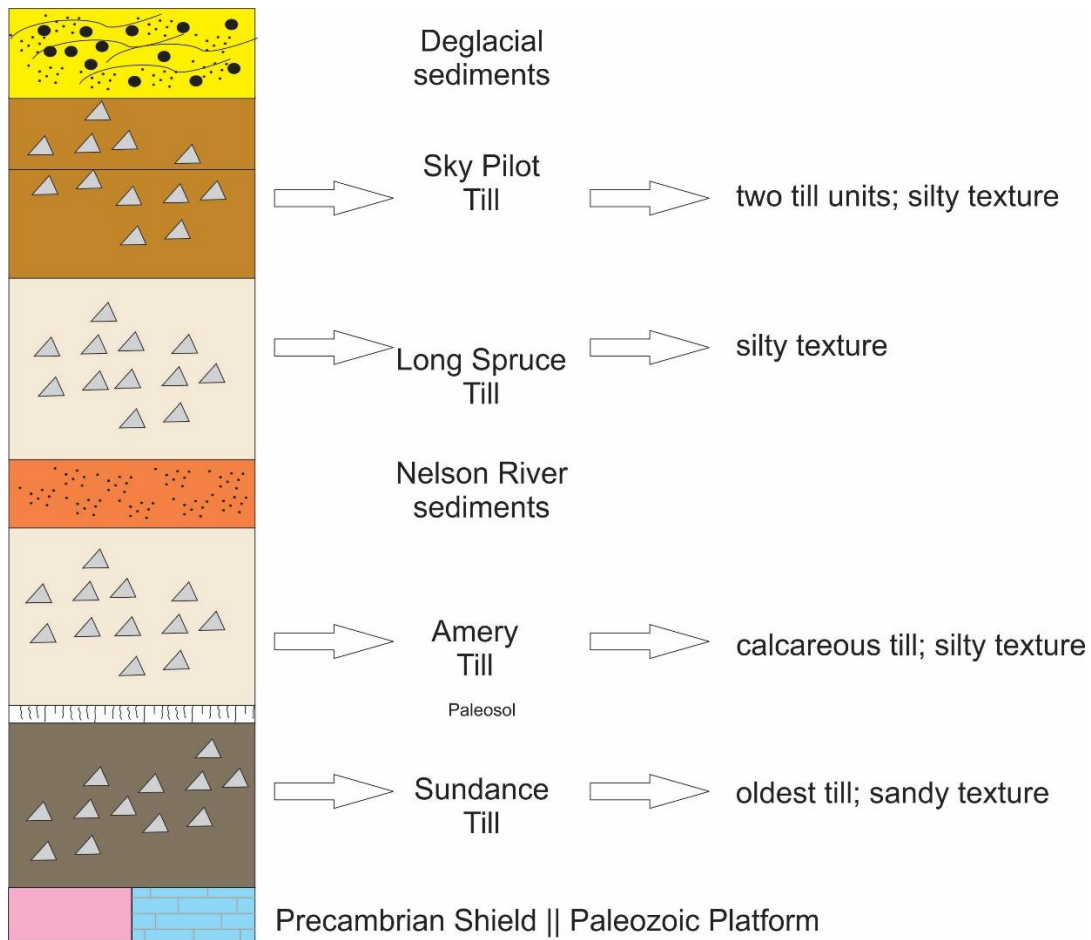




**Figure 3-4** Map showing distinctive bedrock geology in northern and central Canada (from Dredge and McMartin, 2011)

### 3.1.3 Manitoba HBL four till stratigraphy

Four till units are named within the Manitoba HBL. These tills have been described qualitatively based on stratigraphic context, till color, clast lithology content and clast-fabric data (e.g. Nielsen and Dredge, 1982; Nielsen et al. 1986; Dredge and Nielsen, 1987; Klassen, 1986; Roy, 1998). Importantly, most of the tills were classified and named based on type-sections situated within just 6 km<sup>2</sup>, along the Nelson River near the Limestone dam (Figure 3-1). Dredge and McMartin (2011) have published a detailed summary of the local stratigraphy: Sundance Till is regarded as the oldest till in the region, followed by Amery Till, Long Spruce Till, and Sky Pilot Till (Figure 3-5).



**Figure 3-5** Simplified stratigraphic column from northeastern Manitoba (modified from Dredge and McMartin, 2011).

The Sundance Till has a light olive grey color (Munsell color 5Y 5/2; Nielsen et al. 1986) or dark grayish brown color (Munsell 2.5Y 5/2; Roy, 1998). The type-section is the Sundance section (Nielsen and Dredge, 1982; Nielsen et al., 1986). This till is stratigraphically the oldest till and rests directly on the Paleozoic platform at the two sites where it outcrops: Moondance and Sundance sections (Nielsen and Dredge, 1982, Roy, 1998). The Sundance Till contains 45-53% Precambrian clasts, and 40- 55% calcareous clasts (Nielsen and Dredge, 1982; Nielsen et al., 1986; Roy, 1998; Dredge and McMartin, 2011), with a small percentage of distinctive Omarolluk Formation erratics of eastern Hudson Bay provenance. Red Dubawnt clasts from northern Nunavut are also present in this till (Dredge and McMartin 2011). Striations to 245° and 260° were mapped at the base of the Sundance section (Nielsen and Dredge 1982), while striations to 160° were

mapped at the base of the Moondance section (Roy 1998). Clast-fabric data from the Sundance till indicates southeast-trending ice flow direction (Nielsen et al., 1986; Roy 1998). Because of the elevated proportion of Precambrian clasts, the Dubawnt erratics, and the clast-fabric measurements, this till has been regarded as the product of northern-sourced ice. However, the small amount of Omar erratics, together with a small number of foraminifera in the till and the southwest-trending striae suggest that the Sundance till may have re-entrained older sediment derived from an eastern source area (Nielsen et al., 1986; Dredge and McMartin, 2011).

The Amery Till is light olive grey (5Y 6/1) or olive grey (5Y 4/2 or 5Y 5/2), and contains more silt (40- 66%) than the Sundance Till (32- 45%) (Nielsen et al., 1986; Klassen, 1986; Roy, 1998). The type-section is section 20 of Klassen (1986), situated along the Nelson River 2 km upstream of the Sundance section. The Amery Till has a different clast composition than the Sundance. It contains 66-87% calcareous clasts, abraded marine shell fragments, as well as a minor greywacke contribution presumably from the Omarolluk Fm. in eastern Hudson Bay (Nielsen et al., 1986, Roy, 1998). The fabric data from Nielsen and Dredge (1982) from Sundance section indicated the Amery till was deposited by the NW- trending flowing ice. However, a SW-trending ice-flow direction was interpreted from four clast fabrics, while a NW-trending ice-flow direction was interpreted from a fifth (Roy, 1998). Overall, the fabric data suggested a W-trending ice flow direction. The decreased proportion of Precambrian shield clasts, combined with the presence of shell fragments and clasts of the Omarolluk Fm. in the till, indicates an eastern provenance. The Amery till has been assigned to the Illinoian glaciation because it underlies the Nelson River Sediments, which are interpreted as interglacial sediments similar to the Sangamonian Missinaibi Formation interglacial sediments in Ontario (Nielsen et al., 1986, Skinner, 1973).

The Long Spruce Till is described as light olive grey (5Y 6/1) color (Nielsen et al., 1986), dark grey (5Y 4/1) color (Roy, 1998) and olive grey (Dredge and McMartin, 2011). The type-section is the Henday section (Figure 3-1; Nielsen et al. 1986). This till has similar grain size and clast lithology to the Amery Till (Nielsen and Dredge, 1982; Nielsen et al., 1986; Roy, 1998; Dredge and McMartin, 2011). The differentiation between these two units is thus based on their stratigraphic position relative to an interglacial bed; the Nelson River Sediments (cf. Nielsen et al., 1986) that lies between them. However, such a stratigraphic situation is only found at a limited

number of sites (Gauthier et al., 2017), making it difficult to differentiate between Amery and Long Spruce Till away from the type section where this stratigraphy was established. Clast fabric data from Long Spruce Till has been interpreted as NW-, W-, and SW – trending (Nielsen and Dredge, 1982; Nielsen et al., 1986; Roy, 1998; Nielsen, 2001; Dredge and McMartin, 2011). Nielsen and Dredge (1982) stated that this till is associated with the NW-trending ice flow based on fabric measurements, striations on the underlying bedrock and the greywacke clasts associated with an eastern provenance. Dredge and McMartin (2011) summarized the ice flow as having a W-trending direction. Roy (1998) suggested a NW-trending ice flow direction because of Kipalu erratics (not Omars) which are erratics of oolitic jasper from the Belcher Island Group (Prest et al., 2000).

The Sky Pilot Till is a brown till (10YR 6/2, Nielsen and Dredge, 1982; Nielsen et al., 1986) or olive brown to brown (Dredge and McMartin, 2011), which is often associated with sand and gravel lenses (Dredge and Cowan 1989). It was named by Nielsen et al. (1986), and though a specific type section was not identified, the till outcrops along Sky Pilot Creek and is the surface till. This till has similar grain size and clast lithology to the Amery Till and the Long Spruce Till (Nielsen and Dredge, 1982; Roy, 1998; Dredge and McMartin, 2011). The fabric data shows W-trending ice flow direction (Nielsen and Dredge, 1982). The fabric data and small amount of foraminifera indicated the Sky Pilot Till was deposited from Hudson Bay (Nielsen and Dredge, 1982). Nielsen et al. (1986) suggested that the Sky Pilot Till comprises two different tills, based on till fabrics and orientation of drumlins indicating a shift from a west-trending to southwest-trending ice flow direction associated with this uppermost till. However, Trommelen (2013), Trommelen et al., (2014) and Gauthier et al. (2016) have shown that the youngest till along the Sky Pilot Creek is associated with a transition from west-trending to northwest-trending ice flow. Moreover, the relative abundance of greywacke in the upper till units (5%) is smaller than that in the lower till unit (20%) (Nielsen et al., 1986). The upper till unit contains more clay than the lower unit (Dredge & McMartin, 2011). Hence, assigning these till sheets to a single stratigraphic unit (Sky Pilot Till) may not reflect the observed internal variability.



## 3.2 Methods

### 3.2.1 Field and Laboratory Work and QA/QC

The field area comprises 7380 km<sup>2</sup> in northeastern Manitoba (Figure 3-1). Till-sample sites were accessed by truck, boat, and helicopter over three field seasons. In total, 245 till samples were collected, plus 9 field duplicates. 119 samples are from the C-horizon at the surface, collected from hand-dug holes by shovel or dutch auger. 126 are subsurface samples, collected by shovel from semi-vertical Quaternary sections. Each sample weighed about 2-3 kg, half of which was archived. Samples were sent to Saskatchewan Research Council (SRC) Geoanalytical Laboratories for grain size analysis and till-matrix geochemical analysis, while clasts were sent to Manitoba Geological Survey (MGS) for clast-lithology analysis. The analysis of grain size distribution was done on the materials less than 2 mm by SRC. Materials less than 2 mm were deflocculated using Calgon<sup>®</sup> and sieved through a 2 mm screen into a graduated cylinder to get two aliquots of samples: one was removed from the cylinder immediately and the other one was obtained after the settling occurred. The aliquots of materials and sieved sand were dried and re-weighed to determine the grain size distribution. Till-matrix geochemistry was run on the <63 micron size-fraction, using total digestion (HF:HNO<sub>3</sub>:HClO<sub>4</sub> acid) and ICP-MS and ICP-OES analyses. Total digestion was used in this study, as it is important to recognize the signature of minerals like feldspar and other silicate minerals that are not easily dissolved by *aqua regia* or other partial digestions (Koljonen et al., 1992). An analysis on the total digestion is expected to provide a more complete picture of the mineralogy that controls the geochemical composition of the till matrix and is thus useful for this type of regional provenance analysis (e.g. Nikkarinen et al., 1984; Koljonen et al., 1992; McClenaghan and Kjarsgaard, 2007; McClenaghan et al., 2013; McMartin et al., 2016).

It is important to conduct quality assurance and quality control in both field sampling and geochemical analysis (Evans, 1995; Piercey, 2014). First, our sample collection in the field was carried out using a clean shovel/auger and samples were sealed in thick plastic bags with duplicate labels inside and outside. The sample bags were sealed in plastic pails and sent to the lab. Second, two sample bags were collected at the same site (field duplicates) every 40 samples, to test variability within the field. Third, standard materials were inserted into the batch every 20 samples at SRC.

We assessed the quality of our data using duplicate scatterplots and Thompson-Howarth methods (Thompson & Howarth, 1978; Piercey, 2014). Duplicate scatterplots employ original data plotted against duplicate data (Piercey, 2014), whereas the Thompson-Howarth method uses the mean of duplicates as the x-axis and the absolute difference between duplicates as the y-axis plotted against a control line (e.g. 95<sup>th</sup> percentile; Thompson & Howarth, 1978; Piercey, 2014). The 49 elements were tested using these methods, and Ytterbium (Yb) was the only element not precise enough to include in the further analysis.

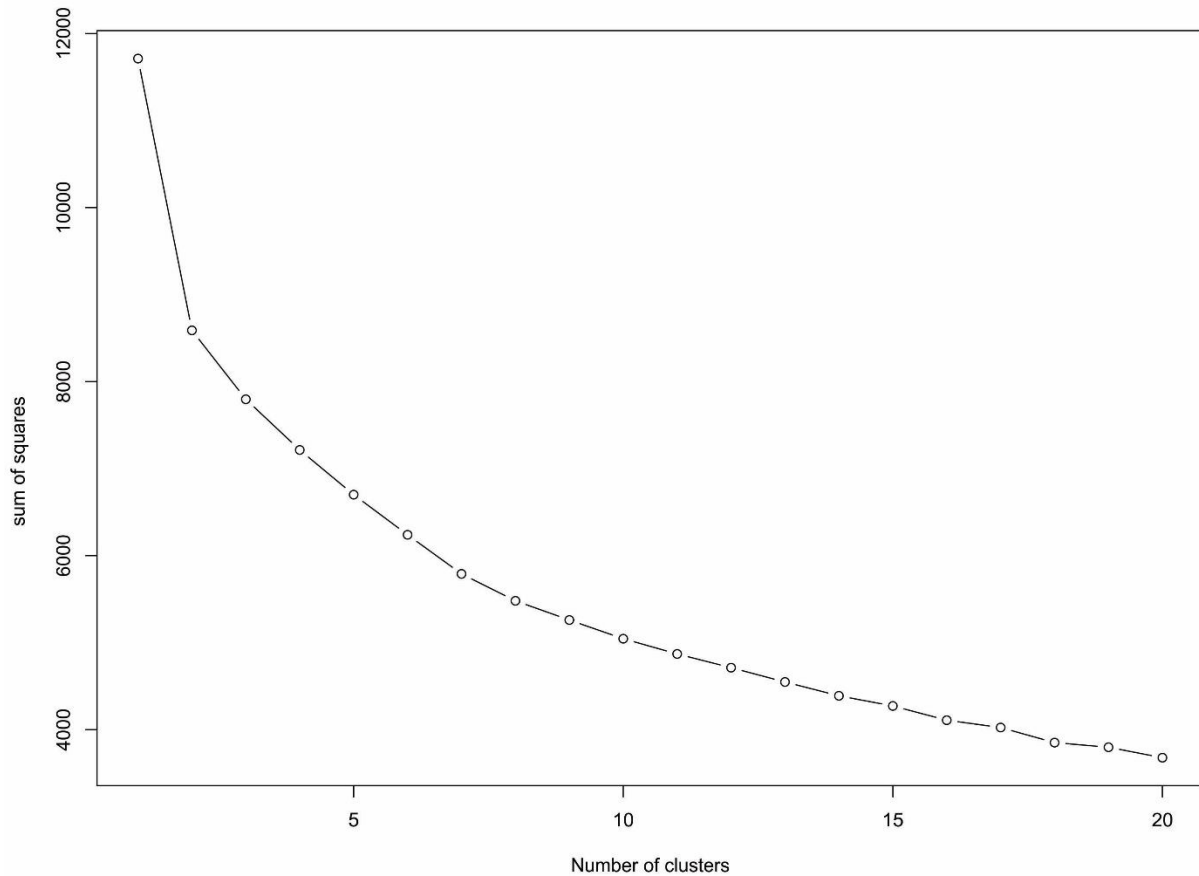
### **3.2.2 Multivariate Analysis**

To prepare the geochemical dataset, the replacement of censored data was applied to remove elements that have mostly censored values (i.e., below the detection limit). In this study, bismuth was removed. Next, a centred log-ratio transformation was conducted to address a problem referred to as the “problem of closure”; Aitchison, 1984, 1986; Grunsky, 2010). Moreover, in an effort to examine the distribution of carbonate rocks in the study area, a “carbonate ratio” (carb ratio), specifically  $(Ca+Mg)/(Na+K+Al)$  is used since Ca can be derived from either carbonate rocks or plagioclase feldspars, and Mg can be derived from either carbonate rocks or ferromagnesian silicate minerals and K can be derived from alkali feldspar (e.g. Ross et al., 2011; Dredge and McMartin, 2011; McMartin et al., 2016). Therefore, by dividing by the sodium, potassium, and aluminum, the ratio will remove any noise coming from silicate source. Additionally, Rare Earth Elements (REE) in till are good indicators of a shield provenance because they belong to the group of lithophile elements which are concentrated in silicate rocks of the Precambrian Shield (e.g. Dredge and Pehrsson, 2006; Dredge & McMartin, 2011; McMartin et al., 2016); carbonates have comparatively low REE content (Rose et al. 1979). The carb ratio is used to compare with the concentration of the Rare Earth Elements (REE).

Multivariate analyses, including k-means cluster analysis and Principal Component Analysis (PCA), were then performed on the geochemical dataset using R, an open-source statistical software (<https://www.r-project.org/>).

### 3.2.2.1 Cluster analysis

K-means cluster analysis is an approach that selects a set number of  $k$  centroids randomly, and then iterates until data clusters minimize the distance between data points and their associated centroid (Tan et al., 2005; Grunsky, 2010). Different techniques can be used to determine an appropriate number of centroids, and thus of clusters. In this study, the number of centroids/clusters was determined by examining a bi-plot that compares the sum of the squared distance between each member of a cluster and its centroid (sum of squared errors; SSE), to a sequential number of clusters (e.g. Tan et al., 2005). There should be a decreasing trend of the values of SSE with increasing number of clusters and, sometimes, a clear break or inflexion point is apparent in the decreasing slope at a specific cluster level (e.g. Tan et al., 2005). Figure 3-6 shows the bi-plot for our dataset, using R. Although the clearest break in slope is at cluster #2, the decrease continues until about cluster #6, beyond which it levels off. As the break point in the plot is ambiguous between 6 and 7, we also examined the data using 7 clusters and found no substantial impact on the total SSE and thus adding the additional cluster is not meaningful for the classification problem at hand. The analysis was thus conducted using six centroids or clusters.



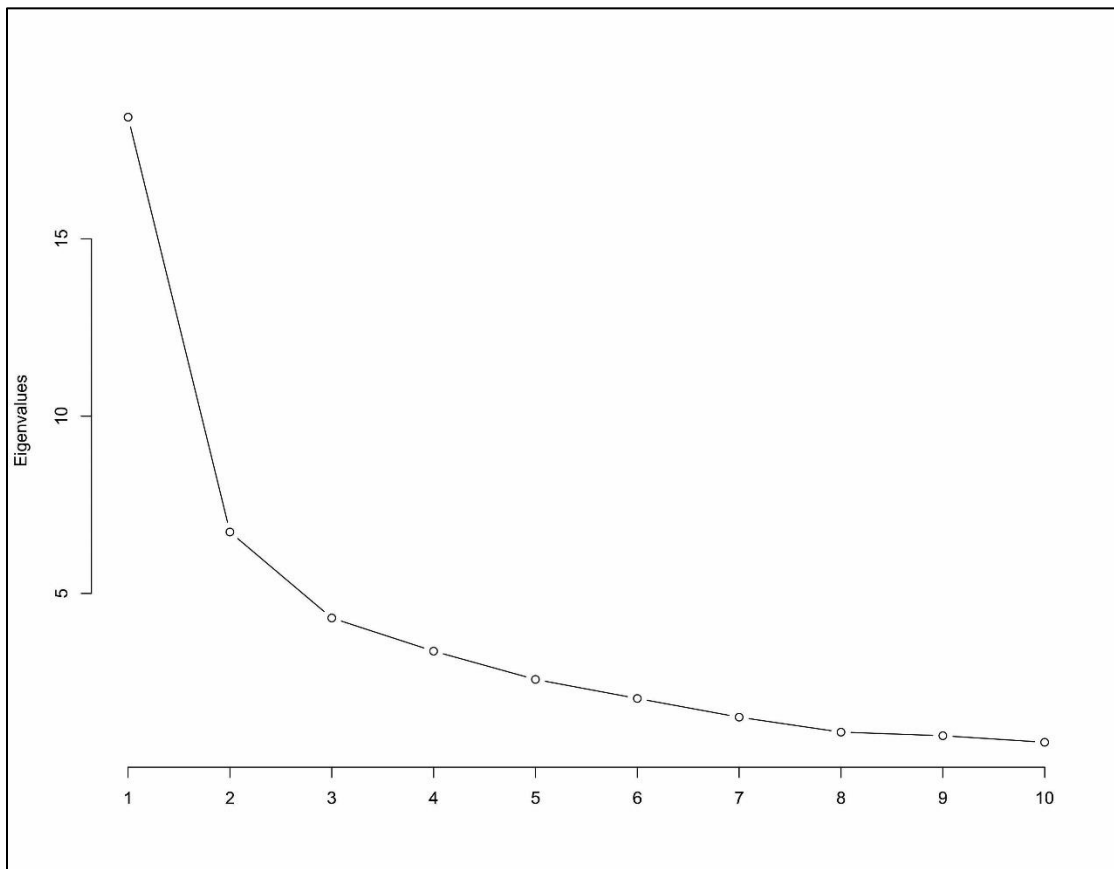
**Figure 3-6** K-means sum of squared errors (SSE) plot. SSE associated with each number of clusters is shown on the y-axis. The less number of clusters has the bigger SSE. The inflexion point here is at number 6 which is applied in this study.

### 3.2.2.2 Principal component analysis

Principal component analysis (PCA) is an eigenvector-based multivariate analysis method that uses an orthogonal linear transformation to convert a set of observations into uncorrelated principal components (Grunsky, 2010). The new coordinate system projects the data in a way that the first component accounts for most of the variance in the dataset, while the succeeding components have decreasing variance. By plotting only the first few principal components, the dimensionality of a multivariate dataset is reduced without losing important information. Figure 3-7 shows the scree plot of our data through R. The clearest inflexion point is at #3. Therefore, the first three components (PC1, PC2, PC3) are chosen to be considered for this data. The results of a

PCA include component *scores*, which are the transformed or projected values of the original data onto the principal axes, and *loadings*, which are the weights of the variables' contribution to each principal component.

Till-geochemistry groups are identified using k-means cluster analysis and samples on the PCA biplots are color-coded according to their k-means cluster membership to examine element combinations responsible for the groupings. The combination of the methods is also used to interpret the geological meaning of the groupings (e.g. dominant bedrock provenance, mixed sources, sediment re-entrainment) and their stratigraphic arrangement (chemostratigraphy).



**Figure 3-7** Principal Component Analysis (PCA) scree plot. Eigenvalues associated with each principal component is shown on the y-axis. First principal component has the largest eigenvalue which explains the most variance within the dataset (e.g. Grunsky, 2010). The inflexion point (“elbow” shape) here is at number 3 which is used in this study.

### 3.3 Results

Using multivariate statistical analyses on the 245 till samples, the data can be constrained into six till-geochemistry groups. These groups are first discussed statistically, to determine the validity of these groupings. Second, the six groups are discussed spatially, to determine what their relationship is to the geological world.

#### 3.3.1 Cluster analysis results

Table 3-1 shows the main results from the k-means method. The largest group contains 80 samples and the smallest group contains 2 samples. In addition, the average distance between data points within the group and its corresponding centroid is listed in Table 3-1. Each group is defined by its centroid and the different distance between sample points and the centroid within one group indicates how strong a sample point is related to the group features. If one group has a larger average distance to its centroid, this group will be less well-defined compared to the others group (Tan et al., 2005). In Figure 3-1 of the dataset from this study, Group a and Group e are less well-defined than the other four groups derived using k-means clustering analysis. In addition, Group a is the weakest group by virtue of very small number of samples and large average distance to its centroid.

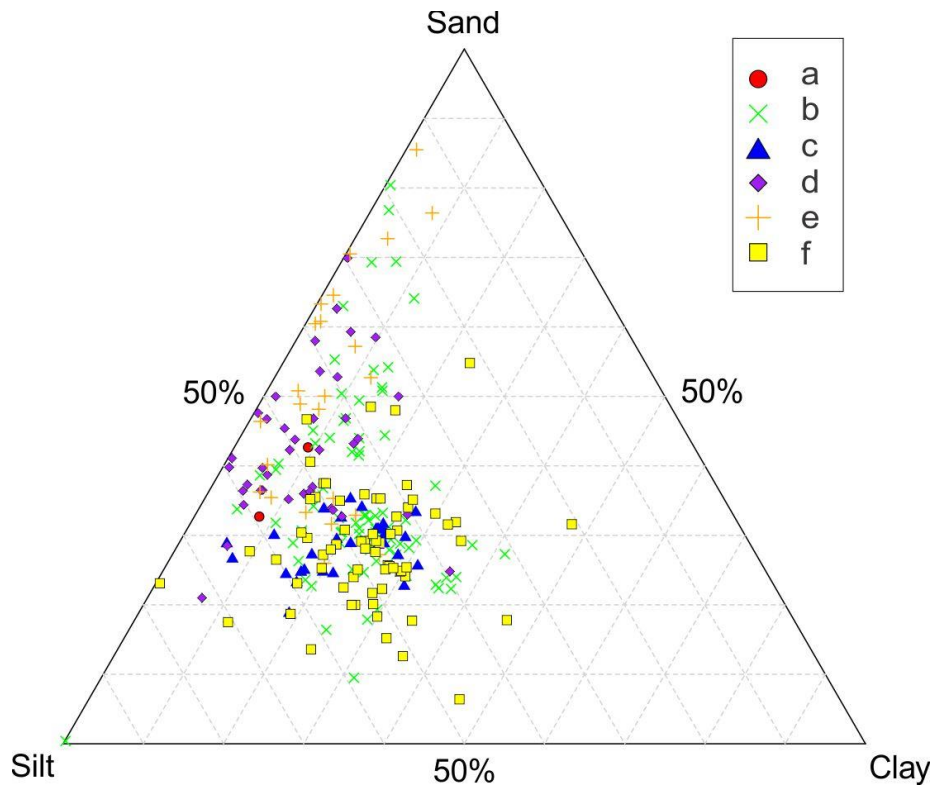
**Table 3-1** Results from k-means method.

Group #	<i>n</i>	Average distance to its centroid
Group a	2	19.29
Group b	80	1.14
Group c	31	4.41
Group d	41	4.56
Group e	24	8.96
Group f	67	5.21

#### 3.3.2 Grain size results

Some trace element concentrations (e.g. Sn, W, Zn) can vary according to the proportion of clay in the sediment (Shilts, 1995). To test whether clay is responsible for the clustering, the six till-geochemistry groups were plotted by till-matrix texture. Grain size results for whole samples

are presented in Figure 3-8. Grain size results on the <2 mm size fraction of the till matrices indicate that the till samples contain 0.1 to 47.6% clay (average = 17.8%). The ternary diagrams show that grain size varies within each of the six till-geochemistry groups. In Figure 3-8, the majority of samples from Group c and Group f contain more clay than the samples from Group d and Group e, which indicates some trace elements might have higher values in Group f and Group c than those in Group d and Group e. Hence, texture may have some influence on the cluster analysis.



**Figure 3-8** Ternary plots of grain size results for each group.

### 3.3.3 Principal Component Analysis

Table 3-2 shows the proportion of explained variance for the first 10 principal components. From that table, we see that the first three components account for 61% of the total variance, and PC3 also corresponds to the position of an inflexion point on the scree plot (Figure 3-7). We will therefore focus our analysis on the first three components; PC1, PC2, and PC3. The next step is to identify the elements that contribute the most to each of the first three principal components. Table

3-3 shows the loadings of the main elements with the strongest loadings highlighted for each of the PCs. Large positive or negative loadings indicate that the element has a strong effect on that principal component.

### 3.3.4 Integrating the methods

After independently applying PCA to the dataset, the next step is to combine these results with the cluster analysis results. K-means cluster analysis has separated the dataset into six till-geochemistry groups. However, this cluster analysis does not provide detailed information within each group. Therefore, the next step is to examine how the major and trace elements are separated between the groups.

In the PCA bi-plots (Figure 3-9), all samples are color-coded by the six till-geochemistry cluster analysis groups. The elements are labelled through the *ggbiplot* R package. The positions of the elements are based on the loadings: if an element has a large loading value, far from the centre, this element contributes significantly to one principal component. The examination of the loadings table (Table 3-3) reveals information as follows:

- Group a is defined by elements that have strong positive loadings for PC2 and negative loadings for PC1. These are Al, Ga, and Rb.
- Group b samples fall in the central portion of the bi-plots. The group thus has an average chemical makeup relative to the entire dataset; neither strong enrichment nor depletion of any element.
- Group c is defined by the elements that have strong negative loadings for PC2; mainly Ca and Mg. Most samples belonging to Group c are also plotted in positive PC3 space, with the exception of four samples. Samples within positive PC3 space adds Mo as a contributor to Group c. Samples within Group c appear to be uncorrelated to PC1 since no elements with strong loadings in PC1 are associated with this group.
- Group d is defined by the elements that have positive loadings for PC1 and negative loadings for PC3. A close look at the bi-plots and loadings table indicates that Ca, Cd, Er, Eu, Ho, K, Mg, Mn, Na, P, Sr, and Ti are in PC1 and PC3 space, and all



contribute to Group d. However, samples within Group d are uncorrelated to PC2 since all samples within this group are situated around the PC2 axis.

- Group e is defined by the elements that have strong positive loadings for PC1 and PC3. Although it is variable within the group, the strongest PC3 loadings are within that group. The elements that are contributing to Group e are Gd, which is a heavy rare earth element (HREE), as well as Nd, Pr, and Sm, which are light rare earth elements (LREE), as well as Hf and Zr. Group e is uncorrelated to PC2 since all samples within this group are situated near the PC2 axis.
- Group f is defined by moderately strong negative loadings for PC1 and positive PC2, but it appears to be uncorrelated to PC3. The main elements contributing to this group are Be, Co, Cr, Cs, Cu, Fe, Ga, Li, Ni, Rb, Sc, Sn, V, and Zn.

**Table 3-2** Summary of principal components

Number#	PC1	PC2	PC3	PC4	PC5	PC6	PC7	PC8	PC9	PC10
Standard deviation	4.288	2.454	2.072	1.832	1.597	1.416	1.218	1.043	0.959	0.890
Proportion of Variance	0.391	0.128	0.091	0.071	0.054	0.043	0.032	0.023	0.020	0.017
Cumulative Proportion	0.391	0.519	0.611	0.682	0.736	0.779	0.811	0.834	0.853	0.870

**Table 3-3** Individual element loadings of first 3 PCs. Loadings of  $\pm 0.5$  is the threshold for elements that contribute strongly to PCs (red bold fonts).

Elements	PC1	PC2	PC3	Elements	PC1	PC2	PC3
Al	-0.27	<b>0.59</b>	<b>-0.54</b>	Ho	<b>0.82</b>	0.25	-0.04
Ca	0.47	<b>-0.72</b>	-0.05	La	0.32	0.43	<b>0.54</b>
Fe	<b>-0.89</b>	0.30	0.18	Li	<b>-0.96</b>	0.03	0.06
K	0.23	0.28	<b>-0.69</b>	Mo	-0.17	-0.38	0.45
Mg	0.49	<b>-0.70</b>	-0.07	Nb	0.06	<b>0.52</b>	-0.41
Mn	0.08	-0.36	-0.08	Nd	<b>0.62</b>	<b>0.53</b>	0.34
Na	<b>0.74</b>	0.19	-0.37	Ni	<b>-0.77</b>	-0.12	0.04
P	<b>0.54</b>	-0.19	-0.16	Pb	0.22	0.11	0.23
Ti	0.41	<b>0.61</b>	-0.18	Pr	<b>0.60</b>	0.48	0.45
Ag	-0.07	-0.20	-0.17	Rb	<b>-0.73</b>	0.45	-0.15
Ba	<b>0.51</b>	0.36	-0.31	Sc	<b>-0.76</b>	0.45	-0.25
Be	<b>-0.58</b>	0.22	-0.13	Sm	<b>0.69</b>	0.32	0.44
Cd	<b>0.54</b>	-0.40	-0.12	Sn	<b>-0.80</b>	0.26	0.14
Ce	0.09	0.36	<b>0.64</b>	Sr	<b>0.75</b>	-0.24	-0.37
Co	<b>-0.87</b>	0.16	-0.07	Ta	0.18	<b>0.56</b>	0.01
Cr	<b>-0.56</b>	0.23	0.05	Tb	<b>0.85</b>	0.25	0.02
Cs	<b>-0.95</b>	0.11	0.12	Th	-0.11	0.31	<b>0.61</b>
Cu	<b>-0.74</b>	-0.06	-0.04	U	0.12	-0.30	0.14
Dy	<b>0.73</b>	0.24	-0.01	V	<b>-0.83</b>	0.31	0.17
Er	<b>0.69</b>	0.21	-0.21	W	-0.26	-0.11	-0.28
Eu	<b>0.71</b>	0.36	-0.45	Y	<b>0.75</b>	0.30	-0.13
Ga	<b>-0.60</b>	<b>0.60</b>	-0.35	Zn	<b>-0.92</b>	-0.01	0.07
Gd	<b>0.63</b>	0.21	<b>0.51</b>	Zr	<b>0.84</b>	0.20	0.18
Hf	<b>0.85</b>	0.21	0.20				





**Table 3-4** Summary table of the average concentration and standard deviation of each element, calculated for each of the six till-geochemistry groups. Rare earth elements (REE) are highlighted in yellow, and are included as a summed group at the end of the table. Light orange shaded boxes delimit the highest mean concentrations of a specific element, relative to the six till-geochemistry groups. Light green shaded boxes likewise delimit the lowest mean concentrations of a specific element, relative to the six till-geochemistry groups. Box plots are plotted for several elements (Appendix D).

## Major elements

Group #	Sample no.	Al (%)	Ca (%)	Fe (%)	K (%)	Mg (%)	Mn (%)	Na (%)	P (%)	Ti (%)	Ca+Mg/ Al+Na+K
<b>a</b>	average	6.72	1.02	2.75	2.14	0.79	0.03	1.41	0.02	0.39	0.18
	standard Dev	0.48	0.05	0.25	0.12	0.11	0.00	0.07	0.01	0.01	0.00
<b>b</b>	average	4.66	13.82	1.88	1.85	4.12	0.04	1.08	0.05	0.25	2.41
	standard Dev	0.47	2.18	0.27	0.18	0.76	0.01	0.13	0.01	0.03	0.52
<b>c</b>	average	4.74	14.96	2.15	1.73	4.77	0.04	0.95	0.05	0.24	3.09
	standard Dev	1.02	2.51	0.51	0.38	1.68	0.01	0.25	0.01	0.06	2.10
<b>d</b>	average	4.11	14.38	1.38	1.69	4.45	0.03	1.16	0.05	0.22	2.73
	standard Dev	0.34	1.51	0.23	0.11	0.38	0.00	0.09	0.00	0.02	0.39
<b>e</b>	average	4.06	13.38	1.50	1.61	4.11	0.03	1.10	0.05	0.25	2.67
	standard Dev	0.61	2.29	0.29	0.21	0.66	0.01	0.14	0.00	0.04	0.68
<b>f</b>	average	5.95	11.53	2.73	2.23	3.61	0.04	1.08	0.06	0.30	1.68
	standard Dev	0.72	2.61	0.47	0.24	0.59	0.00	0.13	0.01	0.03	0.46


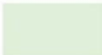

## Trace elements

Group #	Sample no.	Ag (ppm)	Ba (ppm)	Be (ppm)	Cd (ppm)	Ce (ppm)	Co (ppm)	Cr (ppm)	Cs (ppm)	Cu (ppm)	Dy (ppm)
<b>a</b>	average	0.23	594.00	1.55	0.20	48.50	11.68	55.00	2.70	12.35	2.50
	standard Dev	0.01	8.00	0.05	0.00	5.50	2.72	6.00	0.60	3.65	0.26
<b>b</b>	average	0.18	416.71	1.01	0.23	40.63	8.15	49.23	1.97	14.64	2.43
	standard Dev	0.04	44.31	0.14	0.04	6.72	1.14	5.67	0.36	4.40	0.24
<b>c</b>	average	0.24	412.13	1.18	0.22	45.48	8.79	49.16	2.62	16.44	2.50
	standard Dev	0.19	86.32	0.25	0.07	11.47	2.08	12.86	0.71	4.22	0.51
<b>d</b>	average	0.20	390.00	0.91	0.23	35.71	5.99	34.05	1.31	10.60	2.25
	standard Dev	0.14	25.60	0.15	0.05	8.31	1.13	6.36	0.34	2.57	0.22
<b>e</b>	average	0.17	401.00	0.87	0.25	45.21	6.12	38.67	1.27	10.33	2.51
	standard Dev	0.06	52.00	0.18	0.06	10.19	1.46	7.21	0.42	4.06	0.42
<b>f</b>	average	0.25	482.06	1.44	0.23	53.16	11.63	65.12	3.41	22.10	2.91
	standard Dev	0.05	61.01	0.24	0.05	9.59	2.10	10.12	0.76	5.16	0.34

Group #	Sample no.	Er (ppm)	Eu (ppm)	Ga (ppm)	Gd (ppm)	Hf (ppm)	Ho (ppm)	La (ppm)	Li (ppm)	Mo (ppm)	Nb (ppm)
<b>a</b>	average	1.44	0.87	16.25	3.15	6.05	0.46	25.50	36.50	0.47	12.25
	standard Dev	0.09	0.01	3.05	0.55	1.65	0.03	2.50	8.50	0.12	1.15
<b>b</b>	average	1.37	0.87	10.45	3.49	4.04	0.47	26.53	25.31	0.42	7.51
	standard Dev	0.14	0.08	1.29	0.45	0.74	0.05	2.71	4.46	0.13	0.97
<b>c</b>	average	1.38	0.83	10.33	3.35	3.62	0.45	27.68	33.74	0.60	7.77
	standard Dev	0.28	0.17	2.45	0.70	0.86	0.09	5.89	7.80	0.17	1.80
<b>d</b>	average	1.28	0.82	8.73	2.96	3.84	0.43	22.54	16.88	0.30	6.90
	standard Dev	0.13	0.07	1.01	0.34	0.66	0.04	2.63	3.78	0.08	0.72
<b>e</b>	average	1.40	0.85	8.65	3.79	5.35	0.49	27.67	16.58	0.42	7.43
	standard Dev	0.25	0.12	1.84	0.60	0.99	0.08	4.93	5.77	0.19	1.79
<b>f</b>	average	1.64	1.04	14.39	3.99	3.90	0.55	32.93	42.31	0.49	9.52
	standard Dev	0.17	0.11	2.29	0.54	0.56	0.06	4.24	7.97	0.16	1.16

Group #	Sample no.	Nd (ppm)	Ni (ppm)	Pb (ppm)	Pr (ppm)	Rb (ppm)	Sc (ppm)	Sm (ppm)	Sn (ppm)	Sr (ppm)	Ta (ppm)
<b>a</b>	average	22.05	33.05	17.50	5.85	78.55	8.20	3.80	1.35	203.00	0.86
	standard Dev	2.35	9.35	1.00	0.55	5.95	0.90	0.60	0.23	10.00	0.08
<b>b</b>	average	22.29	24.16	12.28	6.12	65.67	5.74	3.98	0.96	207.33	0.54
	standard Dev	2.12	2.76	1.15	0.62	8.09	0.80	0.46	0.13	16.73	0.06
<b>c</b>	average	22.26	29.70	13.12	6.01	68.65	6.25	3.76	1.10	201.23	0.58
	standard Dev	4.77	5.26	2.18	1.29	16.92	1.54	0.80	0.24	36.91	0.13
<b>d</b>	average	19.63	17.80	10.77	5.35	53.78	4.78	3.42	0.76	225.46	0.49
	standard Dev	2.12	2.21	1.18	0.62	6.27	0.61	0.37	0.12	22.43	0.06
<b>e</b>	average	23.29	18.18	12.22	6.41	52.96	4.75	4.28	0.84	205.29	0.56
	standard Dev	3.93	3.40	1.71	1.10	11.54	0.89	0.66	0.21	16.59	0.12
<b>f</b>	average	27.34	34.04	14.90	7.50	92.65	8.12	4.60	1.37	209.99	0.68
	standard Dev	3.25	6.81	2.21	0.91	15.67	1.30	0.56	0.23	15.12	0.09

Group #	Sample no.	Tb (ppm)	Th (ppm)	U (ppm)	V (ppm)	W (ppm)	Y (ppm)	Zn (ppm)	Zr (ppm)	REE
<b>a</b>	average	0.39	10.72	2.34	70.00	4.90	11.55	52.50	210.50	134.26
	standard Dev	0.04	1.48	0.09	10.40	3.40	0.35	8.50	48.50	11.91
<b>b</b>	average	0.41	9.60	1.87	49.93	0.75	12.83	41.28	139.19	127.14
	standard Dev	0.04	1.27	0.67	6.25	0.24	1.25	6.09	25.51	14.09
<b>c</b>	average	0.40	11.22	2.41	53.60	2.09	11.60	49.90	121.10	131.95
	standard Dev	0.08	2.82	0.56	11.51	4.33	2.35	9.06	28.86	29.31
<b>d</b>	average	0.38	8.09	2.43	36.35	0.81	11.50	31.24	128.24	111.05
	standard Dev	0.04	1.31	4.44	6.04	0.23	1.09	5.39	22.77	15.05
<b>e</b>	average	0.43	10.44	2.01	39.76	0.70	12.95	31.25	184.75	134.02
	standard Dev	0.07	2.32	0.48	7.41	0.30	2.14	7.30	34.45	24.50
<b>f</b>	average	0.49	12.86	2.21	70.88	1.14	14.74	61.87	127.43	158.99
	standard Dev	0.05	2.43	0.55	11.70	0.37	1.56	10.60	18.37	21.24

 high
  low
  elements belong to REE

### 3.3.5.1 Group a

PCA shows that group a is defined by the elements Al, Ga, and Rb. A close look at Table 3-4 shows that group a samples indeed have the higher mean concentrations of these elements than most other groups, but also other elements including Ba, Be, Co, Hf, K, Na, Nb, Sc, Pb, V, and Zr. Group a samples also have the lowest concentration of Ca, Mg and carb ratio.

### 3.3.5.2 Group b

PCA shows that group b has a blended signature with no element contributing strongly to defining the group. A close look at Table 3-4 shows that group b samples do not contain any highest or lowest mean concentrations of any elements.

### 3.3.5.3 Group c

PCA shows that group c is defined by the elements Ca, Mg, and Mo. A close look at Table 3-4 shows that group c samples have the highest mean concentrations of Ca, Mg and the carbonate ratio. Moreover, group c has the highest mean concentration of Mo. Group c has the lowest mean concentrations of Hf, Na, Sr, and Zr.

#### 3.3.5.4 Group d

PCA shows that group d is defined by the elements Ca, Cd, Eu, Ho, K, Mg, Mn, Na, P, Sr and Ti. A close look at Table 3-4 shows that group d samples have the highest mean concentrations of Sr, and the second highest mean concentrations of Ca, Mg, and the carbonate ratio. While PCA includes Cd, Eu, Ho, K, Mn, P and Ti within group e, the mean concentrations of these elements are similar to other groups and are not the highest or the lowest. Group d samples also have the lowest mean concentrations of Be, Cr, Co, Fe, Ga, Li, Mo, Nb, Pb, Th, V, Zn and REE (Ce, Gd, La, Pr, Sc, Sm, and Y).

#### 3.3.5.5 Group e

PCA shows that group e is defined by the elements Gd, Hf, Nd, Pr, Sm, and Zr. A close look at Table 3-4 shows that group e samples have the second highest mean concentrations of Gd, Hf, Nd, Pr, Sm, and Zr. Group e samples also have the lowest mean concentrations of Al, Cu, Ga, K, Li, Rb, Sc, and Zn.

#### 3.3.5.6 Group f

PCA shows that group f is defined by the elements Be, Co, Cr, Cs, Cu, Ga, Li, Ni, Rb, Sc, Sn, V and Zn. A close look at Table 3-4 shows that group f samples have the highest mean concentrations of Co, Cr, Cu, Fe, K, La, Li, Ni, Rb, Th, V, Zn and REE. Group f samples do not have any lowest mean concentrations of elements.

### 3.4 Discussion

#### 3.4.1 Interpreting the source of the six till-geochemistry groups

Cluster analysis, PCA, and single-variate element statistics have generated six clusters, with various element relationships. There are some spatial patterns within the 6 groups, namely groups a and d overlie the Precambrian Shield, but most of the groups are widespread across the study area and were sampled from both surface and subsurface tills. At the most basic level, till is derived from the sediments and/or bedrock that a glacier entrains, transports and deposits down ice (Eyles, 1985). In the study area, there have been at least three glacial cycles (Nielsen et al., 1986), leading to potential additional geochemical inputs from different sediment and bedrock



source areas, as well as re-entrainment of older till and both glacial and nonglacial fluvial, lacustrine and marine sediments.

The Paleozoic carbonate platform in the Hudson Bay consists of limestone and dolomite (Trommelen, 2012; Nicolas and Young, 2014) and McMartin et al. (2016) stated that the Paleozoic carbonate clasts are enriched in Ca, Mg, Te  $\pm$  Mn. Additionally, the ratio of Ca+Mg/ Na has been used in McMartin et al. (2016) to highlight the carbonate content in the tills. Therefore, the carb ratio (Ca+Mg/Al+K+Na) established to remove the feldspars contribution is applied in this study to examine the range of the carbonate content within each group. The Precambrian shield can be simplified into metasedimentary/metavolcanic rocks, and granitic/gneissic rocks. The metasedimentary rocks are expected to have ferromagnesian elements with a depleted REE and high field strength elements (HFSE) (except for Zn) geochemical signature (Asiedu et al., 2004). The HFSE belong to incompatible elements and contain intense electrostatic field due to strong charges and small ionic radius (Albarède, 2009). However, the metasedimentary rocks can have great variability in compositions (e.g. McLennan et al., 1984; Gibbs et al., 1986; Ahmad et al., 2016). The metavolcanic rocks can have a notable trace elements relationship: high Zr/Y and low abundance of HFSE with high value in Sr concentrations (Leshner et al., 1986). The granitic rocks are expected to have a higher Al, K, Na, Zr and HFSE content (Frost et al., 2001). The gneissic rocks might contain hornblende, biotite, muscovite, plagioclase and quartz with high K, Na and Al and variable Sr and Zr (e.g. Lal et al., 2011; Hartlaub et al., 2004).

The tills also have a known component of far-travelled Dubawnt Supergroup erratics from northern Nunavut and Omar erratics from the Belcher Islands in eastern Hudson Bay. Detritus transported by a glacier south from Nunavut would cross several rock types including feldspar porphyry, red arkose, pink and white quartzite and conglomerate (Nielsen and Dredge, 1982; Figure 3-3). Geochemical signatures would be similar to those of the Precambrian shield locally. Detritus transported by a glacier west from the Belcher Islands would cross several rock types including greywacke, carbonate rocks, siltstone and quartz-sandstone (Dredge and McMartin, 2011; Figure 3-3). Clast lithology indicates that some detritus in the study area have travelled 600 km from the Dubawnt Supergroup and 800 km from the Belcher Island Group (Shilt, 1982; Prest et al., 2000). However, the bedrock between both of these areas has not been mapped in detail, but

generally includes Precambrian Shield in the north and the Hudson Bay basin in the east (Manitoba Energy and Mines, 1992). Detailed geochemistry from these far-away source areas is difficult to interpret, based on the lack of detailed bedrock mapping.

#### 3.4.1.1 Group a

Group a is defined by high concentrations of Al, Ga, Rb and sum of REE, all of which are associated with felsic igneous rocks (Salminen et al., 2005; De Vos et al., 2006). The dominant host minerals for Al and Ga are feldspar and mica (Salminen et al., 2005; De Vos et al., 2006), which are part of the minerals that are much more abundant in felsic rocks (e.g. granites and certain metasedimentary rocks) than mafic rocks. Together with the lowest carbonate ratio, this data indicates that Group a samples are likely derived from felsic rocks of the Precambrian Shield.

#### 3.4.1.2 Group b

Group b is defined as a mixed group due to lack of specific element signatures from both PCA and single element concentrations. This suggests a mixed composition from a variety of sources. Compositional blend in sediments can occur due to a number of processes, but this characteristic generally indicates re-entrainment and mixing of pre-existing sediments of different provenances (Weltje and von Eynatten, 2004).

#### 3.4.1.3 Group c

Group c is defined by the highest concentrations of Ca, Mg, Mo and carbonate ratio from PCA and single element concentrations. This signature clearly indicates that till samples classified within Group c have a carbonate rock provenance. The low Sr concentration associated with this group is likely because Sr cannot replace a huge amount of Ca in calcite since the ionic radii of these two elements have a large difference, but Mg can substitute for Ca in calcite (Appelo and Postma, 2004). In addition, carbonates can lose Sr during diagenesis, including the transformation of aragonite to calcite (e.g. Morse and Mackenzie, 1990; Jones et al., 1995). Therefore, this group has a carbonate rock provenance, but is low in Sr. However, the range of the carb ratio within Group c shows a wide spread, and the Al, Ca, Mg, and the sum of REEs are higher than that in Group d (Figure 3-10; Appendix D). These elemental signatures suggest variable proportions of

multiple sources within Group c. Additionally, Mo is an element which is enriched in shale and siltstone (Salminen et al., 2005; De Vos et al., 2006), and Mo will be enriched in organic-rich mudrocks deposited in sulfidic environments (Scott and Lyons, 2012). This could possibly indicate some input of siliciclastic rocks (Salminen et al., 2005; De Vos et al., 2006). Therefore, Group c represents a mixed carbonate-siliciclastic provenance.

#### 3.4.1.4 Group d

Group d is defined by the second highest concentrations of Ca, Mg, and carb ratio and the highest concentration of Sr, together with the lowest sum of REE values. Sr and Ca are strongly associated in calcareous rocks; thus, the Sr-Ca-Mg associations could indicate a calcareous provenance (Salminen et al., 2005). In addition, Sr can replace Ca in aragonite which is a rock-forming mineral of limestone (Appelo and Postma, 2004). Sum of REE is usually high in igneous rocks (Salminen et al., 2005; De Vos et al., 2006) and low in carbonate rocks (e.g. Rose et al., 1979). As the sum of REE is lowest for Group d (Table 3-4; Figure 3-10; Appendix D), igneous rocks are likely not a contributing source. Group c is also interpreted to have a carbonate rock provenance. Group d is different from Group c because Group d has highest Sr and lowest Mo while Group c shows the opposite results of these two elements. The contrast in Sr behavior between Group c and Group d suggests multiple carbonate provenance with different depositional and/or diagenetic histories.

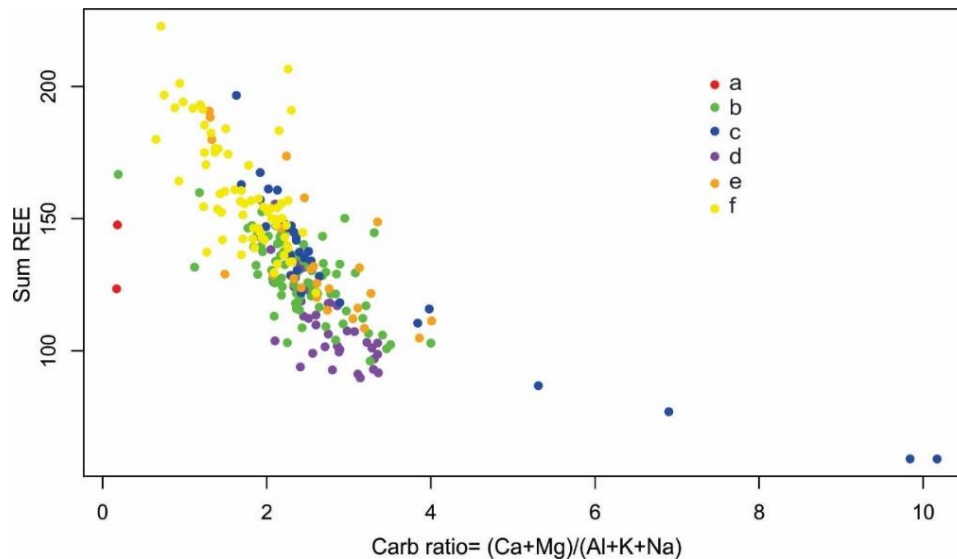
#### 3.4.1.5 Group e

Group e is defined by Gd, Hf, Nd, Pr, Sm, and Zr by comparing PCA and single element concentrations. Zr and Hf shows very similar geochemical properties; therefore, minerals containing Zr will generally have Hf (Salminen et al., 2005). Granitic rocks tend to have the highest concentrations of Hf and Zr than the mafic and metamorphic rocks (Salminen et al., 2005). Moreover, Gd, Nd, Pr, and Sm which are REEs shows high concentrations in granite and granodiorite (Salminen et al., 2005). Thus, Group e samples are interpreted to have a dominant felsic (granitic) source, albeit a different one than that defining Group a. However, the carbonate ratio box plot indicates the carbonate concentration within this group is similar to Group c and

Group d; therefore, this group has a carbonate input mixed with felsic source (Figure 3-10; Appendix D).

#### 3.4.1.6 Group f

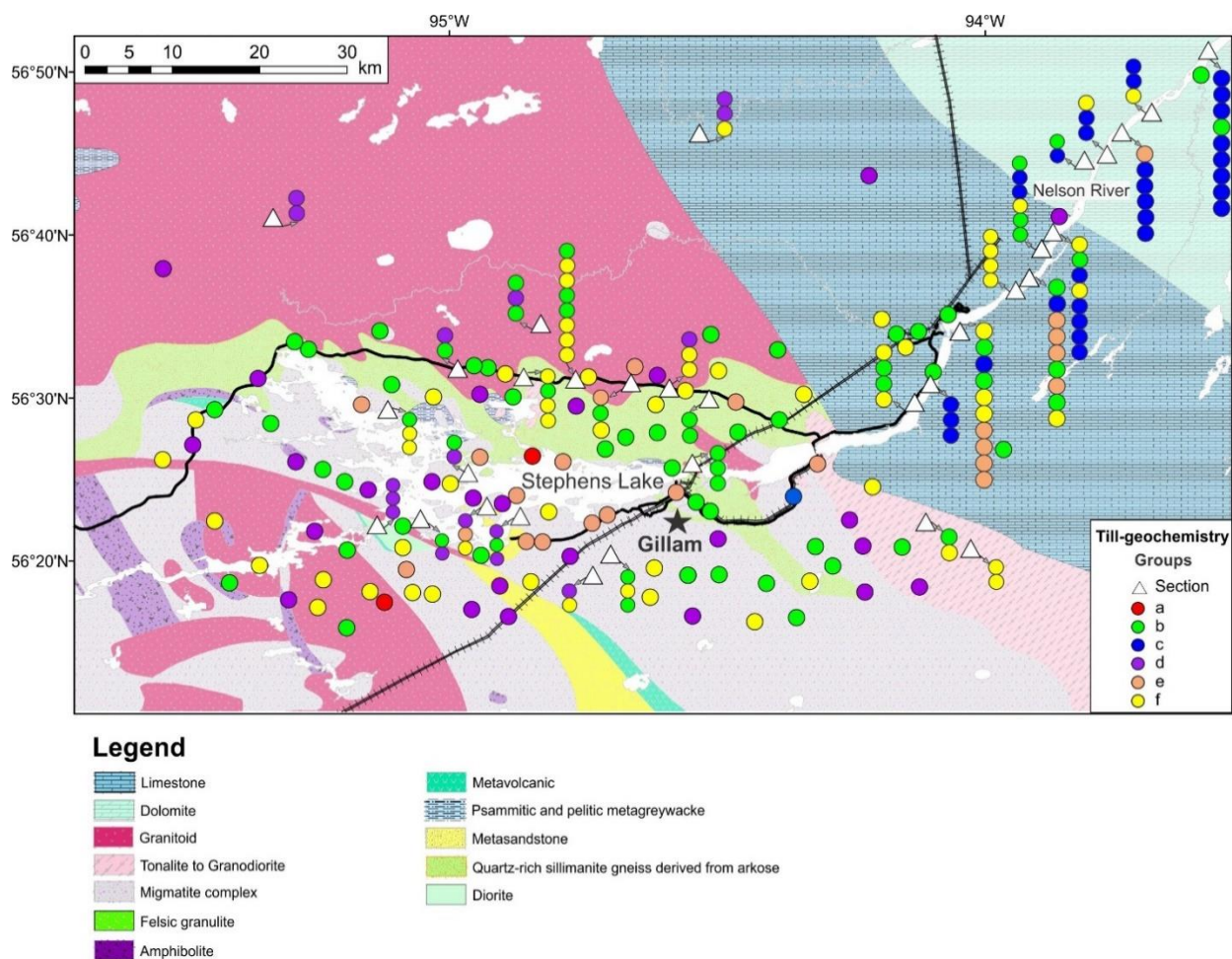
Group f is defined by Be, Co, Cr, Cs, Cu, Ga, Li, Ni, Rb, Sc, Sn, V and Zn. Thus, Group f has a clear metal signature with elements like Co, Cr, Cs, Cu, Li, Ni, Rb, and Zn. Group f contains more clay compared to group a, group d and group e (Figure 3-8), which can increase the amount of metals (e.g. Shilts, 1995). Additionally, carbonates transported from the Hudson Bay platform have the potential to mask or dilute the signal from Precambrian Shield rocks in thick till sequences (McMartin et al., 2016). Group f has a low to medium carbonate ratio (Figure 3-10) which is likely to cause enrichment in the Precambrian Shield source for this group due to lack of carbonate to dilute the signal from Precambrian Shield rocks (e.g. McMartin et al., 2016). However, Group f still has a higher carbonate ratio than Group a (Figure 3-10; Appendix D), which indicates Group f still has some variation in provenance contributions within the group.



**Figure 3-10** Color-coded geochemical groups classified from till matrix geochemistry by k-means cluster analysis: scatterplot of carb ratio vs. sum of REEs. Group a: lowest in carb ratio and medium value of sum of REEs; Group b: medium values in both carb ratio and REEs; Group c: highest value in carb ratio with a large spread, and a large spread in REEs; Group d: high in carb ratio and lowest in REEs; Group e: large spreads in both carb ratio and REEs; Group f: low- medium value in carb ratio and highest in REEs.

### 3.4.1.7 Spatial distribution

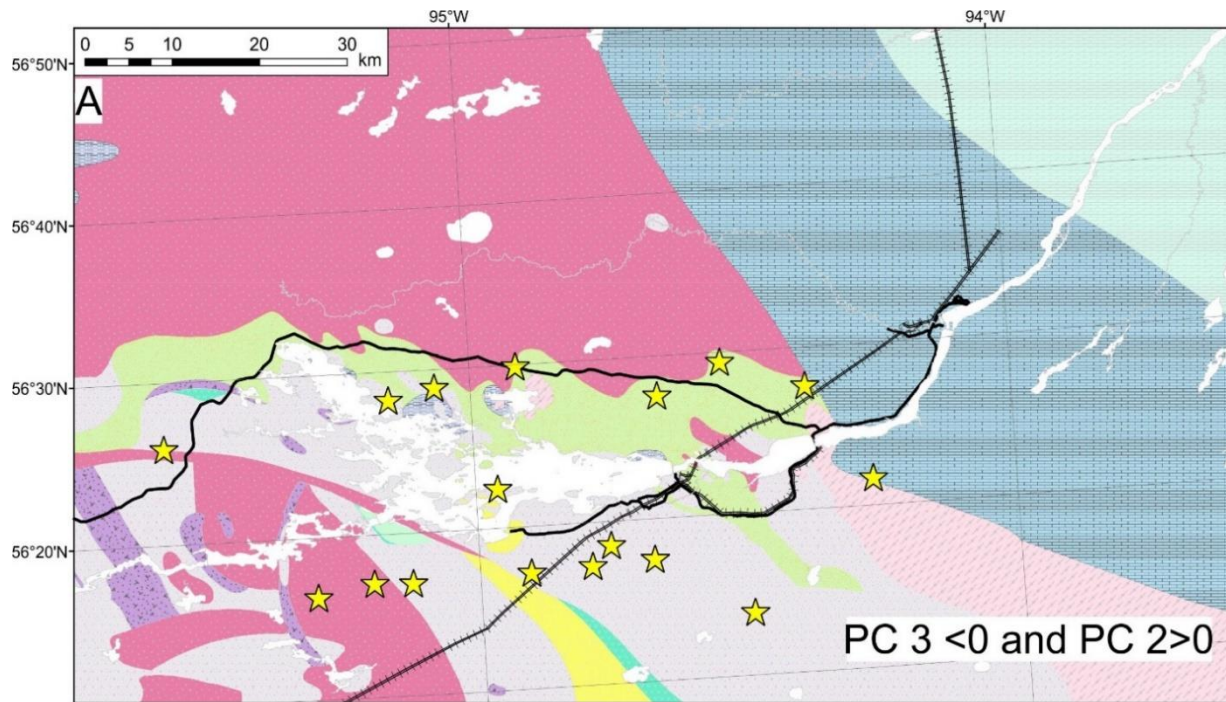
It is important to look at the data spatially because till geochemistry closely relates to the underlying and/or transported bedrock and sediment (Figure 3-11; Grunsky and Kjarsgaard, 2016). The classification from the multivariate analysis should resemble the geospatial pattern in the area where the samples were collected (“Geospatial coherence”; Grunsky and Kjarsgaard, 2016). All samples have been color-coded and displayed on a map to examine spatial patterns (Figure 3-11). Group a (2 samples) contains only surficial samples, and is situated in the western part of the study area overlying the Precambrian Shield. Group b (80 samples) contains both surficial and sub-surface samples, and is widespread across both the Precambrian Shield and Hudson Bay platform. Not surprisingly, this complex hybrid group does not show any obvious spatial pattern, appearing in samples across the field area. Group c (31 samples) mainly contains samples in sections except for one surficial sample. Samples within sections are all in the Hudson Bay platform, while the one surficial sample is located on the Precambrian Shield. However, Group c has carbonate mixed with siliciclastic rocks. The spatial patterns correlate with the carbonate provenance but do not show a relationship with the siliciclastic rocks input. Group d (41 samples) contains both surficial and sub-surface samples, is situated on the Precambrian Shield except for 4 samples in the Hudson Bay platform. Group e (24 samples) also contains both surficial and sub-surface samples. The sub-surface samples within this group are located in the Hudson Bay platform except for one sample which occurs in a section on the Precambrian Shield, while the surficial samples within this group are all present on the Precambrian Shield. Group f (67 samples) is another group containing both surficial and sub-surface samples, and is spread across the study area. Group f is enriched in the Precambrian Shield source mix with carbonate rocks input, which can be demonstrated by the spatial pattern shown by principal component scores (PC scores). PC scores are the new values of individual samples in the PCA space, which are associated with groups of elements (e.g. Grünfeld, 2007; Dempster et al., 2013; Salmirinne et al., 2013; Grunsky and Kjarsgaard, 2016).



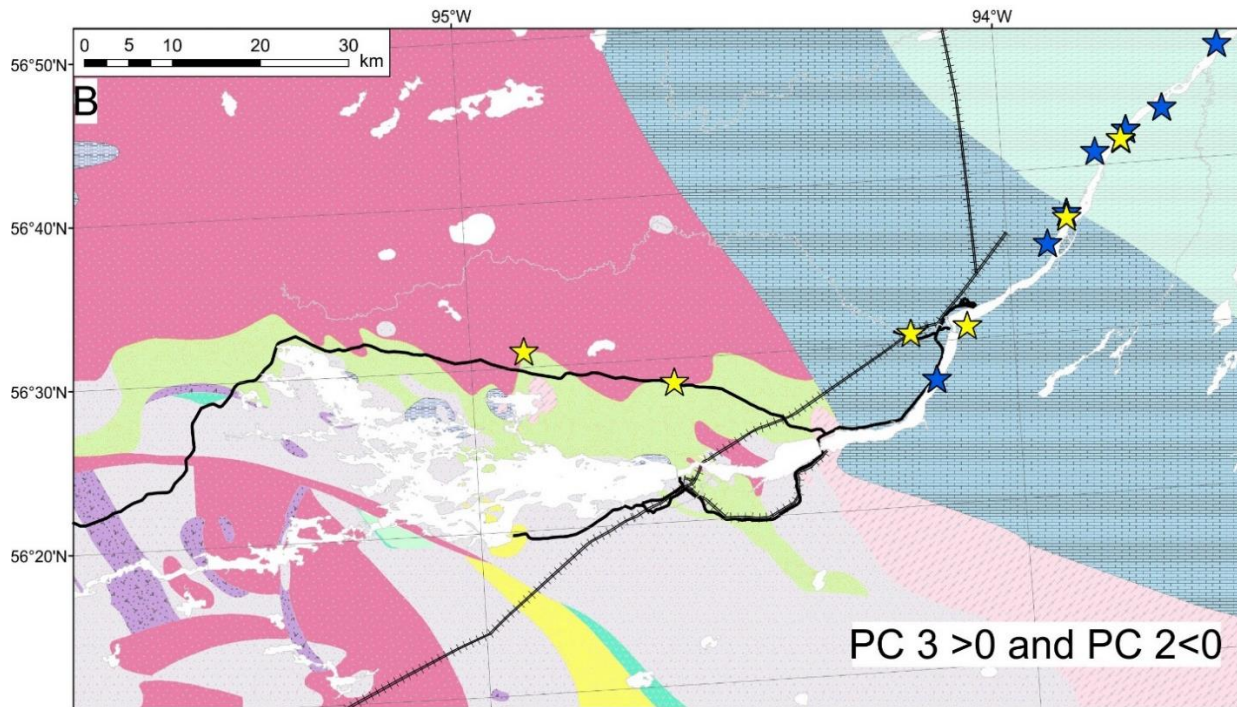
**Figure 3-11** The spatial distribution of till-geochemistry groups. Locations of sections are denoted by hollow triangles, and stacked dots show individual till samples with those sections (unpublished digital bedrock geology compilation from MGS, 2016).

Till samples classified as Group f have a widespread distribution in PCA space; however, this group plots mainly in negative PC1 space and mostly in positive PC2 space, with a relatively even distribution in both positive and negative PC3 space. In positive PC3 space, Group f is plotted mixed with Group c. Therefore, PC3 scores of samples in this group can reveal some compositional change within the group (Figure 3-12). Figure 3-12A shows that group f samples with PC3 scores <0 and PC2 scores > 0 (i.e. close to Group a on the PC1 vs. PC2 plot and away from Group c on the PC1 vs. PC3 plot) are all located on the Precambrian Shield (Figure 3-12A). In contrast, samples within Group c and Group f with PC3 score >0 and PC2 score <0 (i.e. close to Group c on

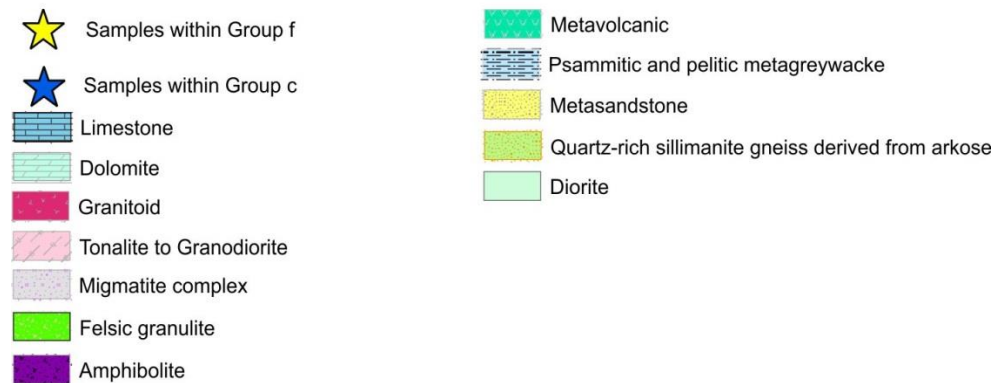
both the PC1 vs. PC2 plot and PC1 vs. PC3 plot) are all located on the carbonate platform (Figure 3-12B). Therefore, the compositional changes within Group f indeed correlate with the spatial locations of the samples. The overlaps between Group f and Group c in terms of both PCA and spatial patterns might indicate a carbonate input associated with Group f.







## Legend



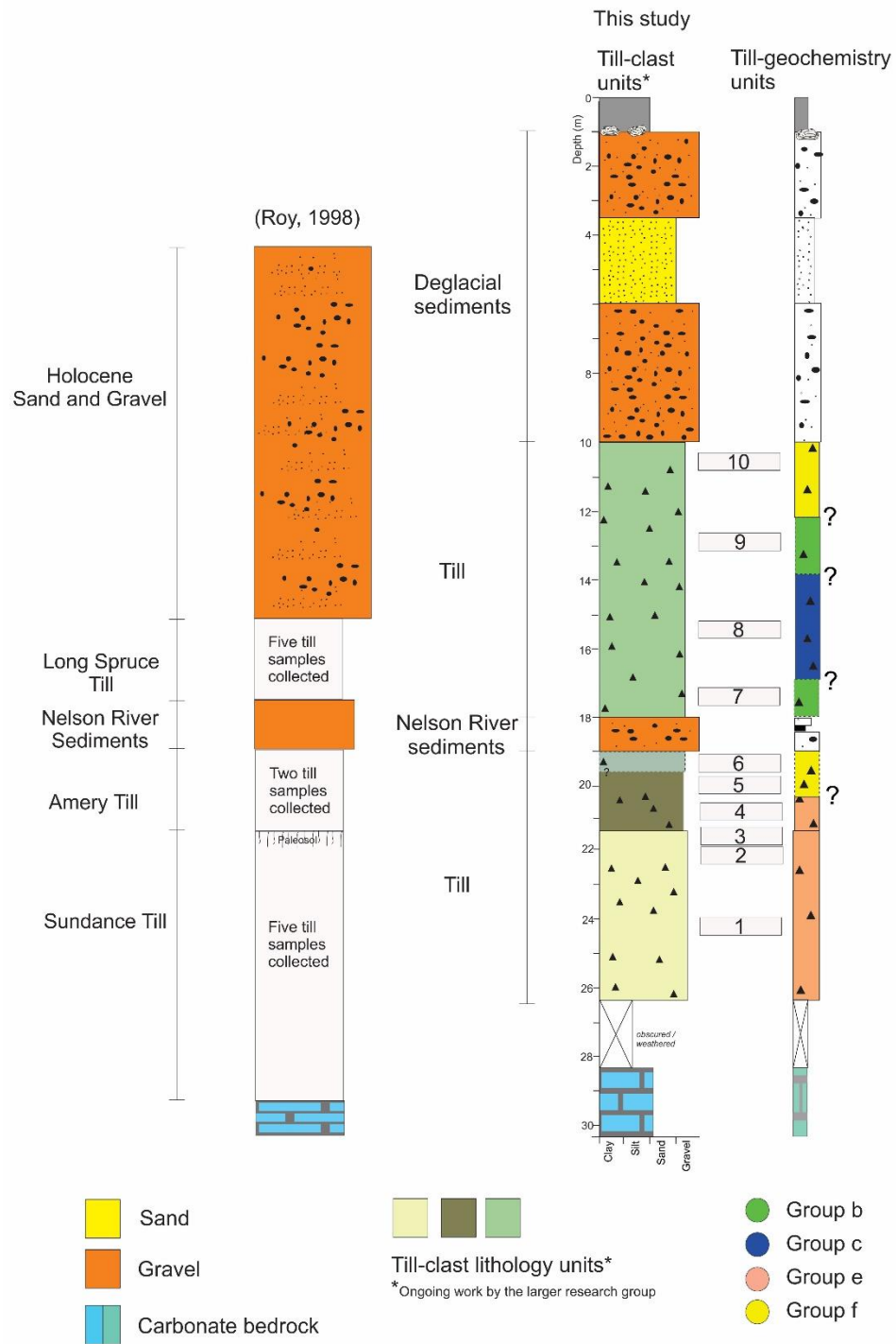
**Figure 3-12** A) Spatial characteristics within Group f (yellow stars) showing only those samples with PC3 scores <0 and PC2 scores >0; B) spatial relationship between Group f and Group c of samples with PC3 scores >0 and PC2 scores <0 (unpublished digital bedrock geology compilation from MGS, 2016).

### 3.4.2 Vertical stratigraphic trends in Moondance section

The interpreted six geochemical groups from this paper are applied to stratigraphic sections to examine the vertical trends within individual sections and make a comparison with existing till stratigraphy in the region. The thick till stratigraphy within the Manitoba HBL allows us to look



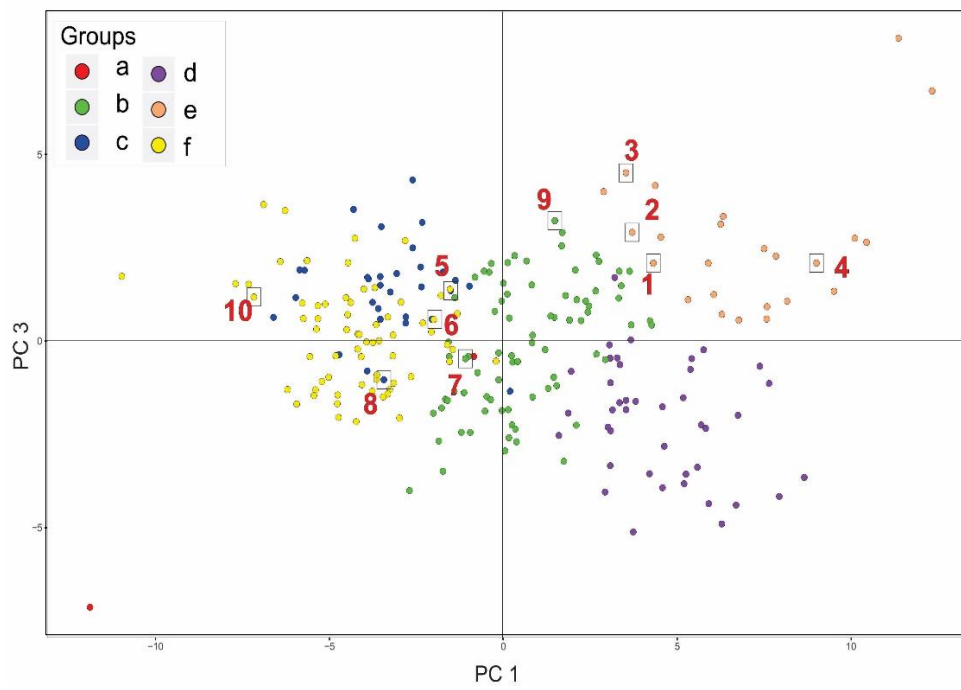
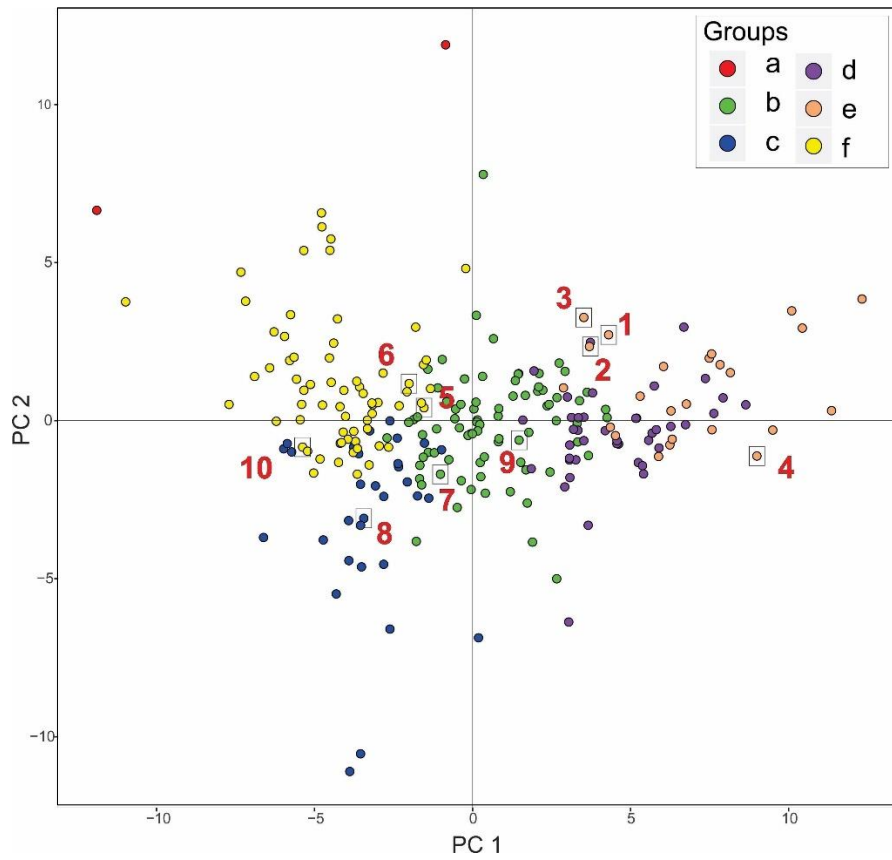
at the vertical till-geochemistry relationships in addition to the horizontal spatial trends. The Moondance section is examined herein, as this section has been described, sampled and analyzed by multiple researchers (Moondance section - Roy 1998, and section 13115MT281/14115MT001 by this research group). It consists of three till units (e.g. Sundance Till, Amery Till and Long Spruce Till), a paleosol that separates the Sundance Till and Amery Till, Nelson River Sediments that separate the Amery Till and Long Spruce Till, and Holocene sand and gravel at the top (Figure 3-13; Roy, 1998). According to the till clast lithology, our research team also characterized three till units, Nelson River Sediments and deglacial sediments at the top. Moondance section is located near the Limestone dam north east of the Gillam townsite, and is accessible by road (Figure 3-2).



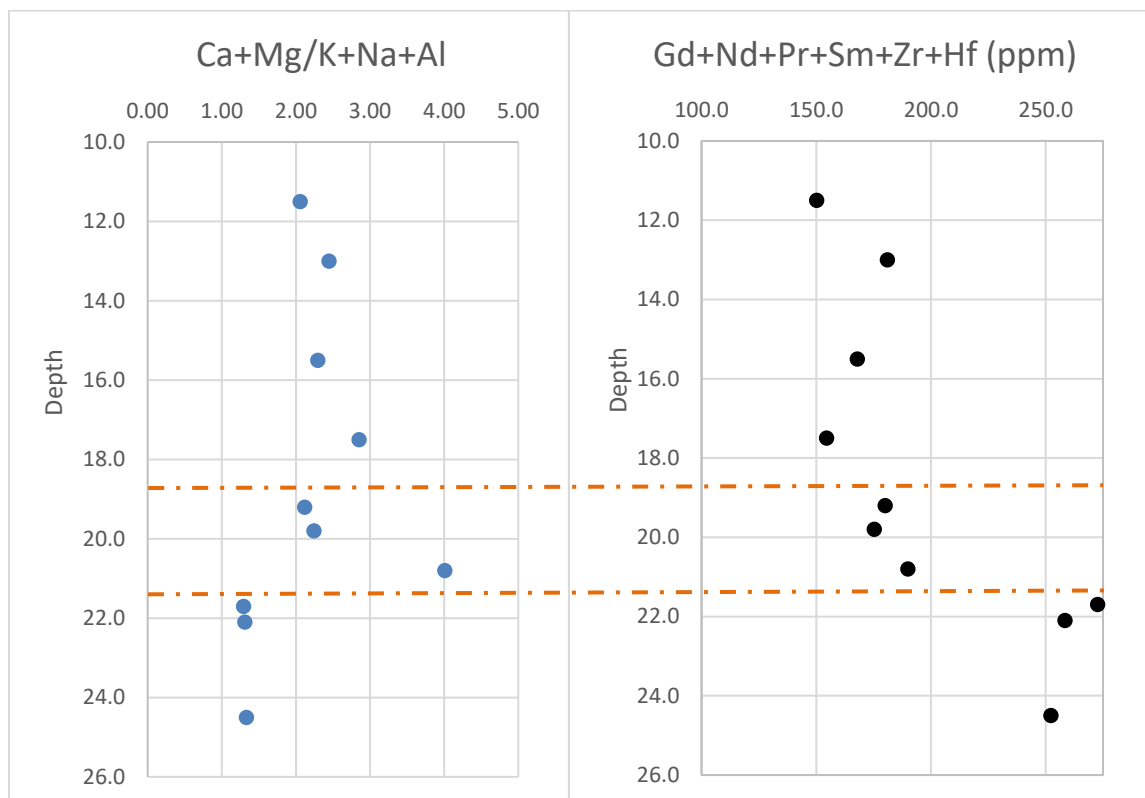
**Figure 3-13** Moondance section till-clast units logged by research team and till-geochemistry units based on the multivariate analysis (this study) compared with stratigraphy generated from Roy (1998). Sample locations are revealed by their labels (e.g. 1 to 10).

10 geochemical samples were taken from this section and three geochemical groups are shown in the stratigraphy (Figure 3-13). The Sundance Till at the base of the section was identified by Roy (1998) based on the high abundance of Precambrian clast and SE-trending ice flow direction from fabric data. In the till geochemistry units (Figure 3-13), the Sundance Till samples are not fully differentiated, but are included with one sample above it into Group e. Group e is characterized by Hf, Zr and certain REEs (Gd, Nd, Pr, and Sm), and the Sundance Till samples are sample #1, sample #2 and sample #3 within Group e space (Figure 3-14). The Sundance Till is characterized by a high abundance of Precambrian clasts and less carbonate clasts by previous researchers (e.g. Nielsen and Dredge, 1982; Nielsen et al., 1986; Roy, 1998). Therefore, the geochemistry signature related to this till will have high concentrations in REEs and low in carbonate related elements (e.g. Rose et al., 1979; Salminen et al., 2005; McMartin et al., 2016). In the PCA biplot, these three samples are plotted close together in both PC1 vs. PC2 and PC1 vs. PC3 spaces associated with Hf, Zr, and REEs such as Gd, Nd, Pr, and Sm. Combined with the concentrations of these elements, the three lower samples, correlated to the Sundance Till, are indeed higher in Gd+Hf+Nd+Pr+Sm+Zr, and lower in carbonate ratio (Figure 3-15) relative to the other samples at the Moondance section. However, the fourth sample (sample #4), which is also plotted in Group e in the PCA biplot, has much higher carbonate ratio values and lower value of the elements associated with Group e in PCA. Additionally, this sample fell into a different till unit (Amery Till) due to the presence of the paleosol on top of the Sundance Till based on Roy (1998) and it shows different lithology in the stratigraphic work compared to the lower three samples in this study (Figure 3-13). The cause of the sudden increase in carbonates could be due to a change in ice flow direction with enough inheritance from the underlying till (Sundance) to keep it in Group e, or a change in subglacial conditions that brought more local rocks (carbonates) into that Group e geochemical group. The above two till samples (sample #5 and sample #6), separated by the Nelson River Sediments with samples collected from the upper till units, are in Group f which is different from the geochemical groups the upper till units fall into. The upper till samples (sample #7 to sample #10), which were characterized as the Long Spruce Till by a previous worker (Roy, 1998), fall within three groups: Group b, Group c and Group f. This

suggests a mixed signature with variable inputs from different sources (e.g. carbonates, Precambrian Shield) for that till.



**Figure 3-14** PCA biplots show the position of samples collected from Moondance section.



**Figure 3-15** Concentration plots for carbonate ratio and certain REEs (Gd, Nd, Pr, Sm) with Hf and Zr for the Moondance samples. Orange dashed lines indicate the contacts between the major till units according to Roy (1998).

### 3.4.3 Implications

#### 3.4.3.1 Till stratigraphy

Till matrix geochemistry provides complementary information in identifying compositional changes in the tills of the HBL. However, the spatial and compositional variability is surprisingly complex, and leads to ambiguity in the interpretation. At a minimum, it is clear that there are not four distinct tills in a layered sequence (c.f. Nielsen and Dredge, 1982; Nielsen et al., 1986; Roy, 1998). Instead, six geochemical groups are identified from the multivariate analysis. The Gillam area of the HBL is a complex region where thick multi-till stratigraphy over the carbonate platform transitions to thin drift cover on the Precambrian Shield, implying the glacier deposited a lot of sediments in a topographic depression, and depositions were not much when the

depression was gone. However, the geochemistry of till matrix still preserves valuable information about the till provenance. A total of six till matrix geochemical groups have been identified and analyzed: 1) Group a shows a felsic rock signature; 2) the other five groups show considerable compositional overlap statistically; however, most of these five groups has a dominant provenance: 1) Group b contains a mixture of sources; 2) Group c has a dominantly carbonate provenance with a siliciclastic rocks input; 3) Group d contains mainly carbonates; 4) Group e shows a dominant granitic source with some carbonate input; 5) Group f has a dominant metal signature such as Co, Fe, Ni, Cu, and Zn, mixed with a carbonate input which is demonstrated through the spatial distribution.

Till matrix geochemistry provides several new insights into the tills of northeastern Manitoba as well as hints on possible provenance and/or processes. First, six geochemical groups are defined by different elements in the PCA, from which interpretations on till provenance can be drawn. Second, the considerable overlaps among the geochemical groups suggests tills in the study area are the products of overprinting and inheritance.

The proposed interpretations can be tested with additional studies of these tills. For instance, a study of till fabric and pebble lithology classifications could help refine the proposed provenances. Additionally, other supervised multivariate data techniques can be applied such as the random forest method (Breiman, 2001).

### **3.5 Conclusion**

The Hudson Bay Lowland in Manitoba has preserved complex till stratigraphy due to the glacial dynamics that occurred during the past glacial cycles; thus, the study of this region has met the limits on till provenance and regional correlation studies of traditional facies analysis such as clast lithology, clast fabric, color, etc. The aim of this study is to obtain extra information on till matrix geochemistry to help understand the stratigraphic framework in the region.

The understanding of till matrix geochemistry adds new insight to the existing Quaternary stratigraphic framework. Results show that there is considerable overlap in the till geochemical makeup. The dominant group of samples is best described as a geochemical hybrid that overlaps with all the other groups identified by the analysis. This means that the tills appear to form a compositional continuum across and within identified till sheets. The results thus indicate that the

till units of the original four-till stratigraphy proposed for the region (e.g. Sundance Till, Amery Till, Long Spruce Till, and Sky Pilot Till) cannot be discriminated and identified on the basis of their composition in a way that would allow identification and correlation of units away from type sections. Therefore, the tills in Manitoba HBL are interpreted as the product of compositional overprinting and inheritance, and cannot be easily differentiated into individual layered till sheets.

Analysis of the till matrix geochemistry provides some details about certain processes (e.g. sediment re-entrainment); the base of a till sheet defined by qualitative logging methods can be compositionally similar to the underlying unit, for example. However, vertical trends from the till matrix geochemistry are complex. Processes like sediment re-entrainment can play a role, but some trends will require more research for interpretation.

Till matrix geochemistry alone may not be sufficient to establish the stratigraphic framework in the study area, but it provides complementary information to the existing knowledge of the regional stratigraphy. The classification from this study still needs to be compared to other information (e.g. clast fabric and clast lithology) to generate a revised till stratigraphy for the region.



## **Chapter 4 Conclusion**

### **4.1 Statistical analysis of the till geochemistry of the Gillam area**

This work is focused on the statistical analysis of the till matrix geochemistry in the Nelson River area, and uses both field work and multivariate data analysis. The section below details the main contributions of the thesis.

#### **4.1.1 Thesis Contributions**

The most significant contributions are as follows:

1. The tills of northeastern Manitoba are, for the first time, described and analyzed rigorously on the basis of their till matrix geochemistry. Six geochemical groups are identified, and their geochemical makeup described and interpreted in terms of possible bedrock provenance and relative degree of mixing. Most till samples show mixing of shield and carbonate (platform) compositional signatures.
2. Results indicate considerable compositional overlap of till matrix. This strongly suggests that despite the identification of distinct till sheets in some sections, most tills exhibit a high degree of compositional similarity. For example, samples from the Long Spruce Till identified at the Moondance section fall within three geochemical groups. This means that a single till sheet recognized through stratigraphic techniques can have samples falling in several different geochemical groups indicating that there is a comparable degree of compositional variation within a till sheet than across different tills separated by stratigraphic bounding surfaces.
3. Results of this thesis support the interpretation that most tills in northeastern Manitoba formed through complex processes involving ice flow shifts and re-entrainment of pre-existing sediment to various degrees. This has major implications not only for understanding glacial processes, but also for reconstructing the regional glacial history, as well as for drift prospecting used in mineral exploration.
4. The findings of this thesis suggest that drift prospecting techniques cannot be applied in a straightforward manner in the region. Detailed ice flow, stratigraphic and compositional analyses are necessary to understand results and identify possible source

- areas for any indicator minerals found in the tills of the study area. Overall, the region presents significant exploration challenges which can best be overcome through detailed research.
5. This study is the first attempt to differentiate till units based on till matrix geochemistry in the region. The study shows that the till matrix geochemistry can provide information about certain processes such as sediment mixing through re-entrainment; the base of a till sheet defined by the standard logging methods may be compositionally similar to an underlying unit, for example. Additionally, the section examined in this study indicates that the vertical trends in till matrix geochemistry are complex. Processes involving sediment re-entrainment can explain certain trends, but some trends will require more research.
  6. This study also provides a case for more detailed bedrock mapping which would include more detailed litho-geochemistry information on each of the bedrock types. This would allow for a more robust connection between till composition and the possible source rocks.
  7. Multi-elements signature from the six geochemical groups can provide meaningful patterns including compositional change and spatial trends in an area where the regional till stratigraphy is complex. This will help the interpretation of the provenances and processes associated with different till sheets with more data integration.

## Bibliography

- Abzalov, M. (2008). Quality control of assay data: a review of procedures for measuring and monitoring precision and accuracy. *Exploration and Mining Geology*, 17(3-4), 131-144.
- Ahmad, I., Mondal, M. E. A., & Satyanarayanan, M. (2016). Geochemistry of Archean metasedimentary rocks of the Aravalli craton, NW India: Implications for provenance, paleoweathering and supercontinent reconstruction. *Journal of Asian Earth Sciences*, 126, 58-73.
- Aitchison, J. (1982). The statistical analysis of compositional data. *Journal of the Royal Statistical Society. Series B (Methodological)*, 139-177.
- Aitchison, J. (1984). The statistical analysis of geochemical compositions. *Journal of the International Association for Mathematical Geology*, 16(6), 531-564.
- Albarède, F. (2009). *Geochemistry: an introduction*. Cambridge University Press.
- Andrews, J. T., Shilts, W. W., & Miller, G. H. (1983). Multiple deglaciations of the Hudson Bay Lowlands, Canada, since deposition of the Missinaibi (Last-integlacial?) formation. *Quaternary Research*, 19(1), 18-37.
- Appelo, C. A. J., & Postma, D. (2004). *Geochemistry, groundwater and pollution*. CRC press.
- Asiedu, D. K., Dampare, S. B., Sakyi, P. A., Banoeng-Yakubo, B., Osa, S., Nyarko, B. J. B., & Manu, J. (2004). Geochemistry of Paleoproterozoic metasedimentary rocks from the Birim diamondiferous field, southern Ghana: Implications for provenance and crustal evolution at the Archean-Proterozoic boundary. *Geochemical Journal*, 38(3), 215-228.
- Benn, D. I. (2007). Glacial landforms, sediments: Till Fabric Analysis. *Encyclopedia of Quaternary Science*, pp. 954–959.
- Berger, G. W., & Nielsen, E. (1991). Evidence from thermoluminescence dating for Middle Wisconsinan deglaciation in the Hudson Bay Lowland of Manitoba. *Canadian Journal of Earth Sciences*, 28(2), 240-249.
- Bostock, H. (1970). *Physiographic subdivisions of Canada*. Ottawa: Geological Survey of Canada, Department fo Energy, Mines and Resources.
- Boston, C. M., Evans, D. J., & Cofaigh, C. Ó. (2010). Styles of till deposition at the margin of the Last Glacial Maximum North Sea lobe of the British–Irish Ice Sheet: an assessment based on geochemical properties of glacial deposits in eastern England. *Quaternary Science Reviews*, 29(23), 3184-3211.
- Breiman, L. (2001). Random forests. *Machine learning*, 45(1), 5-32.
- Buccianti, A., Mateu-Figueras, G., & Pawlowsky-Glahn, V. (Eds.). (2006). *Compositional data analysis in the geosciences: from theory to practice*. Geological Society of London.

- Carlson, A. E., Jenson, J. W., & Clark, P. U. (2004). Sedimentological observations from the Tiskilwa till, Illinois, and Sky Pilot till, Manitoba. *Géographie physique et Quaternaire*, 58(2-3), 229-239.
- Clark, P. U., Licciardi, J. M., MacAyeal, D. R., & Jenson, J. W. (1996). Numerical reconstruction of a soft-bedded Laurentide Ice Sheet during the last glacial maximum. *Geology*, 24(8), 679-682.
- Davies, T., & Fearn, T. (2004). Back to basics: the principles of principal component analysis. *Spectroscopy Europe*, 16(6), 20.
- De Vos, W., Tarvainen, T., Salminen, R., Reeder, S., De Vivo, B., Demetriades, A., ... & O'connor, P. J. (2006). *Geochemical Atlas of Europe: Part 2: Interpretation of geochemical maps, additional tables, figures, maps, and related publications*. Geological Survey of Finland.
- Dempster, M., Dunlop, P., Scheib, A., & Cooper, M. (2013). Principal component analysis of the geochemistry of soil developed on till in Northern Ireland. *Journal of Maps*, 9(3), 373-389.
- Detlefs, J. (2016). *Principal Component Analysis (PCA) [0.16.0]*. GNU Public License v3.
- Dinse, G. E., Jusko, T. A., Ho, L. A., Annam, K., Graubard, B. I., Hertz-Picciotto, I., ... & Weinberg, C. R. (2014). Accommodating measurements below a limit of detection: a novel application of Cox regression. *American journal of epidemiology*, 179(8), 1018-1024.
- Doornbos, C., Heaman, L. M., Doupé, J. P., England, J., Simonetti, A., & Lajeunesse, P. (2009). The first integrated use of in situ U–Pb geochronology and geochemical analyses to determine long-distance transport of glacial erratics from mainland Canada into the western Arctic Archipelago. *Canadian Journal of Earth Sciences*, 46(2), 101-122.
- Dredge, L. A., & Cowan, W. R. (1989). Quaternary geology of the southwestern Canadian Shield. *Quaternary Geology of Canada and Greenland*. Geological Survey of Canada, Ottawa, 214-235.
- Dredge, L. A., & McMartin, I. (2011). Glacial stratigraphy of northern and central Manitoba; Geological Survey of Canada, Bulletin 600, 27 p. doi: 10.4095/288561
- Dredge, L. A., & Nielsen, E. (1985). Glacial and interglacial deposits in the Hudson Bay Lowlands: a summary of sites in Manitoba. *Current Research, Part A*, Geological Survey of Canada, Paper, 85(1), 247-257.
- Dredge, L. A., & Nielsen, E. (1987). Glacial and interglacial stratigraphy, Hudson Bay Lowlands, Manitoba. *Geological Society of America centennial field guide*. Edited by DL Biggs. Geological Society of America, North Central Section, 3, 43-46.
- Dredge, L. A., & Pehrsson, S.J. (2006). Geochemistry and physical properties of till in northernmost Manitoba; Geological Survey of Canada, Open File 5320, 130 p.
- Dredge, L., Morgan, A., & Nielsen, E. (1990). Sangamon and pre-Sangamon interglaciations in the Hudson Bay Lowlands of Manitoba. *Géographie physique et Quaternaire*, 44(3), 319-336.

- Dubé-Loubert, H., Roy, M., Allard, G., Lamothe, M., & Veillette, J. J. (2012). Glacial and nonglacial events in the eastern James Bay lowlands, Canada. *Canadian Journal of Earth Sciences*, 50(4), 379-396.
- Dyke, A. S., Andrews, J. T., Clark, P. U., England, J. H., Miller, G. H., Shaw, J., & Veillette, J. J. (2002). The Laurentide and Innuitian ice sheets during the last glacial maximum. *Quaternary Science Reviews*, 21(1), 9-31.
- Egozcue, J. J., Pawlowsky-Glahn, V., Mateu-Figueras, G., & Barcelo-Vidal, C. (2003). Isometric logratio transformations for compositional data analysis. *Mathematical Geology*, 35(3), 279-300.
- Evans, A. M. (1995). Ore, mineral economics and mineral exploration. *Introduction to Mineral Exploration*: Oxford, UK, Blackwell Science Ltd, 3-15.
- Evans, D. J., Hiemstra, J. F., & O'Coifagh, C. (2007). An assessment of clast macrofabrics in glaciogenic sediments based on A/B plane data. *Geografiska Annaler: Series A, Physical Geography*, 89(2), 103-120.
- Eyles, N. (1985). *Glacial geology: an introduction for engineers and earth scientists*. Oxford: Pergamon.
- Frost, B. R., Barnes, C. G., Collins, W. J., Arculus, R. J., Ellis, D. J., & Frost, C. D. (2001). A geochemical classification for granitic rocks. *Journal of petrology*, 42(11), 2033-2048.
- Gamboa, A., Montero-Serrano, J. C., St-Onge, G., Rochon, A., & Desjage, P. A. (2017). Mineralogical, geochemical, and magnetic signatures of surface sediments from the Canadian Beaufort Shelf and Amundsen Gulf (Canadian Arctic). *Geochemistry, Geophysics, Geosystems*, 18(2), 488-512.
- Garrett, R. G., & Thorleifson, L. H. (1996). Kimberlite indicator mineral and soil geochemical reconnaissance of the Canadian Prairie region. *Searching for Diamonds in Canada*, (eds.) AN LeCheminant, DG Richardson, RNW DiLabio and KA Richardson, 205-211.
- Garrett, R. G., & Grunsky, E. C. (2003). S and R functions for the display of Thompson–Howarth plots. *Computers & Geosciences*, 29(2), 239-242.
- Gauthier, M., Hodder, T.J., Kelly, S.E., Wang, Y., Ross, M. (2016). Drift exploration techniques in the Gillam area - year 4 (NTS 54D, 54C). Manitoba Growth, Enterprise and Trade, Manitoba Geological Survey, Manitoba Mining and Minerals Convention 2016, Winnipeg, Manitoba, November 16–18, 2016, poster presentation.
- Gauthier, M., Kelly, S.E., Hodder, T.J., Wang, Y., Ross, M. (2017). Till composition inheritance and overprinting in the Hudson Bay Lowland and across the Precambrian shield. Presentation presented at the 2017 GAC-MAC annual meeting, Kingston, ON.
- Gibbs, A. K., Montgomery, C. W., O'Day, P. A., & Erslev, E. A. (1986). The Archean-Proterozoic transition: Evidence from the geochemistry of metasedimentary rocks of Guyana and Montana. *Geochimica et Cosmochimica Acta*, 50(10), 2125-2141.

- Grünfeld, K. (2007). The separation of multi-element spatial patterns in till geochemistry of southeastern Sweden combining GIS, principal component analysis and high-dimensional visualization. *Geochemistry: Exploration, Environment, Analysis*, 303-318.
- Grunsky, E. (2010). The interpretation of geochemical survey data. *Geochemistry: Exploration, Environment, Analysis*, 27-74.
- Grunsky, E. C., & Kjarsgaard, B. A. (2008). Classification of distinct eruptive phases of the diamondiferous Star Kimberlite, Saskatchewan, Canada based on statistical treatment of whole rock geochemical analyses. *Applied Geochemistry*, 23(12), 3321-3336.
- Grunsky, E. C., Kjarsgaard, B. A. (2016). Recognizing and Validating Structural Processes in Geochemical Data. In *Compositional Data Analysis*, J.A. Martin-Fernandez and S. Thio-Henestrosa (eds.), Springer Proceedings in Mathematics and Statistics, 187. 85-116, 209pp., doi: 10.1007/978-3-319-44811-4\_7.
- Harris, J. R., & Grunsky, E. C. (2015). Predictive lithological mapping of Canada's North using Random Forest classification applied to geophysical and geochemical data. *Computers & Geosciences*, 80, 9-25.
- Hart, J. K., & Smith, B. (1997). Subglacial deformation associated with fast ice flow, from the Columbia Glacier, Alaska. *Sedimentary Geology*, 111(1-4), 177-197.
- Hartlaub, R.P., Böhm, C.O., Kuiper, Y.D., Bowerman, M.S. & Heaman, L.M. (2004). Archean and Paleoproterozoic geology of the northwestern Split Lake Block, Superior Province, Manitoba (parts of NTS 54D4, 5, 6 and 64A1); in Report of Activities 2004, Manitoba Industry, Economic Development and Mines, Manitoba Geological Survey, p. 187–194.
- Hodder, T. J. & Kelley, S. E. (2016). Quaternary stratigraphy and till sampling in the Kaskattama highland region, northeastern Manitoba (parts of NTS 53N, O, 54B, C); in Report of Activities 2016, Manitoba Growth, Enterprise and Trade, Manitoba Geological Survey, p. 187–195.
- Hodder, T.J., Trommelen, M.S., Kelley, S.E., Wang, Y. & Ross, M. (2015). Revisiting the till stratigraphy in the Hudson Bay lowland region of Manitoba; CANQUA 2015, St. John's, Newfoundland, August 16–19, 2015, Program with Abstracts, p. 49–50.
- Jenner, G.A. (1996). Trace element geochemistry of igneous rocks: Geochemical nomenclature and analytical geochemistry, in Wyman, D.A., ed., *Trace Element Geochemistry of Volcanic Rocks: Applications for Massive Sulfide Exploration*, 12, Geological Association of Canada, Short Course Notes, p. 51–77.
- Jeong, D. H., Ziemkiewicz, C., Ribarsky, W., & Chang, R. (2016). Understanding Principal Component Analysis Using a Visual ... Retrieved July 19, 2016, from <http://www.purdue.edu/discoverypark/vaccine/assets/pdfs/publications/pdf/UnderstandingPrincipalComponent.pdf>
- Jolliffe, I. T., & Cadima, J. (2016). Principal component analysis: a review and recent developments. *Phil. Trans. R. Soc. A*, 374(2065), 20150202.

- Jones, C. E., Halliday, A. N., & Lohmann, K. C. (1995). The impact of diagenesis on high-precision UPb dating of ancient carbonates: An example from the Late Permian of New Mexico. *Earth and Planetary Science Letters*, 134(3-4), 409-423.
- Kääriäinen, K. (2016). Reanalysis of the existing regional geochemical data around the Sakatti Ni-Cu-PGE target, Sodankylä, Finland.
- Kelley, S.E., Hodder, T.J., Wang, Y., Trommelen, M.S., & Ross, M. (2015) Preliminary Quaternary geology in the Gillam area, northeastern Manitoba – year 3 (parts of NTS 54D5 – 9, 11, 54C12). in Report of Activities 2015, Manitoba Mineral Resources, Manitoba Geological Survey, p. 169 – 182.
- Klassen, R.W. (1986). Surficial geology of North-Central Manitoba. Geological Survey of Canada. Memoir 419.
- Klassen, R.W., & Netterville, J A. (1980): Surficial geology of Kettle Rapids, east of principal meridian, Manitoba; Geological Survey of Canada, "A" Series Map, Map 1481A, 1 map. scale 1:250 000.
- Koljonen, T., Gustavsson, N., Noras, P. & Tanskanen, H. (1992). In: Koljonen, T. (ed.) The Geochemical Atlas of Finland Part 2: Till. Geological Survey of Finland, Espoo, Finland.
- Lal, S. N., Pandey, M., Hyanki, A., & Prakash, D. (2011). Petrology and Geochemistry of Granitic Gneisses from Main Central Thrust (MCT) Zone, Kumaun Himalaya, India. *Himalayan Geology*, 32(2), 137-147.
- Lisher, C. M., Goodwin, A. M., Campbell, I. H., & Gorton, M. P. (1986). Trace-element geochemistry of ore-associated and barren, felsic metavolcanic rocks in the Superior Province, Canada. *Canadian Journal of Earth Sciences*, 23(2), 222-237.
- Manitoba Energy and Mines, (1992). Bedrock Geology Compilation Map Series, Kettle Rapids, NTS 54D, 1:250 000.
- McClenaghan, M. B., & Kjarsgaard, B. A. (2007). Indicator mineral and surficial geochemical exploration methods for kimberlite in glaciated terrain, examples from Canada. *Mineral Resources of Canada: A Synthesis of Major Deposit-types, District Metallogeny, the Evolution of Geological Provinces and Exploration Methods*. Geological Association of Canada, Special Publication, (5), 983-1006.
- McClenaghan, M. B., Plouffe, A., McMartin, I., Campbell, J. E., Spirito, W. A., Paulen, R. C., ... & Hall, G. E. M. (2013). Till sampling and geochemical analytical protocols used by the Geological Survey of Canada. *Geochemistry: Exploration, Environment, Analysis*, 13(4), 285-301.
- McLennan, S. M., Taylor, S. R., & McGregor, V. R. (1984). Geochemistry of Archean metasedimentary rocks from West Greenland. *Geochimica et Cosmochimica Acta*, 48(1), 1-13.
- McMartin, I., & Campbell, J. E. (2009). Near-surface till sampling protocols in shield terrain, with examples from western and northern Canada. *Application of Till and Stream Sediment Heavy*

- Mineral and Geochemical Methods to Mineral Exploration in Western and Northern Canada. Geological Association of Canada, St. John's, Newfoundland, 61-78.
- McMartin, I., & McClenaghan, M. B. (2001). Till geochemistry and sampling techniques in glaciated shield terrain: a review. Geological Society, London, Special Publications, 185(1), 19-43.
- McMartin, I., Dredge, L. A., Grunsky, E., & Pehrsson, S. (2016). Till Geochemistry in West-Central Manitoba: Interpretation of Provenance and Mineralization Based on Glacial History and Multivariate Data Analysis. Isabelle McMartin Lynda A. Dredge Eric Grunsky Sally Pehrsson; Economic Geology (2016) 111 (4): 1001-1020. DOI: <https://doi.org/10.2113/econgeo.111.4.1001>
- Mellinger, M. (1987). Multivariate data analysis: its methods. Chemometrics and Intelligent Laboratory Systems, 2(1-3), 29-36.
- Morse, J. W., & Mackenzie, F. T. (1990). Geochemistry of sedimentary carbonates (Vol. 48). Elsevier.
- Netterville, J.A. (1974): Quaternary stratigraphy of the lower Gods River region, Hudson Bay Lowlands, Manitoba; unpublished M.Sc. thesis, Department of Geology, University of Calgary, Calgary, Alberta.
- Nicolas, M. P. B., & Young, G. A. (2014). Reconnaissance field mapping of Paleozoic rocks along the Churchill River and Churchill coastal area, northeastern Manitoba (parts of NTS 54E, L, K). Report of Activities, 148-160.
- Nielsen, E. (2001). Quaternary stratigraphy, till provenance and kimberlite indicator mineral surveys along the lower Hayes River. Report of Activities 2001. Manitoba Industry Trade and Mines. Manitoba Geological Survey: 121-125.
- Nielsen, E. (2002b). Quaternary stratigraphy and ice-flow history along the lower Nelson, Hayes, Gods and Pennycutaway rivers and implications for diamond exploration in northeastern Manitoba; in Report of Activities 2002, Manitoba Industry Trade and Mines. Manitoba Geological Survey (ed.), p. 209-215.
- Nielsen, E., & Dredge, L. A. (1982). Quaternary stratigraphy and geomorphology of a part of the lower Nelson River; Geological Association of Canada–Mineralogical Association of Canada, Joint Annual Meeting, Field Trip Guidebook 5.
- Nielsen, E., Morgan, A. V., Morgan, A., Mott, R. J., Rutter, N. W., & Causse, C. (1986). Stratigraphy, paleoecology, and glacial history of the Gillam area, Manitoba. Canadian Journal of Earth Sciences, 23(11), 1641-1661.
- Nikkarinen, M., Kallio, E., Lestinen, P. & Äyräs, M. (1984). Mode of occurrence of copper and zinc in till over three mineralized areas in Finland. Journal of Geochemical Exploration, 21, 239–247.
- Palarea-Albaladejo, J., & Martín-Fernández, J. A. (2015). ZCompositions — R package for multivariate imputation of left-censored data under a compositional approach. Chemometrics and Intelligent Laboratory Systems, 143, 85-96. doi:10.1016/j.chemolab.2015.02.019



- Parent, M., Paradis, S. J., & Boisvert, É. (1995). Ice-flow patterns and glacial transport in the eastern Hudson Bay region: implications for the late Quaternary dynamics of the Laurentide Ice Sheet. *Canadian Journal of Earth Sciences*, 32(12), 2057-2070.
- Pawłowsky-Glahn, V., & Egozcue, J. J. (2006). Compositional data and their analysis: an introduction. Geological Society, London, Special Publications, 264(1), 1-10.
- Peck, D.C., Hulbert, L., Scoates, R.F.J., Syme, E.C., and Theyer, P. (1999). The Fox River Belt project (parts of NTS 53M/16 and 53N/13); in Report of Activities, 1999, Manitoba Industry, Trade and Mines, Geological Services, p. 44-45.
- Peck, D.C., Potter, L., Desharnais, G., Scoates, R.F.J., Corkery, M.T. and Böhm, Ch.O. (2000). Geology of the western part of the Fox River Belt (parts of NTS 53M and 53N); in Report of Activities 2000, Manitoba Industry, Trade and Mines, Manitoba Geological Survey, p. 38-41.
- Piercey, S. J. (2014). Modern Analytical Facilities 2. A review of quality assurance and quality control (QA/QC) procedures for lithochemical data. *Geoscience Canada*, 41(1), 75-88.
- Plouffe, A., Anderson, R. G., Gruenwald, W., Davis, W. J., Bednarski, J. M., & Paulen, R. C. (2011). Integrating ice-flow history, geochronology, geology, and geophysics to trace mineralized glacial erratics to their bedrock source: An example from south-central British Columbia 1 This article is one of a series of papers published in this Special Issue on the theme of New insights in Cordilleran Intermontane geoscience: reducing exploration risk in the mountain pine beetle-affected area, British Columbia. 2 Earth Sciences Sector Contribution Number: 20100079. *Canadian Journal of Earth Sciences*, 48(6), 1113-1129.
- Prest, V. K., Donaldson, J. A., & Mooers, H. D. (2000). The omar story: the role of omars in assessing glacial history of west-central North America. *Géographie physique et Quaternaire*, 54(3), 257-270.
- Refsnider, K. A., & Miller, G. H. (2013). Ice-sheet erosion and the stripping of Tertiary regolith from Baffin Island, eastern Canadian Arctic. *Quaternary Science Reviews*, 67, 176-189.
- Rinne, M.L. (2016) Geological compilation of the Fox River belt, Manitoba; Manitoba Growth, Enterprise and Trade, Manitoba Geological Survey, Manitoba Mining and Minerals Convention 2016, Winnipeg, Manitoba, November 16–18, 2016, poster presentation.
- Rose, A.W., Hawkes, H.E. and Webb, J.S. (1979). *Geochemistry in Mineral Exploration* Academic Press, New York, N.Y.
- Ross, M., Lajeunesse, P., & Kosar, K. G. (2011). The subglacial record of northern Hudson Bay: insights into the Hudson Strait Ice Stream catchment. *Boreas*, 40(1), 73-91.
- Roy, M. (1998): Pleistocene stratigraphy of the lower Nelson River area-implications for the evolution of the Hudson Bay Lowland of Manitoba, Canada; M.Sc. thesis, University of Quebec, Montreal, 220 p

- Roy, M., Hemming, S. R., & Parent, M. (2009). Sediment sources of northern Quebec and Labrador glacial deposits and the northeastern sector of the Laurentide Ice Sheet during ice-rafting events of the last glacial cycle. *Quaternary Science Reviews*, 28(27), 3236-3245.
- Salminen, R., Batista, M. J., Bidovec, M., Demetriades, A., De Vivo, B., De Vos, W., ... & Heitzmann, P. (2005). *Geochemical atlas of Europe, part 1, background information, methodology and maps*. Geological survey of Finland.
- Salmirinne, H., Turunen, P., & Sarapää, O. (2012, May). On prospecting for REE in the Tana Belt, Northern Finland. In *Current Research: GTK Mineral Potential Workshop*, Kuopio (pp. 152-155).
- Sanford, R. F., Pierson, C. T., & Crovelli, R. A. (1993). An objective replacement method for censored geochemical data. *Mathematical Geology*, 25(1), 59-80. doi:10.1007/bf00890676
- Scoates, R.F.J. (1981). *Volcanic rocks of the Fox River Belt, northeastern Manitoba*; Manitoba Energy and Mines, Geological Services, Geological Report GR81-1, 109 p. Scoates, R.F.J. 1990: *The Fox River sill: a major stratiform intrusion*; Manitoba Energy and Mines, Geological Services, Geological Report GR82-3, 192 p.
- Scoates, R.F.J. (1990). *The Fox River sill: a major stratiform intrusion*; Manitoba Energy and Mines, Geological Services, Geological Report GR82-3, 192 p.
- Scott, C., & Lyons, T. W. (2012). Contrasting molybdenum cycling and isotopic properties in euxinic versus non-euxinic sediments and sedimentary rocks: Refining the paleoproxies. *Chemical Geology*, 324, 19-27.
- Shilts, W. W. (1982). Quaternary evolution of the Hudson/James Bay region. *Le naturaliste Canadien*, 109, 309-332.
- Shilts, W.W. (1995). Geochemical partitioning in till. in: Bobrowsky, P.T., Sibbick, S.J., Newell, J.M., Matysek, P.F. (eds.) *Drift exploration in the Canadian Cordillera*. British Columbia Ministry of Energy, Mines and Petroleum Resources, Paper 1995-2, pages 149-163.
- Skinner, R.G. (1973). Quaternary stratigraphy of the Moose River Basin, Ontario; Geological Survey of Canada, *Bulletin 225*, 77p.
- Stanley, C. R. (2003). Thplot. M: a matlab function to implement generalized Thompson–Howarth error analysis using replicate data. *Computers & Geosciences*, 29(2), 225-237.
- Tan, P., Steinbach, M., & Kumar, V. (2005). *Introduction to data mining*. Boston: Pearson Addison Wesley.
- Thompson, M., & Howarth, R. J. (1978). A new approach to the estimation of analytical precision. *Journal of Geochemical Exploration*, 9(1), 23-30.
- Thorleifson, L., Wyatt, P., Shilts, W., & Nielsen, E. (1992). Hudson Bay lowland Quaternary stratigraphy: Evidence for early Wisconsinan glaciation centered in Quebec. *Geological Society of America Special Papers. The Last Interglacial- Glacial Transition in North America*, 207-222.

- Trommelen, M.S. (2013): Preliminary Quaternary geology in the Gillam area, northeastern Manitoba (parts of NTS 54D5–9, 11, 54C12); in Report of Activities 2013, Manitoba Mineral Resources, Manitoba Geological Survey, p. 169–182.
- Trommelen, M.S. (2012). Quaternary geology of the Knee Lake area, northeastern Manitoba (NTS 53L14, 15, 53M1, 2); in Report of Activities 2012, Manitoba Innovation, Energy and Mines, Manitoba Geological Survey, p. 178–188.
- Trommelen, M.S., Wang, Y. & Ross, M. (2014). Preliminary Quaternary geology in the Gillam area, northeastern Manitoba (parts of NTS 54D5–11, 54C12) – Year Two; in Report of Activities 2014, Manitoba Mineral Resources, Manitoba Geological Survey, p. 187–195.
- Veillette, J. J., Dyke, A. S., & Roy, M. (1999). Ice-flow evolution of the Labrador Sector of the Laurentide Ice Sheet: a review, with new evidence from northern Quebec. *Quaternary Science Reviews*, 18(8-9), 993-1019.
- Vu, V. Q. (n.d.). Ggbiplot. Retrieved January 16, 2016, from <https://www.rdocumentation.org/packages/ggbiplot/versions/0.55/topics/ggbiplot>
- Weltje, G. J., & von Eynatten, H. (2004). Quantitative provenance analysis of sediments: review and outlook. *Sedimentary Geology*, 171(1), 1-11.

## Appendix A

### R code

“mydata” refers to the dataset which is being analyzed in R

#### **Hierarchical cluster analysis:**

(<http://www.statmethods.net/advstats/cluster.html>)

```
d <- dist(mydata, method = "euclidean")
```

```
fit <- hclust(d, method="ward") (if not clarify, R default run the  
analysis based on complete linkage)
```

```
plot(fit)
```

```
groups <- cutree(fit, k=5)
```

```
rect.hclust(fit, k=5, border="red")
```

#### **K-means method:** (<http://www.statmethods.net/advstats/cluster.html>)

```
wss <- (nrow(mydata)-1)*sum(apply(mydata, 2, var)
```

```
for (I in 2:20)+wss[i] <-
```

```
sum(kmeans(mydata,centres=I,nstart=100,iter.max=1000)$withinss)
```

```
plot(1:20,wss,type="b",xlab="Number of clusters",ylab="within groups  
sum of squares")
```

```
mydata.pca=prcomp(mydata,centre=TRUE, scale.=TRUE)
```

```
plot(mydata.pca, type="l")
```

```
comp <- data.frame(mydata.pca$x[,1:4])
```

```
k=kmeans(comp, 14,nstart=100,iter.max=1000)
```

```
library(RColorBrewer)
```

```
library(scales)
```

```
palette(alpha(brewer.pal(9,"set1"),0.5)
```

```
plot(comp,col=k$cluster,pch=16)
```

```
text(comp$PC1,comp$PC2+0.3,label="'",cex=0.4,col=k$cluster)
```

### **Principal component analysis:**

```
ggbiplot :( http://www.r-bloggers.com/using-r-two-plots-of-principal-component-analysis/)
```

```
library(ggbiplot)
```

```
mydata <- read.csv("~/Desktop/section_groups_sequence_selected.csv")
```

```
selected=scale(section_groups_sequence_selected[,2:24])
```

```
selectedpca=prcomp(selected,centre=TRUE, scale. = TRUE)
```

```
plot(selectedpca,type="l")
```

```
mygroup = c(rep("group 1", 8), rep("group 2", 6), rep("group 3", 24),  
rep("group 6", 18), rep("group 7", 12), rep("group 8", 19), rep("group 9",  
19), rep("group 11", 6), rep("group 12",7))
```

```
ggbiplot(selectedpca,choices=c(1,2), cex = 0.5, groups = mygroup)
```

```
ggbiplot(selectedpca,choices=c(1,3), cex = 0.5, groups = mygroup)
```

```
ggbiplot(selectedpca,choices=c(2,3), cex = 0.5, groups = mygroup)
```

```
library(reshape2)
```

```
library(ggplot2)
```

```
data=matrix(nrow=length(mygroup),ncol=119)
```

```
scores=data.frame(mygroup,selectedpca$x[,1:3])
```

```
PC1.2=qplot(x=PC1,y=PC2,data=scores,colour=factor(mygroup))+them  
e(legend.position="none")
```

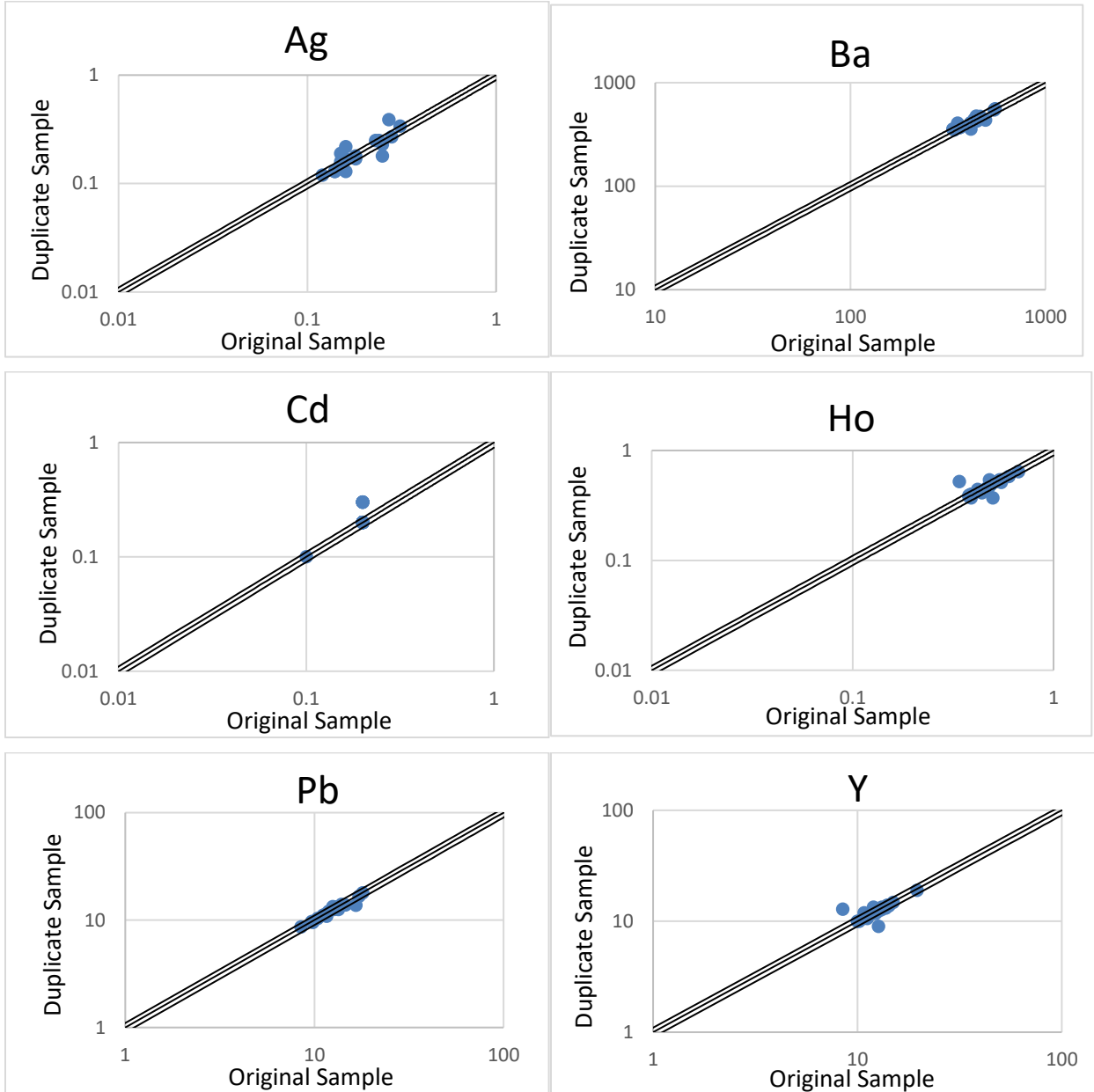
```
PC1.3=qplot(x=PC1,y=PC3,data=scores,colour=factor(mygroup))+them  
e(legend.position="none")
```

```
PC2.3=qplot(x=PC2,y=PC3,data=scores,colour=factor(mygroup))+them  
e(legend.position="none")
```

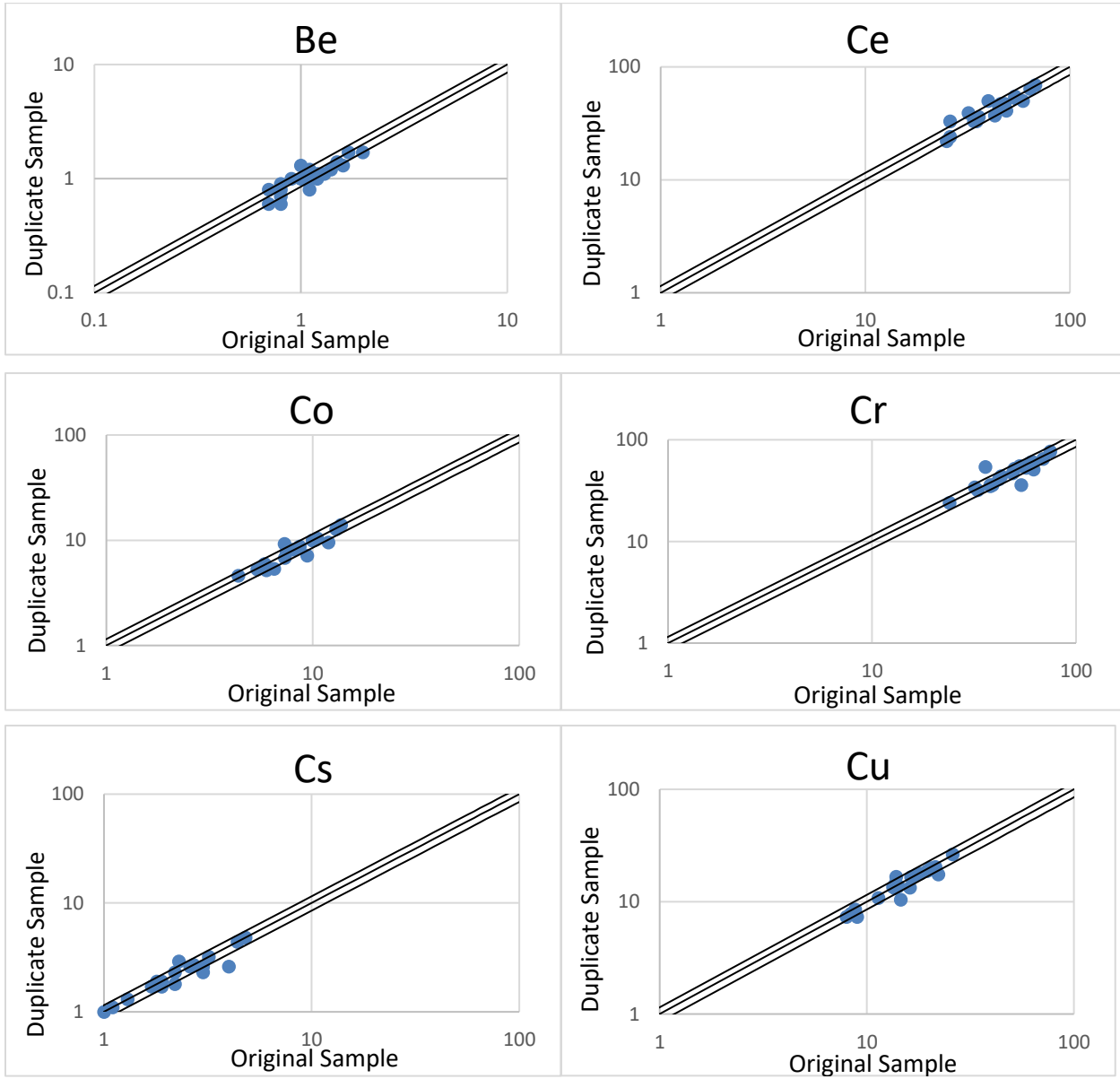
```
print(PC1.2)
print(PC1.3)
print(PC2.3)
name.groups=names(section_groups_sequence_selected[,2:24])
melted=cbind(name.groups,melt(selectedpca$rotation[,1:4]))
barplot <- ggplot(data=melted) +geom_bar(aes(x=Var1, y=value,
fill=name.groups),stat="identity") +
  facet_wrap(~Var2)
print(barplot)
```

## Appendix B

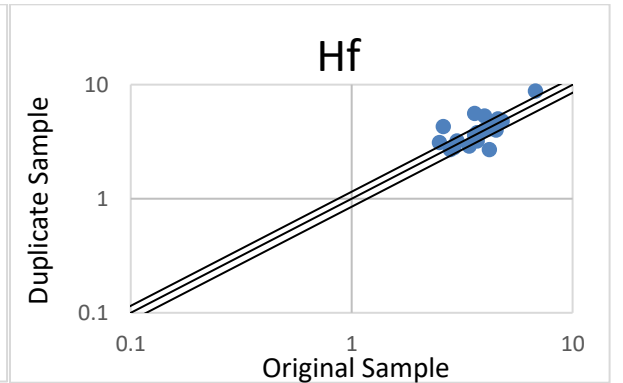
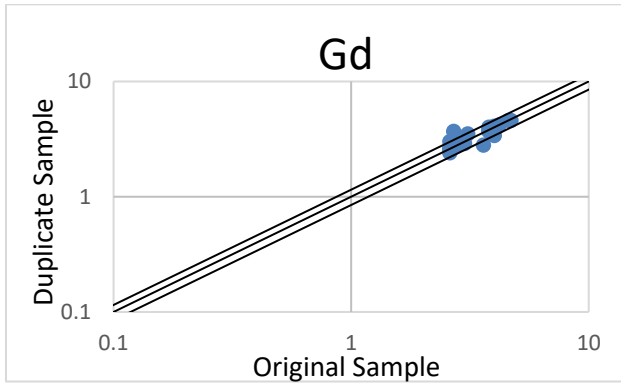
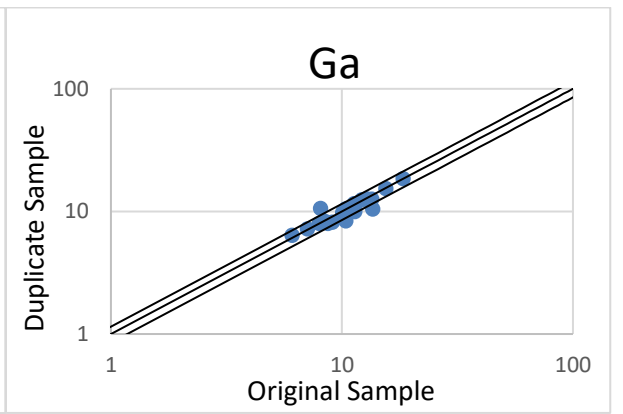
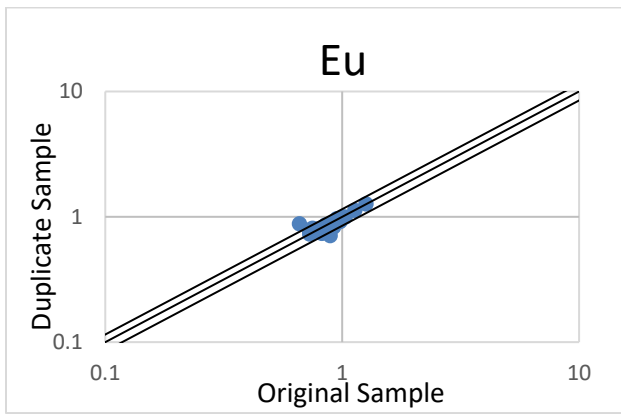
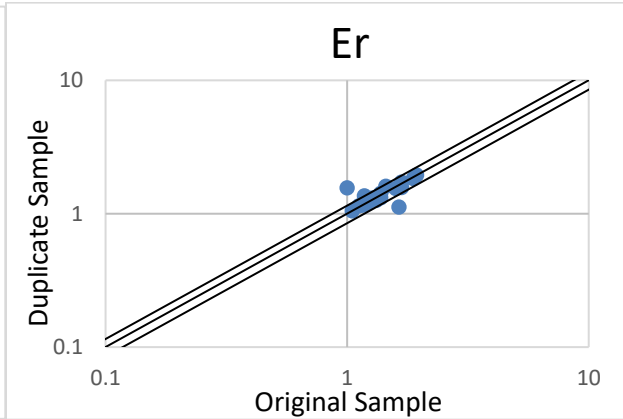
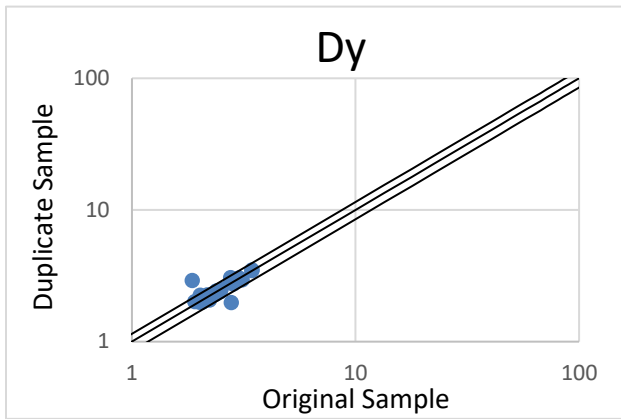
Trace elements: precision 10%

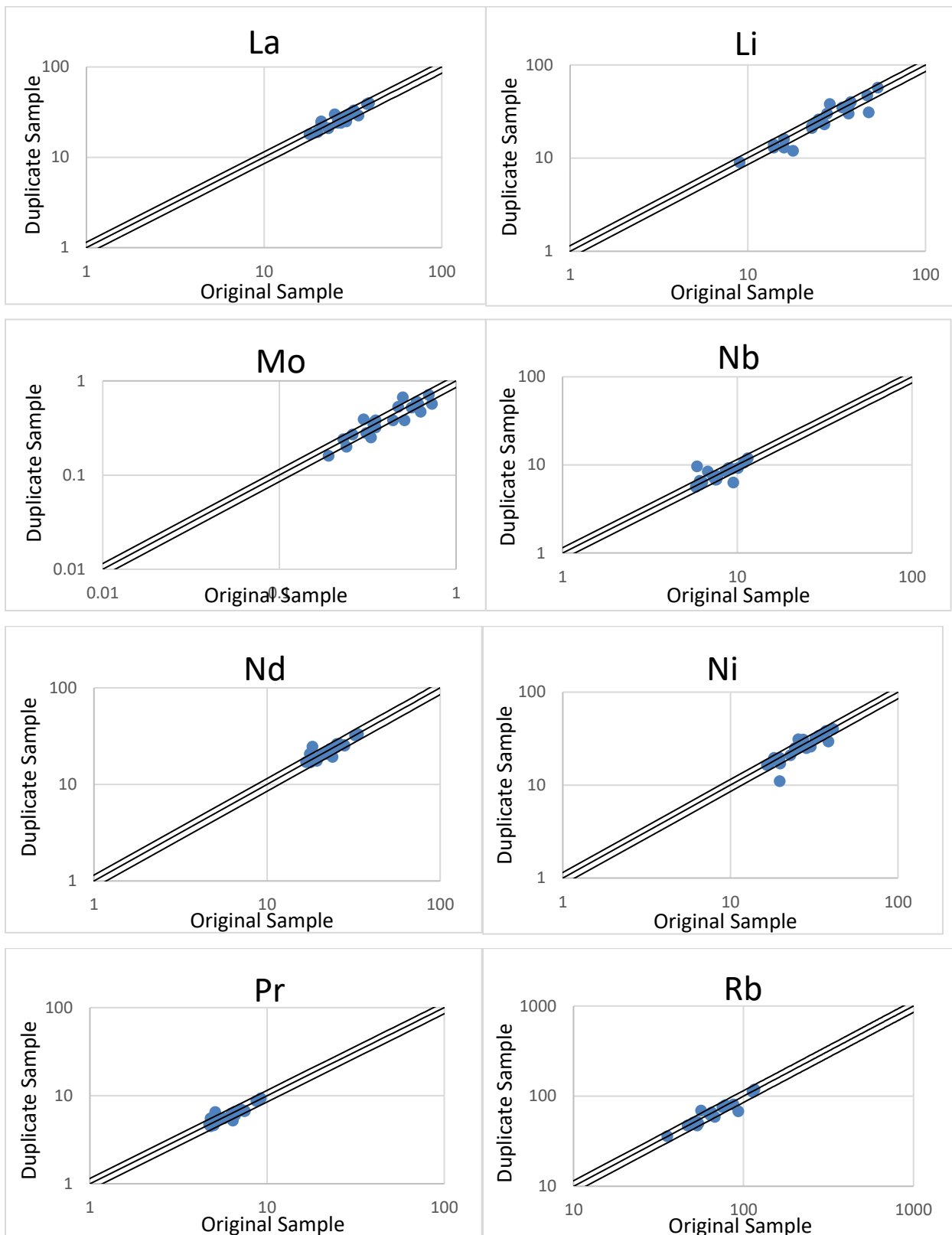


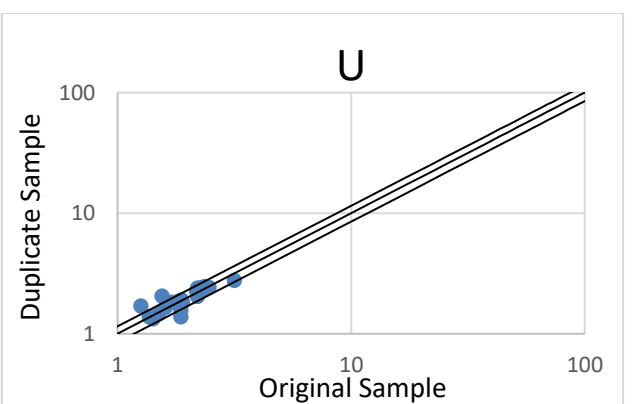
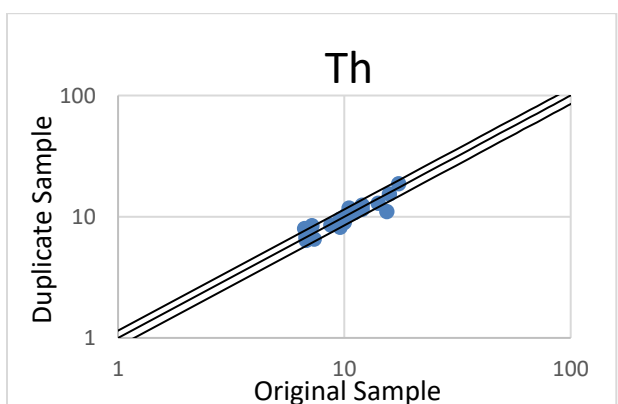
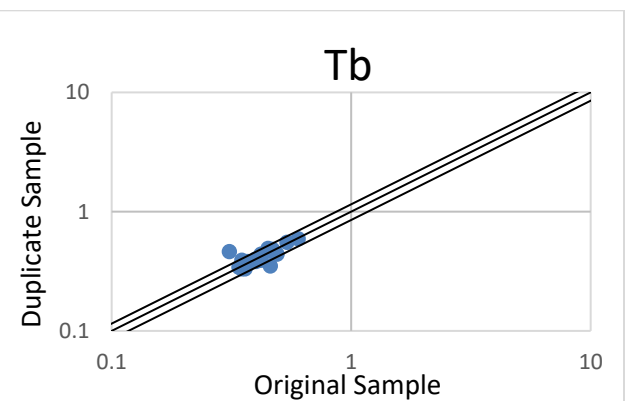
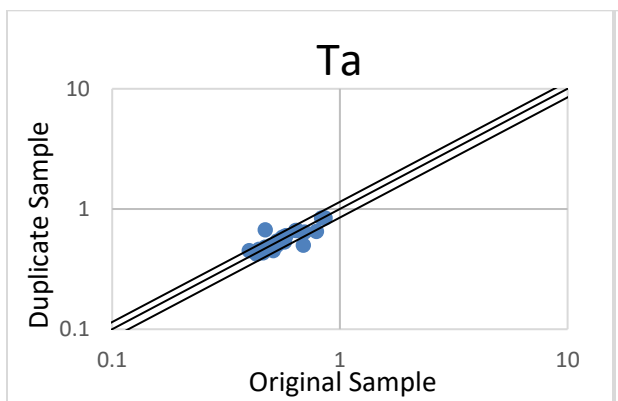
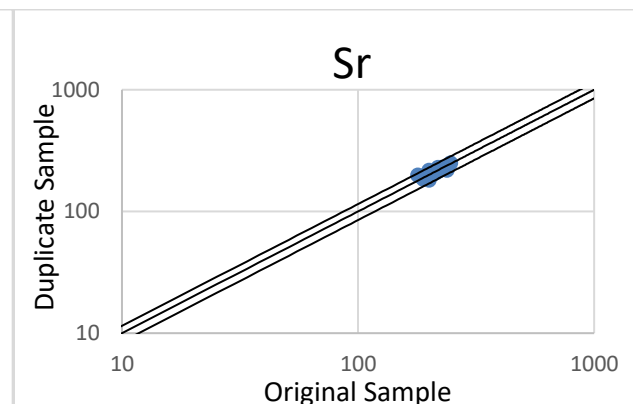
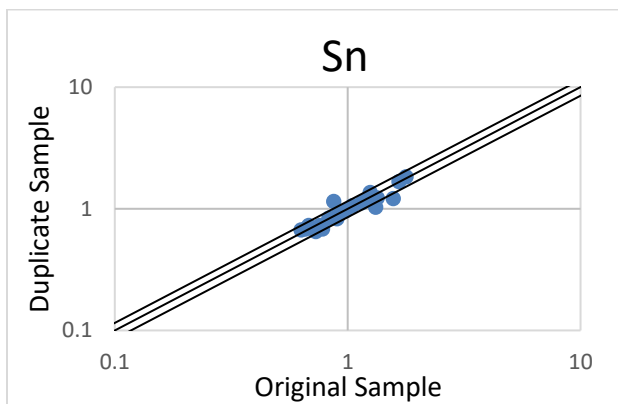
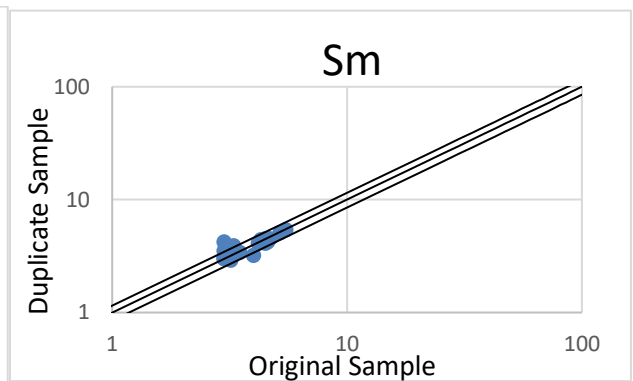
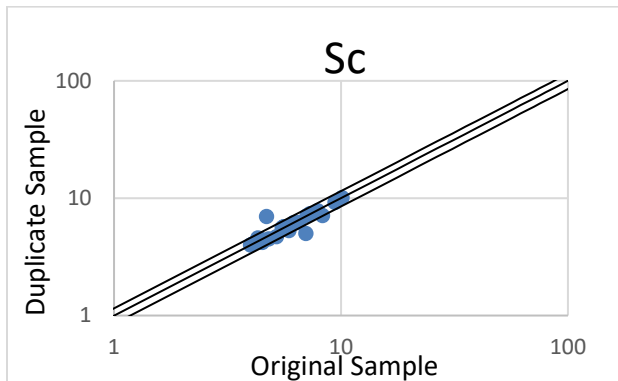
Trace elements: precision 15%

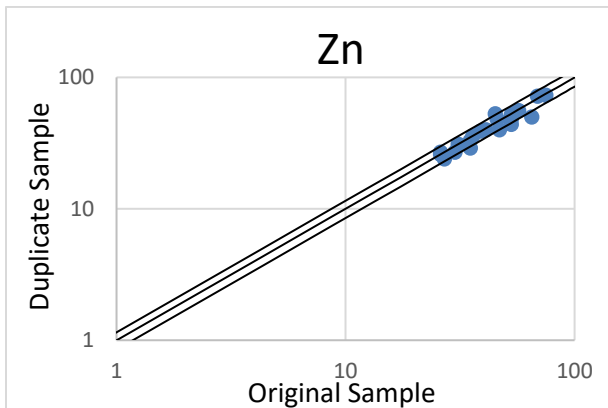
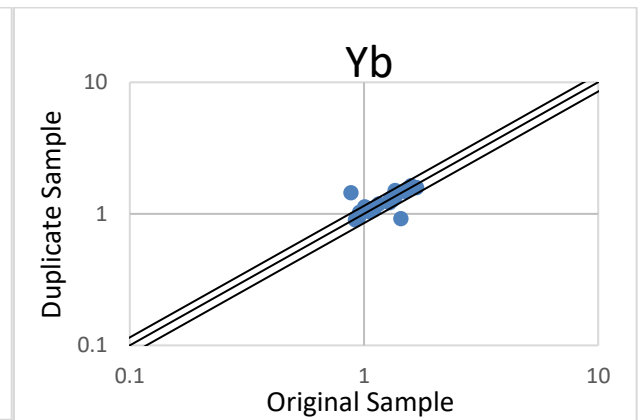
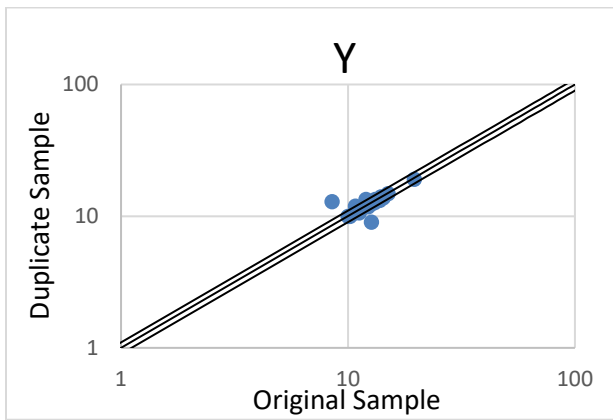
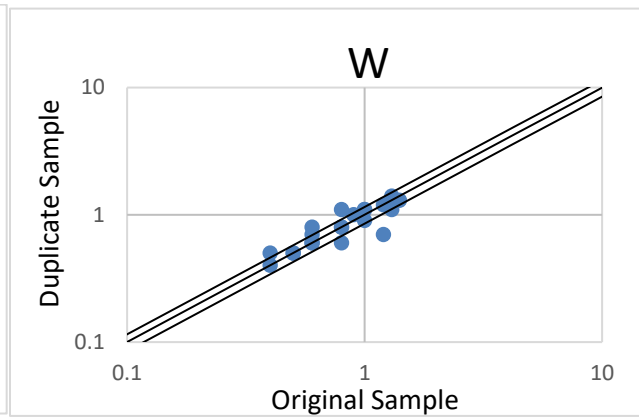
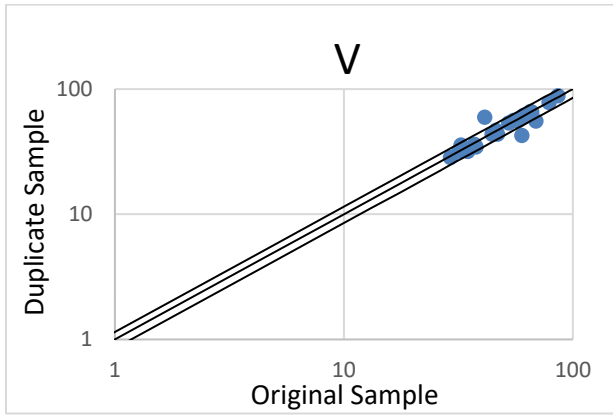




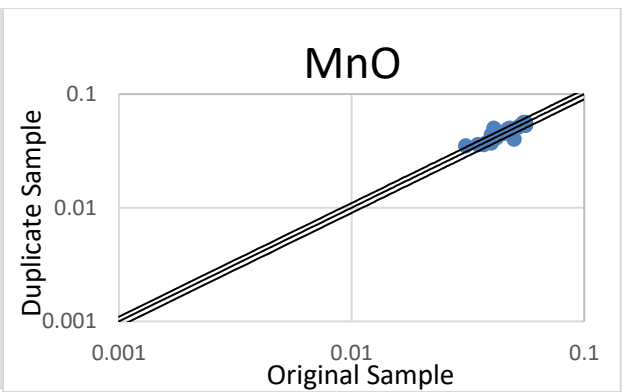
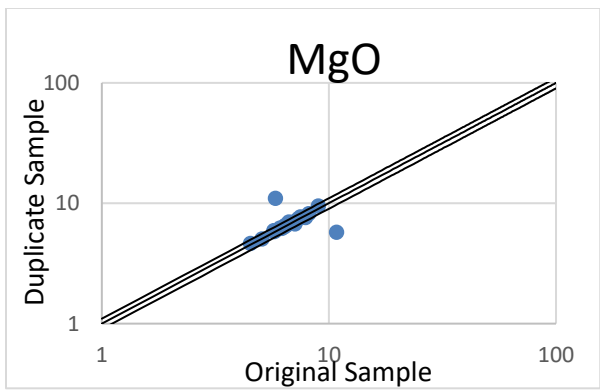
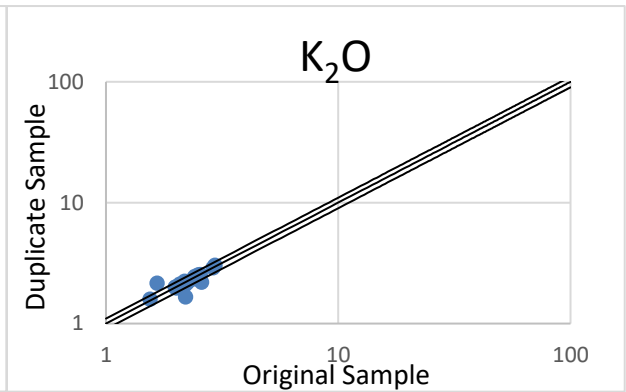
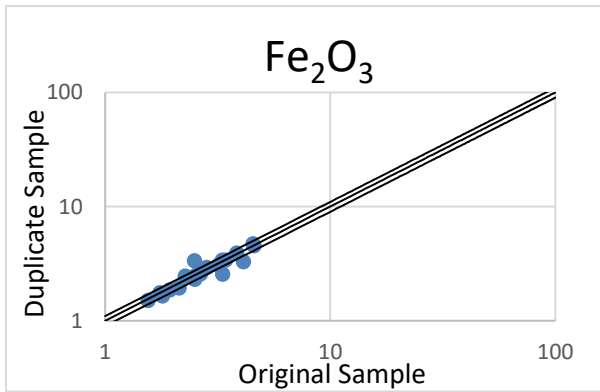
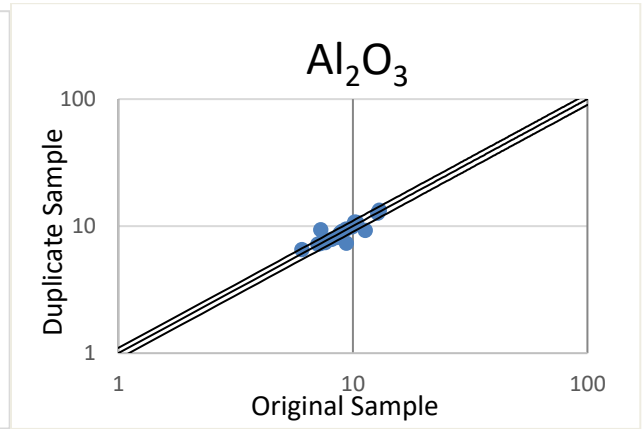
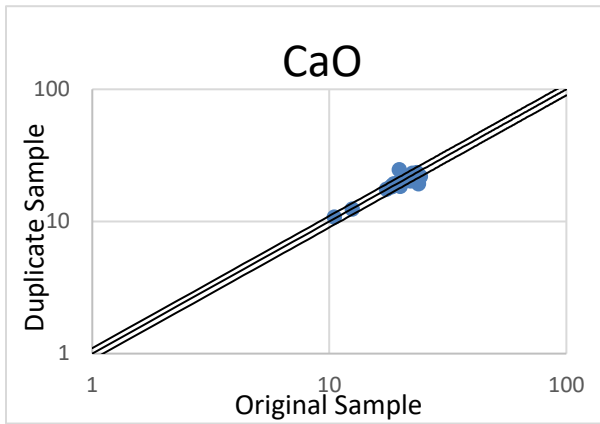


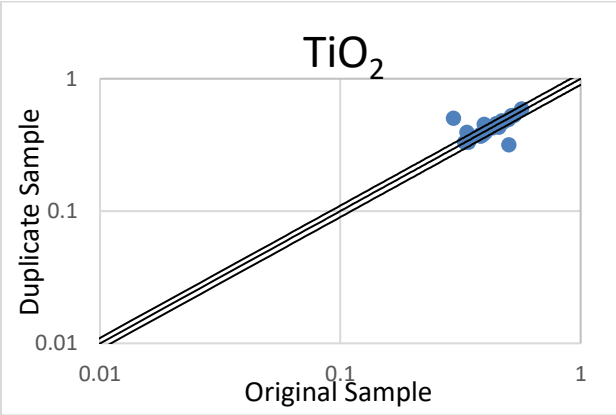
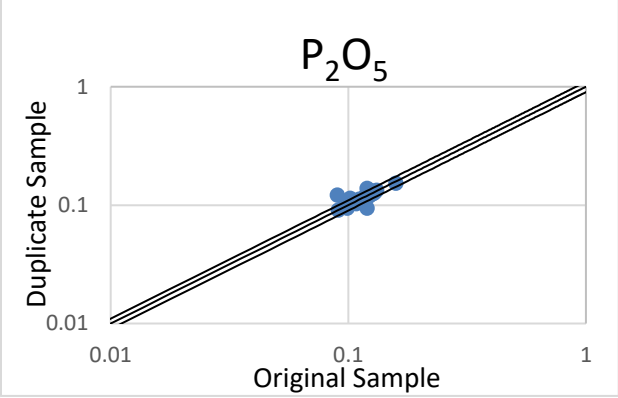
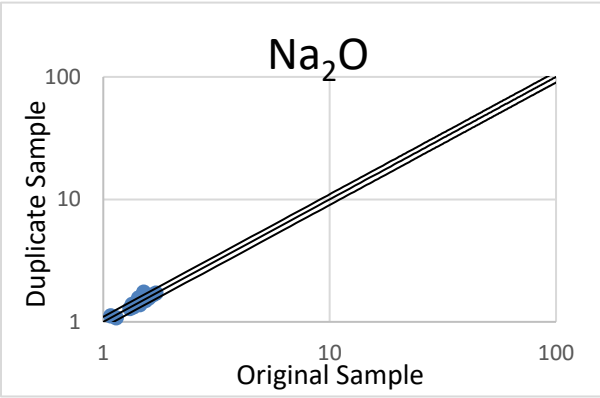




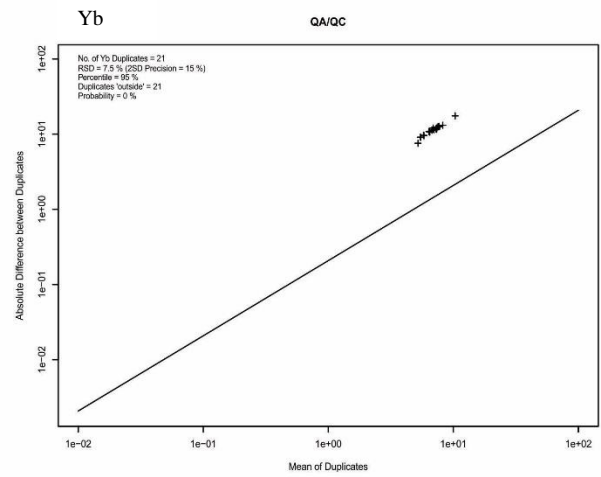
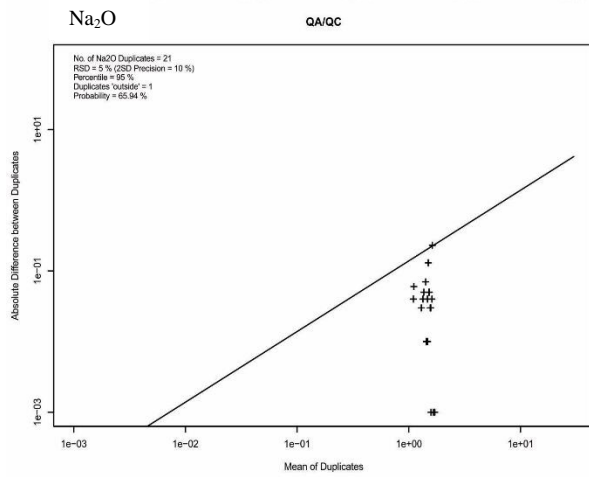
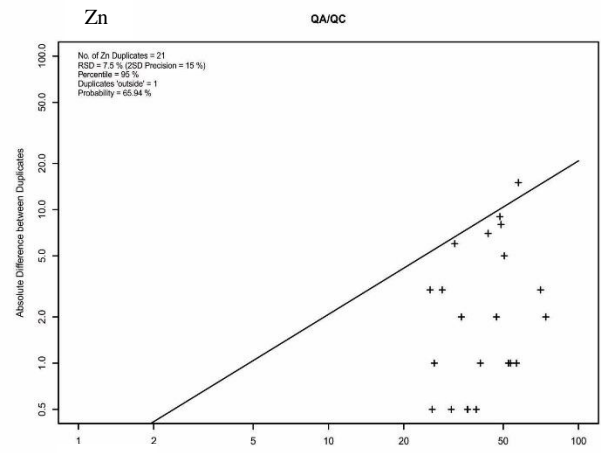
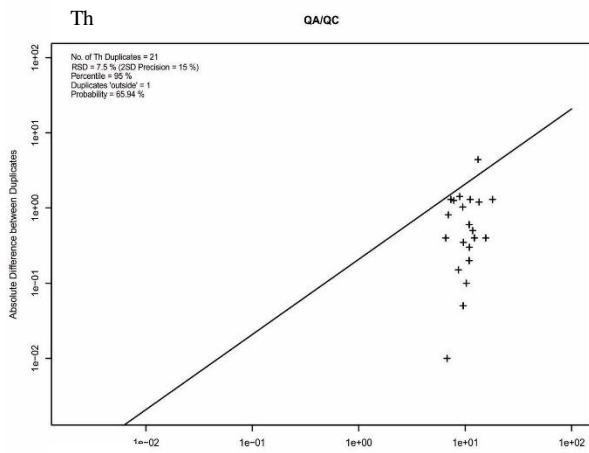
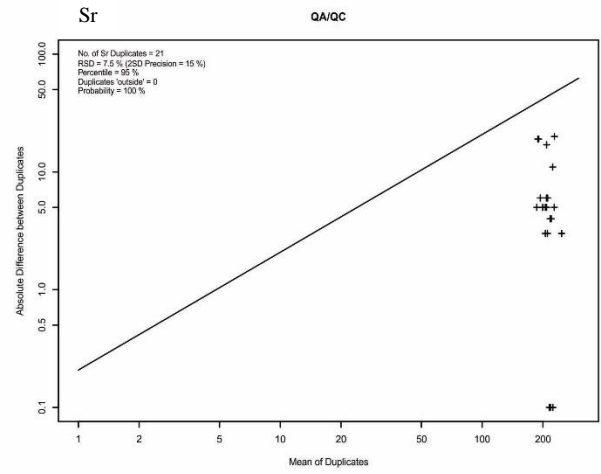
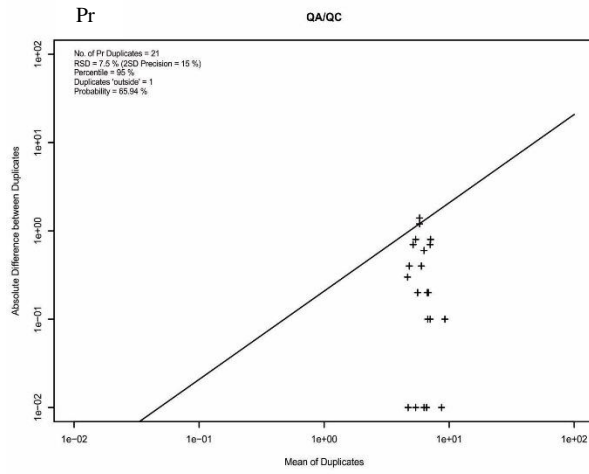


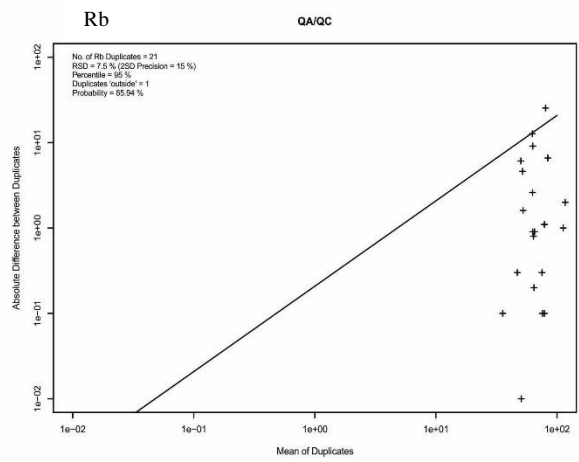
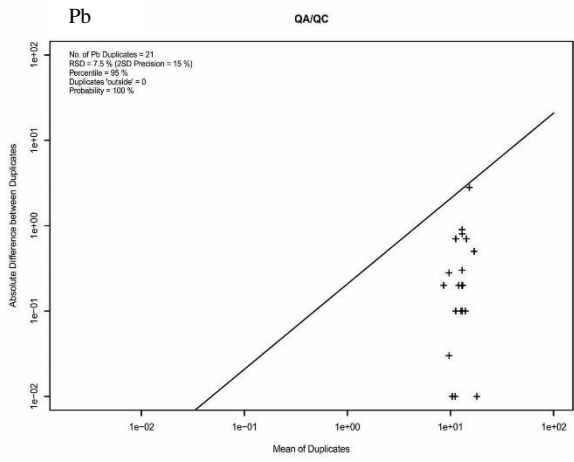
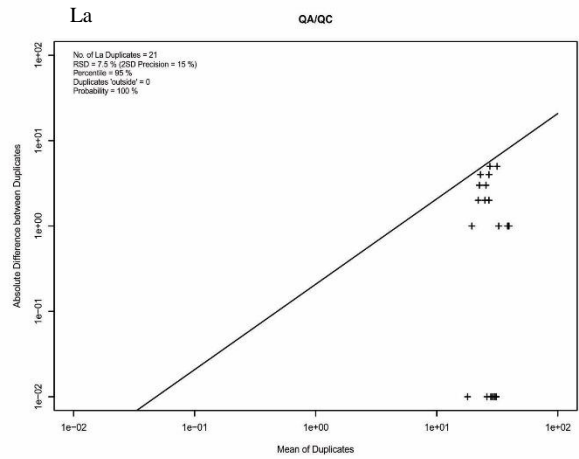
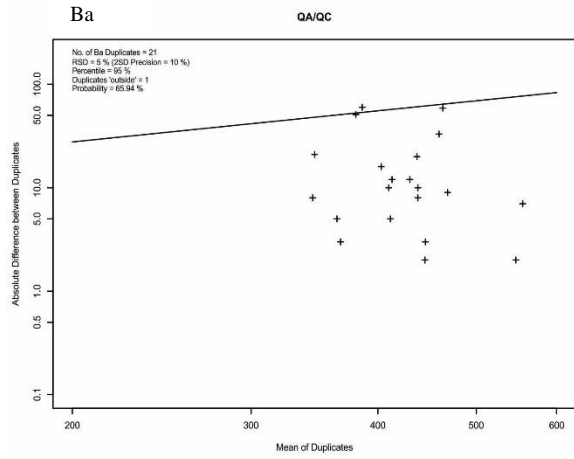
Major elements: precision 10%





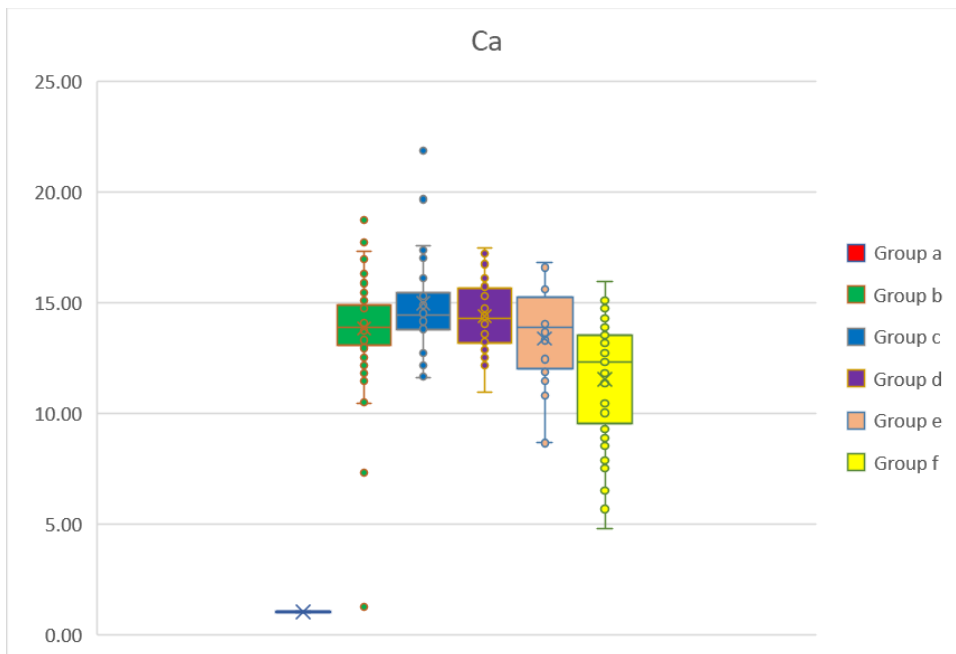
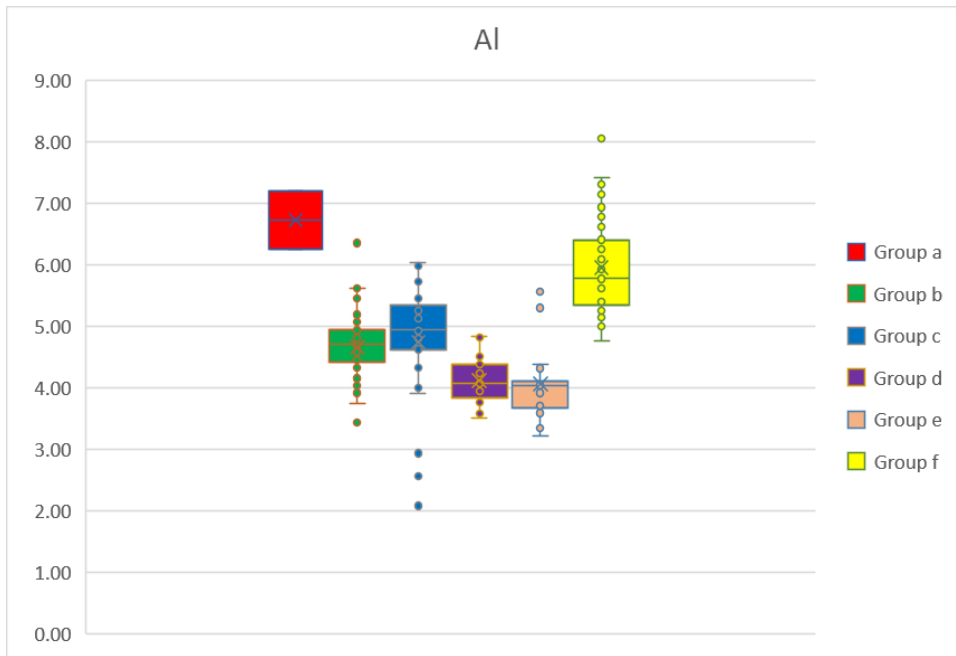
# Appendix C Examples for Thompson-Howarth Plot

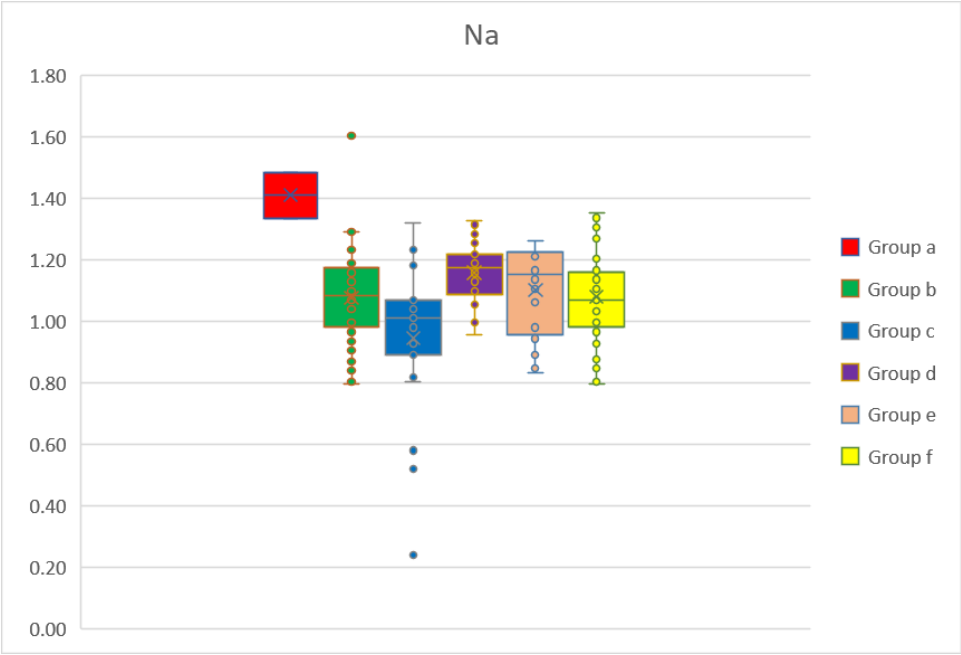
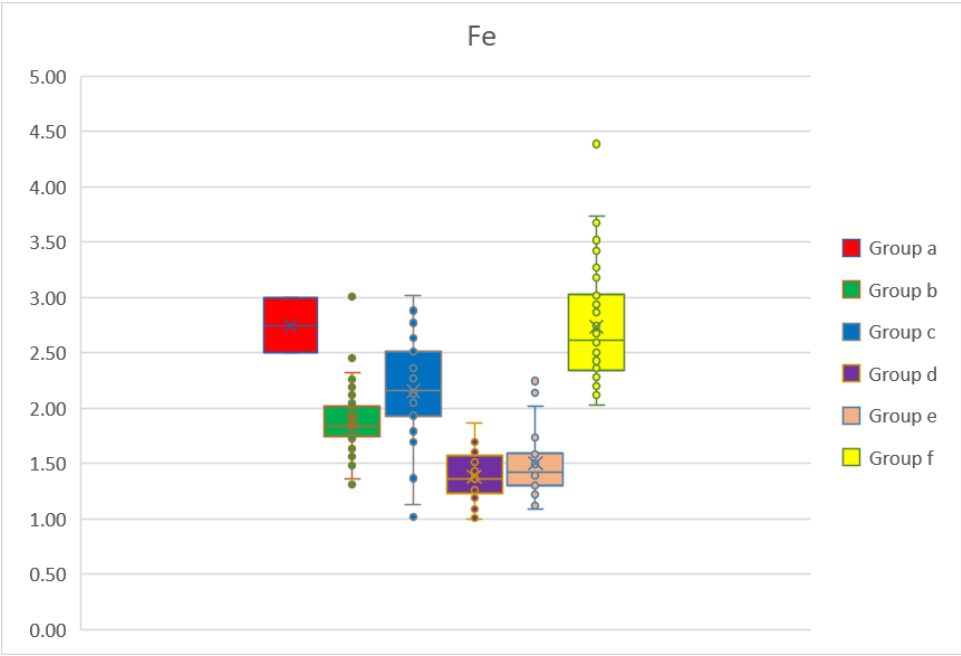


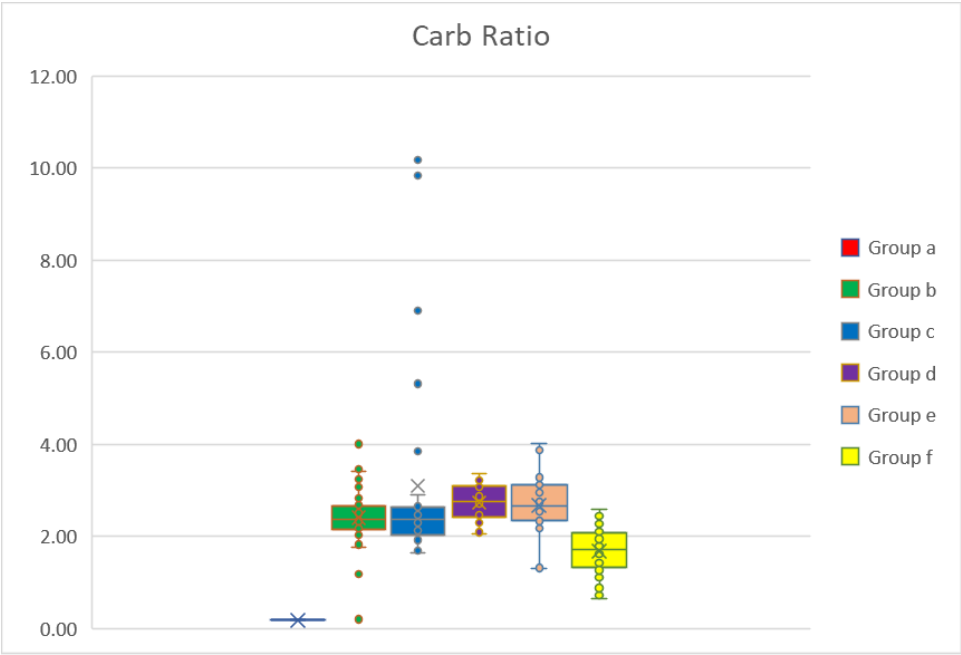
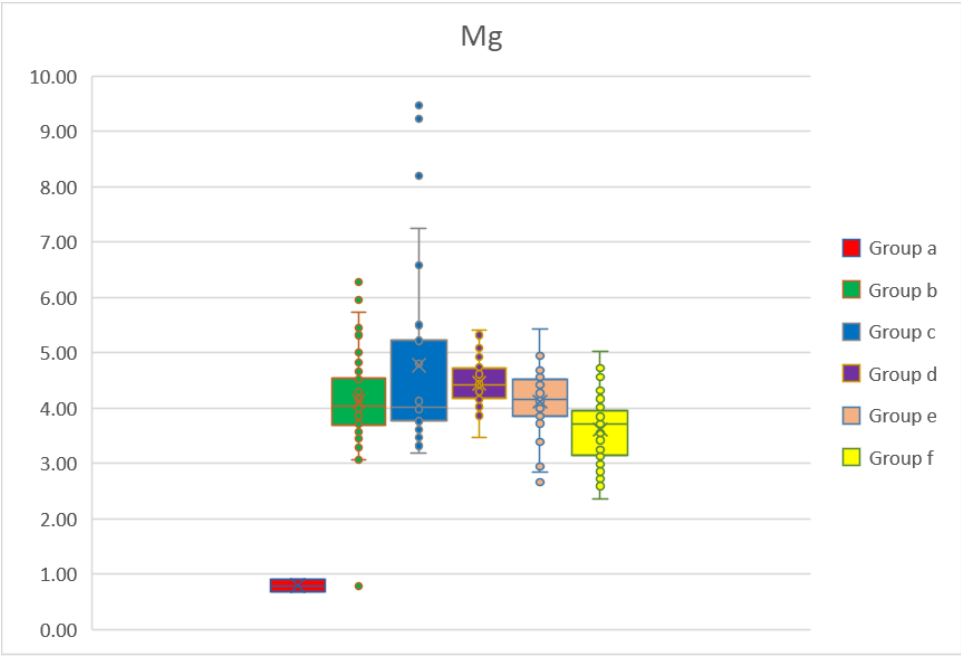


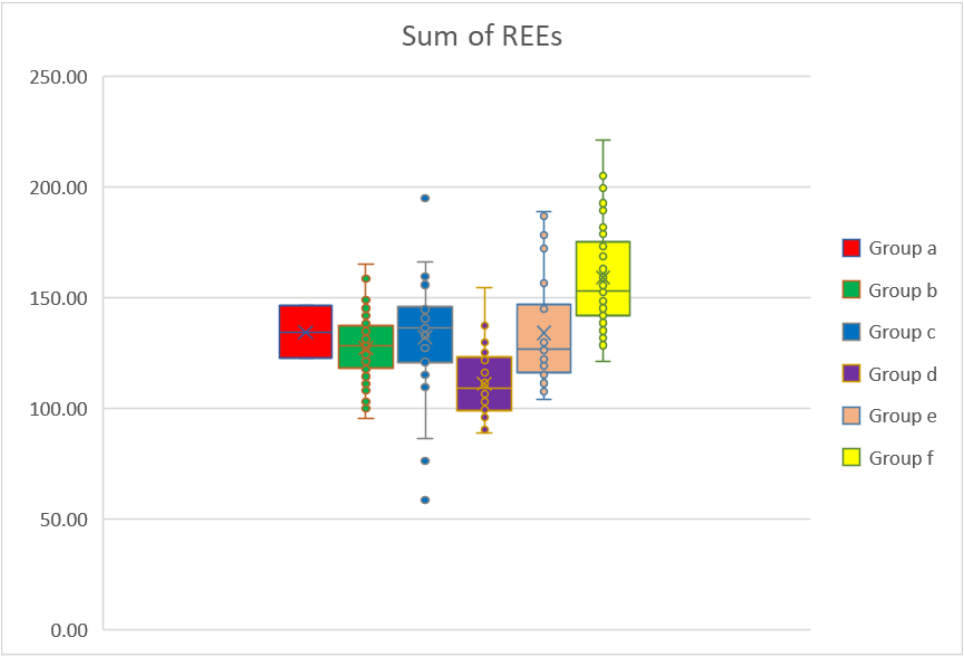


## Appendix D Boxplots of some elements









## Appendix E

Sample no.	Al <sub>2</sub> O <sub>3</sub> (%)	CaO (%)	Fe <sub>2</sub> O <sub>3</sub> (%)	K <sub>2</sub> O (%)	MgO (%)	MnO (%)	Na <sub>2</sub> O (%)
13115 MT206B01	7.39	19.80	1.90	1.92	6.21	0.04	1.44
13115 MT211B01	8.87	18.40	2.60	2.27	6.00	0.05	1.57
13115 MT217B01	6.47	23.00	1.87	1.75	10.40	0.04	1.07
13115 MT217B02	9.80	19.70	3.08	2.49	8.16	0.05	1.35
13115 MT221B01	6.96	21.60	1.85	1.87	8.82	0.03	1.29
13115 MT225A01	8.04	19.20	2.61	1.98	5.88	0.04	1.29
13115 MT225A02	7.55	19.60	2.33	1.99	7.28	0.05	1.31
13115 MT225A03	7.06	22.20	1.94	1.89	9.07	0.04	1.16
13115 MT227A01	12.70	16.50	4.68	2.76	4.84	0.06	1.08
13115 MT227A02	7.55	22.30	2.23	2.06	8.33	0.04	1.22
13115 MT227A03	6.85	20.00	1.90	1.70	7.19	0.04	1.28
13115 MT227A04	7.65	19.80	2.27	1.85	6.41	0.04	1.27
13115 MT227B01	6.34	23.20	1.79	1.68	8.25	0.04	1.12
13115 MT227B02	6.77	21.80	2.01	1.79	6.56	0.04	1.21
13115 MT227C01	8.56	18.90	2.50	2.10	5.07	0.05	1.47
13115 MT233B01	9.27	17.50	2.54	2.28	5.09	0.05	1.74
13115 MT235A01	10.60	14.00	3.58	2.34	4.44	0.05	1.62
13115 MT238B01	8.17	19.00	2.28	2.03	5.53	0.04	1.46
13115 MT239B01	10.60	10.20	3.50	2.44	5.28	0.04	1.69
13115 MT241B01	8.15	19.10	2.14	2.06	6.17	0.04	1.57
13115 MT242A01	7.72	16.00	2.26	1.93	6.78	0.04	1.66
13115 MT248C01	7.76	19.60	1.99	2.00	7.22	0.04	1.70
13115 MT250B01	7.57	19.90	2.15	1.86	6.84	0.04	1.53
13115 MT256B01	6.99	17.40	1.87	1.80	6.92	0.03	1.57

13115 MT259A01	9.02	18.60	2.82	2.18	6.16	0.05	1.60
13115 MT268B01	8.73	20.20	2.42	2.19	6.66	0.05	1.61
13115 MT272B01	6.97	22.00	1.74	1.85	7.56	0.04	1.53
13115 MT276A01	9.00	21.50	2.92	2.25	6.03	0.04	1.27
13115 MT277A01	9.93	20.60	3.42	2.37	6.20	0.05	1.31
13115 MT281B01	8.41	19.20	2.60	2.05	6.32	0.05	1.36
13115 MT281C01	10.50	12.10	3.21	2.46	4.40	0.06	1.52
13115 MT284A01	9.05	18.60	2.64	2.24	6.24	0.04	1.57
13115 MT287A01	8.71	18.80	2.55	2.20	6.60	0.05	1.26
13115 MT287A02	8.91	18.30	2.65	2.22	6.52	0.06	1.54
13115 MT287A03	12.70	14.10	4.70	2.85	4.74	0.06	1.82
13115 MT 287 B01	11.30	19.10	3.84	2.78	6.19	0.05	1.53
13115 MT295B01	8.97	17.90	2.84	2.20	5.08	0.04	1.40
13115 MT298A01	7.39	19.30	1.74	1.93	7.07	0.04	1.63
13115 MT302B01	8.82	18.70	2.75	2.09	5.71	0.05	1.74
13115 MT302D01	9.39	20.10	2.96	2.28	6.25	0.05	1.58
13115 MT304B01	13.00	14.60	5.03	3.21	5.17	0.06	1.50
13115 MT306A01	9.45	18.70	3.14	2.48	6.48	0.05	1.32
13115 MT306B01	12.10	15.90	4.33	2.80	5.50	0.05	1.50
13115 MT309A01	7.63	21.80	1.94	2.02	7.84	0.04	1.59
13115 MT309B01	10.00	16.60	3.11	2.41	6.28	0.04	1.60
13115 MT311B01	9.77	21.10	3.37	2.37	7.82	0.05	1.32
13115 MT312A01	10.60	19.40	3.76	2.54	7.05	0.05	1.37
13115 MT312B01	7.70	19.90	2.29	2.35	6.50	0.05	1.13
13115 MT318A01	7.74	21.20	2.12	2.09	7.91	0.04	1.44
13115 MT319A01	8.38	21.40	2.52	2.11	7.06	0.04	1.50
13115 MT321A01	9.61	18.30	3.16	2.34	6.58	0.05	1.51

13115 MT321B01	7.62	20.80	2.46	1.90	8.40	0.04	1.17
13115 MT323B01	8.82	19.30	2.52	2.15	6.64	0.05	1.74
13115 MT333B01	13.70	12.50	5.25	3.18	5.38	0.06	1.32
13115 MT334A01	8.48	20.90	2.73	2.25	7.57	0.04	1.23
13115 MT335B01	8.05	19.80	2.37	2.33	6.74	0.05	1.26
13115 MT336B01	6.81	22.20	1.63	1.87	7.80	0.04	1.42
13115 MT336C01	9.36	19.90	2.82	2.46	7.90	0.04	1.36
13115 MT342A01	9.08	21.70	2.87	2.29	7.08	0.06	1.40
13115 MT348A01	8.70	19.40	2.65	2.11	6.11	0.05	1.54
13115 MT349B01	9.07	18.30	2.70	2.18	6.40	0.05	1.50
13115 MT355B01	8.69	18.70	2.34	2.05	5.92	0.04	1.61
14115 MT 001 A01	9.32	19.80	3.07	2.32	6.78	0.05	1.46
14115 MT 001 A02	10.60	19.80	3.65	2.52	6.22	0.06	1.34
14115 MT 001 A03	8.66	22.90	2.87	2.46	8.00	0.05	1.08
14115 MT 001 B01	9.45	18.40	3.26	2.34	5.44	0.05	1.09
14115 MT 001 B02	9.44	18.70	3.04	2.30	6.98	0.04	1.25
14115 MT 001 C01	6.31	23.50	1.60	1.58	8.99	0.04	1.20
14115 MT 001 D01	10.50	12.30	3.06	2.60	4.87	0.06	1.66
14115 MT 001 D02	10.00	12.10	2.88	2.52	4.72	0.06	1.66
14115 MT 002 A01	11.10	21.30	3.55	2.88	6.55	0.06	1.49
14115 MT 007 A01	7.28	23.40	1.75	1.99	8.16	0.04	1.48
14115 MT 008 B01	10.20	18.90	3.27	2.63	6.73	0.05	1.54
14115 MT 009 A01	7.39	24.20	2.13	1.99	7.50	0.04	1.51
14115 MT 012 A01	9.93	21.60	3.30	2.47	8.65	0.05	1.23
14115 MT 012 B01	8.84	22.50	3.05	2.23	9.12	0.05	1.25
14115 MT 012 B02	10.40	17.80	3.64	2.62	6.65	0.06	1.41
14115 MT 013 A01	7.29	24.40	1.88	2.06	7.93	0.04	1.43

14115 MT 020 A01	8.42	19.90	2.61	2.25	7.73	0.05	1.40
14115 MT 020 A03	9.71	20.00	3.21	2.51	7.30	0.04	1.34
14115 MT 020 B01	9.41	19.80	3.13	2.86	6.42	0.05	1.13
14115 MT 020 B02	9.87	20.80	3.31	2.62	7.56	0.05	1.35
14115 MT 020 B03	9.00	17.90	3.17	2.57	6.16	0.05	1.14
14115 MT 020 B04	9.85	18.00	3.29	2.86	6.30	0.05	1.18
14115 MT 021 B01	9.97	21.20	3.30	2.48	6.58	0.05	1.36
14115 MT 021 C01	8.35	22.20	2.60	2.06	7.31	0.05	1.35
14115 MT 022 A01	11.00	19.20	3.71	2.72	6.30	0.06	1.54
14115 MT 022 A02	7.79	21.40	2.34	2.09	8.29	0.04	1.32
14115 MT 022 B01	11.90	18.10	4.34	3.17	6.30	0.05	1.30
14115 MT 022 B02	11.80	17.50	4.31	3.42	5.81	0.06	1.14
14115 MT 023 A01	7.52	22.10	1.77	1.93	7.88	0.04	1.51
14115 MT 025 A01	7.16	24.10	1.84	1.90	7.09	0.03	1.52
14115 MT 027 A01	8.12	18.80	2.42	2.04	6.40	0.04	1.56
14115 MT 034 A01	13.00	10.50	4.54	2.95	4.52	0.05	1.54
14115 MT 035 A01	10.70	11.00	3.27	2.46	5.23	0.04	1.72
14115 MT 037 A01	7.65	18.80	2.21	1.94	6.74	0.04	1.65
14115 MT 047 A01	13.10	11.90	4.58	3.07	5.25	0.06	1.47
14115 MT 054 A01	10.80	18.40	3.41	2.55	6.22	0.05	1.44
14115 MT 055 A01	7.88	21.80	1.84	2.04	7.50	0.04	1.58
14115MT061A01	7.48	17.50	1.55	1.92	6.57	0.04	1.71
14115MT062A01	7.81	22.20	1.98	2.04	6.90	0.05	1.50
14115MT062A02	10.90	18.10	3.48	2.50	5.92	0.05	1.56
14115MT063A01	9.69	19.70	3.03	2.30	6.17	0.05	1.52
14115MT063A02	11.10	17.20	3.74	2.56	5.67	0.06	1.58
14115MT063A03	8.99	18.80	2.57	2.26	6.00	0.05	1.58



14115MT066A01	13.60	1.36	4.28	2.72	1.49	0.04	1.80
14115MT067A01	8.36	19.40	2.29	2.13	6.30	0.04	1.44
14115MT068A01	13.50	6.68	4.58	3.07	3.90	0.05	1.80
14115MT072A01	15.20	7.92	6.27	3.51	4.72	0.06	1.35
14115MT076A01	9.55	22.30	2.90	2.30	8.32	0.05	1.49
14115MT077A01	12.50	9.29	4.12	2.94	4.73	0.04	1.59
14115MT078B01	8.14	22.00	1.80	2.17	6.67	0.04	1.59
14115MT081A01	8.94	18.10	2.52	2.19	7.12	0.04	1.62
14115MT082A01	6.78	17.60	1.45	1.82	7.79	0.04	1.44
14115MT083A01	10.10	12.30	3.03	2.32	5.56	0.04	1.41
14115MT084A01	8.46	22.20	2.47	2.17	8.82	0.05	1.27
14115MT085A01	8.86	19.70	2.55	2.23	7.09	0.05	1.45
14115MT086A01	8.38	19.40	2.56	2.13	8.13	0.05	1.31
14115MT087A01	9.02	20.80	2.64	2.19	5.55	0.05	1.36
14115MT088A01	8.60	18.80	2.40	2.08	6.75	0.05	1.56
14115MT089A01	10.30	14.80	3.32	2.51	6.54	0.05	1.41
14115MT090A01	7.14	19.30	1.76	1.94	7.64	0.05	1.36
14115MT093A01	11.40	13.30	3.73	2.45	5.86	0.06	1.41
14115MT094A01	8.16	15.30	1.84	2.05	7.18	0.03	1.69
14115MT096A01	6.91	19.50	1.55	1.88	8.19	0.03	1.32
14115MT099A01	10.70	18.50	3.35	2.56	6.76	0.05	1.52
14115MT099B01	10.60	18.20	3.19	2.48	6.02	0.10	1.63
14115MT100A01	7.84	20.80	2.14	2.04	7.57	0.04	1.36
14115MT103A01	9.02	19.90	2.47	2.23	6.90	0.05	1.58
14115MT104A01	9.73	18.80	2.89	2.31	6.89	0.05	1.56
14115MT106A01	13.30	9.11	4.96	2.85	4.53	0.06	1.53
14115MT107A01	9.80	16.00	2.70	2.34	6.99	0.04	1.58
14115MT113A01	8.28	19.20	2.29	2.12	7.44	0.04	1.72
14115MT115A01	9.93	17.80	3.23	2.45	6.17	0.04	1.61

14115MT116A01	8.64	20.60	2.58	2.20	6.76	0.04	1.52
14115MT117A01	9.93	19.60	3.19	2.54	6.46	0.04	1.53
14115MT119A01	9.27	18.10	2.84	2.32	6.59	0.05	1.67
14115MT120A01	7.99	19.60	2.20	2.03	6.83	0.04	1.72
14115MT121A01	11.80	16.10	4.21	2.88	5.46	0.07	1.44
14115MT129A01	12.00	14.10	4.13	2.83	5.89	0.05	1.65
14115MT136A01	8.56	21.10	2.86	2.20	6.81	0.06	1.34
14115MT139A01	9.46	20.80	3.10	2.48	7.16	0.05	1.37
14115MT140A01	9.58	21.60	3.12	2.43	7.55	0.05	1.44
14115MT140A02	11.10	18.60	3.82	2.69	6.25	0.06	1.54
14115MT140A03	10.10	19.70	3.22	2.50	6.31	0.05	1.56
14115MT149A01	10.90	14.60	3.66	2.54	4.98	0.05	1.50
14115MT151A01	8.01	21.60	2.16	2.16	7.12	0.05	1.54
14115MT155A01	7.70	26.20	2.61	2.01	7.05	0.05	1.33
14115MT156A01	8.02	22.80	2.56	2.02	9.88	0.04	1.27
14115MT156A02	9.85	19.20	3.41	2.38	7.68	0.05	1.28
14115MT159A01	7.26	22.50	1.51	1.94	7.87	0.03	1.60
14115MT161A01	9.57	19.50	3.12	2.80	6.06	0.06	1.19
14115MT161B01	7.66	20.50	1.97	2.00	7.29	0.04	1.64
14115MT161B02	8.98	18.90	2.81	2.21	6.94	0.05	1.60
14115MT168A01	8.80	19.70	2.73	2.16	8.14	0.04	1.40
14115MT169A01	9.08	16.50	2.54	2.34	7.50	0.04	1.56
14115MT172A01	12.30	14.40	4.34	2.95	6.22	0.04	1.41
14115MT175A01	11.20	16.60	3.93	2.70	6.42	0.04	1.40
14115MT183A01	9.19	17.00	2.82	2.46	8.14	0.04	1.35
14115MT186A01	10.60	15.90	3.38	2.81	7.15	0.05	1.49
14115MT187A01	8.94	19.00	2.58	2.47	7.91	0.04	1.46
14115MT188A01	7.11	22.40	1.55	2.08	8.97	0.03	1.34

14115MT190A01	6.75	20.60	1.44	1.83	7.65	0.03	1.51
14115MT193A01	9.32	14.70	2.73	2.57	9.03	0.04	1.52
14115MT194A01	7.65	17.80	1.95	2.22	7.92	0.03	1.45
14115MT196A01	8.44	17.00	2.51	2.04	7.02	0.03	1.35
14115MT200A01	7.46	23.70	2.30	1.96	9.49	0.04	1.20
14115MT200A02	9.54	18.90	3.28	2.40	6.91	0.05	1.28
14115MT205A01	10.30	17.40	3.20	2.50	5.82	0.06	1.66
14115MT206A01	14.00	8.31	4.93	3.08	4.29	0.06	1.82
14115MT207A01	8.16	20.10	2.08	2.16	7.76	0.04	1.64
14115MT207A02	9.12	17.50	2.67	2.34	7.15	0.05	1.66
14115MT208A01	8.32	18.50	2.34	2.20	7.64	0.04	1.52
14115MT209A01	11.80	13.00	3.92	2.75	5.21	0.05	1.80
14115MT210A01	9.09	17.40	2.51	2.27	6.68	0.05	1.79
14115MT210B01	8.32	18.70	2.44	2.10	5.74	0.05	1.45
14115MT210B02	10.70	16.70	3.84	2.58	5.14	0.06	1.57
14115MT211A01	9.09	17.50	2.45	2.23	6.73	0.04	1.73
14115MT214A01	10.30	18.40	3.48	2.45	7.76	0.05	1.32
14115MT214A02	10.30	19.30	3.59	2.53	7.90	0.06	1.25
14115MT221A01	12.00	1.74	4.30	2.99	1.30	0.10	2.16
14115MT228A01	9.62	17.70	3.04	2.51	6.74	0.04	1.49
14115MT228B01	7.14	22.70	1.63	1.93	7.89	0.03	1.53
14115MT232A01	8.52	19.40	2.32	2.16	6.82	0.04	1.64
14115MT234A01	8.27	19.00	2.22	2.12	7.31	0.04	1.58
14115MT234B01	7.67	18.60	2.01	1.98	7.26	0.04	1.58
14115MT234B02	10.30	16.90	3.32	2.49	6.16	0.05	1.63
14115MT235A01	6.62	21.40	1.42	1.79	8.43	0.03	1.44
14115MT236A01	7.21	20.60	1.70	1.86	7.92	0.03	1.60

14115MT236B04	8.46	19.30	2.33	2.14	6.83	0.05	1.59
14115MT236C01	9.71	16.60	3.14	2.32	6.05	0.05	1.60
14115MT237A01	7.11	22.00	1.86	1.84	7.77	0.04	1.65
14115MT239A01	11.50	14.40	4.20	2.73	4.95	0.05	1.41
14115MT251A01	9.37	19.70	2.87	2.38	6.63	0.05	1.62
14115MT254A01	7.65	21.70	2.02	1.91	7.01	0.04	1.71
14115MT254A02	7.69	21.60	2.05	1.96	7.06	0.04	1.60
14115MT254B01	7.45	20.00	1.80	1.96	7.35	0.04	1.60
14115MT258A01	8.31	19.80	2.20	2.15	7.26	0.04	1.56
14115MT269A01	8.04	18.00	2.05	2.03	6.95	0.04	1.77
14115MT270A01	7.47	18.40	1.75	1.94	7.44	0.03	1.64
14115MT270A02	7.93	24.80	2.50	2.03	7.26	0.04	1.36
15112TH404B01	9.87	17.80	3.11	2.27	6.74	0.05	1.78
15112TH404B02	10.10	17.00	3.77	2.28	6.36	0.05	1.44
15112TH404C01	9.31	16.20	3.00	2.14	6.24	0.05	1.67
15112TH409B01	13.80	10.60	5.34	3.05	4.43	0.07	1.41
15112TH410B01	8.26	18.90	2.48	1.96	6.63	0.04	1.49
15112TH412B01	11.80	1.49	3.57	2.44	1.13	0.03	2.00
15112TH412D01	9.92	20.10	3.47	2.32	5.88	0.05	1.39
15112TH412E01	11.50	18.60	4.13	2.61	5.41	0.06	1.39
15112TH413B01	7.48	16.60	2.05	1.86	6.38	0.04	1.66
15112TH417B01	6.08	19.90	2.27	1.55	7.33	0.04	1.43
15112TH423B01	10.40	18.10	3.79	2.33	5.50	0.05	1.39
15112TH423B02	8.92	20.00	3.10	2.04	6.60	0.05	1.37
15112TH423B03	9.68	20.30	3.42	2.20	6.65	0.05	1.36
15112TH423B04	7.64	19.30	2.49	1.83	6.60	0.04	1.30
15112TH423D01	9.26	20.00	3.24	2.11	6.63	0.05	1.32

15112TH423D02	9.13	21.40	3.08	2.14	6.84	0.05	1.40
15112TH423D03	10.30	20.40	3.59	2.30	6.73	0.05	1.41
15112TH423D04	9.42	20.20	3.06	2.15	6.58	0.05	1.39
15112TH423D05	9.06	19.50	3.06	2.10	6.58	0.04	1.36
15112TH425C01	7.76	15.10	2.51	1.91	5.62	0.04	1.14
15112TH425C02	9.24	18.20	2.93	2.07	7.97	0.04	1.27
15112TH425D01	5.54	23.80	1.95	1.27	12.00	0.03	0.78
15112TH425D02	4.84	27.50	1.61	1.15	13.60	0.03	0.70
15112TH425D03	4.05	30.60	1.46	0.96	15.70	0.03	0.33
15112TH425D04	3.92	30.70	1.45	0.91	15.30	0.04	0.32
15112TH426B01	8.17	19.80	2.76	1.88	6.24	0.04	1.20
15112TH426B03	7.37	24.60	2.56	1.67	11.00	0.04	1.08
15112TH426B04	10.10	19.40	3.78	2.30	5.43	0.05	1.07
15112TH428B01	9.12	14.60	3.16	2.09	5.44	0.05	1.60
15112TH429B01	9.94	19.30	3.34	2.18	6.65	0.06	1.28
15112TH429B03	9.37	19.30	3.37	2.17	5.74	0.05	1.12
15112TH429B04	7.54	24.30	2.58	1.72	10.90	0.04	1.10
15112TH431A01	10.40	18.70	3.84	2.41	5.73	0.06	1.45
15112TH431A02	9.23	18.10	3.31	2.17	5.74	0.05	1.48
15112TH431A03	10.90	17.00	3.97	2.53	5.28	0.06	1.59
15112TH431A04	13.10	14.10	5.30	2.79	4.84	0.07	1.64
15112TH431A05	11.40	16.30	4.32	2.58	6.10	0.06	1.66
15112TH431A06	10.80	20.80	3.96	2.50	6.44	0.05	1.38
15112TH431A07	11.00	20.20	4.02	2.53	5.98	0.05	1.37
15112TH431A08	11.30	19.90	4.12	2.58	5.74	0.06	1.44
15112TH432A01	13.20	12.50	4.89	3.02	6.38	0.06	1.73

15112TH432A02	12.00	13.30	4.29	2.74	6.70	0.05	1.71
15112TH432A03	11.60	12.40	4.10	2.68	6.53	0.06	1.76
15112TH432A04	12.80	12.50	4.58	2.89	6.37	0.05	1.71

P <sub>2</sub> O <sub>5</sub> (%)	TiO <sub>2</sub> (%)	Ag (ppm)	Ba (ppm)	Be (ppm)	Bi (ppm)	Cd (ppm)	Ce (ppm)	Co (ppm)	Cr (ppm)
0.10	0.34	0.13	391.00	0.80	<0.1	0.20	35.00	5.85	43.00
0.11	0.42	0.16	452.00	1.00	0.1	0.20	45.00	7.79	50.00
0.08	0.31	0.31	309.00	0.70	<0.1	0.30	32.00	6.30	42.00
0.10	0.39	0.17	452.00	1.30	0.2	0.30	51.00	8.89	58.00
0.09	0.34	1.06	359.00	0.70	<0.1	0.20	32.00	5.24	39.00
0.11	0.44	0.20	381.00	1.00	0.1	0.20	40.00	7.35	48.00
0.11	0.40	0.14	378.00	0.70	<0.1	0.20	39.00	6.98	45.00
0.09	0.32	0.13	353.00	0.70	0.1	0.30	31.00	6.70	40.00
0.14	0.57	0.20	477.00	1.50	0.2	0.20	66.00	12.70	83.00
0.10	0.39	0.16	369.00	0.80	<0.1	0.20	34.00	6.70	43.00
0.10	0.40	0.14	371.00	0.70	<0.1	0.20	38.00	5.52	41.00
0.11	0.43	0.15	395.00	0.80	0.1	0.20	41.00	6.29	43.00
0.09	0.35	0.12	329.00	0.60	<0.1	0.20	32.00	5.17	36.00
0.11	0.42	0.13	346.00	0.80	<0.1	0.20	38.00	5.91	42.00
0.10	0.34	0.14	415.00	1.10	0.1	0.20	32.00	7.31	42.00
0.12	0.47	0.14	467.00	1.00	0.1	0.30	47.00	7.46	54.00
0.13	0.50	0.19	495.00	1.40	0.2	0.20	49.00	10.10	67.00
0.10	0.38	0.14	415.00	0.80	0.1	0.20	39.00	6.89	41.00
0.14	0.55	0.21	499.00	1.00	0.2	0.20	56.00	8.86	65.00
0.11	0.40	0.14	420.00	1.00	<0.1	0.20	40.00	5.58	48.00
0.13	0.51	0.16	421.00	0.80	<0.1	0.30	61.00	4.75	43.00
0.11	0.38	0.12	423.00	0.80	<0.1	0.20	42.00	4.99	37.00
0.11	0.37	0.12	395.00	0.90	<0.1	0.20	35.00	5.77	38.00
0.11	0.37	0.11	381.00	0.80	<0.1	0.20	38.00	4.91	34.00
0.12	0.44	0.13	440.00	1.00	0.1	0.20	47.00	7.57	50.00

0.11	0.41	1.24	455.00	0.90	0.1	0.50	39.00	7.02	47.00
0.10	0.33	0.14	380.00	0.80	<0.1	0.20	35.00	4.78	34.00
0.11	0.45	0.17	405.00	1.10	0.1	0.20	42.00	7.16	55.00
0.12	0.45	0.16	442.00	1.20	0.2	0.20	46.00	10.00	61.00
0.11	0.40	0.15	401.00	0.90	0.1	0.20	43.00	7.84	51.00
0.13	0.57	0.20	540.00	1.30	0.2	0.30	68.00	9.50	54.00
0.12	0.42	0.15	463.00	0.90	0.1	0.20	49.00	7.43	47.00
0.12	0.41	0.15	431.00	0.90	0.1	0.20	38.00	8.12	51.00
0.12	0.46	0.15	447.00	1.10	0.1	0.20	46.00	8.52	57.00
0.15	0.55	0.20	571.00	1.50	0.2	0.20	62.00	13.40	84.00
0.13	0.51	0.30	459.00	1.30	0.2	0.30	49.00	11.50	67.00
0.12	0.48	0.18	423.00	1.00	0.1	0.20	43.00	7.83	53.00
0.11	0.37	0.11	402.00	0.80	<0.1	0.20	42.00	5.09	33.00
0.13	0.44	0.15	446.00	0.90	<0.1	0.20	44.00	7.45	51.00
0.13	0.45	0.14	459.00	1.10	0.1	0.20	48.00	7.98	58.00
0.14	0.58	0.22	579.00	1.80	0.2	0.30	75.00	13.90	85.00
0.12	0.45	0.16	428.00	1.20	0.1	0.20	45.00	9.16	59.00
0.14	0.51	0.19	561.00	1.40	0.2	0.20	64.00	11.70	73.00
0.11	0.39	0.12	411.00	0.70	<0.1	0.20	43.00	5.38	38.00
0.13	0.45	0.13	482.00	1.10	0.1	0.20	52.00	7.29	54.00
0.12	0.44	0.16	434.00	1.20	0.2	0.30	46.00	8.85	61.00
0.12	0.45	0.17	476.00	1.30	0.2	0.20	47.00	10.10	68.00
0.11	0.45	0.15	345.00	0.90	0.1	0.20	39.00	8.15	46.00
0.10	0.39	0.13	398.00	0.80	<0.1	0.20	37.00	6.20	40.00
0.11	0.44	0.14	413.00	0.90	0.1	0.20	43.00	7.86	48.00
0.13	0.45	0.16	451.00	1.20	0.1	0.20	48.00	8.79	59.00
0.10	0.36	0.13	364.00	1.00	0.1	0.20	35.00	6.43	47.00



0.11	0.39	0.14	448.00	1.00	0.1	0.20	43.00	7.21	45.00
0.14	0.58	0.22	558.00	1.70	0.2	0.20	67.00	14.90	88.00
0.10	0.41	0.14	390.00	1.00	0.1	0.30	43.00	7.92	52.00
0.11	0.47	0.16	375.00	0.90	0.1	0.30	40.00	6.81	47.00
0.10	0.36	0.13	364.00	0.70	<0.1	0.20	29.00	4.65	34.00
0.11	0.43	0.15	436.00	1.30	0.1	0.20	48.00	7.47	53.00
0.11	0.41	0.14	432.00	1.00	0.1	0.20	43.00	8.67	51.00
0.12	0.45	0.16	422.00	0.90	0.1	0.20	42.00	8.63	52.00
0.12	0.44	0.15	433.00	0.90	0.1	0.20	45.00	8.07	50.00
0.11	0.43	0.17	452.00	1.00	<0.1	0.20	40.00	7.14	46.00
0.12	0.43	0.38	407.00	1.20	0.2	0.20	39.00	9.09	74.00
0.13	0.46	0.29	429.00	1.30	0.2	0.20	47.00	12.40	63.00
0.11	0.41	0.22	369.00	1.10	0.1	0.30	38.00	8.81	49.00
0.13	0.52	0.30	377.00	1.10	0.2	0.20	46.00	10.20	60.00
0.12	0.48	0.27	397.00	1.20	0.2	0.20	47.00	9.07	60.00
0.10	0.35	0.21	325.00	0.60	<0.1	0.30	33.00	4.70	34.00
0.14	0.57	0.33	502.00	1.30	0.2	0.40	63.00	9.67	53.00
0.13	0.56	0.33	502.00	1.10	0.2	0.40	60.00	9.47	52.00
0.12	0.49	0.29	455.00	1.20	0.2	0.20	47.00	12.40	63.00
0.09	0.34	0.15	362.00	0.80	0.1	0.20	36.00	5.86	24.00
0.12	0.47	0.26	443.00	1.20	0.2	0.20	48.00	10.50	56.00
0.10	0.34	0.18	366.00	0.80	<0.1	0.20	26.00	6.51	39.00
0.11	0.43	0.25	405.00	1.20	0.2	0.40	41.00	9.72	63.00
0.11	0.39	0.21	371.00	1.10	0.2	0.30	34.00	10.00	59.00
0.13	0.47	0.31	449.00	1.40	0.2	0.30	44.00	12.10	74.00
0.10	0.35	0.21	360.00	0.80	<0.1	0.20	26.00	6.00	39.00
0.10	0.39	0.21	382.00	1.10	0.1	0.30	37.00	9.14	55.00

0.12	0.45	0.36	406.00	1.20	0.2	0.30	40.00	9.28	64.00
0.13	0.52	0.27	371.00	1.20	0.2	0.30	40.00	9.07	59.00
0.12	0.44	0.25	420.00	1.20	0.2	0.20	41.00	9.58	61.00
0.12	0.46	0.26	378.00	1.20	0.2	0.30	40.00	9.60	64.00
0.13	0.49	0.26	389.00	1.20	0.2	0.30	42.00	10.20	65.00
0.13	0.46	0.26	404.00	1.20	0.2	0.30	42.00	10.40	63.00
0.12	0.43	0.23	404.00	0.90	0.1	0.30	37.00	8.66	55.00
0.13	0.48	0.28	483.00	1.40	0.2	0.30	50.00	12.00	63.00
0.11	0.40	0.22	360.00	1.00	0.1	0.20	33.00	7.88	47.00
0.14	0.55	0.30	459.00	1.40	0.2	0.30	51.00	11.50	69.00
0.14	0.57	0.33	432.00	1.40	0.2	0.20	50.00	13.00	68.00
0.11	0.37	0.19	370.00	0.80	<0.1	0.30	32.00	5.21	35.00
0.10	0.36	0.21	367.00	0.90	<0.1	0.20	25.00	5.44	35.00
0.12	0.39	0.22	405.00	0.90	<0.1	0.30	36.00	7.44	44.00
0.13	0.57	0.31	552.00	1.70	0.2	0.20	64.00	13.70	75.00
0.11	0.51	0.28	497.00	1.30	0.2	0.20	49.00	8.80	54.00
0.12	0.41	0.22	393.00	0.80	<0.1	0.30	40.00	6.36	41.00
0.14	0.57	0.33	542.00	1.70	0.3	0.30	65.00	14.60	76.00
0.13	0.48	0.39	476.00	1.40	0.2	0.20	45.00	10.10	58.00
0.12	0.37	0.15	408.00	1.00	0.1	0.20	27.00	6.08	38.00
0.12	0.33	0.10	413.00	0.80	<0.1	0.20	27.00	4.39	31.00
0.11	0.36	0.14	398.00	0.80	0.1	0.20	27.00	7.17	39.00
0.14	0.45	0.16	480.00	1.30	0.2	0.20	44.00	9.66	60.00
0.13	0.44	0.15	442.00	1.20	0.1	0.20	38.00	9.58	58.00
0.14	0.47	0.18	496.00	1.30	0.2	0.20	44.00	12.10	62.00
0.13	0.42	0.16	429.00	1.00	0.1	0.20	35.00	8.86	54.00
0.06	0.68	0.22	602.00	1.60	0.2	0.20	43.00	14.40	61.00

0.12	0.37	0.13	391.00	0.80	0.1	0.20	31.00	6.73	48.00
0.12	0.64	0.22	628.00	1.60	0.2	0.20	60.00	13.40	72.00
0.17	0.62	0.27	625.00	2.30	0.4	0.20	78.00	21.70	96.00
0.11	0.36	0.16	464.00	1.10	0.2	0.20	37.00	9.83	51.00
0.14	0.57	0.22	577.00	1.80	0.2	0.10	47.00	11.50	69.00
0.12	0.38	0.16	414.00	0.80	<0.1	0.10	26.00	5.97	38.00
0.13	0.44	0.15	437.00	1.00	0.1	0.20	41.00	7.44	47.00
0.11	0.35	0.12	357.00	0.70	<0.1	0.20	25.00	4.79	32.00
0.15	0.44	0.18	481.00	1.40	0.2	0.20	46.00	9.03	52.00
0.11	0.39	0.15	387.00	0.90	0.2	0.20	30.00	8.80	49.00
0.12	0.40	0.15	419.00	1.00	0.1	0.20	35.00	8.45	49.00
0.13	0.43	0.13	385.00	1.10	0.1	0.20	35.00	8.84	47.00
0.12	0.44	0.15	407.00	1.20	0.1	0.20	32.00	9.06	50.00
0.13	0.40	0.15	427.00	1.00	0.1	0.20	34.00	8.42	46.00
0.15	0.49	0.18	457.00	1.00	0.2	0.20	43.00	10.50	59.00
0.11	0.37	0.14	362.00	0.80	<0.1	0.20	27.00	6.32	37.00
0.14	0.47	0.17	485.00	1.50	0.3	0.30	52.00	12.30	59.00
0.12	0.39	0.13	425.00	0.90	0.1	0.20	30.00	5.16	32.00
0.11	0.34	0.12	367.00	0.80	<0.1	0.20	34.00	5.60	32.00
0.14	0.45	0.18	485.00	1.20	0.2	0.20	46.00	10.70	59.00
0.14	0.47	0.16	504.00	1.10	0.1	0.20	40.00	10.80	59.00
0.11	0.35	0.14	387.00	1.00	0.1	0.20	29.00	7.08	44.00
0.12	0.38	0.14	444.00	1.10	0.1	0.20	34.00	8.65	43.00
0.13	0.42	0.15	461.00	1.20	0.2	0.20	39.00	9.67	50.00
0.14	0.58	0.20	593.00	1.90	0.3	0.20	63.00	14.40	74.00
0.13	0.42	0.14	465.00	1.10	0.2	0.20	40.00	9.38	51.00
0.12	0.38	0.21	412.00	0.80	0.2	0.20	33.00	6.52	41.00
0.12	0.46	0.25	453.00	1.00	0.2	0.30	50.00	9.96	55.00
0.11	0.40	0.22	402.00	0.90	0.1	0.20	38.00	7.69	47.00

0.12	0.44	0.22	449.00	1.00	0.2	0.20	40.00	9.31	54.00
0.12	0.42	0.24	439.00	1.00	0.2	0.20	39.00	8.22	49.00
0.12	0.40	0.20	394.00	1.00	<0.1	0.20	38.00	5.80	40.00
0.14	0.52	0.29	490.00	1.40	0.2	0.30	58.00	13.90	72.00
0.14	0.51	0.27	511.00	1.50	0.2	0.20	59.00	11.70	69.00
0.11	0.41	0.23	388.00	0.90	0.1	0.20	37.00	8.57	49.00
0.11	0.43	0.22	409.00	1.10	0.2	0.30	42.00	9.66	53.00
0.12	0.47	0.24	402.00	1.10	0.1	0.30	44.00	8.91	54.00
0.13	0.47	0.26	453.00	1.50	0.2	0.20	47.00	11.80	68.00
0.12	0.44	0.24	429.00	1.10	0.2	0.20	39.00	9.81	61.00
0.13	0.55	0.27	462.00	1.30	0.2	0.30	52.00	10.80	61.00
0.12	0.38	0.20	399.00	0.90	0.1	0.20	35.00	6.51	41.00
0.11	0.36	0.19	363.00	0.90	0.1	0.30	29.00	7.84	44.00
0.10	0.37	0.18	357.00	0.80	0.1	0.20	31.00	7.80	50.00
0.12	0.44	0.25	413.00	1.20	0.2	0.30	43.00	10.20	61.00
0.10	0.34	0.19	363.00	0.70	<0.1	0.20	24.00	4.39	32.00
0.12	0.52	0.26	370.00	1.10	0.2	0.30	40.00	9.99	52.00
0.11	0.35	0.18	394.00	0.90	0.1	0.20	31.00	5.65	38.00
0.12	0.42	0.22	411.00	1.20	0.2	0.20	44.00	9.66	56.00
0.12	0.41	0.22	389.00	1.00	0.1	0.20	37.00	8.29	49.00
0.12	0.42	0.23	425.00	1.00	0.2	0.30	41.00	8.04	47.00
0.14	0.53	0.28	464.00	1.60	0.2	0.20	44.00	10.70	77.00
0.13	0.49	0.26	438.00	1.30	0.2	0.20	48.00	11.00	68.00
0.12	0.42	0.23	405.00	1.00	0.2	0.20	46.00	8.37	50.00
0.13	0.47	0.24	468.00	1.40	0.2	0.20	52.00	10.80	58.00
0.12	0.41	0.23	408.00	1.10	0.3	0.20	37.00	6.78	45.00
0.10	0.33	0.18	341.00	0.80	<0.1	0.20	25.00	4.36	32.00
0.10	0.33	0.19	363.00	0.80	<0.1	0.20	25.00	4.76	32.00

0.13	0.45	0.25	420.00	1.00	0.2	0.30	44.00	6.86	46.00
0.11	0.38	0.20	387.00	0.90	<0.1	0.20	33.00	5.76	38.00
0.11	0.46	0.27	417.00	1.10	0.2	0.20	38.00	6.24	46.00
0.10	0.36	0.18	333.00	0.80	0.1	0.20	29.00	6.56	47.00
0.12	0.45	0.23	392.00	1.40	0.2	0.20	43.00	9.81	60.00
0.12	0.48	0.24	444.00	1.10	0.2	0.20	47.00	10.00	60.00
0.14	0.59	0.31	586.00	1.70	0.2	0.20	64.00	14.20	84.00
0.11	0.36	0.21	401.00	0.80	0.1	0.20	34.00	5.85	39.00
0.13	0.43	0.20	433.00	1.20	0.2	0.30	57.00	8.54	39.00
0.11	0.40	0.29	396.00	1.00	0.1	0.30	47.00	7.53	34.00
0.15	0.52	0.25	514.00	1.60	0.2	0.30	61.00	12.60	59.00
0.12	0.41	0.21	445.00	1.10	0.2	0.30	50.00	8.07	35.00
0.11	0.43	0.20	389.00	1.30	0.1	0.30	44.00	7.85	43.00
0.14	0.51	0.24	464.00	1.40	0.2	0.30	57.00	12.60	54.00
0.11	0.39	0.20	439.00	1.20	0.1	0.30	44.00	7.97	36.00
0.11	0.44	0.21	413.00	1.50	0.2	0.30	54.00	11.50	51.00
0.11	0.43	0.21	410.00	1.40	0.2	0.30	54.00	12.10	50.00
0.17	0.61	0.22	604.00	1.40	0.2	0.30	58.00	12.00	52.00
0.12	0.44	0.18	452.00	1.10	0.2	0.30	50.00	8.90	45.00
0.10	0.34	0.16	366.00	1.00	<0.1	0.20	36.00	4.78	24.00
0.12	0.41	0.18	408.00	1.10	0.1	0.30	46.00	6.63	37.00
0.11	0.39	0.18	408.00	1.20	0.1	0.20	47.00	7.12	35.00
0.12	0.39	0.16	385.00	0.90	<0.1	0.30	48.00	6.16	30.00
0.13	0.46	0.20	468.00	1.40	0.2	0.30	56.00	9.97	48.00
0.09	0.30	0.13	345.00	0.70	<0.1	0.20	32.00	3.95	19.00
0.10	0.33	0.14	366.00	1.00	<0.1	0.20	39.00	5.24	23.00
0.11	0.40	0.18	409.00	1.00	0.1	0.30	46.00	7.52	37.00

0.12	0.43	0.20	439.00	1.30	0.2	0.30	52.00	10.10	44.00
0.11	0.39	0.17	367.00	0.80	<0.1	0.30	47.00	5.65	26.00
0.16	0.53	0.27	498.00	1.60	0.2	0.30	64.00	12.70	59.00
0.12	0.41	0.19	463.00	1.10	0.2	0.30	53.00	8.77	41.00
0.10	0.33	0.14	393.00	0.90	<0.1	0.30	42.00	5.82	25.00
0.10	0.34	0.16	385.00	0.90	0.3	0.30	42.00	6.36	25.00
0.10	0.34	0.15	375.00	0.90	0.1	0.20	43.00	5.41	24.00
0.11	0.40	0.16	399.00	1.00	0.2	0.20	43.00	6.92	32.00
0.12	0.38	0.16	415.00	0.90	<0.1	0.30	46.00	5.30	28.00
0.11	0.34	0.16	384.00	0.90	<0.1	0.20	39.00	5.04	24.00
0.10	0.37	0.17	366.00	0.90	0.1	0.30	42.00	8.22	32.00
0.13	0.42	0.17	502.00	1.20	0.2	0.20	52.00	8.50	45.00
0.12	0.46	0.20	460.00	1.20	0.2	0.20	52.00	10.60	62.00
0.12	0.40	0.19	479.00	1.20	0.2	0.20	51.00	8.35	45.00
0.11	0.60	0.26	590.00	1.90	0.3	0.20	72.00	14.90	81.00
0.13	0.42	0.17	432.00	1.10	0.1	0.30	57.00	7.44	37.00
0.03	0.63	0.23	586.00	1.50	0.1	0.20	54.00	8.95	49.00
0.13	0.48	0.23	452.00	1.30	0.2	0.20	55.00	9.72	49.00
0.12	0.52	0.23	503.00	1.50	0.2	0.20	61.00	11.70	63.00
0.13	0.39	0.18	411.00	1.00	<0.1	0.20	44.00	5.33	31.00
0.12	0.40	0.16	336.00	0.70		0.20	54.00	5.81	33.00
0.13	0.51	0.24	462.00	1.40	0.2	0.20	55.00	10.20	58.00
0.12	0.42	0.20	428.00	1.10	0.2	0.20	47.00	8.36	48.00
0.12	0.44	0.22	447.00	1.30	0.2	0.20	51.00	9.54	53.00
0.11	0.38	0.19	394.00	1.00	0.1	0.20	46.00	6.90	38.00
0.12	0.41	0.20	424.00	1.20	0.2	0.20	48.00	8.86	47.00
0.12	0.42	0.19	437.00	1.00	0.2	0.20	47.00	8.70	47.00
0.13	0.46	0.25	464.00	1.30	0.2	0.20	51.00	9.71	52.00

0.12	0.43	0.21	440.00	1.10	0.2	0.20	51.00	8.98	49.00
0.12	0.42	0.23	422.00	1.20	0.2	0.20	45.00	7.97	47.00
0.11	0.47	0.20	390.00	0.90	0.2	0.20	52.00	7.04	38.00
0.11	0.43	0.22	452.00	1.10	0.2	0.20	50.00	8.69	44.00
0.08	0.25	0.13	269.00	0.80	0.1	0.10	30.00	5.42	30.00
0.07	0.21	0.13	245.00	0.90	0.1	0.10	26.00	4.62	25.00
0.06	0.19	0.10	180.00	0.60	<0.1	0.20	17.00	4.31	18.00
0.06	0.19	0.08	174.00	0.70	<0.1	0.20	18.00	4.58	23.00
0.11	0.41	0.22	392.00	1.20	0.1	0.20	45.00	7.67	41.00
0.09	0.32	0.18	356.00	1.00	0.2	0.20	41.00	7.14	36.00
0.13	0.53	0.25	416.00	1.40	0.2	0.20	54.00	9.88	57.00
0.13	0.45	0.22	493.00	1.30	0.1	0.20	52.00	8.66	50.00
0.12	0.46	0.23	443.00	1.30	0.2	0.20	50.00	10.20	54.00
0.12	0.50	0.19	406.00	1.30	0.2	0.20	50.00	9.26	54.00
0.09	0.31	0.16	372.00	1.00	0.2	0.20	38.00	7.06	37.00
0.13	0.52	0.23	464.00	1.40	0.2	0.20	54.00	10.50	61.00
0.13	0.51	0.22	437.00	1.10	0.1	0.20	50.00	9.06	54.00
0.14	0.55	0.24	490.00	1.40	0.3	0.20	57.00	11.30	61.00
0.15	0.57	0.27	558.00	1.90	0.4	0.20	64.00	15.60	83.00
0.15	0.53	0.29	541.00	1.60	0.3	0.30	71.00	12.00	61.00
0.12	0.48	0.24	478.00	1.50	0.3	0.20	56.00	11.70	57.00
0.12	0.48	0.29	469.00	1.70	0.3	0.20	56.00	11.80	58.00
0.13	0.50	0.25	493.00	1.60	0.3	0.20	59.00	11.90	62.00
0.15	0.54	0.30	566.00	1.70	0.3	0.20	69.00	13.70	70.00
0.15	0.50	0.26	525.00	1.70	0.2	0.20	62.00	11.90	57.00
0.15	0.51	0.25	525.00	1.60	0.2	0.20	66.00	11.50	57.00
0.16	0.53	0.28	548.00	2.00	0.3	0.20	68.00	13.00	69.00

Cs (ppm)	Cu (ppm)	Dy (ppm)	Er (ppm)	Eu (ppm)	Ga (ppm)	Gd (ppm)	Hf (ppm)	Ho (ppm)	La (ppm)
1.20	9.00	1.95	1.08	0.77	8.10	3.20	3.20	0.39	22.00
1.90	11.80	2.36	1.36	0.86	10.20	4.00	4.30	0.46	28.00
1.30	9.70	1.98	1.11	0.64	7.20	3.10	3.20	0.39	21.00
2.40	14.80	2.45	1.33	0.83	11.90	4.10	4.00	0.50	31.00
1.20	8.20	1.99	1.06	0.72	7.70	3.20	3.80	0.39	21.00
1.80	12.70	2.42	1.32	0.83	9.50	3.70	4.60	0.48	25.00
1.60	11.50	2.17	1.18	0.80	8.50	3.50	4.40	0.43	25.00
1.30	11.20	1.92	1.08	0.67	7.80	3.10	3.30	0.39	21.00
4.00	21.60	2.76	1.53	1.04	15.70	4.80	3.50	0.56	39.00
1.60	12.20	2.22	1.22	0.76	8.60	3.50	3.80	0.43	23.00
1.10	9.90	2.11	1.21	0.74	7.60	3.40	5.20	0.41	24.00
1.30	9.50	2.22	1.27	0.80	8.40	3.70	5.40	0.45	25.00
1.00	8.90	2.01	1.10	0.71	6.90	3.20	4.10	0.38	22.00
1.20	10.30	2.36	1.32	0.80	7.70	3.80	5.50	0.48	24.00
1.90	11.40	1.91	1.05	0.73	10.10	3.10	3.40	0.38	21.00
1.80	14.00	2.42	1.32	0.93	10.50	4.00	4.00	0.48	28.00
2.80	20.20	2.68	1.55	1.02	13.60	4.60	4.90	0.54	30.00
1.70	10.10	2.22	1.19	0.82	9.40	3.50	3.80	0.42	24.00
2.40	14.80	2.71	1.49	0.96	12.70	4.40	5.50	0.54	32.00
1.30	8.80	2.30	1.23	0.88	8.70	3.80	4.60	0.48	25.00
1.10	7.40	2.97	1.64	0.94	8.70	5.10	8.30	0.60	35.00
1.10	7.80	2.29	1.20	0.80	8.40	3.60	5.00	0.44	26.00
1.30	10.40	2.27	1.25	0.81	8.70	3.80	5.20	0.45	23.00
0.90	6.50	2.30	1.29	0.81	7.60	3.90	5.60	0.46	24.00
1.70	14.40	2.41	1.38	0.90	10.50	4.20	4.80	0.48	29.00



1.70	12.10	2.21	1.22	0.88	9.80	3.80	3.90	0.44	25.00
0.90	7.70	1.95	1.09	0.73	7.40	3.40	4.00	0.40	23.00
2.30	14.10	2.42	1.36	0.88	10.80	3.90	4.00	0.48	27.00
2.70	17.50	2.38	1.34	0.90	12.20	4.00	3.70	0.48	29.00
2.00	13.90	2.73	1.33	0.90	10.50	4.00	4.40	0.50	27.00
2.10	17.20	3.24	1.82	1.09	13.00	5.40	6.40	0.66	38.00
2.00	25.10	2.41	1.32	0.94	10.90	4.00	4.70	0.46	30.00
2.00	13.10	2.41	1.33	0.83	10.10	3.80	4.00	0.47	24.00
2.20	14.20	2.36	1.32	0.92	11.40	3.90	4.20	0.47	28.00
3.50	25.70	2.82	1.50	1.09	16.30	4.80	3.80	0.53	35.00
3.40	20.80	2.90	1.60	1.04	14.10	3.80	4.00	0.53	34.00
2.10	14.20	2.52	1.42	0.92	11.10	4.00	5.30	0.51	27.00
1.00	7.10	2.33	1.27	0.83	8.30	4.00	4.80	0.46	26.00
1.40	12.80	2.37	1.31	0.89	10.10	4.00	5.80	0.46	26.00
2.00	14.80	2.48	1.36	0.90	10.60	4.00	4.40	0.50	29.00
4.70	29.10	3.21	1.72	1.21	18.40	5.70	4.20	0.61	41.00
2.60	16.40	2.36	1.47	0.90	11.70	3.90	3.60	0.47	28.00
3.70	23.20	2.91	1.53	1.11	16.10	4.80	4.20	0.56	38.00
1.10	8.80	2.17	1.19	0.77	8.50	3.80	4.30	0.44	27.00
2.20	15.00	2.46	1.36	0.90	11.70	4.10	4.70	0.50	32.00
2.70	16.90	2.43	1.34	0.88	12.00	3.80	3.90	0.48	29.00
3.20	20.60	2.45	1.34	0.95	14.10	4.10	3.20	0.48	30.00
2.00	11.40	2.64	1.40	0.88	8.90	4.20	4.40	0.52	24.00
1.40	12.00	2.24	1.17	0.80	8.70	3.50	3.90	0.44	24.00
1.70	13.20	2.38	1.35	0.86	9.70	3.90	5.20	0.49	27.00
2.40	15.70	2.45	1.36	0.89	11.80	4.20	4.40	0.50	29.00
1.90	12.40	2.07	1.18	0.75	9.50	3.40	3.60	0.42	23.00

1.60	12.50	2.25	1.23	0.84	9.90	3.90	4.50	0.44	27.00
4.60	30.20	3.16	1.80	1.20	18.60	5.30	3.70	0.64	37.00
2.20	16.40	2.25	1.21	0.82	10.50	3.90	3.60	0.46	27.00
1.80	10.60	2.56	1.47	0.86	9.00	4.10	5.00	0.52	25.00
0.90	7.60	2.02	1.12	0.72	7.40	3.20	3.90	0.42	20.00
2.20	13.80	2.50	1.38	0.85	11.30	4.20	4.20	0.49	30.00
2.00	14.60	2.25	1.18	0.87	11.00	3.70	3.10	0.43	27.00
1.70	13.60	2.46	1.38	0.90	10.40	3.90	4.60	0.47	26.00
1.90	13.40	2.40	1.36	0.90	10.40	4.10	4.60	0.49	28.00
1.60	11.80	2.32	1.35	0.84	9.90	3.80	4.10	0.44	25.00
2.30	16.00	2.39	1.40	0.90	11.50	3.30	3.80	0.48	28.00
3.30	21.10	2.67	1.56	1.01	14.10	3.70	3.50	0.51	32.00
2.20	14.50	2.48	1.48	0.88	10.80	3.30	3.60	0.49	28.00
2.90	16.90	2.82	1.63	1.00	12.40	3.80	4.40	0.54	30.00
2.60	15.00	2.70	1.55	0.96	12.20	3.70	4.20	0.53	31.00
0.80	8.20	2.09	1.22	0.72	6.80	3.00	4.70	0.41	25.00
2.10	15.40	3.52	2.08	1.15	13.50	4.60	6.40	0.68	39.00
2.00	14.10	3.43	1.91	1.13	12.90	4.50	6.10	0.68	37.00
3.20	21.70	2.75	1.62	1.04	14.00	3.80	3.10	0.55	34.00
1.30	16.40	2.01	1.16	0.77	8.00	2.60	2.80	0.39	18.00
2.80	19.20	2.77	1.56	1.00	13.00	3.90	3.70	0.54	33.00
1.20	14.60	2.02	1.18	0.74	8.70	2.60	3.60	0.42	21.00
2.70	17.10	2.69	1.50	0.90	12.10	3.60	3.70	0.51	31.00
2.70	17.10	2.30	1.32	0.83	11.60	3.20	3.20	0.45	25.00
3.30	20.90	2.76	1.62	1.02	14.20	3.70	4.00	0.54	30.00
1.30	10.20	2.07	1.25	0.76	8.60	2.80	3.00	0.41	21.00
2.00	13.50	2.50	1.47	0.84	10.30	3.30	4.20	0.50	26.00

3.00	17.90	2.57	1.52	0.94	12.60	3.50	3.60	0.51	28.00
2.90	22.80	2.88	1.64	0.96	11.20	3.70	4.20	0.55	28.00
2.90	18.80	2.56	1.47	0.93	12.40	3.40	3.20	0.50	28.00
2.90	16.50	2.85	1.54	0.92	11.70	3.50	3.60	0.52	27.00
3.40	18.20	2.98	1.72	0.99	13.10	3.80	3.90	0.58	28.00
2.80	21.40	2.96	1.49	0.95	12.60	3.50	4.10	0.52	28.00
1.80	12.00	2.33	1.36	0.82	10.10	3.00	4.50	0.46	27.00
3.40	21.90	2.82	1.60	1.03	14.40	4.00	3.80	0.53	34.00
1.80	13.00	2.40	1.41	0.86	9.60	3.10	4.20	0.47	24.00
4.10	23.20	3.08	1.76	1.07	15.40	4.00	3.70	0.61	32.00
4.50	36.50	3.24	1.81	1.13	15.50	4.20	3.90	0.63	32.00
1.10	8.10	2.16	1.24	0.78	7.90	2.80	4.10	0.41	23.00
1.20	12.00	2.14	1.22	0.80	8.10	2.80	3.40	0.43	21.00
1.60	14.30	2.36	1.40	0.89	9.90	3.20	4.20	0.48	24.00
4.40	26.00	3.45	1.94	1.26	18.40	4.70	4.80	0.67	38.00
2.90	18.50	2.99	1.73	1.08	14.40	3.90	6.00	0.60	31.00
1.20	7.90	2.58	1.48	0.91	9.20	3.50	5.00	0.48	28.00
4.60	24.10	3.40	1.90	1.18	18.20	4.50	4.40	0.62	40.00
2.60	18.80	2.74	1.57	1.00	12.60	3.40	3.60	0.51	33.00
1.10	9.60	2.17	1.22	0.81	8.30	2.60	3.30	0.40	23.00
0.80	6.50	2.05	1.12	0.73	7.80	2.40	3.90	0.37	20.00
1.20	11.70	2.15	1.23	0.78	8.30	2.60	3.40	0.40	23.00
2.50	19.50	2.65	1.53	0.98	13.20	3.20	3.60	0.50	30.00
2.10	17.80	2.54	1.51	0.93	11.50	3.10	3.60	0.47	27.00
2.80	22.60	2.71	1.52	1.00	14.10	3.40	3.40	0.50	30.00
1.70	13.90	2.53	1.42	0.91	10.40	3.00	3.80	0.46	26.00
3.30	16.00	2.24	1.35	0.88	19.30	2.60	4.40	0.43	23.00

1.60	12.50	2.16	1.23	0.78	9.70	2.70	2.80	0.38	25.00
3.50	28.40	3.38	1.94	1.21	17.80	4.00	4.70	0.61	37.00
6.00	39.50	3.72	2.04	1.38	23.10	4.80	3.80	0.64	46.00
2.50	15.60	2.17	1.21	0.82	12.30	2.80	2.60	0.39	28.00
3.50	24.90	3.16	1.83	1.15	17.50	3.90	4.10	0.57	36.00
1.20	9.00	2.22	1.21	0.82	9.10	2.60	2.50	0.39	23.00
1.50	12.30	2.58	1.45	0.91	10.10	3.10	4.70	0.47	29.00
0.80	5.80	2.17	1.21	0.76	7.20	2.50	3.90	0.40	20.00
2.40	17.40	2.67	1.52	0.92	12.50	3.30	3.90	0.50	30.00
1.80	13.60	2.24	1.26	0.81	9.90	2.80	2.90	0.41	25.00
1.80	14.20	2.47	1.38	0.88	10.70	3.00	3.70	0.44	26.00
1.70	11.60	2.48	1.45	0.89	10.00	3.10	4.20	0.46	26.00
2.00	15.10	2.42	1.38	0.85	10.90	2.80	3.00	0.44	25.00
1.60	11.80	2.42	1.38	0.89	10.30	2.90	4.20	0.44	25.00
2.60	17.10	2.65	1.52	0.96	13.10	3.30	3.60	0.48	28.00
1.10	9.10	2.18	1.23	0.78	8.00	2.70	3.90	0.39	21.00
2.80	22.60	2.97	1.90	1.02	14.60	3.70	4.00	0.53	33.00
1.00	7.10	2.28	1.33	0.82	8.90	2.70	4.40	0.41	22.00
1.00	8.70	2.19	1.24	0.74	7.70	2.80	3.80	0.41	25.00
2.60	18.00	2.57	1.42	0.94	13.00	3.30	3.50	0.47	31.00
2.20	18.20	2.54	1.47	0.95	12.60	3.10	3.20	0.48	29.00
1.60	12.70	2.27	1.22	0.78	9.40	2.70	3.20	0.41	22.00
1.70	13.70	2.37	1.27	0.86	10.40	2.80	3.00	0.42	26.00
2.10	16.10	2.43	1.39	0.88	11.70	3.10	3.50	0.44	27.00
4.00	23.10	3.40	1.92	1.21	18.60	4.40	4.90	0.61	41.00
2.10	15.40	2.48	1.41	0.91	11.70	3.00	3.70	0.44	28.00
1.30	15.50	2.32	1.27	0.84	9.20	3.10	3.80	0.43	24.00
2.30	22.50	2.75	1.47	0.95	12.30	3.80	4.90	0.54	32.00
1.90	14.10	2.49	1.36	0.88	10.50	3.20	3.60	0.46	26.00

2.40	17.80	2.54	1.38	0.94	11.90	3.50	3.60	0.49	29.00
2.10	15.30	2.51	1.38	0.89	11.20	3.20	3.80	0.47	26.00
1.20	10.60	2.44	1.38	0.83	9.00	3.20	4.90	0.47	26.00
3.90	23.20	3.11	1.70	1.11	15.50	4.20	3.90	0.58	36.00
3.60	23.80	2.95	1.63	1.10	15.60	4.20	4.40	0.57	37.00
2.10	14.80	2.36	1.37	0.87	10.50	3.30	3.50	0.46	25.00
2.50	16.20	2.58	1.47	0.89	11.60	3.50	3.70	0.49	29.00
2.30	15.40	2.67	1.50	0.94	10.90	3.50	3.70	0.51	30.00
3.20	21.70	2.68	1.52	0.98	13.90	3.60	3.20	0.50	30.00
2.60	42.60	2.51	1.45	0.91	12.30	3.30	3.20	0.49	27.00
2.90	18.20	3.12	1.73	1.10	13.60	4.00	5.00	0.62	32.00
1.60	10.60	2.37	1.31	0.84	9.20	3.20	3.70	0.46	25.00
1.80	42.60	2.14	1.26	0.77	9.00	2.90	2.50	0.42	24.00
2.00	13.20	2.10	1.24	0.79	9.50	2.80	3.10	0.42	23.00
3.00	19.10	2.47	1.46	0.92	12.70	3.40	3.50	0.50	30.00
0.90	8.20	1.87	1.13	0.74	7.30	2.60	3.00	0.37	19.00
3.10	25.90	2.96	1.72	0.99	11.40	3.80	3.50	0.58	29.00
1.20	12.40	2.16	1.28	0.80	8.50	2.90	4.10	0.42	23.00
2.00	14.20	2.47	1.45	0.91	10.80	3.40	4.20	0.49	29.00
2.00	14.00	2.33	1.35	0.85	10.50	3.10	4.00	0.46	25.00
2.00	13.20	2.52	1.44	0.91	10.80	3.40	4.10	0.51	27.00
3.90	22.70	2.97	1.72	1.09	16.10	4.00	3.50	0.60	33.00
3.60	23.90	2.72	1.56	1.00	14.80	3.60	3.50	0.57	31.00
2.20	12.60	2.71	1.56	0.93	11.20	3.70	3.90	0.52	30.00
3.00	27.60	2.75	1.59	0.99	13.20	3.80	4.10	0.54	32.00
2.00	12.80	2.52	1.52	0.92	10.70	3.50	3.60	0.50	26.00
1.00	8.00	2.06	1.12	0.73	7.10	2.60	2.90	0.38	20.00
1.00	8.00	1.93	1.10	0.75	7.60	2.60	3.10	0.38	19.00

2.00	11.60	2.50	1.41	0.88	10.80	3.50	4.40	0.50	29.00
1.30	8.90	2.38	1.36	0.84	8.80	3.20	4.40	0.45	23.00
2.30	12.90	2.75	1.57	0.97	10.40	3.40	4.00	0.54	26.00
1.70	15.60	2.12	1.23	0.73	8.80	2.70	3.20	0.40	22.00
2.90	20.60	2.58	1.50	0.92	12.20	3.40	4.00	0.49	28.00
2.60	18.10	2.75	1.59	1.01	12.80	3.80	4.50	0.55	30.00
4.20	24.90	3.60	1.98	1.32	18.90	4.90	4.60	0.69	40.00
1.50	10.40	2.25	1.26	0.84	9.20	2.90	3.50	0.43	24.00
1.90	13.80	2.75	1.66	0.97	10.70	3.90	5.10	0.52	30.00
1.70	12.30	2.48	1.40	0.89	9.70	3.40	4.40	0.49	25.00
3.20	23.40	3.04	1.78	1.13	15.20	4.20	4.70	0.59	32.00
1.80	13.80	2.66	1.50	0.95	10.50	3.50	4.80	0.51	26.00
1.80	13.30	2.52	1.43	0.91	9.40	3.30	4.50	0.49	22.00
3.00	21.80	2.76	1.64	1.04	13.60	3.80	3.80	0.55	29.00
1.90	14.30	2.45	1.40	0.94	10.90	3.30	4.00	0.47	24.00
3.00	20.10	2.66	1.51	0.95	13.00	3.50	3.50	0.51	29.00
3.10	20.70	2.69	1.55	0.96	13.50	3.60	3.30	0.52	28.00
2.60	8.70	3.20	1.86	1.19	15.90	4.20	6.80	0.62	31.00
2.30	17.50	2.56	1.47	0.97	12.00	3.50	4.20	0.50	27.00
1.10	8.60	2.03	1.20	0.77	8.00	2.60	2.90	0.39	19.00
1.60	12.00	2.44	1.44	0.91	9.90	3.30	4.00	0.47	26.00
1.60	11.00	2.45	1.41	0.90	9.80	3.30	4.40	0.47	25.00
1.20	9.40	2.44	1.37	0.85	8.70	3.30	4.60	0.48	25.00
2.70	19.10	2.82	1.54	1.04	13.10	3.80	3.90	0.53	31.00
0.90	8.50	1.81	1.06	0.71	7.20	2.40	2.70	0.35	17.00
1.00	8.70	2.03	1.19	0.78	7.80	2.70	3.40	0.39	20.00
1.70	12.30	2.49	1.44	0.92	10.00	3.30	4.10	0.49	26.00

2.40	18.40	2.64	1.49	0.95	12.30	3.50	4.20	0.50	27.00
0.90	9.50	2.50	1.43	0.83	7.80	3.40	5.60	0.49	25.00
3.60	24.40	3.14	1.80	1.12	14.80	4.20	4.10	0.61	34.00
2.20	18.30	2.48	1.39	0.92	11.10	3.40	3.70	0.48	28.00
1.10	11.60	2.20	1.27	0.80	8.70	2.90	4.60	0.43	23.00
1.30	12.40	2.23	1.26	0.78	8.90	2.80	4.10	0.42	23.00
1.10	8.80	2.17	1.24	0.77	8.20	3.00	3.80	0.42	22.00
1.70	14.10	2.36	1.33	0.89	9.50	3.20	3.40	0.46	23.00
1.20	9.70	2.40	1.41	0.89	9.00	3.20	5.40	0.47	24.00
1.10	8.40	2.17	1.22	0.79	8.30	2.90	4.10	0.41	20.00
1.90	13.10	2.21	1.28	0.82	9.30	3.00	2.70	0.44	21.00
2.40	16.50	2.65	1.46	0.90	10.90	3.50	4.30	0.46	31.00
3.10	20.80	2.69	1.40	0.88	11.80	3.40	3.40	0.46	30.00
2.30	16.20	2.62	1.42	0.88	10.40	3.60	4.20	0.46	29.00
5.20	27.20	3.56	1.94	1.15	16.90	4.60	3.80	0.65	41.00
2.00	25.60	2.88	1.54	0.87	8.70	4.20	5.70	0.51	32.00
2.10	8.70	2.76	1.52	0.86	13.20	3.70	7.70	0.49	28.00
2.80	17.10	2.99	1.65	0.96	11.10	3.70	3.70	0.53	31.00
3.60	22.60	3.10	1.60	0.96	12.80	4.00	3.20	0.53	35.00
1.10	9.20	2.63	1.46	0.80	7.70	3.40	6.10	0.46	25.00
0.70	8.40	2.76	1.45	0.75	6.10	3.80	6.80	0.48	31.00
3.30	19.80	3.05	1.70	0.96	12.00	3.90	4.80	0.52	31.00
2.40	15.30	2.54	1.45	0.81	10.00	3.40	4.50	0.47	28.00
2.80	18.20	2.60	1.64	0.90	10.80	3.60	4.20	0.46	30.00
1.80	11.70	2.41	1.39	0.76	8.20	3.20	4.30	0.42	27.00
2.70	17.00	2.57	1.39	0.82	10.40	3.50	3.70	0.47	28.00
2.40	16.00	2.52	1.42	0.84	10.10	3.30	3.90	0.46	28.00
3.00	19.20	2.77	1.57	0.91	11.30	3.70	3.60	0.50	31.00

2.70	16.80	2.60	1.47	0.87	10.40	3.60	3.50	0.48	29.00
2.50	16.50	2.48	1.38	0.81	9.80	3.20	3.70	0.44	27.00
2.00	11.10	2.68	1.52	0.83	8.60	3.50	5.20	0.49	30.00
2.50	16.60	2.63	1.48	0.87	10.00	3.40	3.70	0.47	29.00
1.80	10.00	1.70	0.88	0.50	6.30	2.10	2.10	0.27	19.00
1.40	8.50	1.45	0.80	0.49	5.50	1.90	2.10	0.26	16.00
1.20	7.60	1.32	0.78	0.42	4.30	1.70	1.60	0.24	13.00
1.20	7.60	1.32	0.74	0.40	4.20	1.70	1.60	0.24	12.00
2.30	13.40	2.45	1.36	0.80	9.20	3.20	3.60	0.44	26.00
2.30	13.30	1.98	1.12	0.71	8.40	2.80	2.70	0.37	25.00
3.40	18.60	2.97	1.65	0.93	11.50	3.80	3.80	0.53	31.00
2.40	16.60	2.80	1.55	0.92	10.40	3.60	4.90	0.50	29.00
2.90	19.20	2.66	1.48	0.87	11.40	3.50	2.90	0.52	29.00
2.90	16.70	2.90	1.56	0.88	10.60	3.70	4.30	0.52	30.00
2.40	13.60	2.01	1.11	0.71	8.40	2.70	2.80	0.34	24.00
3.20	20.40	3.01	1.66	0.95	11.50	3.90	4.00	0.54	31.00
2.40	16.00	3.02	1.59	0.87	10.20	3.80	5.50	0.51	30.00
3.30	22.30	3.13	1.68	1.03	12.30	4.10	4.30	0.55	33.00
4.60	30.50	3.51	1.82	1.14	16.10	4.60	4.00	0.61	37.00
3.80	23.50	3.49	1.89	1.10	13.70	4.80	5.50	0.60	40.00
3.80	21.60	2.90	1.60	0.95	12.80	3.80	3.70	0.52	34.00
4.00	21.80	2.96	1.64	1.02	13.50	3.80	3.80	0.56	33.00
4.00	22.20	3.11	1.68	0.98	13.60	4.00	4.00	0.54	34.00
5.00	22.60	3.43	1.87	1.13	16.10	4.60	4.00	0.61	39.00
4.20	19.40	3.20	1.82	1.08	14.20	4.40	4.50	0.58	36.00
3.80	18.00	3.37	1.80	1.05	13.60	4.60	4.70	0.58	37.00
4.80	21.50	3.44	1.88	1.13	15.50	4.60	4.20	0.60	39.00



Li (ppm)	Mo (ppm)	Nb (ppm)	Nd (ppm)	Ni (ppm)	Pb (ppm)	Pr (ppm)	Rb (ppm)	Sc (ppm)	Sm (ppm)
15.00	0.69	5.70	19.00	19.40	10.60	5.40	52.40	4.30	3.70
23.00	0.54	6.80	23.40	24.40	13.10	6.60	66.70	5.20	4.50
18.00	0.50	5.20	17.90	21.20	10.80	5.10	47.10	3.80	3.60
34.00	0.88	7.20	23.80	31.80	14.20	6.90	81.60	5.50	4.50
16.00	0.36	5.60	17.90	17.40	10.90	5.00	51.20	4.10	3.40
23.00	0.45	7.20	21.40	23.40	12.30	6.00	59.40	5.30	4.20
20.00	0.51	6.40	20.80	20.90	11.10	5.80	54.30	4.80	4.10
19.00	0.60	5.50	17.10	21.60	10.90	4.80	51.10	4.00	3.40
55.00	1.17	9.80	29.20	42.40	16.70	8.50	98.90	8.00	5.40
19.00	0.42	6.40	19.80	22.20	13.60	5.50	56.40	4.70	3.80
15.00	0.68	6.70	19.40	17.30	12.50	5.50	46.80	4.00	4.00
20.00	0.66	7.00	20.80	20.10	13.20	5.80	51.00	4.50	4.10
15.00	0.38	5.90	18.50	17.10	10.60	5.20	42.80	4.00	3.60
16.00	0.52	7.00	21.70	19.50	12.30	6.00	45.40	4.50	4.30
23.00	0.56	5.80	17.70	22.80	12.70	5.00	64.10	4.80	3.30
21.00	0.63	7.40	23.50	24.70	13.40	6.70	64.50	5.70	4.50
30.00	0.44	8.50	26.60	32.00	15.60	7.40	82.90	7.50	5.00
20.00	0.48	6.50	19.90	20.60	13.00	5.70	62.50	4.70	3.90
30.00	0.64	8.60	25.80	27.60	15.00	7.30	79.80	6.70	5.00
17.00	0.62	6.60	21.40	19.30	11.50	5.90	54.00	4.70	4.20
13.00	0.35	8.20	29.20	15.80	13.90	8.20	51.80	4.80	5.80
13.00	0.40	5.90	21.40	15.90	11.80	6.10	51.50	4.20	4.10
15.00	0.27	6.20	20.70	17.80	12.30	5.70	52.40	4.50	4.00
11.00	0.25	5.70	21.30	14.00	11.40	5.90	45.60	4.10	4.40
21.00	0.32	7.10	23.90	23.20	14.00	6.80	62.70	5.60	4.60

21.00	0.44	6.60	20.90	22.50	13.70	5.90	62.90	5.00	4.10
12.00	0.25	5.20	18.50	14.60	10.80	5.20	45.30	3.50	3.70
29.00	0.35	7.50	22.60	25.20	12.90	6.30	69.40	5.90	4.30
36.00	0.60	7.60	23.20	32.00	14.60	6.60	78.60	6.50	4.50
25.00	0.78	6.70	23.00	27.20	13.20	6.60	64.40	5.50	4.50
29.00	0.60	10.20	31.00	25.80	17.30	8.80	80.10	6.50	5.80
25.00	0.39	7.10	24.60	23.50	14.30	7.00	70.90	5.50	4.70
24.00	0.54	6.90	21.00	24.70	11.90	5.90	64.90	5.40	4.10
27.00	0.61	7.60	22.80	28.40	13.10	6.60	63.50	5.90	4.40
43.00	0.62	8.70	28.20	41.00	16.50	8.00	104.00	8.40	5.30
44.00	0.50	9.40	27.60	32.80	14.40	7.60	92.20	7.70	4.50
25.00	0.42	7.90	22.90	25.80	13.10	6.50	68.40	6.00	4.60
12.00	0.27	6.20	22.70	15.20	11.70	6.40	51.80	4.00	4.60
19.00	0.48	6.80	23.00	22.30	14.90	6.50	58.90	5.50	4.40
25.00	0.60	7.10	23.80	25.80	12.90	6.60	65.90	5.70	4.70
53.00	0.45	10.10	33.60	44.90	19.40	9.80	124.00	9.40	6.10
31.00	0.47	7.30	23.10	28.50	13.00	6.50	76.40	6.20	4.50
43.00	0.47	9.10	30.00	37.60	16.80	8.80	109.00	8.00	5.60
14.00	0.26	6.30	22.30	16.50	11.30	6.20	53.30	4.10	4.20
29.00	0.41	7.20	24.20	24.30	13.50	6.90	76.70	5.80	4.70
35.00	0.42	7.20	23.20	29.70	13.00	6.60	77.00	6.20	4.30
40.00	0.43	7.80	24.40	34.40	14.40	7.00	91.60	7.00	4.60
21.00	0.70	7.30	22.40	23.80	11.10	6.10	60.10	5.50	4.50
17.00	0.36	6.40	19.70	19.20	11.60	5.60	57.50	4.50	4.00
20.00	0.33	7.10	23.00	22.50	12.70	6.50	60.80	5.00	4.40
30.00	0.43	7.30	23.70	28.10	13.50	7.00	75.30	6.20	4.60
24.00	0.61	6.10	19.90	22.80	12.10	5.60	61.30	4.80	3.80

20.00	0.36	6.30	21.80	22.30	13.20	6.10	61.50	5.00	4.20
56.00	0.49	9.90	30.60	48.00	18.90	8.70	123.00	9.80	5.80
26.00	0.34	6.80	22.60	25.00	12.50	6.40	69.40	5.50	4.30
21.00	0.46	7.70	21.70	20.50	11.50	6.10	60.00	5.30	4.40
12.00	0.29	5.90	17.50	14.80	10.40	4.90	45.80	3.80	3.60
28.00	0.44	7.40	24.30	24.80	12.80	6.90	75.10	5.60	4.70
27.00	0.60	6.50	22.10	26.90	12.20	6.20	70.50	5.40	4.10
22.00	0.39	7.20	22.00	24.80	12.80	6.20	61.00	5.50	4.40
24.00	0.30	7.40	22.80	24.20	12.90	6.30	64.90	5.50	4.40
19.00	0.34	7.00	21.20	21.80	12.10	5.90	58.10	5.10	4.20
33.00	0.60	8.10	22.60	29.20	11.90	6.20	71.60	6.10	3.70
45.00	0.71	9.40	26.70	29.00	13.50	7.30	90.50	7.60	4.20
35.00	0.48	8.10	23.30	21.40	11.10	6.30	69.00	5.90	3.80
39.00	0.44	10.30	26.60	27.60	12.80	7.20	76.60	7.00	4.30
35.00	0.70	9.60	26.20	25.50	13.00	7.20	77.10	6.60	4.20
13.00	0.25	7.20	20.60	11.40	10.90	5.60	41.00	3.70	3.40
30.00	0.99	12.40	32.40	24.30	16.10	9.00	81.00	6.90	5.40
27.00	0.57	12.00	31.10	23.50	15.10	8.60	79.40	6.60	5.20
42.00	0.32	9.50	27.10	32.60	13.40	7.60	91.50	7.70	4.50
16.00	0.23	6.30	16.80	19.70	10.40	4.70	50.70	4.40	3.00
37.00	0.38	8.90	27.00	27.70	12.70	7.60	84.80	7.00	4.40
18.00	0.35	6.10	17.70	19.70	9.66	4.80	53.40	4.50	3.00
42.00	0.74	8.20	24.10	31.20	12.60	6.60	75.90	6.50	4.00
36.00	0.57	7.50	21.90	30.50	13.40	6.10	75.40	6.10	3.60
43.00	0.60	9.00	26.10	35.50	13.40	7.00	90.40	7.80	4.20
17.00	0.30	6.80	18.80	16.20	11.30	5.10	55.60	4.50	3.90
27.00	0.43	7.60	22.00	23.50	11.40	5.90	63.90	5.50	3.70

38.00	0.46	8.40	24.20	28.20	12.40	6.70	80.70	7.00	4.00
34.00	0.62	9.50	24.50	25.80	11.60	6.60	74.20	7.00	4.10
37.00	0.48	8.20	23.80	26.70	12.10	6.50	79.40	6.90	4.00
34.00	0.54	8.80	23.80	27.50	11.40	6.50	76.90	6.80	4.10
37.00	0.61	9.40	25.80	27.80	13.00	7.00	85.30	7.60	4.50
37.00	0.82	9.00	24.10	30.20	12.90	6.60	79.30	6.90	3.90
28.00	0.47	8.30	21.20	22.10	12.30	5.80	60.90	5.10	3.50
42.00	0.39	9.40	27.60	31.20	14.50	7.60	94.60	7.80	4.40
23.00	0.37	7.40	21.10	20.30	10.90	5.80	60.00	5.30	3.60
49.00	0.59	10.30	28.20	34.30	14.60	7.60	100.00	8.70	4.60
50.00	0.92	10.80	27.90	33.40	14.90	7.60	102.00	9.10	4.90
14.00	0.25	6.70	19.60	12.20	9.63	5.40	48.50	4.20	3.30
14.00	0.20	6.80	18.70	12.30	10.10	5.00	49.40	4.30	3.10
20.00	0.24	7.30	21.60	18.10	11.70	5.80	59.70	5.30	3.70
54.00	0.34	11.50	33.50	37.20	17.20	9.20	116.00	10.10	5.50
34.00	0.30	10.20	27.50	22.50	15.10	7.50	89.80	7.60	4.60
14.00	0.25	7.90	23.90	16.20	11.40	6.40	54.00	5.00	4.00
57.00	0.38	11.40	32.30	38.50	15.60	9.00	118.00	9.80	5.30
36.00	0.38	9.00	25.40	30.80	13.20	6.70	80.70	7.40	4.10
16.00	0.29	6.90	19.20	17.80	10.30	5.10	50.40	4.80	3.30
10.00	0.26	6.00	17.10	13.20	10.60	4.50	45.80	4.00	2.90
17.00	0.29	6.60	18.40	20.50	11.10	4.80	50.20	4.80	3.00
36.00	0.39	8.60	24.00	31.30	13.40	6.40	79.10	7.50	4.00
28.00	0.28	8.20	22.90	29.90	12.40	5.90	70.10	6.80	3.70
38.00	0.37	8.90	25.00	34.60	14.00	6.70	85.30	8.10	4.00
24.00	0.44	7.80	22.00	29.40	12.10	5.70	61.60	6.20	3.60
45.00	0.58	13.40	19.70	42.40	18.50	5.30	84.50	9.10	3.20

22.00	0.32	7.00	19.20	24.90	10.60	5.10	57.70	5.50	3.20
47.00	0.40	11.90	30.30	39.20	17.50	8.00	106.00	10.10	4.80
75.00	0.66	12.80	36.60	62.60	21.40	9.90	151.00	13.00	5.70
33.00	0.38	7.70	21.60	32.00	13.10	5.90	84.90	6.40	3.40
44.00	0.29	11.40	29.30	40.40	16.30	7.70	104.00	10.00	4.80
16.00	0.19	7.50	19.40	19.80	9.81	5.00	54.20	5.20	3.20
22.00	0.30	8.00	23.50	24.60	11.60	6.20	60.00	5.80	3.90
11.00	0.21	6.30	17.20	14.10	9.55	4.50	42.20	4.10	3.00
35.00	0.29	8.60	24.20	27.80	12.80	6.50	76.40	6.90	4.00
26.00	0.28	7.90	20.40	26.90	11.40	5.30	61.10	5.80	3.30
25.00	0.33	7.70	21.80	25.50	11.60	5.70	64.40	6.20	3.50
23.00	0.26	8.00	21.90	26.40	11.60	5.70	61.30	6.00	3.70
26.00	0.31	8.20	21.00	28.20	11.40	5.50	64.50	6.60	3.40
20.00	0.23	7.70	21.70	24.00	12.10	5.70	60.00	5.80	3.60
35.00	0.39	9.10	23.20	33.00	20.50	6.20	80.70	7.70	3.80
15.00	0.37	7.20	18.60	19.40	9.91	4.80	49.20	4.80	3.30
38.00	0.44	9.80	27.30	37.80	15.50	7.10	88.30	8.10	4.40
14.00	0.19	7.20	18.40	15.40	10.60	4.80	51.40	4.70	3.20
16.00	0.26	6.40	20.10	18.00	10.60	5.30	47.10	4.40	3.20
35.00	0.25	8.50	24.40	31.00	13.00	6.50	82.00	7.30	3.90
31.00	0.25	8.60	22.70	33.00	12.50	5.90	73.20	7.30	3.70
21.00	0.25	6.80	19.20	22.50	11.10	5.00	58.40	5.40	3.10
23.00	0.24	7.30	20.60	24.30	11.90	5.40	64.70	5.60	3.40
29.00	0.33	8.00	22.60	28.80	12.80	5.90	72.60	6.50	3.60
52.00	0.36	11.50	32.40	43.50	17.50	8.50	112.00	10.40	5.20
28.00	0.19	8.20	22.40	27.30	13.10	5.90	72.40	6.50	3.60
17.00	0.29	6.60	20.80	17.10	10.80	5.60	58.80	5.20	3.50
30.00	0.55	8.40	26.80	26.10	13.10	7.30	78.40	6.80	4.50
23.00	0.28	8.00	23.50	20.50	11.00	6.30	68.20	5.70	3.90

32.00	0.28	8.10	24.10	23.80	11.90	6.60	78.80	6.70	4.10
25.00	0.33	7.90	22.50	22.50	12.10	6.00	73.90	5.90	3.70
16.00	0.27	7.30	22.60	15.20	10.50	6.10	54.90	5.00	3.90
48.00	0.45	10.20	30.50	36.60	15.80	8.40	104.00	8.60	4.90
45.00	0.42	9.70	30.50	34.80	15.00	8.20	99.90	8.30	4.80
27.00	0.41	7.70	22.40	22.50	11.30	6.00	66.80	5.80	3.70
33.00	0.40	8.10	24.40	25.40	12.40	6.60	77.10	6.30	4.00
31.00	0.33	8.20	24.50	24.90	11.80	6.80	67.30	6.20	4.20
45.00	0.43	8.70	25.40	33.50	13.10	6.90	86.00	7.80	4.30
37.00	0.38	8.10	23.30	27.70	11.90	6.30	75.50	7.00	3.80
38.00	0.40	10.10	28.20	27.40	14.20	7.60	83.50	7.80	4.60
21.00	0.21	7.00	21.80	17.30	10.60	5.90	59.30	5.00	3.60
24.00	0.29	6.70	19.50	26.00	11.30	5.30	58.00	5.00	3.20
28.00	0.31	6.80	19.40	24.10	10.80	5.20	61.50	5.20	3.20
40.00	0.40	8.30	24.60	28.80	12.90	6.80	82.00	6.90	4.10
12.00	0.24	6.30	17.20	16.20	8.88	4.50	45.90	4.00	2.90
33.00	0.53	9.40	25.50	23.70	11.90	6.80	75.30	7.40	4.40
16.00	0.32	6.30	19.40	18.20	10.50	5.20	52.00	4.40	3.30
27.00	0.37	7.70	24.30	24.60	12.80	6.50	67.10	5.80	4.00
26.00	0.34	7.40	21.90	21.30	11.70	5.90	64.10	5.60	3.60
26.00	0.46	8.30	22.80	23.70	13.40	6.20	68.60	5.70	3.90
52.00	0.45	9.90	27.70	36.90	13.30	7.40	102.00	9.00	4.60
43.00	0.38	9.30	26.70	36.70	13.60	7.40	99.40	8.10	4.50
30.00	0.35	7.90	25.10	22.40	12.30	6.80	69.40	6.00	4.20
39.00	0.40	8.80	27.20	29.00	13.50	7.50	86.90	7.00	4.30
28.00	0.37	7.90	22.90	20.20	11.50	6.20	69.50	5.80	3.90
14.00	0.31	6.10	17.80	18.20	8.48	4.80	46.90	4.00	3.00
13.00	0.26	6.20	17.50	22.10	9.37	4.70	47.80	4.00	3.00

28.00	0.41	8.70	24.30	24.10	11.60	6.70	71.70	5.70	4.00
19.00	0.33	6.90	20.70	18.60	10.30	5.50	56.00	4.60	3.60
23.00	0.44	9.00	23.50	18.20	11.50	6.20	65.20	6.00	4.00
24.00	0.39	6.70	18.60	24.10	9.82	5.10	55.50	4.90	3.10
36.00	0.46	8.40	24.20	26.90	12.40	6.60	78.40	6.80	4.00
34.00	0.34	8.60	26.20	27.20	13.00	7.10	78.20	7.10	4.30
56.00	0.41	11.00	34.40	40.50	16.60	9.40	114.00	10.50	5.60
20.00	0.31	6.80	21.00	18.70	10.90	5.60	58.40	4.80	3.60
25.00	0.49	8.10	25.40	19.20	13.20	7.20	66.30	6.00	4.50
22.00	0.44	7.70	21.80	16.10	11.90	6.00	60.10	5.50	3.80
38.00	0.58	10.00	27.70	29.00	14.90	8.00	92.90	8.70	4.80
22.00	0.48	8.00	22.70	17.90	13.50	6.30	65.80	5.70	4.00
23.00	0.46	7.80	20.70	19.10	11.30	5.70	56.60	5.70	3.60
38.00	0.62	9.60	25.40	29.00	14.20	7.10	81.70	7.90	4.30
23.00	0.33	7.80	20.70	17.20	12.80	5.80	66.00	5.80	3.60
39.00	0.35	8.70	23.90	28.50	13.40	6.80	80.20	7.40	4.10
42.00	0.55	8.80	24.50	28.70	13.30	6.90	83.00	7.70	4.00
35.00	0.51	11.80	27.30	22.20	16.80	7.60	100.00	8.40	4.80
29.00	0.32	8.30	23.20	20.10	11.80	6.60	71.80	7.20	4.10
15.00	0.24	6.70	17.00	18.00	9.23	4.80	48.90	4.60	3.00
21.00	0.27	7.70	22.10	18.90	10.70	6.10	58.50	5.60	3.70
20.00	0.39	7.60	21.70	18.70	11.20	6.10	59.50	5.40	3.70
16.00	0.32	7.40	21.80	16.10	10.80	6.00	52.30	4.90	3.80
34.00	0.46	9.00	25.50	23.30	14.50	7.20	81.00	7.30	4.30
12.00	0.24	5.80	15.10	18.00	8.68	4.20	44.10	3.90	2.70
13.00	0.25	6.30	17.60	18.30	10.10	4.90	47.20	4.20	3.10
22.00	0.37	7.80	21.00	19.80	11.60	6.00	60.50	5.40	3.70
30.00	0.56	8.40	23.10	21.50	13.30	6.60	74.30	6.80	4.00

11.00	0.29	7.10	21.70	19.20	11.30	6.10	44.50	4.60	3.90
42.00	0.58	10.50	28.20	32.20	15.60	8.10	92.30	8.40	4.90
28.00	0.36	7.90	23.40	19.20	12.50	6.50	71.90	6.30	3.90
14.00	0.30	6.20	18.80	19.30	10.90	5.30	52.00	4.50	3.40
17.00	0.34	6.60	18.80	21.50	13.10	5.30	54.00	4.70	3.30
15.00	0.32	6.50	19.80	19.60	10.20	5.50	51.30	4.40	3.50
20.00	0.22	7.30	20.60	19.10	11.70	5.60	61.10	5.30	3.60
15.00	0.25	7.20	21.20	19.20	13.00	5.90	53.80	4.70	3.70
14.00	0.28	6.40	18.30	19.00	10.30	5.10	49.80	4.40	3.20
23.00	0.30	7.10	19.50	27.90	11.70	5.40	58.40	5.40	3.40
29.00	0.65	7.80	23.80	27.50	14.00	6.40	74.5	6.6	4.2
38.00	0.88	8.30	23.50	36.40	13.60	6.30	78.5	7.6	3.9
26.00	0.51	7.50	23.70	27.10	13.40	6.40	71.7	6.3	3.9
57.00	0.37	11.70	32.90	47.20	18.60	8.80	119	10.9	5.4
21.00	0.28	7.80	27.00	22.60	12.10	7.00	60.4	5.7	4.6
28.00	0.35	11.10	24.40	23.70	16.50	6.40	72.6	7.3	4.4
33.00	0.31	8.80	25.90	30.70	13.30	6.80	73	7.5	4.4
43.00	0.32	9.50	28.00	37.10	14.70	7.40	86	8.4	4.6
13.00	0.24	7.10	21.80	17.10	11.10	5.80	47.3	4.8	3.8
9.00	0.51	6.80	25.30	16.90	11.10	6.80	35.6	4.3	4.3
40.00	0.63	9.80	26.00	34.80	14.40	7.00	78.9	8	4.3
31.00	0.76	7.70	22.00	29.60	13.20	5.90	65.3	6.4	3.7
37.00	0.84	8.20	24.00	33.70	13.40	6.40	72	6.8	3.9
23.00	0.57	7.10	21.70	24.50	11.50	5.80	52.5	5.2	3.6
35.00	0.66	7.70	22.90	30.10	13.00	6.10	68.7	6.6	3.8
33.00	0.51	7.60	21.50	29.10	12.80	5.80	67.1	6.3	3.6
39.00	0.45	8.40	24.20	33.00	14.00	6.50	74.9	7.3	4.1



33.00	0.48	8.00	23.40	29.30	13.50	6.20	69.2	6.5	4
32.00	0.57	7.60	21.40	27.50	12.60	5.70	64.8	6.3	3.8
26.00	0.58	9.10	24.40	22.00	12.20	6.40	56.7	5.7	4.2
33.00	0.43	8.20	23.60	27.90	13.60	6.20	65.5	6.4	3.9
23.00	0.39	4.70	14.30	20.40	9.81	3.90	42.3	3.7	2.5
20.00	0.26	4.20	13.40	19.40	9.08	3.60	36.9	3.3	2.2
20.00	0.38	3.80	10.20	21.60	7.70	2.70	26.6	2.8	1.8
20.00	0.28	3.70	10.40	21.70	7.69	2.70	26	2.8	1.8
30.00	0.68	7.90	21.40	26.10	12.60	5.80	59.3	5.8	3.5
30.00	0.47	6.30	19.20	25.80	12.60	5.20	58.6	5	3.2
43.00	0.57	10.30	25.40	33.10	14.40	6.80	74.9	7.7	4.3
27.00	0.44	8.30	24.50	27.40	13.30	6.60	68.3	6.5	4.1
37.00	0.39	8.70	23.70	33.50	13.60	6.30	72.4	7.1	4
38.00	0.67	9.60	24.50	31.00	13.40	6.50	69	7	4.2
30.00	0.43	6.30	18.50	25.80	12.30	5.00	59	4.9	2.9
38.00	0.47	8.90	25.10	33.80	13.90	6.80	75.8	7.9	4.3
29.00	0.50	9.00	24.50	28.30	13.00	6.50	64.2	6.9	4.2
40.00	0.79	10.20	26.50	34.80	15.30	7.10	80.2	8.2	4.6
52.00	0.86	10.80	31.10	48.80	18.00	8.40	107	10.7	5.1
43.00	0.73	10.60	33.10	38.40	17.50	8.90	96	8.6	5.5
47.00	0.62	9.80	26.40	37.80	15.80	7.10	91.1	8	4.4
48.00	0.63	10.20	26.70	38.00	16.00	7.20	92.3	8.3	4.4
48.00	0.73	10.10	28.00	38.40	16.60	7.40	93.2	8.3	4.6
50.00	0.83	11.00	32.30	42.60	19.30	8.80	120	9.7	5.3
42.00	0.70	10.00	29.60	37.20	17.60	8.00	105	8.5	5
38.00	0.68	9.90	29.90	33.90	17.50	8.10	96.9	8.3	5
47.00	0.70	10.90	32.20	40.90	18.00	8.70	113	9.4	5.2

Sn (ppm)	Sr (ppm)	Ta (ppm)	Tb (ppm)	Th (ppm)	U (ppm)	V (ppm)	W (ppm)	Y (ppm)	Yb (ppm)
0.70	204.00	0.44	0.35	7.12	1.83	39.70	0.50	11.00	1.03
0.95	212.00	0.55	0.42	9.90	1.65	50.40	0.60	12.80	1.24
0.70	162.00	0.39	0.34	7.71	1.59	36.00	0.40	10.90	1.06
1.17	182.00	0.57	0.42	11.50	1.87	55.90	0.60	13.60	1.33
0.71	186.00	0.43	0.34	7.82	1.46	36.30	0.40	10.80	1.05
0.91	203.00	0.51	0.41	8.24	1.89	51.70	0.50	13.10	1.36
0.84	196.00	0.47	0.39	7.97	1.76	44.20	0.40	12.30	1.28
0.71	172.00	0.41	0.33	7.23	1.49	38.20	0.40	10.90	1.10
1.55	203.00	0.70	0.49	13.20	2.39	93.60	0.80	15.20	1.50
0.82	185.00	0.50	0.39	8.64	2.16	42.70	0.60	11.80	1.20
0.74	191.00	0.53	0.37	8.34	1.85	36.80	0.40	11.80	1.25
0.84	200.00	0.55	0.38	8.77	2.08	44.20	0.50	12.20	1.28
0.73	181.00	0.43	0.34	7.34	1.68	35.60	0.40	10.70	1.11
0.84	194.00	0.48	0.40	9.10	1.84	39.60	0.60	12.70	1.36
0.90	219.00	0.46	0.34	7.18	1.70	46.90	0.40	10.70	1.05
0.94	230.00	0.53	0.45	9.40	2.18	52.60	0.50	13.10	1.38
1.18	211.00	0.65	0.48	11.20	1.61	69.30	0.60	14.50	1.51
0.90	211.00	0.50	0.37	9.10	1.49	43.30	0.50	11.80	1.20
1.18	199.00	0.64	0.46	11.00	1.79	66.90	0.60	15.00	1.50
0.81	214.00	0.47	0.39	8.26	1.86	43.00	0.40	12.30	1.24
0.94	204.00	0.62	0.55	12.80	2.28	43.60	1.00	16.20	1.64
0.75	216.00	0.46	0.39	9.45	1.60	38.10	0.40	11.80	1.16
0.77	203.00	0.58	0.40	8.89	1.59	40.50	0.40	12.20	1.28
0.69	195.00	0.44	0.41	8.97	1.60	36.30	0.40	12.10	1.24
0.98	215.00	0.53	0.42	9.98	1.91	54.50	0.50	13.10	1.31

0.97	219.00	0.51	0.39	8.39	2.11	46.00	6.10	11.90	1.19
0.62	209.00	0.40	0.35	7.90	1.44	32.60	0.50	10.60	1.09
1.03	207.00	0.58	0.41	9.82	1.61	57.60	0.60	12.90	1.30
1.19	207.00	0.56	0.42	10.20	2.18	66.20	0.60	13.10	1.36
0.98	202.00	0.51	0.44	10.80	2.09	52.80	0.50	13.20	1.33
1.34	201.00	0.78	0.61	14.80	3.28	60.20	1.00	17.90	1.87
0.93	225.00	0.54	0.42	11.30	1.76	50.40	0.60	12.80	1.25
0.95	211.00	0.50	0.40	8.31	1.78	49.50	0.50	12.90	1.27
0.98	214.00	0.53	0.42	8.70	1.90	57.60	0.50	13.10	1.30
1.41	233.00	0.64	0.50	12.20	1.90	86.40	0.60	15.40	1.48
1.35	240.00	0.66	0.50	13.00	2.55	68.80	1.20	14.70	1.38
1.09	204.00	0.54	0.43	9.08	1.79	56.50	0.60	18.00	1.45
0.74	208.00	0.48	0.43	9.35	1.56	35.00	0.40	12.50	1.26
0.87	227.00	0.51	0.42	8.53	1.51	53.40	0.50	12.90	1.30
0.96	219.00	0.60	0.42	8.90	1.72	57.50	0.70	13.30	1.30
1.81	207.00	0.80	0.55	17.10	3.60	97.00	0.80	17.00	1.64
1.12	196.00	0.55	0.41	9.47	1.57	61.20	0.60	13.20	1.33
1.46	217.00	0.68	0.50	14.80	1.85	80.00	0.70	16.00	1.48
0.76	212.00	0.47	0.40	9.59	1.87	37.20	0.40	12.30	1.16
1.02	214.00	0.57	0.42	10.90	1.68	58.10	0.50	13.50	1.29
1.12	203.00	0.55	0.41	10.20	1.76	64.50	0.60	13.00	1.30
1.28	200.00	0.58	0.42	10.80	1.60	71.20	0.60	13.70	1.30
0.95	175.00	0.55	0.45	8.25	1.67	46.30	0.60	14.30	1.46
0.78	200.00	0.48	0.40	9.02	1.43	40.20	0.50	12.00	1.18
0.89	211.00	0.52	0.43	10.30	1.63	47.40	0.60	13.20	1.29
1.03	216.00	0.56	0.44	10.30	2.04	60.40	0.50	13.60	1.39
0.88	176.00	0.46	0.35	9.18	1.90	47.20	0.40	11.70	1.12

0.83	226.00	0.49	0.40	9.21	2.24	48.80	0.40	12.10	1.21
1.78	194.00	0.75	0.56	13.80	2.17	98.20	0.80	17.70	1.73
0.97	186.00	0.49	0.40	9.72	1.75	50.90	0.50	12.60	1.18
0.97	188.00	0.57	0.44	8.09	1.83	47.60	0.60	14.50	1.52
0.65	200.00	0.44	0.36	6.48	1.42	31.90	0.40	11.30	1.15
1.05	189.00	0.53	0.42	11.00	1.81	55.10	0.50	14.00	1.34
0.96	211.00	0.49	0.38	10.10	1.83	52.20	0.50	11.90	1.12
0.96	215.00	0.52	0.42	8.65	1.48	52.40	0.40	13.30	1.37
0.92	205.00	0.57	0.42	9.79	1.60	52.50	0.60	13.20	1.34
0.88	217.00	0.50	0.40	8.10	1.67	50.60	0.80	12.50	1.21
1.09	216.00	0.54	0.42	9.64	1.94	56.50	1.90	12.80	1.16
1.38	211.00	0.62	0.46	11.90	2.45	70.90	1.00	14.10	1.24
1.06	198.00	0.52	0.42	9.75	2.15	51.70	0.90	13.50	1.21
1.31	197.00	0.67	0.47	10.90	1.96	62.80	1.20	14.80	1.37
1.20	203.00	0.67	0.46	11.50	2.24	61.20	1.00	14.10	1.30
0.65	191.00	0.48	0.36	9.03	1.76	29.70	0.70	11.10	1.09
1.34	211.00	0.88	0.60	15.80	2.73	55.50	1.40	18.30	1.72
1.30	208.00	0.83	0.56	14.10	3.12	51.40	1.30	17.50	1.69
1.39	226.00	0.67	0.48	12.10	1.91	67.10	1.50	14.50	1.30
0.68	246.00	0.44	0.35	6.75	1.37	31.80	1.00	10.00	0.92
1.22	217.00	0.63	0.47	12.00	2.04	61.30	1.30	14.10	1.29
0.78	218.00	0.40	0.35	6.68	1.26	37.80	0.60	10.80	1.01
1.22	198.00	0.56	0.46	10.90	2.57	61.60	1.00	13.50	1.28
1.17	204.00	0.52	0.40	10.10	2.01	53.80	0.90	11.90	1.11
1.30	220.00	0.63	0.48	11.00	1.98	68.00	1.10	14.20	1.37
0.85	213.00	0.46	0.36	7.46	2.39	35.90	1.00	10.80	0.95
0.97	197.00	0.53	0.43	9.83	1.50	45.90	0.90	12.90	1.21

1.22	202.00	0.60	0.45	10.30	2.33	59.80	1.10	13.00	1.24
1.24	190.00	0.64	0.47	9.02	2.10	57.90	1.30	14.60	1.41
1.16	208.00	0.54	0.44	9.91	2.07	60.60	1.00	13.00	1.19
1.23	181.00	0.60	0.46	9.42	1.76	56.70	1.10	13.60	1.23
1.41	186.00	0.63	0.49	10.30	2.16	62.30	3.20	15.10	1.40
1.22	217.00	0.62	0.45	10.00	2.52	62.10	1.30	13.50	1.26
0.98	215.00	0.57	0.41	9.33	1.70	46.60	0.90	12.40	1.15
1.39	220.00	0.67	0.48	12.60	1.68	68.70	1.10	14.30	1.34
0.89	195.00	0.51	0.39	8.24	1.82	42.50	0.80	12.40	1.21
1.63	206.00	0.72	0.52	11.70	1.98	77.90	1.30	15.90	1.52
1.75	194.00	0.74	0.55	11.10	2.15	80.00	1.40	16.40	1.50
0.70	212.00	0.46	0.36	7.49	1.32	33.00	0.80	11.00	1.02
0.74	211.00	0.46	0.36	6.51	1.43	33.00	0.80	11.10	1.03
0.89	210.00	0.51	0.42	7.94	1.43	44.40	0.70	12.50	1.14
1.78	197.00	0.83	0.60	15.80	1.84	86.10	1.30	19.60	1.59
1.36	202.00	0.75	0.50	12.00	1.79	60.80	1.10	15.10	1.41
0.84	211.00	0.55	0.45	9.06	1.64	39.30	0.70	13.10	1.20
1.81	197.00	0.83	0.60	15.20	2.45	85.50	1.30	16.60	1.52
1.23	211.00	0.66	0.44	12.40	2.05	61.70	1.20	13.80	1.22
0.72	222.00	0.49	0.36	7.52	1.78	35.30	0.80	10.90	0.96
0.61	221.00	0.41	0.34	6.61	1.63	27.80	0.60	10.50	0.89
0.67	213.00	0.44	0.34	7.71	1.54	36.90	0.70	11.00	0.96
1.07	221.00	0.60	0.42	10.70	2.25	62.00	1.00	16.00	1.18
1.00	220.00	0.55	0.40	9.68	1.65	53.60	1.30	13.10	1.14
1.18	223.00	0.60	0.43	11.00	2.03	66.20	1.00	13.80	1.20
0.89	224.00	0.51	0.40	8.72	2.63	47.60	0.90	12.70	1.11
1.58	193.00	0.93	0.35	9.24	2.25	80.40	8.30	11.20	1.12

0.77	207.00	0.47	0.34	8.62	1.38	41.80	0.80	11.20	0.96
1.51	211.00	0.83	0.53	14.80	2.07	83.10	1.60	16.60	1.52
2.08	184.00	0.90	0.60	20.60	4.85	109.00	1.70	18.50	1.89
1.04	203.00	0.56	0.35	12.30	1.83	48.60	0.80	11.00	0.89
1.46	198.00	0.81	0.51	14.60	2.42	75.60	1.20	16.80	1.47
0.73	222.00	0.51	0.35	7.35	1.87	34.80	0.80	11.20	0.95
1.02	216.00	0.57	0.42	10.20	1.80	45.30	0.80	13.10	1.18
0.62	189.00	0.43	0.36	6.38	1.81	27.30	0.60	10.60	0.99
1.08	206.00	0.64	0.45	12.30	2.98	55.20	0.90	13.80	1.19
0.86	194.00	0.51	0.36	9.22	1.80	45.50	0.80	11.50	1.02
0.90	208.00	0.57	0.40	10.00	2.20	46.20	0.80	12.70	1.10
0.86	190.00	0.54	0.40	9.64	2.12	45.60	1.40	13.30	1.17
0.90	213.00	0.53	0.39	8.46	1.82	49.70	0.90	12.50	1.11
0.82	214.00	0.55	0.39	9.18	1.58	44.50	0.70	12.60	1.10
1.12	192.00	0.62	0.42	10.60	3.35	60.30	0.90	13.90	1.20
0.67	192.00	0.50	0.35	7.39	1.60	33.00	0.60	11.40	1.04
1.18	183.00	0.68	0.49	13.80	2.24	64.10	1.20	15.50	1.37
0.71	204.00	0.49	0.35	7.39	1.49	33.80	0.60	11.70	1.08
0.66	185.00	0.45	0.36	11.00	1.99	30.90	0.70	11.40	1.02
1.11	215.00	0.57	0.41	11.70	1.95	59.40	1.00	13.40	1.17
0.97	224.00	0.57	0.42	9.22	1.66	60.40	1.30	13.60	1.19
0.83	195.00	0.46	0.36	8.76	1.93	39.70	0.80	11.60	1.00
0.83	218.00	0.50	0.37	9.60	1.50	44.40	0.80	11.90	0.96
0.95	217.00	0.54	0.38	10.70	1.71	50.70	0.80	12.60	1.07
1.59	198.00	0.80	0.56	18.20	2.34	84.00	1.30	17.80	1.52
0.95	204.00	0.56	0.40	10.50	1.74	50.40	0.90	12.80	1.06
0.74	218.00	0.46	0.38	8.81	1.60	40.70	0.70	11.60	1.02
1.12	211.00	0.60	0.49	13.80	2.13	59.10	1.10	14.00	1.21
0.93	212.00	0.58	0.42	9.99	1.56	47.40	0.80	12.50	1.08

1.10	215.00	0.58	0.44	10.50	1.59	57.20	0.90	13.00	1.14
1.18	217.00	0.56	0.41	9.73	1.50	50.00	0.90	12.50	1.15
0.75	223.00	0.52	0.40	9.88	1.66	40.30	1.10	12.90	1.11
1.50	207.00	0.74	0.51	15.30	2.01	77.60	1.30	15.40	1.37
1.47	213.00	0.70	0.51	14.50	1.89	75.40	1.30	15.00	1.33
1.01	208.00	0.54	0.40	9.44	1.76	50.50	0.90	12.30	1.11
1.10	199.00	0.57	0.44	11.10	1.66	54.90	0.90	13.10	1.20
1.03	212.00	0.55	0.47	10.50	1.62	55.40	0.90	13.70	1.23
1.22	222.00	0.57	0.46	11.10	1.65	69.50	1.00	14.00	1.31
1.07	225.00	0.54	0.42	9.92	2.00	60.60	0.90	12.90	1.18
1.42	209.00	0.68	0.52	12.00	1.90	68.20	1.70	15.60	1.42
0.83	227.00	0.47	0.41	8.72	1.66	40.10	1.20	12.00	1.06
0.82	211.00	0.46	0.35	8.35	1.37	44.60	0.80	11.10	1.01
0.85	187.00	0.50	0.36	8.65	1.37	46.80	0.80	10.90	1.00
1.18	189.00	0.58	0.43	11.50	1.63	63.40	1.00	13.00	1.22
0.60	217.00	0.43	0.33	6.17	1.22	28.50	0.60	10.20	0.91
1.31	181.00	0.66	0.51	9.40	1.95	57.70	1.30	15.40	1.43
0.70	216.00	0.45	0.38	8.01	1.52	36.60	0.60	11.10	0.99
0.98	217.00	0.55	0.44	11.20	2.04	51.00	0.80	12.80	1.19
0.95	198.00	0.52	0.40	9.38	1.48	49.80	0.80	12.10	1.15
0.98	199.00	0.56	0.45	10.50	7.26	46.90	0.90	13.40	1.22
1.52	194.00	0.69	0.51	12.20	1.78	81.10	1.10	15.60	1.38
1.40	201.00	0.64	0.46	12.80	2.35	71.10	1.00	14.50	1.29
0.97	181.00	0.55	0.45	11.20	1.79	49.80	1.00	13.80	1.25
1.25	209.00	0.62	0.49	12.60	2.45	61.90	1.40	14.20	1.28
1.11	200.00	0.60	0.47	10.50	1.99	46.70	1.00	12.70	1.15
0.66	191.00	0.43	0.36	6.77	1.42	29.20	0.60	10.20	0.93
0.63	202.00	0.43	0.34	6.58	1.67	28.40	0.80	10.00	0.90

1.36	178.00	0.60	0.44	10.90	2.55	48.50	0.90	13.40	1.17
0.74	194.00	0.50	0.42	9.08	1.60	35.30	1.10	12.10	1.13
1.05	186.00	0.63	0.46	9.40	1.81	53.30	1.20	13.90	1.25
0.80	188.00	0.46	0.35	8.04	1.48	42.30	0.70	11.10	1.02
1.18	192.00	0.61	0.43	11.20	1.71	61.60	1.00	13.00	1.24
1.15	224.00	0.58	0.47	11.10	1.88	61.10	0.90	14.20	1.33
1.63	217.00	0.76	0.61	15.50	2.15	89.90	1.30	18.10	1.66
0.78	217.00	0.49	0.40	8.80	1.67	38.80	0.90	11.40	1.04
1.00	250.00	0.61	0.47	12.20	2.55	47.60	1.00	13.80	1.28
0.88	238.00	0.56	0.44	9.75	1.84	41.80	0.80	12.60	1.19
1.36	244.00	0.70	0.52	12.10	3.92	70.80	1.10	15.50	1.45
0.97	262.00	0.62	0.46	10.60	3.24	43.50	0.90	12.80	1.24
0.90	242.00	0.54	0.44	8.01	1.90	45.50	0.90	12.20	1.28
1.27	251.00	0.66	0.48	11.20	2.40	66.30	1.10	14.20	1.37
0.95	257.00	0.62	0.43	9.29	1.74	43.20	0.80	12.10	1.16
1.21	221.00	0.62	0.47	11.60	1.69	61.20	1.00	13.70	1.24
1.26	217.00	0.61	0.46	11.60	1.78	62.10	1.00	14.00	1.21
1.37	232.00	0.84	0.53	12.40	2.27	65.00	1.20	16.50	1.54
1.05	231.00	0.55	0.45	9.49	2.02	54.00	0.90	14.70	1.19
0.70	250.00	0.46	0.35	6.71	1.71	30.70	0.80	10.50	0.96
0.88	252.00	0.55	0.41	8.62	1.67	42.20	0.80	14.20	1.13
0.88	242.00	0.56	0.41	8.99	2.22	40.50	0.80	12.60	1.19
0.78	237.00	0.51	0.44	10.50	1.67	36.30	0.80	12.40	1.14
1.28	250.00	0.66	0.49	11.70	2.17	58.70	1.20	14.00	1.26
0.57	231.00	0.40	0.31	5.86	1.23	26.00	0.60	9.30	0.85
0.64	241.00	0.46	0.36	7.97	1.64	30.10	0.70	10.30	0.96
0.88	252.00	0.55	0.43	9.22	1.91	42.60	0.90	12.60	1.18
1.10	242.00	0.59	0.43	10.90	2.58	54.40	1.00	13.30	1.23



0.72	258.00	0.51	0.43	9.37	1.90	33.60	0.80	12.80	1.21
1.43	225.00	0.75	0.53	13.00	2.16	74.90	1.30	15.90	1.49
1.06	256.00	0.57	0.44	11.40	2.00	49.50	0.90	12.40	1.13
0.70	260.00	0.45	0.38	9.21	1.61	34.00	0.70	11.30	1.06
0.76	253.00	0.45	0.38	8.50	30.40	35.30	0.90	11.10	1.01
0.69	243.00	0.47	0.39	9.15	2.66	32.00	1.70	10.90	1.01
0.87	245.00	0.53	0.41	8.11	1.84	40.90	0.80	11.80	1.12
0.82	251.00	0.62	0.43	8.95	1.56	36.20	0.70	12.20	1.17
0.74	243.00	0.45	0.37	7.59	1.44	31.70	0.90	10.90	1.02
0.84	242.00	0.51	0.38	8.22	1.42	42.70	0.80	11.20	1.03
1.2	234.00	0.61	0.41	12.00	3.04	51.40	24.90	12.30	1.31
1.22	208.00	0.61	0.41	11.70	2.43	62.50	5.30	12.00	1.28
1	217.00	0.58	0.41	12.40	1.73	49.30	1.70	11.90	1.27
1.87	196.00	0.89	0.56	18.00	2.44	88.90	1.70	16.00	1.70
0.84	205.00	0.56	0.48	12.50	2.39	44.60	1.00	12.70	1.35
1.11	213.00	0.78	0.43	12.20	2.42	59.60	1.50	11.90	1.45
1.16	212.00	0.66	0.46	12.90	1.86	58.80	1.30	13.50	1.37
1.28	213.00	0.69	0.49	14.60	1.89	69.20	1.20	13.60	1.44
0.79	214.00	0.57	0.44	9.84	1.77	34.20	0.70	11.60	1.33
0.63	200.00	0.70	0.45	14.10	2.20	32.50	1.20	12.00	1.36
1.2	220.00	0.72	0.48	13.10	2.61	64.30	1.20	13.70	1.54
0.98	214.00	0.57	0.42	11.80	2.22	53.30	0.90	11.70	1.31
1.17	217.00	0.63	0.40	12.00	2.35	58.50	0.90	11.90	1.26
0.8	201.00	0.53	0.38	11.20	1.89	42.00	0.80	10.70	1.20
1.03	212.00	0.57	0.40	11.70	2.60	54.10	0.80	11.50	1.28
1.01	222.00	0.57	0.39	10.60	2.43	52.90	0.80	11.60	1.31
1.21	224.00	0.62	0.43	12.10	2.48	63.80	1.00	12.60	1.40

1.13	217.00	0.60	0.41	11.80	2.39	55.80	1.00	11.90	1.33
1.04	212.00	0.54	0.37	10.60	2.39	53.50	0.90	11.40	1.23
1.1	179.00	0.61	0.44	11.80	2.46	43.60	0.80	12.70	1.43
1.07	191.00	0.61	0.42	11.20	2.33	53.00	1.10	12.10	1.34
1.01	138.00	0.36	0.24	8.29	1.69	33.00	0.60	7.00	0.72
0.62	132.00	0.34	0.24	7.45	1.58	29.20	0.80	6.60	0.74
0.59	98.00	0.28	0.20	4.69	1.39	29.50	0.50	6.30	0.69
0.54	97.00	0.26	0.21	4.43	1.42	27.90	0.70	6.10	0.70
0.91	205.00	0.59	0.40	10.40	2.76	47.80	1.00	10.80	1.20
1.03	181.00	0.50	0.35	11.20	2.40	42.70	0.90	9.00	0.92
1.28	203.00	0.69	0.46	11.90	2.55	66.40	1.10	13.10	1.48
0.99	222.00	0.65	0.45	11.80	2.07	52.00	0.80	12.50	1.40
1.12	206.00	0.61	0.42	11.00	2.13	61.60	1.00	12.10	1.33
1.15	198.00	0.67	0.46	11.80	2.46	59.70	1.10	12.90	1.45
0.89	183.00	0.51	0.31	10.70	2.16	44.70	0.80	9.00	1.00
1.25	225.00	0.64	0.47	12.00	2.34	65.30	1.00	13.30	1.50
1.13	219.00	0.65	0.45	11.10	2.46	55.30	0.90	13.40	1.56
1.42	243.00	0.74	0.49	12.50	3.52	67.40	1.20	13.90	1.56
1.66	239.00	0.79	0.53	16.20	3.06	85.70	1.30	15.20	1.61
1.43	240.00	0.80	0.53	19.10	3.23	69.70	1.20	15.40	1.69
1.42	230.00	0.78	0.46	15.20	3.60	65.80	1.20	13.20	1.45
1.54	231.00	0.75	0.48	15.10	3.23	67.10	1.30	13.70	1.47
1.57	238.00	0.79	0.46	15.40	3.17	68.90	1.30	13.80	1.54
1.68	219.00	0.86	0.53	18.20	2.52	83.00	1.50	15.20	1.60
1.54	214.00	0.81	0.52	17.00	2.31	72.90	1.30	14.30	1.59
1.39	218.00	0.76	0.50	16.00	2.49	69.00	1.10	14.60	1.60
1.66	215.00	0.86	0.54	17.40	2.47	78.70	1.40	15.00	1.68

Zn (ppm)	Zr (ppm)
27.00	106.00
35.00	152.00
30.00	114.00
51.00	145.00
29.00	135.00
40.00	163.00
33.00	160.00
31.00	117.00
72.00	123.00
33.00	135.00
27.00	191.00
32.00	196.00
27.00	141.00
32.00	182.00
35.00	116.00
40.00	145.00
55.00	162.00
32.00	133.00
48.00	193.00
30.00	164.00
28.00	294.00
26.00	173.00
29.00	178.00
22.00	188.00
37.00	175.00

37.00	134.00
25.00	145.00
44.00	138.00
54.00	131.00
42.00	143.00
47.00	221.00
41.00	160.00
42.00	142.00
47.00	148.00
75.00	136.00
58.00	133.00
45.00	181.00
24.00	167.00
39.00	194.00
45.00	160.00
85.00	135.00
53.00	125.00
70.00	140.00
30.00	153.00
46.00	172.00
54.00	135.00
66.00	107.00
35.00	149.00
32.00	138.00
35.00	185.00
50.00	152.00
42.00	114.00

37.00	161.00
78.00	120.00
45.00	119.00
36.00	175.00
28.00	138.00
46.00	147.00
44.00	106.00
39.00	163.00
41.00	175.00
35.00	140.00
49.00	132.00
61.00	109.00
48.00	118.00
54.00	138.00
51.00	134.00
26.00	156.00
48.00	206.00
46.00	202.00
55.00	100.00
31.00	85.00
51.00	120.00
35.00	116.00
55.00	120.00
53.00	98.00
63.00	122.00
31.00	95.00
40.00	143.00

55.00	111.00
48.00	141.00
56.00	101.00
52.00	113.00
56.00	117.00
64.00	124.00
41.00	153.00
58.00	117.00
38.00	134.00
67.00	117.00
69.00	117.00
27.00	141.00
30.00	109.00
35.00	138.00
69.00	144.00
51.00	182.00
32.00	165.00
78.00	137.00
48.00	126.00
28.00	120.00
22.00	147.00
29.00	123.00
54.00	133.00
46.00	127.00
59.00	117.00
40.00	137.00
61.00	162.00

36.00	105.00
66.00	171.00
108.00	121.00
49.00	93.00
63.00	142.00
27.00	91.00
34.00	177.00
23.00	141.00
46.00	143.00
39.00	107.00
39.00	132.00
46.00	158.00
44.00	109.00
36.00	148.00
56.00	127.00
29.00	143.00
61.00	140.00
26.00	161.00
27.00	138.00
53.00	131.00
50.00	120.00
37.00	114.00
36.00	112.00
46.00	132.00
71.00	176.00
43.00	134.00
31.00	132.00
45.00	164.00
37.00	118.00

45.00	122.00
41.00	131.00
31.00	168.00
68.00	120.00
63.00	146.00
41.00	117.00
46.00	126.00
43.00	128.00
59.00	105.00
50.00	103.00
53.00	165.00
36.00	127.00
39.00	86.00
45.00	106.00
57.00	111.00
25.00	98.00
46.00	117.00
28.00	143.00
41.00	138.00
39.00	131.00
39.00	141.00
68.00	114.00
62.00	106.00
41.00	128.00
57.00	134.00
39.00	117.00
26.00	95.00
26.00	101.00



43.00	147.00
31.00	145.00
47.00	127.00
37.00	101.00
53.00	129.00
53.00	145.00
72.00	142.00
37.00	115.00
41.00	165.00
39.00	145.00
64.00	149.00
39.00	151.00
38.00	138.00
59.00	123.00
40.00	125.00
60.00	111.00
64.00	102.00
61.00	215.00
59.00	133.00
29.00	92.00
36.00	126.00
36.00	140.00
31.00	153.00
56.00	123.00
25.00	86.00
27.00	115.00
37.00	131.00

51.00	135.00
27.00	185.00
65.00	128.00
46.00	119.00
30.00	149.00
33.00	133.00
29.00	122.00
33.00	110.00
29.00	180.00
27.00	132.00
42.00	86.00
46.00	150.00
60.00	113.00
46.00	147.00
74.00	121.00
37.00	202.00
44.00	259.00
46.00	126.00
56.00	109.00
28.00	212.00
26.00	243.00
56.00	158.00
46.00	150.00
52.00	145.00
36.00	149.00
49.00	122.00
47.00	133.00
55.00	124.00

50.00	122.00
47.00	128.00
43.00	179.00
49.00	124.00
35.00	73.00
32.00	72.00
36.00	52.00
35.00	54.00
44.00	118.00
44.00	91.00
60.00	125.00
48.00	161.00
56.00	97.00
53.00	143.00
43.00	91.00
57.00	135.00
48.00	186.00
62.00	145.00
83.00	122.00
64.00	175.00
60.00	119.00
62.00	121.00
65.00	131.00
78.00	119.00
67.00	141.00
63.00	156.00
75.00	130.00